

**Development of tools for the study of enzymes in ammonia oxidising
archaea**

Arne Schatteman

**A thesis submitted to the school of Biology in fulfilment of the requirements
for the degree of Doctor in Philosophy.**

September 2022

University of East Anglia

School of Biology

Norwich, UK

© This copy of the thesis has been supplied on condition that anyone who consults it is understood to recognise that its copyright rests with the author and that use of any information derived therefrom must be in accordance with current UK copyright law. In addition, any quotation or extract must include full attribution.

Abstract

Ammonia-oxidizing archaea (AOA) and bacteria (AOB) perform key steps in the global nitrogen cycle, the oxidation of ammonia to nitrite. While the ammonia oxidation pathway is well characterized in AOB, many knowledge gaps remain about the metabolism of AOA. In addition, AOA are hard to grow, and laboratory techniques are poorly developed. The main aim of this thesis was to identify the unknown proteins in the archaeal ammonia oxidation pathway and an additional goal was to improve the methods for growing and working with the model organism '*Ca. N. franklandus*'.

A bioreactor system was explored to grow '*Ca. N. franklandus*'. A continuous cultivation system with biomass retention was shown to be a promising way to culture this organism. If successfully deployed, it would provide permanent access to high quality biomass in sufficient quantities for physiological experiments. In addition, a cell breakage protocol was optimised, and a proteome of cells grown on urea and ammonia was determined.

To investigate the ammonia oxidation pathway, substrates and inhibitors of the hydroxylamine oxidation mechanism were identified and characterised. Hydrazine and phenylhydrazine were shown to interfere with ammonia and hydroxylamine oxidation in AOA. Furthermore, '*Ca. N. franklandus*' oxidized hydrazine into dinitrogen, coupling this reaction to ATP production and O₂ uptake.

Furthermore, activity-based protein profiling (ABPP) probes were evaluated for the labelling of the ammonia monooxygenase and the hydroxylamine oxidation enzyme. To this end, 1,5-hexadiyne and an aryl-hydrazine probe, respectively, were evaluated. The diyne probe has been successfully used to label the AMO of AOA and the aryl probe shows promising results which may lead to the identification of the hydroxylamine oxidation enzyme.

Finally, several observations in this thesis led to the identification of a catalase isozyme. First, a DNA protection during starvation protein was very abundant in the proteome. Second, this protein was identified when a catalase staining method was used and catalase activity was observed while no catalase is encoded in the genome of '*Ca. N. franklandus*'. Sequence analysis supported the hypothesis that it was a DPS-like protein with catalase activity.

Access Condition and Agreement

Each deposit in UEA Digital Repository is protected by copyright and other intellectual property rights, and duplication or sale of all or part of any of the Data Collections is not permitted, except that material may be duplicated by you for your research use or for educational purposes in electronic or print form. You must obtain permission from the copyright holder, usually the author, for any other use. Exceptions only apply where a deposit may be explicitly provided under a stated licence, such as a Creative Commons licence or Open Government licence.

Electronic or print copies may not be offered, whether for sale or otherwise to anyone, unless explicitly stated under a Creative Commons or Open Government license. Unauthorised reproduction, editing or reformatting for resale purposes is explicitly prohibited (except where approved by the copyright holder themselves) and UEA reserves the right to take immediate 'take down' action on behalf of the copyright and/or rights holder if this Access condition of the UEA Digital Repository is breached. Any material in this database has been supplied on the understanding that it is copyright material and that no quotation from the material may be published without proper acknowledgement.

Table of contents

1	Introduction	1
1.1	Nitrogen (N)	1
1.2	The microbial nitrogen cycle	1
1.2.1	Nitrogen fixation	2
1.2.2	Nitrification	3
1.2.3	Denitrification	3
1.2.4	Anammox	4
1.2.5	Assimilation and mineralisation	4
1.3	Humans and the nitrogen cycle	4
1.4	Nitrification inhibitors	5
1.5	Nitrogen in wastewater treatment	6
1.6	Ammonia oxidising organisms	7
1.6.1	Ammonia oxidising bacteria (AOB)	7
1.6.2	Ammonia oxidising archaea (AOA)	8
1.6.3	Complete ammonia oxidising bacteria (comammox)	10
1.6.4	Heterotrophic ammonia oxidisers	10
1.7	Enzymology of AOM	11
1.7.1	Ammonia oxidising bacteria and comammox	12
1.7.2	Ammonia oxidising archaea	14
2	Materials and methods	19
2.1	Materials	19
2.2	Growth of microorganisms	19
2.2.1	Growth conditions	19
2.2.2	Media composition	20
2.3	Cell counts	22
2.4	Cell harvesting and preparation	22
2.5	Nitrogen quantification	23

2.5.1	Nitrite determination	23
2.5.2	Ammonia determination.....	23
2.5.3	Hydroxylamine determination	23
2.5.4	¹⁵ N stable isotope analysis	24
2.6	Inhibition, activity, recovery and growth assays.....	24
2.6.1	96-well inhibition assays	24
2.6.2	Activity, inhibition and growth assays	25
2.6.3	Recovery.....	25
2.7	ATP assay.....	25
2.8	Oxygen consumption experiments	26
2.9	Protein analysis and cell extract preparation	26
2.9.1	Cell extract preparation	26
2.9.2	SDS-PAGE	27
2.9.3	Colourless native PAGE	27
2.9.4	Blue native PAGE.....	27
2.9.5	Coomassie stain	28
2.9.6	Sypro ruby stain	28
2.9.7	Catalase activity stain.....	28
2.9.8	Protein precipitation	28
2.9.9	Protein fractionation.....	29
2.9.10	Preparation of gel slices for trypsin digestion	29
2.9.11	Protein identification	30
2.9.12	Protein quantification	30
2.10	Activity based protein profiling (ABPP).....	31
2.10.1	Treatment with bifunctional inhibitor probes	31
2.10.2	Copper catalysed azide-alkyne cycloaddition (CuAAC).....	31
3	Optimising growth and laboratory methods of the model AOA <i>Nitrosocosmicus franklandus</i> C13	

3.1	Introduction	33
3.2	Results.....	34
3.2.1	Growth of <i>N. franklandus</i> in a bioreactor	34
3.2.2	Evaluation of breakage methods	41
3.2.3	Making cell-free protein extract and developing a hydroxylamine oxidation assay	43
3.2.4	Proteomics using growth on urea and ammonia.....	52
3.3	Discussion.....	58
3.3.1	A bioreactor system for the growth of AOA	58
3.3.2	Hydroxylamine oxidation in cell extract	58
3.3.3	Proteome of <i>N. franklandus</i> grown with urea and ammonia.....	59
4	Hydrazines as substrates and inhibitors of the archaeal ammonia oxidation pathway	60
4.1	Introduction	60
4.2	Results.....	62
4.2.1	The effect of phenylhydrazine on NH ₃ and hydroxylamine-dependent nitrite production by ammonia oxidisers	62
4.2.2	The effect of hydrazine on NH ₃ and hydroxylamine-dependent NO ₂ ⁻ production	64
4.2.3	Recovery of NO ₂ ⁻ production by ' <i>Ca. Nitrosocosmicus franklandus</i> ' following inhibition with phenylhydrazine or hydrazine.....	67
4.2.4	Hydrazine-dependent O ₂ consumption in ' <i>Ca. Nitrosocosmicus franklandus</i> '	69
4.2.5	ATP production in response to hydrazine and phenylhydrazine	74
4.2.6	N ₂ is a product of hydrazine oxidation in ' <i>Ca. Nitrosocosmicus franklandus</i> '	76
4.3	Discussion.....	77
4.3.1	Hydrazines as inhibitors of AOA.....	77
4.3.2	Hydrazine as a substrate in AOA.....	78
4.4	Outlook for applications of hydrazines in ammonia oxidation research.....	79
5	Identification of novel enzymes in the archaeal ammonia oxidation pathway using activity-based protein profiling (ABPP)	80
5.1	Introduction	80

5.2	Results.....	82
5.2.1	Inhibition of ammonia oxidation in the archaeon ' <i>Ca. N. franklandus</i> ' by 1,5-Hexadiyne (15HD)	83
5.2.2	15HD inhibition is AMO-specific	84
5.2.3	15HD inhibition is irreversible.....	84
5.2.4	A fluorescent tag reveals labelled cells by fluorescent microscopy	87
5.2.5	Fluorescent SDS-PAGE	88
5.2.6	Hydrazine-based ABPP probes.....	90
5.2.7	Inhibition of ' <i>Ca. N. franklandus</i> ' by biotin-hydrazides.....	91
5.2.8	Hydrazine-alkyne ABPP probes	92
5.2.9	Inhibition of ' <i>Ca. N. franklandus</i> ' by a hydrazine-alkyne	93
5.2.10	Click-fluorescence	94
5.3	Discussion.....	95
5.3.1	Labelling of the archaeal AMO with 1,5-Hexadiyne	95
5.3.2	Labelling of archaeal hydroxylamine oxidising enzymes using hydrazine probes.....	96
6	Identification of a Catalase isozyme from ' <i>Ca. N. franklandus</i> ' C13	98
6.1	Introduction	98
6.2	Results.....	100
6.2.1	' <i>Ca. N. franklandus</i> ' has a H ₂ O ₂ detoxification enzyme	100
6.2.2	Partial purification of the catalase enzyme	101
6.2.3	Identification of the candidate catalase isozyme	105
6.2.4	Sequence analysis	108
6.2.5	Blue native polyacrylamide gel electrophoresis (BN-PAGE)	109
6.2.6	Growth with pyruvate and catalase.....	110
6.3	Discussion.....	113
7	Conclusions and prospects for future research	115
7.1	Development of ' <i>Ca. N. franklandus</i> ' as a model organism.....	115
7.2	Hydrazines as inhibitors in the AOA.....	116

7.3	Activity based protein profiling in AOA.....	117
7.4	The role of a H ₂ O ₂ detoxification mechanism in ' <i>Ca. N. franklandus</i> '	117
7.5	Prospects for future research	118
	References	119

List of tables

Table 2-1 – growth conditions of ammonia oxidisers.....	19
Table 3-1 Overview of tested breakage methods and their effectivity.....	41
Table 3-2 – Electron acceptors tested with cell extract from ' <i>Ca N. franklandus</i> '	43
Table 3-3 – The ten most abundant proteins identified in the samples cut out from an SDS-PAGE ...	49
Table 5-1 – Identification of proteins by MALDI-TOF from excised SDS-PAGE protein bands.	90
Table 6-1 - Protein concentrations of different fractions after $(\text{NH}_4)_2\text{SO}_4$ precipitation.....	101
Table 6-2 - Protein concentrations of different fractions after anion exchange fractionation	104
Table 6-3 - MALDI-TOF analysis results.....	106
Table 6-4 - The top five most abundant identified proteins in each sample.....	107

List of Figures

Figure 1-1 – Overview of the biogeochemical cycling of nitrogen from (Kuypers <i>et al.</i> , 2018)	2
Figure 1-2 – Pathways of ammonia oxidation in bacteria (A) and archaea (B-C)	12
Figure 3-1 – Schematic of reactor set-up (A), picture of reactor (B), DAPI stained picture of biofilm (C), picture of turbid reactor with biofilm formation on filter (D).	35
Figure 3-2 – Overview of the first two successful reactor runs.	38
Figure 3-3 – Activity assay of batch-grown cells compared to reactor grown cells.	39
Figure 3-4 – Overview of successful Runs 3 (A) and 4 (B).	40
Figure 3-5 – SDS-PAGE profiles of identical <i>N. franklandus</i> protein samples lysed with different techniques.	42
Figure 3-6 – pH optimum of the reduction of ferricyanide in cell free extracts of ‘ <i>Ca. N. franklandus</i> ’ when using 200 µg protein in 50 mM Tris buffer.	44
Figure 3-7 – The reduction of ferricyanide in cell free extracts of ‘ <i>Ca. N. franklandus</i> ’ and <i>N. europaea</i> when using different protein concentrations in 50 mM Tris buffer.	45
Figure 3-8 – Profile of the activity in the different fractions after anion exchange fractionation	46
Figure 3-9 – Profile of the activity in the different fractions after cation exchange fractionation	47
Figure 3-10 – SYPRO Ruby stain of active fractions after cation exchange fractionation	48
Figure 3-11 – Size exclusion fractionation of active fractions using spin tubes	51
Figure 3-12 – Details of the urease operon in ‘ <i>Ca. N. franklandus</i> ’ in cells grown on urea vs ammonia.	53
Figure 3-13 – All significantly up or downregulated proteins that were detected in the proteome of ‘ <i>Ca. N. franklandus</i> ’	55
Figure 3-14 – The normalised absolute abundances of the 50 most highly expressed proteins detected in (A) ammonia grown cells and (B) urea grown cells.	57
Figure 4-1 - Percentage NO_2^- production compared to the uninhibited control (C) after 1 h incubation with different concentrations of phenylhydrazine using 100 µM NH_4^+ as substrate	62
Figure 4-2 - NO_2^- production after 1 h incubation with different concentrations of phenylhydrazine using 100 µM NH_2OH as substrate for <i>N. europaea</i> and ‘ <i>Ca. Nitrosotalea sinensis</i> ’ and 200 µM for ‘ <i>Ca. Nitrosocosmicus franklandus</i> ’ and <i>N. viennensis</i>	63
Figure 4-3 - Percentage NO_2^- production compared to the uninhibited control (C) after 1 h incubation with different concentrations of hydrazine using 100 µM NH_4^+ as substrate.	65
Figure 4-4 - NO_2^- production after 1 h incubation with different concentrations of N_2H_4 using 100 µM NH_2OH as substrate for <i>N. europaea</i> and ‘ <i>Ca. Nitrosotalea sinensis</i> ’ and 200 µM for ‘ <i>Ca. Nitrosocosmicus franklandus</i> ’ and <i>N. viennensis</i>	66

Figure 4-5 - Time course of the recovery of NO ₂ ⁻ production from 1 mM NH ₄ ⁺ in ‘ <i>Ca. Nitrosocosmicus franklandus</i> ’ after removal of 100 μM phenylhydrazine (A) or 1 mM and 10 mM N ₂ H ₄ (B) by washing	68
Figure 4-6 - Time course of the recovery of NO ₂ ⁻ production in <i>N. europaea</i> with 1 mM NH ₄ ⁺ or 0.5 mM NH ₂ OH as substrate after removal of 100 μM phenylhydrazine by washing.	68
Figure 4-7 - Oxygen uptake measurements in cell suspensions of ‘ <i>Ca. Nitrosocosmicus franklandus</i> ’.	70
Figure 4-8 - Oxygen uptake measurements by cell suspensions of ‘ <i>Ca. Nitrosocosmicus franklandus</i> ’.	71
Figure 4-9 - Initial rates of oxygen consumption in cell suspensions of ‘ <i>Ca. Nitrosocosmicus franklandus</i> ’ after addition of different concentrations of N ₂ H ₄ (red triangles)	73
Figure 4-10 - Oxygen uptake measurements by cell suspensions of <i>N. europaea</i>	74
Figure 4-11 - Relative ATP-dependent luminescence, with NH ₄ ⁺ controls normalised to 1	75
Figure 4-12 - ³⁰ N ₂ /total N ₂ ratio after 1 h incubation of cell suspensions of ‘ <i>Ca. Nitrosocosmicus franklandus</i> ’ (A) and <i>N. europaea</i> (B) with 500 μM ¹⁵ N-N ₂ H ₄	76
Figure 5-1 – Chemical structures of 1,7-octadiyne (A) and 1,5-hexadiyne (B).	81
Figure 5-2 – ABPP schematic for enzyme labelling using bifunctional inhibitor-alkyne probes.....	82
Figure 5-3 – Time course of the inhibition of NO ₂ ⁻ production (A) and NH ₃ consumption (B) from 1 mM NH ₄ ⁺ in ‘ <i>Ca. Nitrosocosmicus franklandus</i> ’ after addition of 100 μM 15HD and 100 μM pentane.....	83
Figure 5-4 – Time course of the inhibition of NO ₂ ⁻ production (A) and NH ₂ OH consumption (B) from 200 μM NH ₂ OH in ‘ <i>Ca. Nitrosocosmicus franklandus</i> ’ after addition of 100 μM 15HD and 100 μM pentane	84
Figure 5-5 – Six (A) and 21 (B) hour time course of the recovery of NO ₂ ⁻ production from 1 mM NH ₄ ⁺ in ‘ <i>Ca. Nitrosocosmicus franklandus</i> ’ after removal of 100 μM 15HD with and without 200 μg mL ⁻¹ CHX	85
Figure 5-6 – Time course of the inhibition of NO ₂ ⁻ production with different concentrations of CHX (A) and recovery of NO ₂ ⁻ production from 1 mM NH ₄ ⁺ in ‘ <i>Ca. Nitrosocosmicus franklandus</i> ’ after removal of 20 μM acetylene with and without 1000 μg mL ⁻¹ CHX (B).....	86
Figure 5-7 - ABPP-based fluorescent labelling of active ‘ <i>Ca. N. franklandus</i> ’ (A and B) and <i>N. europaea</i> (C and D).....	87
Figure 5-8 – Fluorescent SDS-PAGE of cell extracts of <i>N. europaea</i>	88
Figure 5-9 – Fluorescent (left) and Coomassie stained (right) SDS-PAGE gel.....	89
Figure 5-10 - Chemical structures of the two biotin-hydrazine probes used.	91

Figure 5-11 - Percentage NO_2^- production compared to the uninhibited control (C) after 1 h incubation with different concentrations of biotin-hydrazine probe using 100 μM NH_4^+ or 200 μM NH_2OH as substrate	91
Figure 5-12 – Chemical structures of hydrazine probes: (A): prop-2-yn-1-ylhydrazine (alkyl probe); (B): N-(But-3-yn-1-yl)-4-hydrazineylbenzamide (aryl probe).	92
Figure 5-13 – Relative NO_2^- production compared to the control after 1 h incubation with different concentrations of aryl probe using 100 μM NH_4^+ or 200 μM NH_2OH as substrate	93
Figure 5-14 – Abiotic nitrite measurements with different concentrations of Aryl probe.....	94
Figure 5-15 - Fluorescent labelling profiles by the aryl probe after clicking (left) and corresponding expression profiles after Coomassie staining (right) of protein extract from ‘ <i>Ca. N. franklandus</i> ’ (1-4) and <i>N. europaea</i> (5-7).....	95
Figure 6-1 - Colourless native PAGE (10%) stained with Coomassie (A) and activity stained (B).....	100
Figure 6-2 Coomassie-stained 10% SDS-PAGE gel with $(\text{NH}_4)_2\text{SO}_4$ precipitated fractions.....	102
Figure 6-3 – Colourless native PAGE (10%) activity stained for catalase activity (A) and Coomassie stained (B)	103
Figure 6-4 - Colourless native PAGE (5%) activity stained for catalase activity (A) and Coomassie stained (B).....	104
Figure 6-5 - Colourless native PAGE (5%) Coomassie-stained..	105
Figure 6-6 - Sequence alignment of three representative sequences of the Ferritins, bacterioferritins (BFR), Dps and DpsL proteins.....	109
Figure 6-7 - BN-PAGE from different fractions of protein with catalase activity. Activity stain (left) destained (right).....	110
Figure 6-8 - Growth, quantified by nitrite accumulation, of three separate experiments (A, B, C) where triplicate cultures of each treatment were grown	111
Figure 6-9 – Growth, quantified by nitrite accumulation, of the Figure 6-8 A and C experiments over a longer time, A and B, respectively where triplicate cultures of each treatment were grown.	112
Figure 6-10 – SDS-PAGE of protein extracts from ‘ <i>Ca. N. franklandus</i> ’ cells grown in normal growth conditions (1), with 0.5 mM pyruvate (2) or 1 μM catalase	113

Declaration

I declare that the work presented in this thesis was conducted by me under the direct supervision of Laura Lehtovirta-Morley. Results obtained by, or with help from, others have been acknowledged in the relevant sections. None of the work presented has been previously submitted for any other degree. The data in Chapter 4 have been published (Schatteman *et al.*, 2022), some of the data in Chapter 5 have also been published (Wright *et al.*, 2020).

Arne Schatteman

Acknowledgements

I would like to thank the Royal Society for the funding of this PhD project. I am grateful to my supervisory team Laura Lehtovirta-Morley, Colin Murrell, and Andrew Crombie for guidance during my PhD. Most importantly, I would like to thank the members of the ELSA lab, past and current, for advice and help but most importantly for being friends and making Norwich feel like home.

I want to thank my parents and family, who showed endless patience and support. I want to thank my two grandmothers, who were always ready with tea, coffee, and good conversations whenever I came back to Belgium. Finally, the most important person to thank is Nele, who moved with me to the UK and without whom I would never have finished. Thank you for your endless support, patience and understanding.

Abbreviations

15HD:	1,5-hexadiyne
17OD:	1,7-octadiyne
ABPP:	activity-based protein profiling
alkyl probe:	prop-2-yn-1-ylhydrazine
AMO:	ammonia monooxygenase
Anammox:	anaerobic ammonia oxidation
AOA:	ammonia oxidising archaea
AOB:	ammonia oxidising bacteria
AOM:	ammonia oxidising microorganisms
aryl probe:	N-(But-3-yn-1-yl)-4-hydrazineylbenzamide
ATCC:	American Type Culture Collection
ATP:	adenosine triphosphate
ATU:	allylthiourea
BCA:	bicinchoninic acid
BFR:	bacterioferritin
BHDR:	biotin hydrazide
BNI:	biological nitrification inhibitor
BN-PAGE:	blue native polyacrylamide gel electrophoresis
BPHDR:	Biotin-dPEG [®] 4 -hydrazide
Ca:	candidatus
CHX:	cycloheximide
Comammox:	complete ammonia oxidation
CuAAC:	copper(I)-catalyzed alkyne-azide cycloaddition
CuMMO:	copper membrane monooxygenase
CV:	column volume
DAPI:	4',6-diamidino-2-phenylindole
DCD:	dicyandiamide
DCPIP:	dichlorophenol indophenol
DMPP:	3,4-Dimethylpyrazole phosphate
DNA:	deoxyribonucleic acid

DNRA:	dissimilatory nitrate reduction to ammonium
DPS:	DNA protection during starvation protein
DpsL:	DNA protection during starvation-like protein
FWM:	freshwater medium
HAO:	hydroxylamine dehydrogenase
HDH:	hydrazine dehydrogenase
HEPES:	4-(2-hydroxyethyl)-1-piperazineethanesulfonic acid
HRT:	hydraulic retention time
HZS:	hydrazine synthase
IAA:	iodoacetamide
IPCC:	Intergovernmental Panel on Climate Change
kDa:	kiloDalton
LC-MS:	Liquid chromatography–mass spectrometry
MALDI-TOF:	matrix-assisted laser desorption/ionization time-of-flight mass spectrometer
MCO:	multicopper oxidase
MES:	2-(N-morpholino) ethane sulfonic acid
MOB:	methane oxidising bacteria
NI:	nitrification inhibitor
NirK:	copper containing nitrite reductase
Nitrapyrin:	2-Chloro-6-(trichloromethyl)pyridine
NOB:	nitrite oxidising bacteria
NXR:	Nitrite oxidoreductase
OD:	optical density
PEG:	polyethylene glycol
pMMO:	particulate methane monooxygenase
PMS:	phenazine methosulfate
PTIO:	2-Phenyl-4,4,5,5-tetramethylimidazoline-1-oxyl 3-oxide
RNA:	ribonucleic acid
RT-QPCR:	reverse transcription quantitative real-time PCR
SDS-PAGE:	sodium dodecyl sulfate–polyacrylamide gel electrophoresis
SRT:	solids retention time

TEMED: tetramethylethyleendiamine
THPTA: tris-hydroxypropyltriazolylmethylamine
Tris: tris(hydroxymethyl)aminomethane

1 Introduction

1.1 Nitrogen (N)

Nitrogen is the fifth most abundant element in the universe and the most abundant element in our atmosphere where it mostly exists as dinitrogen gas (N_2). Nitrogen is vital to all living organisms as a component of amino acids and nucleic acids. Despite its overall abundance in the atmosphere, N_2 is highly inert and is inaccessible to most organisms. Reactive nitrogen, mostly ammonia (NH_3) or nitrate (NO_3^-), is limiting in many environments which is the reason why agricultural crops are heavily fertilised with nitrogen. To be accessible, N_2 needs to be “fixed”, that is, be transformed into NH_3 , organic nitrogen or other bioavailable forms of nitrogen. Only certain microorganisms, called diazotrophs, can do this. All other organisms rely on either biologically or abiotically fixed nitrogen. Humans, however, stopped relying on diazotrophs for fixed nitrogen through the discovery of the Haber-Bosch process, an industrial process to create NH_3 from N_2 and hydrogen (H_2). Crucially, roughly half of the world’s human population relies on industrially fixed nitrogen for food production. The industrial production of bioavailable nitrogen has massively increased its input into the environment resulting in severe, long-lasting consequences. To adequately understand these consequences, it is important to understand the underlying mechanisms and dynamics of the microbial nitrogen transformations.

1.2 The microbial nitrogen cycle

Nitrogen exists in several different oxidation states in the environment (Figure 1-1) and microorganisms play a pivotal role in transforming nitrogen from one form to another. Together, these microbial transformations constitute the microbial nitrogen cycle.

Traditionally, the transformations are depicted in a cycle in which there is a sequential order to the processes and every step has an equal flux. This is an oversimplification because these processes may have vastly different fluxes and do not form a perfectly balanced cycle (Kuypers *et al.*, 2018). The microbial nitrogen transformations are complemented by abiotic processes which typically have a smaller, but significant flux (Doane, 2017).

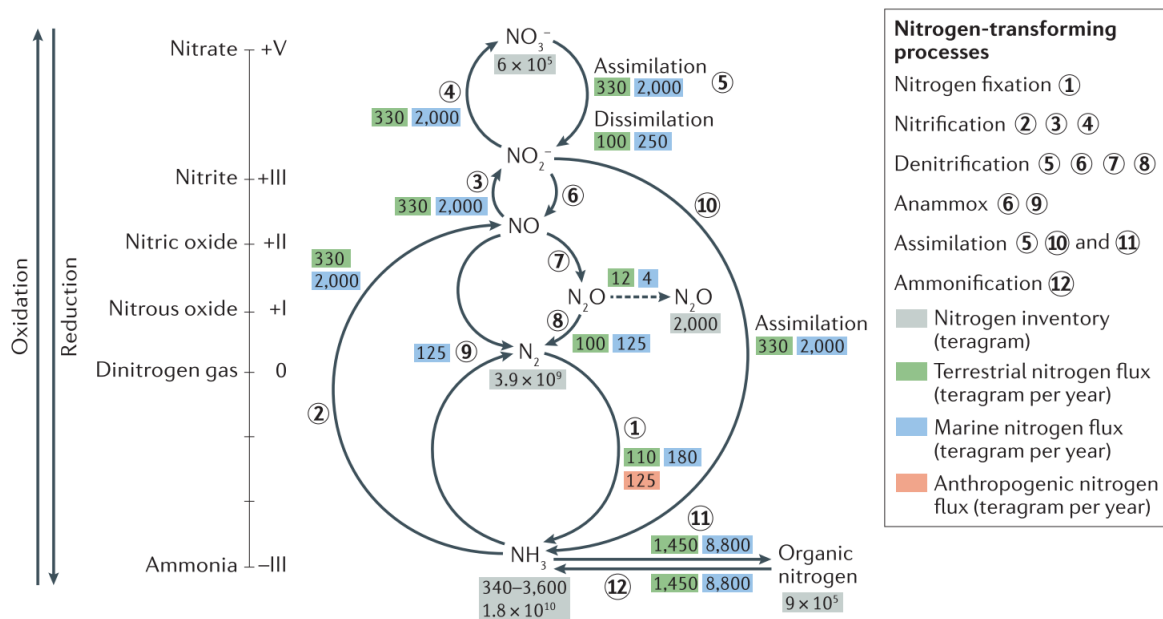


Figure 1-1 – Overview of the biogeochemical cycling of nitrogen from (Kuypers *et al.*, 2018). The total nitrogen inventories are shown in the grey boxes in teragram per year. The six nitrogen transforming processes are highlighted with the encircled numbers and their estimated annual flux in teragrams per year is shown in the coloured boxes

There are six microbial transformations of nitrogen in the nitrogen cycle. It was long thought that each of these was carried out by a distinct group of microorganisms, but it has become clear that there is more metabolic versatility within groups of organisms than originally thought. The traditional classification, by function, is therefore no longer valid, though, sometimes still useful and will be used to discuss the different processes.

1.2.1 Nitrogen fixation

Even though nitrogen is the most abundant element in our atmosphere, it exists mostly in the form of dinitrogen gas (N_2). This highly inert gas is only accessible to organisms called diazotrophs, that carry a nitrogenase enzyme able to fix N_2 into NH_3 . These enzymes are widespread within bacteria and archaea and provide them with a clear competitive advantage in environments where bioavailable nitrogen is limiting. Nitrogen-fixing eukaryotes have not been discovered, but nitrogen fixers often live in tight symbioses with eukaryotes. The best-known example is the fixation of nitrogen in root nodules of legume plants by bacteria (Burriss & Roberts, 1993). Notably, abiotically fixed nitrogen is produced in relatively significant amounts, mostly by lightning, photochemical nitrogen fixation and the Haber-Bosch process (Doane, 2017).

1.2.2 Nitrification

Nitrification, the main subject of this thesis, is the oxidation of ammonia to nitrate (NO_3^-) via nitrite (NO_2^-). The first step of this process, the oxidation of ammonia to nitrite, is carried out by ammonia oxidising archaea (AOA) and bacteria (AOB). The second step, the oxidation of nitrite to nitrate is carried out by nitrite oxidising bacteria (NOB). Recently, organisms capable of carrying out the complete oxidation of ammonia to nitrate (comammox) were discovered (Daims *et al.*, 2015; M. A. H. J. van Kessel *et al.*, 2015). Ammonia oxidation is typically studied using chemolithotrophs that use ammonia as the sole source of energy. However, a wide range of heterotrophic bacteria and fungi are capable of nitrification and are understudied players in nitrification (Papen *et al.*, 1989).

All autotrophic ammonia oxidisers have an ammonia monooxygenase enzyme (AMO) which carries out the oxidation of ammonia (NH_3) to hydroxylamine (NH_2OH). It is a key enzyme and has been used extensively as a biomarker to detect ammonia oxidising microorganisms (AOM) in the environment (see enzymology section). How hydroxylamine is further oxidised to nitrite is not entirely clear in any of the ammonia oxidisers (see enzymology section). The key enzyme in the nitrite oxidisers is the nitrite oxidoreductase (NXR) that converts nitrite into nitrate. In contrast to the autotrophic ammonia oxidisers, nitrite oxidisers are typically more metabolically versatile and can grow on substrates other than nitrite such as formate, hydrogen and sulfide (Daims *et al.*, 2016).

1.2.3 Denitrification

Denitrification is the sequential anaerobic conversion of nitrate (NO_3^-) to nitrite (NO_2^-), to nitric oxide (NO), to nitrous oxide (N_2O) and finally to dinitrogen gas (N_2). Canonical denitrifiers, i.e. organisms that carry out the whole process, are thought to be exceptions rather than the rule (Jones *et al.*, 2013) and it is common for microorganisms to have some of the enzymes from the denitrification pathway. Denitrification can have N_2O or N_2 as end product, so while this process is the main sink for N_2O (discussed below), it can also act as a source of this potent greenhouse gas (CHAPUIS-LARDY *et al.*, 2007).

1.2.3.1 Dissimilatory nitrate reduction to ammonium (DNRA)

DNRA is an alternative denitrification pathway which converts NO_3^- into NH_4^+ via NO_2^- . The process can be considered a short circuit in the nitrogen cycle as it skips both N_2 fixation and denitrification (COLE & BROWN, 1980). Organisms generate energy and can grow using this process by coupling the oxidation of an electron donor to the reduction of nitrate, also termed fermentative ammonification (Rütting *et al.*, 2011). Its importance in the environment is unclear, though, there are conditions in which it is favoured over denitrification e.g. when nitrate is limiting relative to electron donors (Kraft

et al., 2014). As opposed to denitrification, DNRA preserves and recycles N in the system, leading to sustained primary production and nitrification (Marchant *et al.*, 2014).

1.2.4 Anammox

The anaerobic ammonia oxidisers (anammox) were discovered relatively recently (Strous *et al.*, 1999) but have been extensively studied since then. In the anammox process, ammonia and nitrite or nitric oxide are directly combined into dinitrogen gas (Hu *et al.*, 2019). The key enzyme is the hydrazine synthase (HYS) which converts ammonia and nitric oxide into hydrazine (N₂H₄) which is then further converted by the hydrazine dehydrogenase (HDH) to dinitrogen gas. The HYS enzyme is the only known enzyme that can activate ammonia anaerobically (Kartal & Keltjens, 2016). Notably, the anammox pathway evolved a unique prokaryotic organelle called the anammoxosome in which all the catabolic enzymes of the pathway are located (de Almeida *et al.*, 2015).

1.2.5 Assimilation and mineralisation

So far, only the inorganic transformations have been discussed but the largest fluxes in the nitrogen cycle are the assimilation of inorganic ammonia into organic nitrogen compounds and the reverse, called assimilation and mineralisation (or ammonification) respectively (Figure 1-1). Inorganic nitrogen can be taken up as nitrate or ammonia, but nitrate will be converted to ammonia to be incorporated in organic molecules. The enormity of the assimilation and mineralisation fluxes clearly impact the other processes. For example in acidic soils ammonification is thought to drive nitrification carried out by AOA (Levičnik-Höfferle *et al.*, 2012).

1.3 Humans and the nitrogen cycle

The microbial processes described above are in a precarious balance and, as always, when humans get involved, this balance is threatened. To deal with the growing human population, an increase in food production was needed. The Haber-Bosch process, an artificial nitrogen fixation process, was one of the solutions to this problem. Artificial nitrogen fertiliser has massively increased crop yields and is now responsible for feeding over half the human population (Erisman *et al.*, 2008). While this is an amazing feat, nitrogen fixation by the Haber-Bosch process has surpassed terrestrial biological nitrogen fixation, resulting in an imbalance in the nitrogen cycle (more N₂ is fixed than produced by anammox and denitrification) (Kuypers *et al.*, 2018). The consequences of the input of bioavailable nitrogen into the environment are only now becoming clear (Fowler *et al.*, 2013) and we may have already passed the planetary boundaries that define a safe operating space for humanity on Earth (Rockström *et al.*, 2009).

Eutrophication is one of these consequences and is the sudden influx of nutrients into ecosystems which creates a massive disturbance. When bioavailable nitrogen suddenly enters ecosystems,

organisms that can make the best use of the nitrogen dominate, causing (toxic) algal blooms and biodiversity loss. Moreover, when N is provided in excess, other nutrients become limiting. Most notably, more and more ecosystems are driven to phosphorous limitation in this way (Vitousek et al., 2010). Globally, less than 50% of the nitrogen applied to the fields is taken up by the plants (Cassman et al., 2002; Ladha et al., 2005). The rest is transported from the fields, mostly by NO_3^- leaching or NH_3 volatilisation. On average, 18% of the applied nitrogen is volatilised to NH_3 (Pan et al., 2016) and similar amounts (19%) are lost by leaching (H. J. Di & Cameron, 2002). The nitrification process converts NH_3 to negatively charged NO_3^- which does not adhere well to negatively charged soil particles as opposed to NH_4^+ . NO_3^- leaches from the environment and ends up in surface and ground water, contaminating drinking water and causing eutrophication (Grizzetti et al., 2011; Townsend et al., 2003). The cost of fertiliser is significant and with a nitrogen-use efficiency (NUE) as low as 50%, there is a lot of optimisation that can be done.

A second consequence is the production of N_2O which is projected as the most important ozone depleting agent in the 21st century (Ravishankara et al. 2009) and is a very potent greenhouse gas with a global warming potential over 250 times that of CO_2 and an atmospheric lifetime of over a century (IPCC 2014). It is produced biotically and abiotically during nitrification and subsequent denitrification. Due to the excess nitrogen input, both nitrification and denitrification have a larger flux resulting in an increase of atmospheric N_2O . Agricultural soils are the biggest source of anthropogenic N_2O to the environment (Ciais et al., 2014), posing a difficult question regarding food security and climate change: can we reduce N_2O emissions without compromising food security?

1.4 Nitrification inhibitors

To prevent the loss of nitrogen from agricultural systems and to reduce N_2O emissions, nitrification inhibitors (NI) can be applied. They can be mixed with the fertiliser or applied later. Many of the known NIs are thought to be copper chelators that inhibit the AMO enzyme of ammonia oxidisers by binding the copper-catalysed active site of these enzymes.

Commercially available NIs are DCD (dicyandiamide), DMPP (3,4-dimethylpyrazole phosphate) and nitrapyrin (2-chloro-6-(trichloromethyl)pyridine). The first two have a bacteriostatic effect on AOB and are deemed safe for use in soil and animal manure slurry (Amberger, 1989; Guo et al., 2013; Zerulla et al., 2001). Nitrapyrin is used mostly in the US as a pesticide that also functions as a bactericide and nitrification inhibitor (Powell & Prosser, 1986). It has been shown to inhibit the AOB *Nitrosomonas*, while it only has a very weak inhibitory effect on *Nitrosospira multiformis* (Powell et al., 1986; Zacherl et al., 1990; Belser et al., 1981; Shen et al., 2013)). The variation of AOB in susceptibility towards nitrapyrin raises concerns about its efficacy. Moreover, the observation that DCD, nitrapyrin and

allylthiourea (ATU), a copper chelator often used in laboratory conditions to inhibit AOB, had different effects dependent on the AOA strain (Lehtovirta-Morley *et al.*, 2013; Shen *et al.*, 2013) further exacerbates these concerns.

The efficiency of NIs varies depending on the environment (Mkhabela *et al.*, 2006) and their effects are generally of short duration (Ruser & Schulz, 2015). New compounds that not only target some AOB but also AOA, comammox and a broader range of AOB could improve the efficacy of NIs (Beeckman *et al.*, 2018). NIs that are suited for different soil types or production systems would be worth investigating as well (Di & Cameron, 2016).

There are downsides to NIs however, including their additional cost. To be economically viable, the cost of the NI needs to be balanced with increased yield and a reduction in fertiliser application. This is highly variable depending on soil, crop, inhibitor and weather conditions but tends to be positive (Abalos *et al.*, 2014; M. Yang *et al.*, 2016). Another caveat to NIs is their uptake and degradation by soil microorganisms (Marsden *et al.*, 2016) which reduce the efficacy of NIs. Lastly, it has been shown that DCD can enter into our food chain and while the effects are not clear, this is highly undesirable (Marsden *et al.*, 2015).

A more elegant method of inhibiting nitrification was pitched recently: certain plants produce root exudates with a biological nitrification inhibitor (BNI) function, which is thought to have evolved as a mechanism to retain nitrogen in the rhizosphere in low-N ecosystems (Subbarao *et al.*, 2012; Di *et al.*, 2016). The precise release in the rhizosphere and the wide variety of compounds could give an advantage over synthetic NIs. BNIs have been discovered in several strains of economically important crops and could be bred into commercial strains in the future (Coskun *et al.* 2017). A recent evaluation of the effect of six BNI compounds on the ammonia oxidation activity in both AOA and AOB provided a crucial framework for evaluating and testing future BNIs (Kaur-Bhambra *et al.*, 2022). It is important, however, that comammox bacteria are included in these studies as well.

1.5 Nitrogen in wastewater treatment

When the effect of excess nitrogen on the environment became clear, nitrogen-removing systems were developed and added to many wastewater treatment facilities. As opposed to most natural systems where fixed nitrogen is highly valuable, the goal in wastewater treatment is to remove fixed nitrogen from systems by converting it to dinitrogen gas. Therefore, nitrogen removing wastewater treatment systems are per definition characterised by an imbalance in the nitrogen transformations and pose an opportunity to rectify the imbalance introduced by the Haber-Bosch process.

In conventional systems, nitrification is combined with denitrification to reduce nitrate to dinitrogen gas. Nitrification requires extensive aeration and energy input, and the subsequent denitrification requires the addition of organic compounds which comes with a high cost (T. Liu, Hu, & Guo, 2019). Moreover, N₂O is produced during both nitrification and denitrification increasing the emission of this greenhouse gas (Kampschreur *et al.*, 2009).

An alternative strategy using the anammox process has great potential for wastewater treatment. Anammox, combined with partial nitritation by ammonia oxidisers under oxygen-limiting conditions (B. Kartal, Kuenen, and Van Loosdrecht 2010), could reduce N₂O emissions and would omit the extensive aeration requirements as well as the need to add organic compounds in conventional nitrification-denitrification systems. This system is used more and more in ammonium-rich wastewaters but not often in full-scale municipal wastewater treatment which tends to have lower ammonia concentrations. While the process has been shown to be feasible and economically favourable, it comes with a significant start-up cost and set-up time and requires expertise to run (Magri *et al.*, 2021).

Finally, the discovery of new microbial pathways that couple the anaerobic oxidation of methane to the reduction of nitrite (Ettwig *et al.*, 2010) or nitrate (Haroon *et al.*, 2013) has opened the door to new wastewater treatment methods. Combining nitrogen and methane removal by using these new methane oxidation pathways in combination with anammox has already been demonstrated under laboratory conditions (Luesken *et al.*, 2011) and will likely make its way eventually into full-scale wastewater treatment plants in the future. The implementation of new microbiological processes in wastewater treatment plants can transform this industry from an energy consuming source of greenhouse gasses to an energy producing greenhouse gas sink (T. Liu, Hu, Yuan, *et al.*, 2019; M. A. van Kessel *et al.*, 2018).

1.6 Ammonia oxidising organisms

1.6.1 Ammonia oxidising bacteria (AOB)

Ammonia oxidising bacteria were identified over 100 years ago by Sergei Winogradsky (Winogradsky, 1890) and were first isolated in liquid culture by Percy and Grace Frankland (Frankland & Frankland, 1890). The AOB are either β -proteobacteria, represented by the genera of *Nitrosomonas* and *Nitrospira*, or γ -proteobacteria, represented by *Nitrosococcus*, *Nitrosacidococcus* and *Nitrosoglobus*. The most studied model organism for bacterial nitrification is *Nitrosomonas europaea*, an AOB isolated from French and Swiss soils by Winogradsky in 1904 (Meiklejohn, 1950) and the first AOB to have its genome sequenced (Chain *et al.*, 2003). Since their discovery, the AOB have been heavily studied. The central enzyme to their ammonia oxidation pathway, the ammonia

monooxygenase (AMO) which carries out the oxidation of ammonia to hydroxylamine (NH_3), has been used as a molecular marker to study ammonia oxidation in the environment.

1.6.2 Ammonia oxidising archaea (AOA)

In 1992, archaeal sequences belonging to the Crenarchaeota were discovered to be widespread in marine environments (DeLong, 1992; Fuhrman & McCallum, 1992). This was opposed to the dogma that all archaea were extremophiles. Further study determined them to be among the most abundant organisms on the planet, accounting for up to 40% of bacterioplankton in deep ocean waters (Karner *et al.*, 2001). The first indication that these organisms were nitrifiers came from the detection of archaeal AMO-like genes in a shotgun-sequencing study of the Sargasso Sea (Venter *et al.*, 2004). Similar Crenarchaeota were also detected in soil (Bintrim *et al.*, 1997). Additionally, a fosmid clone from a metagenomic library contained homologues to bacterial nitrogen cycling genes (Treusch *et al.*, 2005). The Amo sequence from this clone was too divergent from the AOB to be picked up by PCR and implicated a group of uncultivated Crenarchaeota in the nitrogen cycle. Finally, in 2005 Könneke and colleagues isolated the first archaeal ammonia oxidiser *Nitrosopumilus maritimus* SCM1 from a tropical marine aquarium. As more data became available and more thorough phylogenetic analysis was performed it became clear that the AOA do not belong to the Crenarchaeota but are members of a deep-branching archaeal lineage subsequently assigned to the new phylum Thaumarchaeota (Brochier-Armanet *et al.*, 2008; Spang *et al.*, 2010), although a more recent publication proposed a different organisation where the Thaumarchaeota would be part of the Thermoproteota (Rinke *et al.*, 2021). No stable archaeal phylogeny can be agreed upon for as long as new lineages keep being discovered and due to computational limitations (Tahon *et al.*, 2021). A current consensus is shown in Figure 1-2.

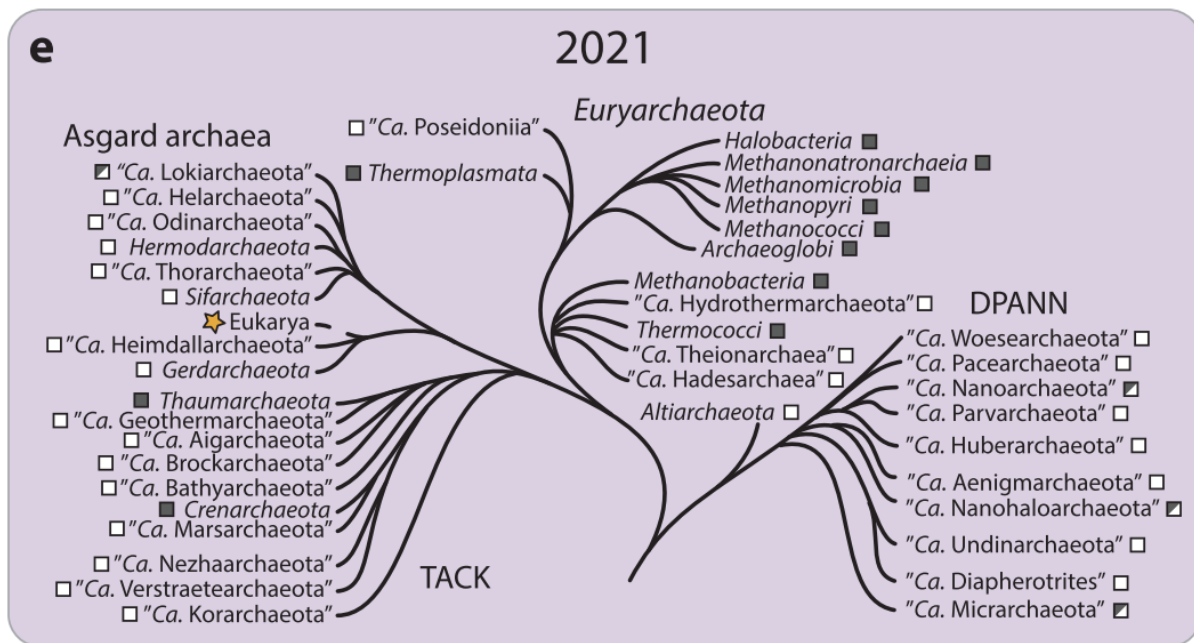


Figure 1-2 – Current consensus on the phylogeny of the Archaea. Figure taken from (Tahon et al., 2021). The position of the Eukarya as a sister-group or member of the Asgard archaea is unconfirmed. White squares indicated no representatives have been cultivated while purple squares have cultured representatives. A half-purple square indicates that a (co)cultivated member is described in the literature.

Since the isolation of *N. maritimus*, a lot of interesting isolates have been obtained, including isolates from soil and marine environments, hot springs, wastewater treatment facilities and arctic soils. The isolation of the obligate acidophilic AOA ‘*Ca. Nitrosotalea devanaterre*’ provides an explanation for the high nitrification rates that are observed in acidic soils where both AOB abundance and ammonia availability are low (Lehtovirta-Morley *et al.*, 2014, 2011). Ammonia, rather than its protonated form ammonium, is the substrate for AMO. Ammonia and ammonium are in a pH-dependent equilibrium and ammonium is the predominant form in acidic pH. A major problem in the progress of AOA research is the difficulty in culturing isolates. It often takes years to isolate a strain and the growth is often slow and difficult (Liu *et al.*, 2019). Many AOA isolates also still retain their *Candidatus* status because culture collections have difficulties growing them. In this thesis, ‘*Ca. Nitrosocosmicus franklandus*’ C13 was predominantly used. It is a ureolytic soil archaeon from agricultural soil that grows relatively easily and tolerates high ammonia concentrations (Lehtovirta-Morley, Ross, *et al.*, 2016).

Many AOA were thought to be mixotrophic due to stimulation of growth by the addition of α -keto acids (Qin *et al.*, 2014; M. Tourna *et al.*, 2011). However, radioactive tracer studies showed that these compounds were barely incorporated into biomass and it was shown that α -keto acids were used to detoxify hydrogen peroxide (H_2O_2) (Kim *et al.*, 2016). The H_2O_2 sensitivity of AOA and their mechanisms

to deal with this are thought to be important factors determining the abundance of AOA in the environment.

1.6.3 Complete ammonia oxidising bacteria (comammox)

Comammox organisms were predicted in 1977 by E. Broda based on evolutionary and thermodynamic grounds. Costa *et al.* (2006) argued that a complete nitrifier would be outcompeted by partial nitrifiers in many environments, based on kinetic theory of optimal pathway length. However, they also argued that under circumstances where maximisation of growth yield is favoured as opposed to growth rate, comammox would be favoured. Conditions characterised by low mixing of substrates, such as biofilms and clonal clusters were posed to be good candidate niches. Indeed, in 2015, two groups simultaneously published clear evidence of complete nitrification by a single microorganism (Daims *et al.*, 2015; M. A. H. J. van Kessel *et al.*, 2015). '*Ca. Nitrospira inopinata*' was enriched from a microbial biofilm on the walls of a pipe under the flow of hot water (Daims *et al.*, 2015) and '*Ca. Nitrospira nitrificans*' and '*Ca. Nitrospira nitrosa*' from an ammonium-oxidizing biofilm, sampled from the anaerobic compartment of a trickling filter connected to a recirculation aquaculture system (M. A. H. J. van Kessel *et al.*, 2015). These complete ammonia oxidisers were shown to be *Nitrospira* bacteria, previously considered to be nitrite oxidisers and showed a high affinity for ammonia and a high growth yield as predicted (Koch *et al.*, 2019). Unexpectedly, comammox bacteria are not confined to low nitrogen environments and have been found to co-occur with AOA and AOB in a wide variety of environments, sketching a complex picture of the interactions between these groups and the environment (Koch *et al.*, 2019).

1.6.4 Heterotrophic ammonia oxidisers

Heterotrophic ammonia oxidisers are a severely understudied group of ammonia oxidisers and are rarely even mentioned in literature. Heterotrophic ammonia oxidisers can oxidise ammonia but cannot grow on it as the only source of energy. Their pathway and intermediates are mostly unknown but nitrite and hydroxylamine have been implicated in their metabolism (Castignetti & Gunner, 1980; Papen *et al.*, 1989). Some heterotrophic nitrifiers possess the capability to also aerobically denitrify (Chen & Ni, 2011) and as a group they are likely to contain new enzymes carrying out new reactions. To emphasise this point, a recent study isolated a novel heterotrophic nitrifier containing no homologues to AMO or HAO, capable of oxidising ammonia to hydroxylamine with nitrogen gas as an end product (M. Wu *et al.*, 2021). The authors of this study were able to identify and express the genes for ammonia oxidation in *E. coli* to further unravel the pathway and decided to name it '*dirammox*' for the direct oxidation of ammonia to dinitrogen gas. It was later shown that hydroxylamine was oxidised to N₂ by a hydroxylamine oxidase that was not homologous to any known hydroxylamine oxidases (M.-R. Wu *et al.*, 2022). This highlights the possibility for new enzymes and chemistry in

heterotrophic nitrifiers and the possibility for its use in wastewater treatment plants where simultaneous nitrogen and carbon consumption is often desired.

1.7 Enzymology of AOM

Ammonia monooxygenase (AMO) is the key enzyme in NH_3 oxidation and is the first enzyme of the NH_3 oxidation pathway in AOB, comammox and AOA. Although the archaeal and bacterial AMOs show deep phylogenetic divergence (Walker *et al.*, 2010), both convert ammonium to hydroxylamine (NH_2OH) (N. Vajjala *et al.*, 2013). The bacterial and archaeal pathways (Figure 1-3) likely diverge after the first step, with a unique enzyme system for each group. Comammox bacteria are thought to be NOB, which have obtained the necessary genes for NH_3 oxidation via a lateral gene transfer from AOB (Daims *et al.*, 2015; Palomo *et al.*, 2018; M. A. H. J. van Kessel *et al.*, 2015) and while their AMO and HAO form a distinct clade from the AOB (Pjevac *et al.*, 2017), their overall enzyme system is thought to be similar. Thus, a sequential conversion of ammonia to hydroxylamine by the AMO, followed by the conversion of hydroxylamine to nitric oxide. As in the AOB, it is not known how nitric oxide is converted to nitrite. The enzymology of the oxidation of nitrite by comammox is not discussed in detail. It is important to note that no physiological experiments have been published unravelling the ammonia oxidation pathway in comammox bacteria, with the exception of the kinetic properties of the AMO (Jung *et al.*, 2021).

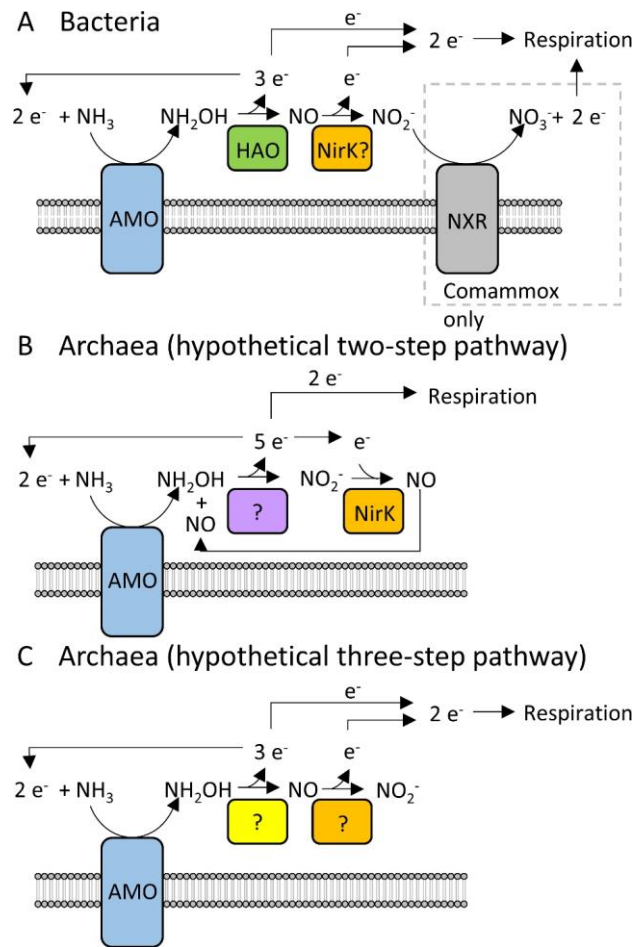


Figure 1-3 – Pathways of ammonia oxidation in bacteria (A) and archaea (B-C). Taken from (Lehtovirta-Morley, 2018). The role of NirK has not been demonstrated in any of the proposed pathways and question marks indicate missing links.

1.7.1 Ammonia oxidising bacteria and comammox

The bacterial NH_3 oxidation pathway is well characterised with only a few remaining gaps (Figure 1-3A). As in all autotrophic AOM, the AMO performs the oxidation of ammonia to hydroxylamine. This enzyme has eluded purification in its active form and knowledge about the mechanism of action is limited. However, while scientists in the field like to emphasise how difficult the purification of the AMO is, it is unclear whether anyone has attempted it in the last 15 years with emerging new techniques. The last reported attempt was an ambiguous paper reporting the purification of a soluble version of the AMO which did not show activity (Gilch, Meyer, *et al.*, 2009). Most structural data is extrapolated from the closely related and better-characterised particulate methane monooxygenase (pMMO) from methane oxidising bacteria (MOB). Data generated directly from the AOB are often obtained from whole cell or cell lysate experiments. Similar to AOA, a lot of functional and structural understanding of the AMO was obtained through work exploring substrate analogues such as alkynes and alkenes (Wright *et al.*, 2020, and references therein).

The bacterial AMO consists of three subunits, AmoA, AmoB and AmoC. Based on the pMMO crystal structure (Hakemian *et al.*, 2008; Lieberman & Rosenzweig, 2005), the AMO subunits are likely arranged in a trimeric, $(\alpha\beta\gamma)_3$, complex composed of three protomers, each containing an AmoA, AmoB and AmoC subunit. The active site of the pMMO is likely a dicopper center in the PmoB subunit (Balasubramanian *et al.*, 2010; Culpepper & Rosenzweig, 2012). The three histidine residues that coordinate the dicopper center in *Methylococcus capsulatus* Bath are conserved in the sequences of methanotrophs, AOB, and AOA (Lehtovirta-Morley, Sayavedra-Soto, *et al.*, 2016). In AOB genomes, AMO is mostly arranged in *amoCAB* operons. The betaproteobacterial NH_3 oxidizers possess an additional divergent *amoC* copy that is not a part of the *amoCAB* operon which is thought to function as part of the stress response (Berube & Stahl, 2012).

After the first step, NH_2OH is further converted to nitric oxide (NO) by hydroxylamine dehydrogenase (HAO, formerly known as hydroxylamine oxidoreductase), a trimeric octaheme enzyme. One of these hemes is the active site cofactor, P460, while the other seven are electron transfer cofactors (Cedervall *et al.*, 2013). For decades, it was thought HAO converted NH_2OH to NO_2^- but recently, purified HAO from *N. europaea* was used to convincingly show it catalysed the conversion of NH_2OH to NO, thereby changing the perception of the bacterial ammonia oxidation pathway (Caranto & Lancaster, 2017). Hydrazine (N_2H_4) is an alternative substrate of the HAO and has been used as a source of electrons to characterise the substrate promiscuity of the bacterial AMO (Michael R. Hyman & Wood, 1984).

While it is possible that the bacterial ammonia oxidation pathway ends in NO, it is unlikely. Non-enzymatic reactions of NO with O_2 would produce N_2O , NO_2^- and NO_3^- . Based on several observations such as the stoichiometric conversion of NH_3 to NO_2^- , the lack of NO_3^- production and the fact that one oxygen atom of NO_2^- originates from water, AOB likely have a third enzyme that catalyses the conversion of NO to NO_2^- (Lancaster *et al.*, 2018). This hypothetical NO oxidoreductase remains unknown, but several candidate enzymes have been proposed. The NO_2^- oxidoreductase, NirK, has been shown to be able to catalyse the reaction in both directions (Wijma *et al.*, 2004), making it a possible candidate. There is some evidence supporting the role of NirK in bacterial ammonia oxidation such as the fact that *nirK* mutants are able to reduce NO_2^- , which suggests NirK has a role other than participating in denitrification, (Kozlowski *et al.*, 2014) as well as the physiological (Cantera & Stein, 2007) and transcriptional (Cho *et al.*, 2006) response of these mutants. However, some AOB lack *nirK* (Kozlowski, Kits, *et al.*, 2016) and the phylogeny of the bacterial *nirK* shows it has multiple evolutionary origins (Lehtovirta-Morley, 2018). Moreover, the kinetics of the reaction are unfavourable in cellular conditions (Kits *et al.*, 2019). It seems that whenever NO may be involved in a pathway NirK-involvement is the immediate reaction, but very little experimental work has been done to reveal the function of this enzyme in either AOA or AOB. Another candidate enzyme is the red copper protein

nitrosocyanin, encoded by the *ncyA* gene. Its role as either an electron transfer protein or a catalytic enzyme has been controversial in the literature (Klotz & Stein, 2014; Lieberman *et al.*, 2001) but it is present in nearly all AOB at concentrations comparable to AMO and HAO and is thought to have an essential function in bacterial NH_3 chemolithotrophy (Klotz & Stein, 2014). Since the discovery of NO as an obligate intermediate in ammonia oxidation (Caranto *et al.* 2017), the hypothesis that nitrosocyanin is involved in the catalysis of NO to NO_2^- has gained some extra traction. However, none of the comammox bacteria possess a nitrosocyanin analogue so they would require a different enzyme (Kits *et al.*, 2019). Neither of these hypotheses are confirmed and this is the greatest remaining question concerning the bacterial ammonia oxidation pathway.

1.7.2 Ammonia oxidising archaea

AOA are notoriously hard to work with due to their low growth rates and yields and high maintenance because there are no reliable methods for preparing freezer stocks. Experiments with cell extracts are challenging with only one paper describing successful lysate experiments carried out in the marine archaeon *Nitrosopumilus maritimus* (Konneke *et al.*, 2014). This combined with the lack of genetic tools is reflected in the limited knowledge of the archaeal ammonia oxidation pathway. NH_2OH (N. Vajrala *et al.*, 2013) and NO (Martens-Habbena *et al.*, 2015) were identified as obligate metabolic intermediates in the archaeal ammonia oxidation pathway. These intermediates are similar to those of AOB and suggest a metabolic pathway similar to that of AOB. However, apart from the AMO enzyme, none of the archaeal ammonia oxidising enzymes have been identified and homologues to the bacterial genes encoding for other enzymes in the ammonia oxidation pathway are lacking.

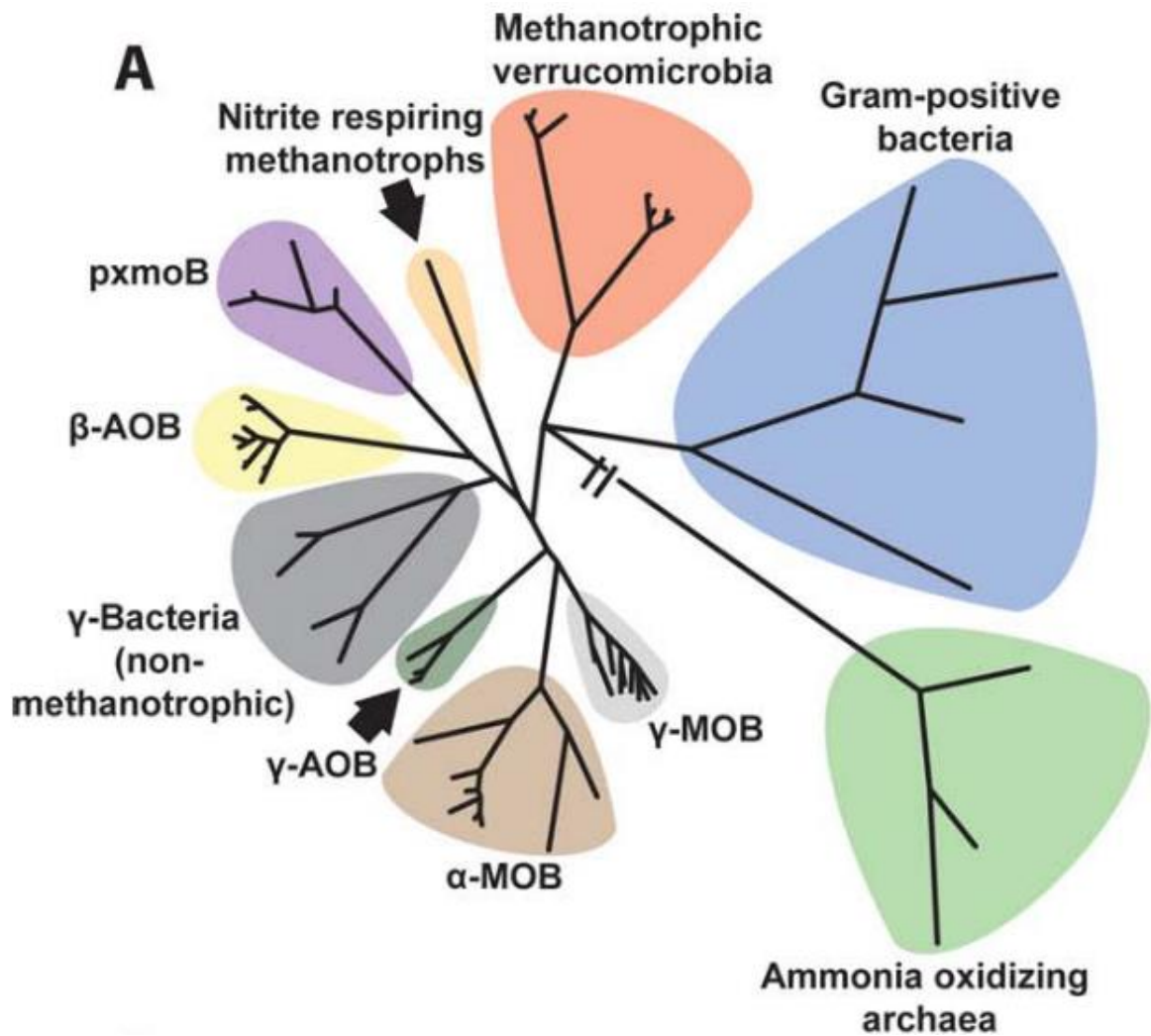


Figure 1-4 – Phylogenetic tree of representative B-subunits of members of the AMO/pMMO superfamily taken from (Lawton et al., 2014). The tree shows the position of the AOA far away from the other Cu-monoxygenases. The phylogenetic tree was constructed by curating 61 Cu-monoxygenase sequences to contain domain 1 only and to remove the putative signal peptides.

The archaeal AMO has a ~40% amino acid identity to bacterial AMO (Könneke *et al.*, 2005; Stahl & de la Torre, 2012). The Archaeal AMO forms a distinct cluster from other Cu-monoxygenases (Figure 1-4). However, amino acid sequence homology and structural homology modelling of the active site(s) of the archaeal and bacterial AMO and the pMMO indicate that the active site(s) may be conserved (Lancaster *et al.*, 2018). This structural conservation is confirmed by the crystal structure of the soluble part of the archaeal AmoB subunit of *Nitrosocaldus yellowstonii* (Lawton *et al.*, 2014). It is striking that the archaeal AmoB C-termini and the AmoC N-termini are significantly truncated compared to the bacterial AMO and pMMO, resulting in ~20 kDa of missing protein (Lehtovirta-Morley, 2018). In addition, the AOA possess a potential fourth subunit, AmoX (Treusch *et al.*, 2005). The gene for this potential subunit, *amoX*, has been found adjacent to *amoA* in all AOA genomes so far (Bartossek *et al.*, 2012; Kerou *et al.*, 2016) and it has been hypothesised to make up for the truncated part of the

enzyme (Lawton *et al.*, 2014). It has also been proposed to be homologous to an exogenous helix of unknown function found in some pMMO structures (Culpepper & Rosenzweig, 2012) but its true function has not been demonstrated. Contrary to AOB and MOB, the archaeal AMO genes are not always organised in *amoCAB* operons. They can be in an *amoAXCB* cluster which is typically the case in marine AOA (Bayer *et al.*, 2016) but the genes are often not clustered (Spang *et al.*, 2012).

Functional and structural understanding of the archaeal AMO has increased mostly through work exploring substrate analogues (Anne E. Taylor *et al.*, 2013; Wright *et al.*, 2020). This also led to techniques such as the use of octyne to distinguish between archaeal and bacterial ammonia oxidation in soil microcosms (Anne E. Taylor *et al.*, 2013), and the use of alkadiynes in combination with click chemistry to label the AMO (Sakoula *et al.*, 2021). For the largest part however, the archaeal AMO remains a mystery and a lot of work needs to be done to characterise this enzyme. Nevertheless, it is the only enzyme of the archaeal ammonia oxidation pathway that has been confidently identified. The rest of the pathway has been a topic of discussion for years, with plenty of hypotheses but a lack of conclusive evidence.

AOA lack homologues to the bacterial HAO and therefore NH_2OH oxidation is expected to be carried out by a novel enzyme (Walker *et al.*, 2010). All known AOA lack the c-heme maturase machinery. Instead, the archaeal respiratory chains are most likely copper based (Schleper & Nicol, 2010). Currently, there are two plausible hypotheses for the continuation of the pathway after the conversion of NH_3 to NH_2OH by the AMO enzyme.

The most popular hypothesis is that a putative “Cu-HAO” converts one molecule of NH_2OH and one molecule of NO into two molecules of NO_2^- (Figure 1-3B) (Kozłowski, Stieglmeier, *et al.*, 2016). In this model, a NO_2^- reducing enzyme, possibly NirK, would supply the NO that is necessary to fuel the reaction. This model was proposed because of the observation that PTIO, a NO scavenger, strongly inhibits AOA (Martens-Habbena *et al.*, 2015). It is further supported by the production and consumption of NO during NH_2OH oxidation (Kozłowski, Stieglmeier, *et al.*, 2016) as well as the isotopic signature of N_2O which indicates that one molecule of N is produced from NH_3 and the second from NO_2^- (Stieglmeier *et al.*, 2014). Some thermophilic AOA as well as a sponge symbiotic AOA do not possess *nirK* however (Abby *et al.*, 2018; Daebeler *et al.*, 2018; Kerou *et al.*, 2016), which is hard to consolidate with this model. Moreover, the AOA *Ca. Nitrosocaldus islandicus* lacks *nirK* but is still inhibited by PTIO, suggesting a different NO production mechanism (Daebeler *et al.*, 2018).

The second model is highly reminiscent of the bacterial pathway where NH_2OH is converted to NO by the unknown Cu-HAO and subsequently to NO_2^- (Figure 1-3C) (Lehtovirta-Morley, 2018). The conversion of NO to NO_2^- may be carried out by NirK which has been shown to be able to catalyse the

reaction in both directions (Wijma *et al.*, 2004), making it possible for this enzyme to participate in both models. The importance of NirK is supported by its high expression levels (Kerou *et al.*, 2016) but its exact function remains unclear. NirK of *Nitrososphaera viennensis* has been heterologously expressed and purified and was shown to be able to convert nitrite to nitric oxide, hydroxylamine to nitric oxide and to produce nitrous oxide from hydroxylamine and nitrite (Kobayashi *et al.*, 2018). However, it is not clear what the role of these different reactions is *in vivo*. Another NO oxidising candidate is a purple cupredoxin isolated from *Nitrosopumilus maritimus* that has been shown to be able to oxidise NO to NO₂⁻ (Hosseinzadeh *et al.*, 2016). The rate of the reaction was slow, however, and may not be physiologically relevant.

Finally, before a lot of the intermediates of the AOA pathway were known, an NO-shuttling pathway was proposed (Stahl & de la Torre, 2012). While the proposed pathway does not exactly fit with some of the experimental evidence obtained since then, it is still possible that an NO-shuttling mechanism is in fact used by the AOA to transport electrons to the AMO for ammonia oxidation and this mechanism would fit with the importance of NO in AOA and their sensitivity to NO scavengers. The hydroxylamine conversion to nitric oxide observed using purified nirK may contribute to this hypothesis (Kobayashi *et al.*, 2018).

The NH₂OH oxidation mechanism is the most sought-after enzyme in the archaeal pathway. One of the prominent “functional HAO” candidates is a multicopper oxidase (MCO1) proposed by Kerou *et al.* (2016). However, this enzyme is not in the core genome repertoire of *Nitrosotalea* species (Herbold *et al.*, 2017). This would require the unlikely loss of the original mechanism and the subsequent evolution of a new NH₂OH oxidation mechanism in *Nitrosotalea*. Alternatively, an enzyme containing an F420 cofactor could be the missing NH₂OH oxidation enzyme (Kerou *et al.*, 2016). The key genes for the synthesis of this cofactor are found in all AOA genomes and large amounts of F420 containing proteins are produced (Spang *et al.*, 2012). An F420 protein has been implicated in the detoxification of reactive nitrogen species in mycobacteria so it could also have a detoxifying role instead (Purwantini & Mukhopadhyay, 2009). Two putative F420-dependent luciferase-like monooxygenase proteins that are part of the core AOA genome were detected in high amounts in the proteomes of *Nitrososphaera viennensis* and *Ca. Nitrosopelagicus brevis* (Kerou *et al.*, 2016). However, a counter-argument for these F420-proteins is the fact that they were predicted to be cytoplasmic while ammonia oxidation most likely occurs extracellularly (Lehtovirta-Morley, Sayavedra-Soto, *et al.*, 2016). Lastly, Lancaster *et al.* (2018) suggested that a non-heme Fe protein could be responsible for the NH₂OH oxidation. None of these hypotheses have been convincingly proven and a lot of work needs to be done to elucidate the archaeal ammonia oxidation pathway.

In this thesis, a focus is placed on (1) improving methods to study the AOA, (2) exploring substrates and inhibitors of known and unknown enzymes in the archaeal ammonia oxidation pathway, (3) developing methods to study the archaeal ammonia oxidation pathway and (4) the identification of enzymes of interest in the AOA. Headway in any of these objectives could massively improve our understanding of these ubiquitous organisms vital to the global nitrogen cycle.

2 Materials and methods

2.1 Materials

Analytical grade chemicals were obtained from Sigma-Aldrich (St Louis, MO, USA), Fisher Scientific (Loughborough, UK), Melford (Ipswich, UK) and Formedium (Hunstanton, UK). ^{15}N -hydrazine sulfate (>98% purity) was purchased from Cambridge Isotope Laboratories (CAS No. 88491-70-7).

2.2 Growth of microorganisms

The glassware used to grow ammonia oxidisers was acid-washed with 10% v/v nitric acid to remove any contaminants adhering to the glass. All solutions were sterilised by autoclaving for 15 minutes at 121 °C at 15 psi or by passage through a 0.2 µm pore-sized disposable Minisart syringe filter (Sigma Aldrich/Sartorius, Germany) for heat-sensitive solutions.

2.2.1 Growth conditions

Unless otherwise specified, the organisms were grown in the growth conditions stated in Table 2-1. Purity of cultures was monitored by microscopy and screening for contaminants on R2A agar plates (Oxoid, Basingstoke, UK). Subculturing was carried out by transfer (0.1-10% inoculum) to fresh medium when NO_2^- reached concentrations specified in Table 2-1, associated with mid-to late exponential phase. This was also when cells were harvested for experiments.

Table 2-1 – growth conditions of ammonia oxidisers

Organism	T (°C)	Agitation	$[\text{NH}_4^+]$ (mM)	Dark/light	$[\text{NO}_2^-]$ (mM) for transfer	Reference
' <i>Ca. Nitrosocosmicus franklandus</i> ' C13	37	/	5	Dark	1 – 1.2	(Lehtovirta-Morley, Ross, et al., 2016)
<i>Nitrososphaera viennensis</i> EN76	37	/	2	Dark	1	(Stieglmeier et al., 2014)
' <i>Ca. Nitrosotalea sinensis</i> ' Nd2	37	/	0.5	Dark	0.1	(Lehtovirta-Morley, Sayavedra-Soto, et al., 2016)
<i>Nitrosomonas europaea</i> ATCC19718	30	200 rpm	50	Dark	15 – 18	(Stein & Arp, 1998)

2.2.2 Media composition

All solutions were prepared in ddH₂O, using acid-washed glassware. To make up the media the following stock solutions were required:

Fresh water medium (FWM) salts contained per litre:

NaCl	1.0 g
MgCl ₂ ·6H ₂ O	0.4 g
CaCl ₂ ·2H ₂ O	0.1 g
KH ₂ PO ₄	0.2 g
KCl	0.5 g

Modified non-chelated trace solution (Könneke *et al.*, 2005) contained per litre :

HCl (12.5 M)	8.0 mL
H ₃ BO ₃	30.0 mg
MnCl ₂ ·4H ₂ O	100.0 mg
CoCl ₂ ·6H ₂ O	190.0 mg
NiCl ₂ ·6H ₂ O	24.0 mg
CuCl ₂ ·2H ₂ O	2.0 mg
ZnSO ₄ ·7H ₂ O	144.0 mg
Na ₂ MoO ₄ ·2H ₂ O	36.0 mg

Vitamin solution (pH 7.0) contained per litre:

Biotin	0.02 g
Folic acid	0.02 g
Pyridoxine HCl	0.10 g
Thiamine HCl	0.05 g
Riboflavin	0.05 g
Nicotinic acid	0.05 g
<i>DL</i> -Pantothenic acid	0.05 g
<i>p</i> -Aminobenzoic acid	0.05 g
Choline Chloride	2.00 g
Vitamin B ₁₂	0.01 g

HEPES buffer (1 M HEPES, 0.6 M NaOH, pH 7.5) contained per litre:

HEPES	119.0 g
NaOH	12.0 g

MES hydrate buffer (0.5 M pH 5.3) contained per litre:

MES hydrate	97.62 g
-------------	---------

2.2.2.1 '*Ca. Nitrosocosmicus franklandus*' C13

The C13 growth medium was prepared by the addition to 1 L FWM mineral salts solution of 1 mL trace element solution, 1 mL vitamin solution, 1 mL FeNaEDTA solution (7.5 mM), 2 mL Sodium Bicarbonate solution (1 M), 10 mL HEPES buffer (1 M HEPES, 0.6 M NaOH) and NH₄Cl solution (1 M) was added as growth substrate (5 mM). 1 mL of phenol red (0.5 g L⁻¹) was added as a pH indicator and the final pH was 7.6

2.2.2.2 *Nitrososphaera viennensis* EN76

The growth medium for *Nitrososphaera viennensis* was identical to that of *Nitrosocosmicus franklandus* with the only differences being the addition of 0.5 mM sodium pyruvate from a 1 M stock, 50 mg L⁻¹ kanamycin and 2 mM NH₄Cl as opposed to 5 mM final concentration.

2.2.2.3 ‘*Ca. Nitrosotalea sinensis*’ ND2

The *Nitrosotalea sinensis* growth medium was prepared by the addition to 1 L FWM mineral salts solution of 1 mL trace element solution, 1 mL FeNaEDTA solution (7.5 mM), 4 mL sodium bicarbonate solution (1 M), 5 mL MES hydrate buffer (0.5 M pH 5.3), 2.5 mL 10% HCl solution and 0.4 mM NH₄Cl from a 1 M stock solution as growth substrate.

2.2.2.4 *Nitrosomonas europaea* ATCC19718 (M R Hyman & Wood, 1985)

N. europaea growth medium was prepared by first adding the following components into 900 mL H₂O to make up the salts: 3.3 g (NH₄)₂SO₄, 0.41 g KH₂PO₄, 0.75 ml 1 M MgSO₄ stock solution, 0.2 ml 1 M CaCl₂ stock solution, 0.33 ml 30 mM FeSO₄ /50 mM EDTA stock solution and 0.01 ml 50mM CuSO₄ stock solution. Then, 100 mL of 500 mM phosphate buffer (pH 8) 8 mL of 5% (w/v) Na₂CO₃ solution were added to the 900 mL salts.

2.3 Cell counts

Cell counts were performed using a protocol adapted from (Lehtovirta-Morley *et al.*, 2014). Briefly, the total cell concentration was determined in 1 mL samples. Thirty microlitres of 200 µg/mL DAPI (4,6-diamidino-2-phenylindole) was added to 1 mL culture, and samples were incubated for 5 min in the dark. Stained cells vacuum filtered onto a Cyclopore 0.22-µm pore-sized black polycarbonate filter (Sigma-Aldrich) and dried filters were mounted on glass slides with immersion oil and a cover slip. Cells were imaged using a Zeiss Axioscope 50 microscope (Carl Zeiss Ltd, Cambridge, UK). Five fields of view were counted on each filter. Depending on the growth stage, samples were diluted to result in 10–500 cells per sample.

2.4 Cell harvesting and preparation

For ‘*Ca. Nitrosocosmicus franklandus*’ and *N. viennensis*, mid- to late-exponential culture (corresponding to 1,000 – 1,500 µM NO₂⁻ accumulation) was harvested via filtration using a 0.22-µm pore-size PES membrane filter (Millipore). ‘*Ca. Nitrosocosmicus franklandus*’ cells were washed three times on the filter using 100 mL 10 mM HEPES-buffered FWM salts (pH 7.5) to remove residual nitrite and ammonia. Harvested cells were resuspended by turning over the filter and flushing with fresh solution to dislodge the cells. *N. viennensis* cells adhered more strongly to the filter than other strains and were scraped from the filter after filtration and subsequently washed three times in 100 mL 10 mM HEPES-buffered FWM salts (pH 7.5) by centrifugation (10 min, 4,000 g), before finally

resuspending in fresh HEPES-buffered FWM salts. For '*Ca. Nitrosotalea sinensis*', mid- to late-exponential culture corresponded to 100 – 200 μM NO_2^- . The cells were washed three times on the filter with 100 mL 2.5 mM MES-buffered FWM salts (pH 5.3) and were resuspended in fresh buffer. For *N. europaea*, 100 mL mid-exponential culture (15-18 mM NO_2^-) was harvested by filtration, washed three times with 100 mL 50 mM sodium phosphate buffer (pH 7.8) containing 2 mM MgCl_2 , and resuspended in fresh buffer. After harvesting, the cells were incubated at their respective growth temperatures for 1 h to consume any remaining ammonia. Background NO_2^- was measured prior to commencing the experiments to determine the baseline levels.

2.5 Nitrogen quantification

2.5.1 Nitrite determination

Growth and activity of the cultures was monitored by nitrite accumulation. Nitrite concentration was determined using a colorimetric assay with Griess reagent in a 96-well plate format (Lehtovirta-Morley *et al.*, 2014). Briefly, 20 μL of sulfanilamide solution (5 g L^{-1} in 2.4 M HCl) was added to 100 μL of sample or standard, followed by the addition of 20 μL N-(1-naphthyl)ethylenediamide solution (3 g L^{-1} in 0.12 M HCl). The detection limit was <1 μM . Absorbance was measured at 540 nm using a VersaMax™ microplate reader (Molecular Devices, California, USA). Standards were prepared in duplicate using KNO_2 solutions ranging from 1.6 to 50 μM .

2.5.2 Ammonia determination

Ammonium (NH_4^+) was determined colorimetrically using a modified indophenol method using 96-well plates. Working reagent was prepared by mixing 1:1 vol/vol ratio sodium salicylate solution (27.6 g L^{-1} sodium salicylate and 0.9 g L^{-1} sodium nitroprusside in 0.5 M NaOH) with sodium hypochlorite solution (3% vol/vol sodium hypochlorite in 1 M NaOH). 100 μL of working reagent was added to 100 μL of sample/standard. Standards were performed in duplicate and prepared using NH_4Cl solution ranging from 10 to 250 μM . The absorbance was measured at 660 nm wavelength using a VersaMax platereader (Molecular Devices, CA, US) after an incubation time of 20 min.

2.5.3 Hydroxylamine determination

To measure hydroxylamine, it was reacted with 8-hydroxyquinoline (quinolinol) to form the stable indooxine (5, 8-quinolinequinone-(8-hydroxy-5quinolylimide)) which absorbs light at 705 nm. Hydroxylamine was measured in 1 mL cuvettes or 96 well plates by reading the absorption at 705 nm. Briefly, the protocol was performed as follows: 200 μL of 50 mM Phosphate buffer pH 7 was added into a 2 mL tube, 160 μL water was added, followed by 200 μL sample and 40 μL 12% w/v trichloroacetic acid in water. Then, 200 μL of 1% w/v 8-hydroxyquinoline (quinolinol) in 100% EtOH was added followed by 200 μL of 1M Na_2CO_3 . The mixture was pipetted up and down and was incubated at 100

°C for 1 minute, after which the absorption at 705 nm was measured. A standard curve was prepared in duplicate, and the linear range was 0.02-0.1 mM hydroxylamine.

2.5.4 ¹⁵N stable isotope analysis

To determine if N₂ is a product of hydrazine oxidation, ¹⁵N-hydrazine sulfate was added to a concentration of 500 μM to cell suspensions as described above and ²⁹N₂ and ³⁰N₂ production was investigated. If N₂ is produced from ¹⁵N-labelled hydrazine, an enrichment in ³⁰N₂ was expected as ²⁹N₂ cannot be a product of this reaction. "*Ca. Nitrosocosmicus franklandus*" and *N. europaea* were harvested, washed, and rested as described above (~3 x 10⁸ and ~4 x 10⁸ cells mL⁻¹ respectively). For abiotic controls, samples containing just the media components were included as well as heat-killed cells (121 °C for 15 min). Additionally, phenylhydrazine treated samples (100 μM, 1 h) were included to see if this would inhibit ³⁰N₂ production. Incubations were carried out in triplicate. ¹⁵N-labelled hydrazine sulfate was added from a concentrated aqueous stock after which the vials were sealed with twice-autoclaved butyl rubber seals and incubated for 1 h at the respective growth temperature of the organisms. The vials were shaken (180 rpm) to ensure gas exchange between the liquid and headspace. Headspace gas (10 mL) was then sampled using a gas-tight syringe fitted with a Luer-lock and injected into pre-evacuated (<0.1 atm) 12 mL exetainers (Labco). Gas samples were analysed using a Sercon CryoPrep gas concentration system interfaced to a Sercon 20-20 isotope-ratio mass spectrometer (Stable Isotope Facility, University of California, Davis, USA). Molar fractions were calculated from the isotope ratios and the N₂ concentration in the vials. The amount of ³⁰N₂ in the liquid was calculated using Henry's law (32) and standard conditions and was added to the total ³⁰N₂ formed. The background amount of ³⁰N₂ from heat-killed cells was subtracted.

2.6 Inhibition, activity, recovery and growth assays

2.6.1 96-well inhibition assays

To test the inhibition of ammonia and hydroxylamine oxidation by several inhibitors, a 96-well microtiter plate was prepared with 5 μl inhibitor from concentrated aqueous stocks or 5 μl dH₂O (controls) in each well. The inhibitors were diluted to their final concentrations with 95 μl cell suspension (~2 x 10⁸, ~3 x 10⁸, ~9 x 10⁸ and ~2 x 10⁸ cells mL⁻¹ for '*Ca. Nitrosocosmicus franklandus*', *N. europaea*, *N. viennensis* and '*Ca. Nitrosotalea sinensis*', respectively). The plate was incubated at the respective growth temperature for 1 h, and after inhibition, 2 μl of substrate (either ammonia or hydroxylamine) was added to each well and the plate was incubated for another hour. Griess reagent was added to stop the reaction and to determine nitrite concentration. Background nitrite at T = 0 was subtracted, and the nitrite production was normalised to the control. NH₂OH-dependent NO₂⁻ accumulation in AOA is not stoichiometric with NH₂OH consumption (Kozłowski, Stieglmeier, *et al.*, 2016) and the threshold for NH₂OH toxicity in AOA is lower than in AOB, leading to low levels of NO₂⁻

accumulation in AOA with this substrate. Therefore, the absolute, rather than relative, NO_2^- accumulation are shown with NH_2OH as substrate. The final ammonia concentration was 100 μM and final hydroxylamine concentrations were 100 μM for *N. europaea* and '*Ca. Nitrosotalea sinensis*', and 200 μM for '*Ca. Nitrosocosmicus franklandus*' and *N. viennensis*. Each assay was carried out at least two times with similar results with three technical replicates for each treatment.

2.6.2 Activity, inhibition and growth assays

Aliquots of 5 mL cell suspension were added to acid-washed 23 mL glass vials and inhibitors were added from concentrated aqueous stocks. The vials were sealed with twice-autoclaved butyl rubber seals and incubated in the respective growth temperature of the organisms. Ammonia and/or nitrite and/or hydroxylamine were assayed at regular intervals. All treatments were performed in triplicate.

2.6.3 Recovery

After 1 hour inhibition as described in the previous section, the cells were washed by filtration and resuspended in their respective media supplied with substrate. The vials were then incubated for 8 h and NO_2^- was measured every 30 min for the first two hours and every 60 min thereafter. All treatments were performed in triplicate.

2.7 ATP assay

To assess the effects of hydrazine and phenylhydrazine on ATP production, cells ($\sim 2 \times 10^8$ and $\sim 3 \times 10^8$ cells mL^{-1} for '*Ca. Nitrosocosmicus*' and *N. europaea* respectively) were first washed and starved without any substrates for 1 h to deplete internal ATP levels. For killed controls, cells were autoclaved at 121 °C for 15 min. Pre-treatment of cells, where necessary, was performed by incubating for 1 h with 100 μM phenylhydrazine at the respective growth temperatures. Experiments were performed in opaque black 96-well plates which were prepared with 5 μl of 20 times concentrated substrate/inhibitor stocks (100 μM final concentration) and 95 μl of alive or dead cell suspension. The cells were mixed with the different inhibitors and substrates by pipetting and were then incubated for 10 min at the respective growth temperatures. ATP accumulation was then measured using a luminescence assay based on the luciferase enzyme (BactTiter Glo; Promega, Wisconsin, USA). BactTiter-Glo reagent (100 μl) was added, and luminescence was measured every 5 min using a Spectramax ID5 plate reader (Molecular Devices, California, USA) with 1 s integration time. The luminescence values reached their maxima after 10 min and remained stable for 5 – 10 min thereafter. Therefore, fluorescence was measured 10 min after addition of the BactTiter-Glo reagent. The data were normalised against the NH_4^+ control (100%) (0.1 mM NH_4Cl). Killed controls were all very similar and were subtracted from their respective live measurements. Each assay was done at least two times with similar results and with three biological replicates for each treatment.

2.8 Oxygen consumption experiments

A Clark-type electrode (Rank Brothers, Cambridge, UK) was used to determine substrate-induced oxygen consumption. The instrument comprised of a 3 mL reaction chamber which was sealed with a stopper containing an injection port. Temperature was maintained by a circulating water bath (Churchill Co. Ltd, Perivale, UK). The temperature was set to the respective growth temperature of each microorganism and the electrode was calibrated as described previously (Green & Hill, 1984). The polarising voltage was set to 0.6V. Cell suspensions (3 mL) were fully oxygenated by stirring for 5 min without the stopper. The chamber was then sealed, and the endogenous rate was established for 2-5 min, and substrate was injected in 15 μL volumes from freshly made concentrated aqueous stocks of NH_4^+ , NH_2OH or N_2H_4 . End-point inhibition assays informed the choice of substrate and inhibitor concentrations for the O_2 uptake experiments. Experiments were carried out with either uninhibited cells or with cells preincubated with 100 μM phenylhydrazine ($\sim 7 \times 10^8$ and $\sim 3 \times 10^8$ cells mL^{-1} for '*Ca. Nitrosocosmicus franklandus*' and *N. europaea* respectively). Nitrite was measured at the end of each O_2 uptake trace. Abiotic controls for all treatments were performed using buffered salts without cells and oxygen consumption never exceeded 0.5 $\mu\text{M min}^{-1}$. Reactions were performed in triplicate with similar results.

2.9 Protein analysis and cell extract preparation

2.9.1 Cell extract preparation

Cell extracts of '*Ca. Nitrosocosmicus franklandus*' C13 were made using two lysis methods. Cells were kept on ice at all times after harvesting or after freezing. Cell extracts were preferably used immediately after lysis, alternatively they were stored frozen ($-20\text{ }^\circ\text{C}$).

2.9.1.1 French press

When using the French press, cells were washed an additional time (before freezing) using HEPES-buffered FWM salts (pH 7.5), diluted 1:7 with H_2O . This osmotic stress enhanced the physical destruction of the cells (Konneke *et al.*, 2014). The cells were suspended in up to 4 mL of precooled buffer and were then passed 3 – 5 times through a chilled ($4\text{ }^\circ\text{C}$) French press cell at 1 000 psi. Finally, the cell extracts were centrifuged (10 min, 17 000 g, $4\text{ }^\circ\text{C}$) to remove any insoluble components and large debris.

2.9.1.2 Bead-beating

When bead-beating, cells were suspended in 1 mL chilled ($4\text{ }^\circ\text{C}$) buffer and added to 2-ml Lysing Matrix E tubes (MP Biomedical, Eschwege, Germany). The cells were bead-beaten for 40 sec at 6 m/sec according to the instructions from the manufacturer. Finally, the cell extracts were centrifuged (10

min, 17 000 g, 4 °C) to remove any insoluble components and large debris, as well as to separate them from the beads.

2.9.2 SDS-PAGE

SDS-PAGE was performed using commercial precast 12% gels and premade buffers (TruPAGE, Sigma Aldrich). To run the gel, protein samples were mixed 3:1 with loading buffer containing 40 % glycerol, 240 mM Tris (pH 6.8), 8 % (w/v) SDS, 2 % (v/v) 2-mercapto-ethanol and bromophenol blue to visualise the sample. The gel along with 500 mL running buffer containing 25 mM Tris, 192 mM glycine and 0.1% SDS (pH 8.6) was added to the gel tank (XCell SureLock Mini-Cell, Thermo Fisher) and up to 15 µL sample (80 µg max) was loaded. The gel was first run at a constant voltage of 100 V for 10 min to ensure samples entered the gel evenly, and then for 60 more min at 160 V.

2.9.3 Colourless native PAGE

Native gels were prepared to 5 or 10 % acrylamide using premixed 40% (w/v) acrylamide/bis (37.5:1) (Sigma Aldrich). Tris buffer (1 M stock, pH 8,8) was used in a final concentration of 180 mM and was mixed with H₂O and acrylamide. Finally, 200 µL of 100 mg mL⁻¹ ammonium persulfate and 20 µL TEMED were added and mixed thoroughly to catalyse acrylamide polymerization. This solution was added to a gel cassette and a comb was fitted. The gel was left to solidify and was either used immediately or could be stored at 4 °C by wrapping with wet tissue and then wrapping with plastic foil.

To run the gel, protein samples were mixed 3:1 with loading buffer containing 40 % glycerol, 240 mM Tris (pH 6.8) and bromophenol blue to visualise the sample. Running buffer was made from a 10x concentrated stock with final concentrations of 25 mM Tris-HCl and 192 mM glycine (pH 8.8). The gel along with 500 mL running buffer was added to the gel tank (XCell SureLock Mini-Cell, Thermo Fisher) and up to 25 µL sample was loaded. The gel was run at a constant current of 20 mA to avoid heating and consequent denaturing of the proteins.

2.9.4 Blue native PAGE

Commercial BN-PAGE 4–16% gels, running buffer (both anode and cathode) and sample buffer were used (NativePAGE, Novex). NativeMark™ unstained protein standard (Novex) was used as a size marker. The gels were run according to the manufacturer's protocols, in a cold room or with pre-chilled running buffers (4 °C) at a constant voltage of 150 V for one hour and then at 250 V for the remainder of the run (30 – 90 min). This results in gels with a deep blue colour due to the included Coomassie G-250. Only the most abundant proteins are visible this way and for visualisation, extra processing is necessary. To do this, the fast-staining protocol provided by the manufacturer was used which has a sensitivity of ~60 ng (when binding to bovine serum albumin). First, the gel was placed in 100 mL fix solution (40% methanol, 10% acetic acid) and microwaved on maximum wattage for 45 sec.

Next, the gel was placed on a rotary shaker for 15 minutes at room temperature. The fix Solution was decanted, and 100 mL de-stain solution (8% acetic acid) was added. It was then microwaved for another 45 sec. Finally, the gel was placed on a rotary shaker at room temperature until the desired background was obtained.

2.9.5 Coomassie stain

Protein staining was carried out using a commercial coomassie mix (InstantBlue, Merck) which did not require a de-staining step. Gels were stained for at least 1 h, and typically overnight on a rotary shaker. The gels were then rinsed and stored in H₂O before visualisation.

2.9.6 Sypro ruby stain

The SYPRO[®] Ruby protein gel stain (Invitrogen, cat no. S12000) was carried out using the instructions from the manufacturer using the basic protocol. First, the gel was fixed using 50% methanol, 7% acetic acid on an orbital shaker for 30 min. This was done twice. Then, the Sypro ruby gel stain was added, and the gel was left on the shaker overnight. Finally, the gel was washed using 10% methanol, 7% acetic acid solution for 30 min. The gel was kept in the dark and visualised using a Typhoon FLA9500 (GE Healthcare) with a 473 nm laser and the LPG filter for detection (optimal excitation is at 450 nm and emission at 640 nm).

2.9.7 Catalase activity stain

This protocol is based on that described in (Woodbury *et al.*, 1971). After the native PAGE gel was run, the gel was washed three times with distilled H₂O on a rotary shaker for 15 min. The gel was then transferred to a 0.003 % H₂O₂ solution for 10 min after which it was briefly rinsed with distilled H₂O. The gel was then transferred to a solution of ferric chloride and potassium ferricyanide (1 % (w/v) each) for 10 min. This solution was prepared fresh every time from 2 % (w/v) stock solutions. The staining solution was poured off and the gel was briefly rinsed with H₂O. The protein bands with catalase activity appeared yellow on a dark green background because H₂O₂ was consumed at these spots. The colour was stable for at least several hours. The gel was stored in H₂O in the dark.

2.9.8 Protein precipitation

The reaction is described for 100 µL protein sample in a 1.5 mL Eppendorf tube but can be scaled up accordingly. First, 400 µL methanol, 100 µL chloroform and 300 µL H₂O were added to the protein sample with vortexing thoroughly in between each addition. After the addition of the water, the mixture became cloudy and started to precipitate. Next, the mixture was centrifuged for 1 min at 14 000 g, resulting in three layers: a large aqueous layer on top, a circular flaky layer of protein in the interphase, and a smaller chloroform layer at the bottom. The top aqueous layer was removed carefully without disturbing the protein layer. Another 400 µL methanol was then added to wash the

protein and the sample was vortexed. Finally, the sample was centrifuged 5 minutes at 20 000 g, which causes the protein precipitate to pellet against the tube wall. The supernatant was removed as much as possible, and the pellet was left to dry or dried under vacuum.

2.9.9 Protein fractionation

Small scale fractionation techniques were used to purify the cell extracts for several experiments. These were carried out in small volumes (5-20 mL) using bench top columns or ammonium sulfate precipitation.

2.9.9.1 Ammonium sulfate precipitation

Ammonium precipitation was carried out by the stepwise addition of ammonium sulfate crystals to the cell extract. The extract was continuously stirred and kept at 4 °C. The amount of crystals to be added to obtain the desired fraction was calculated beforehand using a calculator by Encor Biotechnology (<https://www.encorbio.com/protocols/AM-SO4.htm>). Fractions in steps of 20% were used. When the salt was dissolved and the protein precipitated, the extract was centrifuged (10 min, 10 000 g) and the supernatant was used for further fractionation.

2.9.9.2 Anion/cation exchange chromatography

1 mL columns from Cytiva were used for anion (HiTrap Q) and cation (HiTrap SP) exchange chromatography. The start buffer was 50 mM Tris (pH 9) and the ionic strength was increased by increasing the NaCl concentration in steps of 100 mM. The flow rate was $\sim 1 \text{ mL min}^{-1}$ for all solutions. Columns were first washed with 5 column volumes (CV) of start buffer, followed by 5 CV of 1M NaCl elution buffer and finally the column was equilibrated with 5 more CV of start buffer. The sample was then applied and washed with 5 CV of start buffer to wash away excess protein. Different fractions were then collected by addition of 3-5 CV of different ionic strength buffers. Finally, the column was washed with 5 CV of 1M NaCl elution buffer.

2.9.10 Preparation of gel slices for trypsin digestion

All washing steps were performed in 1 mL volumes for 20 min with strong vortexing unless otherwise specified. Protein bands of interest were cut out from Coomassie stained PAGE gels and were first de-stained in a 1.5 mL Eppendorf tube in 1 mL 30% ethanol for 30 min at 65 °C. This step was repeated until the ethanol was colourless. The gel slices were then washed in 50 mM TEAB in 50% acetonitrile. Next, the samples were incubated with 10 mM DTT in 50 mM TEAB for 30 min at 55 °C. The DTT solution was removed and replaced with 30 mM Iodoacetamide (IAA) in 50 mM TEAB which was incubated for 30 min at room temperature in the dark. The IAA was then removed, and the samples were washed with 50 mM TEAB in 50% acetonitrile. The gel slices were then cut into 1 mm x 1 mm pieces and added to a new tube. The pieces were subsequently washed with 50 mM TEAB in 50%

acetonitrile, and then two times with 100% acetonitrile. Finally, the acetonitrile was removed, and the samples were left open to dry or were dried under vacuum.

2.9.11 Protein identification

2.9.11.1 Preparation of samples for proteomics

Three times three bottles of 1 L '*Ca. Nitrosocosmicus franklandus*' cells were grown as described in section 2.2 and three bottles were pooled to form one replicate. This was done for cells grown with ammonia (5 mM) and urea (2 mM). The inoculum was pre-grown with ammonia or urea to minimise the need for a metabolic shift. In the ammonia grown samples, the pH was adjusted using bicarbonate to mimic the pH change in the urea grown samples and to minimise pH differences. In the urea grown samples, 2 mM urea was added when nitrite reached 0.5 mM to ensure urea was present when the cells were harvested. Cells were harvested and lysed as described in sections 2.4 and 2.9.1.1 respectively. A protease inhibitor mix was included in the buffer (SIGMAFAST™, Sigma Aldrich). The proteins in the protein extract were then precipitated using a methanol chloroform precipitation as described in section 2.9.8. All samples were fractionated and labelled using a TMTsixplex™ Isobaric Label Reagent Set (Thermo Fisher). Samples were analysed by mass spectrometry using an Orbitrap Eclipse™ (Thermo Scientific) system by Dr Gerhard Saalbach (John Innes Centre). Data were processed using Proteome Discoverer software (Thermo Fisher).

2.9.11.2 Matrix-assisted laser desorption/ionization time of flight (MALDI-TOF) analysis

Bands of interest were excised as described in section 2.9.10 and sent for analysis at the Proteomics Facility at the John Innes Centre. Samples were digested with trypsin and analysed by peptide mass fingerprinting using the Bruker Autoflex Speed Maldi-TOF/TOF. An identification was made by using the amino acid sequences from the whole genome sequence.

2.9.12 Protein quantification

Different protein quantification techniques were used depending on the amount of sample required, the sensitivity of the technique and compatibility of reagents with the techniques. Bovine serum albumin was used as a standard in all assays.

2.9.12.1 Bio-Rad protein assay

The Bio-Rad protein assay is based on the Bradford method (Bio-Rad, Temse, BE, cat. no. 5000006) This assay was used with a microplate reader according to the manufacturer's instructions using either the standard procedure which has a sensitivity of 50 µg mL⁻¹ or the microassay procedure which has a sensitivity of 8 µg mL⁻¹ but requires more sample. In the standard procedure, dye reagent was prepared by diluting 1 part dye reagent with 4 parts H₂O. 10 µl of the samples or standards was then pipetted into the wells in triplicate and 200 µL diluted dye reagent was added. In the microassay

procedure, 160 μL of sample or standard was used and 40 μL undiluted dye reagent was added. After mixing thoroughly using a pipet, the sample was incubated for at least 5 min at room temperature. Finally, absorbance was measured at 595 nm using a VersaMax™ microplate reader (Molecular Devices, California, USA).

2.9.12.2 Bicinchoninic acid assay (BCA)

For this assay, a commercial kit was used (Pierce, IL, USA) according to the manufacturers microplate protocol which has a working range of 20-2000 $\mu\text{g mL}^{-1}$. A working reagent was prepared by adding 50 parts of a mix containing sodium carbonate, sodium bicarbonate, bicinchoninic acid and sodium tartrate in 0.1M sodium hydroxide to 1 part of 4% cupric sulfate. Briefly, 25 μL of each standard or unknown sample was pipetted into a microplate well and 200 μL of working reagent was added to each well after which the plate was shaken for 30 sec. The plate was then covered for 30 min and incubated at 37 °C. Finally, the plate was cooled to room temperature and the absorbance was measured at 562 nm using a VersaMax™ microplate reader (Molecular Devices, California, USA). All samples and standards were assayed in triplicate.

2.10 Activity based protein profiling (ABPP)

2.10.1 Treatment with bifunctional inhibitor probes

Cells, inhibited with bifunctional probes as described above, were harvested, and washed as described above and inhibited for 1 hour at their respective growth conditions in their respective buffer solutions (either HEPES or phosphate buffer) using bifunctional inhibitor probes (100 μM). The cells were then harvested and washed again and either used immediately or stored in the freezer (-20 °C) for later use.

Tested probes

1,5-Hexadiyne

Biotin hydrazide

Biotin-dPEG4-hydrazide

N-(But-3-yn-1-yl)-4-hydrazineylbenzamide (aryl probe)

2.10.2 Copper catalysed azide-alkyne cycloaddition (CuAAC)

Cells were suspended in 50 mM phosphate buffer (pH 7.4) containing 2 mM MgCl_2 and the CuAAC reaction was carried out in this buffer. Other conditions were tested and are described in Chapter 5. Reactions are described in a 75 μL volume but can be scaled accordingly. A dye mixture was prepared containing the fluorescein-azide probe, CuSO_4 and Tris((1-hydroxy-propyl-1H-1,2,3-triazol-4-

yl)methyl)amine (THPTA). Ascorbate and aminoguanidine were added to the sample first and the dye mix was added subsequently. The mixture was left to react at room temperature in the dark for 1 hour.

Reagent	Final concentration	Stock concentration	Volume (μL)
Ascorbate	5 mM	100 mM	3.75
Aminoguanidine hydrochloride	5 mM	100mM	3.75
Copper(II) sulfate	0.1 mM	15 mM	5
Tris((1-hydroxy-propyl-1H-1,2,3-triazol-4-yl)methyl)amine (THPTA)	0.5 mM	5 mM	5
Azide-probe	10 μM	0.5 mM	1
H ₂ O			6.5
Sample			50
Final volume			75

2.10.2.1 Fluorescent SDS-PAGE

For fluorescent SDS-PAGE, cells were lysed after inhibition using a French pressure cell or bead-beating. The CuAAC reaction was carried out in a 75 μL volumes for 1 hour at room temperature in the dark with fluorescein azide as the azide probe. The reaction was stopped by adding 25 μL of SDS-PAGE loading buffer, after which the gel was run as described before, except it was run in the dark to avoid degradation of the fluorophore due to exposure to light. After electrophoresis, the gel was always kept in the dark until it was visualised by fluorescence imaging with an excitation laser at 473 nm and a long-pass blue emission filter (Typhoon FLA9500, GE Healthcare).

2.10.2.2 Fluorescence microscopy

Fluorescence microscopy was carried out by Dimitra Sakoula as described in Sakoula *et al.* (2022).

3 Optimising growth and laboratory methods of the model AOA

Nitrosocosmicus franklandus C13

3.1 Introduction

Growing AOA requires a lot of know-how and expertise and may be a barrier for scientists to introduce them into their laboratories. This chapter tries to improve these conditions.

While cultivation on solid media has always been difficult in ammonia oxidisers, AOB can often form microcolonies on plates or form colonies on floating filters (Picone *et al.*, 2021; Wood, 2001). AOA, on the contrary, have not been grown on solid substrates as single colonies. Some creative cultivation methods have been published such as an agar stab method (Chu *et al.*, 2015), the immobilisation of AOA in hydrogel beads (Landreau *et al.*, 2021) and most recently a Liquid-Solid method using phytigel (Klein *et al.*, 2022) but no bona-fide cultivation method on solid medium has been described. The lack of growth on solid media is also a limiting factor for research on genetic manipulation on the AOA as this often requires a way of screening single colonies.

Being able to genetically modify microorganisms is a corner stone of microbiology research. In a similar fashion to the solid media cultivation, generating mutants in AOB is difficult but not impossible. The large amount of established bacterial genetic techniques available can be translated to AOB and have been used to knock out genes of interest (Beaumont *et al.*, 2002, 2004) and even to generate a reporter strain for nitrification inhibitor research (Iizumi *et al.*, 1998). In AOA, however, no genetic techniques have been developed and archaeal research is significantly less mature than bacterial research, making it difficult to translate techniques of other organisms to this group.

The lack of robust and efficient growth methods and standard laboratory practices for AOA considerably limits the scientific progress. First, the lack of methods and tools limits reproducibility between different laboratories. The fact that AOA can be sensitive to the glassware, or the purity of distilled water, makes it difficult to compare data generated in different laboratories. The huge differences in culture media between the AOA with many of them requiring different additives contributes to this challenge. Second, the slow growth and low yield of the AOA limit the number of results that can be generated. Assays that can be done in a 96-well plate in a single day with many organisms can take days or weeks to prepare with AOA. Moreover, if a constant supply of 'experiment-ready' AOA is required, an immense amount of media, glassware, incubator space and labour is necessary. Third, experiments requiring a lot of biomass, be it protein, DNA or otherwise, may be outright impossible. No native purification experiments have been published and hardly any experiments using protein extracts in AOA have been performed, with the notable exception elucidating the AOA carbon fixation pathway (Konneke *et al.*, 2014).

Something as simple as lysing archaea can be more difficult than most bacteria as many of the methods used for bacteria are not compatible with the archaea. For example, lysozyme, which is often added in commercial lysing matrices has no effect on archaea as they do not have peptidoglycan in their cell walls. In general, mechanical breakage methods are more effective in archaea (Salonen *et al.*, 2010).

In this chapter, improvements for the growth and handling of the model AOA *Nitrosocosmicus franklandus* C13 were evaluated. First, the use of bioreactors was explored for the growth of *N. franklandus* in batch, fed-batch and continuous mode with a biomass retention system. Second, methods for obtaining cell extract were evaluated. Third, biomass was used to create cell extracts and an attempt to create a hydroxylamine oxidation enzyme assay was made. Finally, a proteome analysis was performed to compare the growth of the strain with ammonia or urea as substrate and to identify the most highly expressed proteins in '*Ca. N. franklandus*'.

3.2 Results

3.2.1 Growth of *N. franklandus* in a bioreactor

For each experiment carried out in this thesis, several litres (2 L for small experiments ranging to ~20 L for cell extract work) of AOA culture were needed. Due to the difficult growth of the AOA and the high requirements for biomass and protein, an attempt was made to grow *Nitrosocosmicus franklandus* in a bioreactor. A plan was made, where in several runs the complexity of the system would be increased, starting from (Run 1) simply running the bioreactor in batch mode to see the effect of pH and oxygen control on the growth compared to batch cultures without regulation (Figure 3-2A). In Run 2, the bioreactor was run in a fed batch mode but with the addition of a biomass retention system (Figure 3-2B). In Run 3 and 4, the bioreactor was run in a continuous mode (Figure 3-4A & B) where substrate was added at a constant rate and biomass was retained (retentostat). When the desired density and substrate consumption was obtained, a bleed was added to remove dead cells, resulting in a constant supply of active exponentially growing cells (Figure 3-1A).

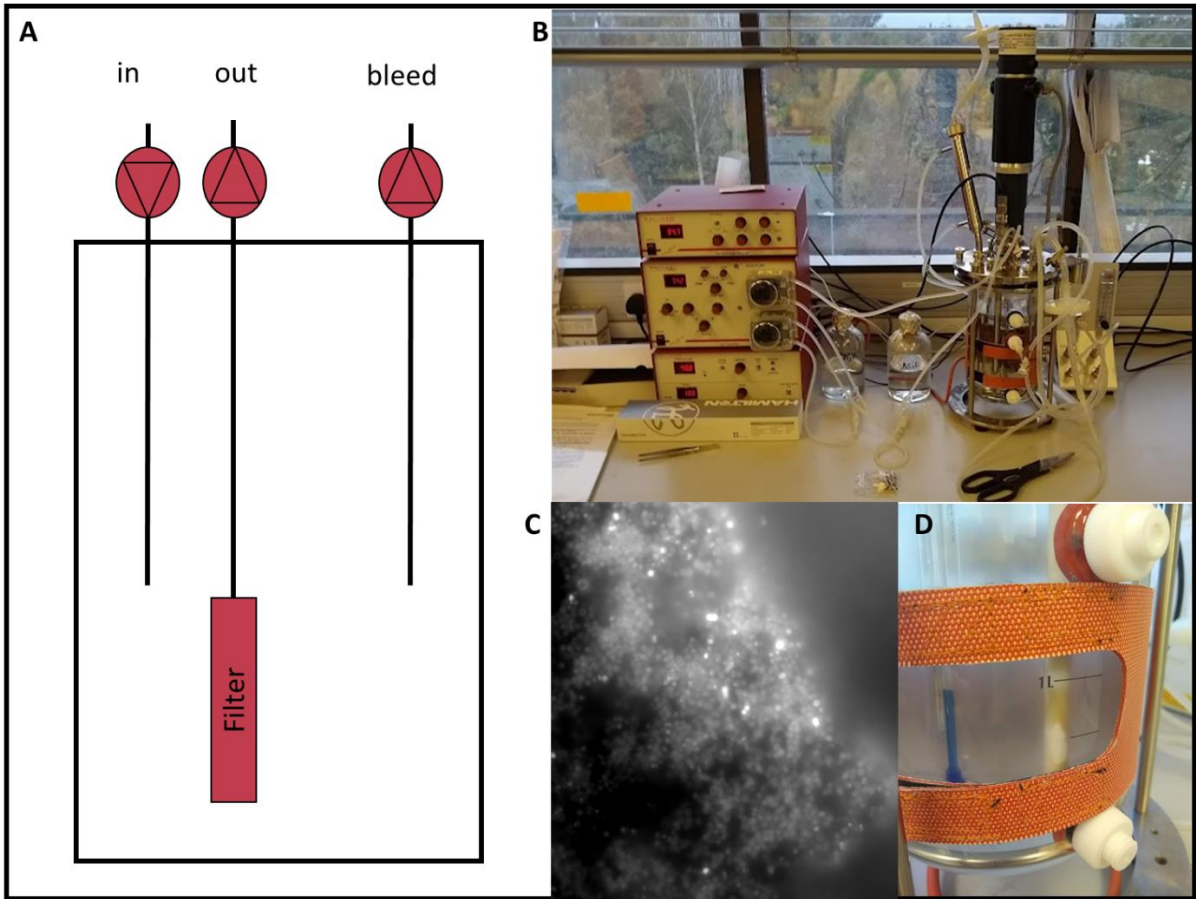


Figure 3-1 – Schematic of reactor set-up (A), picture of Electrolab FerMac200 reactor set-up (Reactor volume was 2.2 L and working volume was 2 L) (B), DAPI stained picture of biofilm taken in run 1 (C), picture of turbid reactor with biofilm formation on filter taken during run 1 (D).

3.2.1.1 Run 1 (batch)

In the first run, the reactor was set up with 2 L of the standard medium with 5mM NH_4^+ at pH 7.5, at 37 °C in the dark. The reactor was initially stirred at 100 rpm and stirring reduced to 50 rpm at day 10. Oxygen was kept at 60% saturation by injecting sterile air. Contamination was observed at day 12 by microscopy and appeared to be small rod-shaped cells. The contaminants, however, did not seem to inhibit nitrification. Once approximately 2 mM nitrite had accumulated, doubling times rapidly decreased and the nitrite doubled every day. Such a fast rate of nitrite accumulation was suspicious because the doubling time of '*Ca. N. franklandus*' is approximately two days, and this could be due to the contaminant being capable of ammonia oxidation. Alternatively, the pH regulation or oxygen regulation could have improved growth. Approximately 2 mM nitrite is the threshold when the pH decreases below seven in batch cultures. In run 1 NaOH was used instead of bicarbonate to regulate the pH. However, because the run was not continuous yet, it is unlikely CO_2 was limiting due to the constant addition of CO_2 from the air and due to the initial 2 mM bicarbonate concentration in the medium.

In earlier samples (day 12-15), the contaminant was much more prominent than *N. franklandus*. In later samples (day 20-25), the contaminant was barely noticeable under the light microscope, although still clearly present. Small brown particles were observed in the reactor. When examined under the microscope, these particles appeared to be *N. franklandus* biofilms (Figure 3-1C). Biofilms could be a potential problem especially when trying to fit a filter in later stages due to potential blockage. This was, however, very promising as it is difficult to get a comparable amount of growth at this rate in unregulated batch cultures. It seems likely that the pH or oxygen in batch cultures limits the growth. When all 5 mM substrate was consumed, additional substrate was added until 15 mM nitrite was reached, which is when nitrite has a negative effect on growth (Figure 3-2A) (Lehtovirta-Morley, Ross, *et al.*, 2016).

3.2.1.2 Run 2 (fed batch / continuous)

To avoid contamination, 50 $\mu\text{g mL}^{-1}$ kanamycin was added in the second run (Figure 3-2B). The pH was adjusted with 1M sodium bicarbonate instead of 0.5M NaOH and 0.5M HCl (nitrite acidifies so pH never needs to be adjusted down). Finally, due to technical problems with the oxygen electrode, saturation was not measured and a constant airflow and stirring speed were applied (5 L/min, 200 rpm).

When the nitrite concentration indicated that most of the ammonia had been consumed (day 14), 500 ml of medium was pumped out through the filter (retaining biomass) and replaced with medium containing 10 mM ammonium and 50 $\mu\text{g/ml}$ kanamycin (resulting in a final concentration of 2.5 mM

NH_4^+ when added in the existing volume of 1.5 L of culture). This was repeated on day 17. No *N. franklandus* cells were observed in the effluent from the membrane showing the biomass retention system worked efficiently. At this point the cells reached a visible turbidity and the reactor was prepared to be run in a continuous mode. In continuous mode, the reactor will always approach a steady state. For example, when the reactor is fed with 5 mM NH_4^+ , the reactor will adjust to this concentration. When the substrate is being converted to NO_2^- , the concentration in the effluent reflects the consumption rate. For example, when the NO_2^- concentration in the effluent is consistently 2 mM, this means 2 mM of the 5 mM NH_4^+ added is continuously being consumed (Tappe *et al.*, 1999).

To set up the continuous mode, 2.85 L of medium without ammonium was pumped through the reactor on day 21 to dilute nitrite and ammonium, at which point medium containing 5 mM ammonium and $50 \mu\text{g mL}^{-1}$ kanamycin was added continuously. The flow rate for the in- and effluent was adjusted to $\sim 1 \text{ L day}^{-1}$, resulting in a hydraulics retention time (HRT) of 2 days while the solid retention time (SRT) was infinite (no solids removed at this point). Because turbidity was now observable, cell counts were carried out by measuring OD540 and comparing this to a standard curve prepared with a known number of cells. However, a biofilm started forming on the filter (Figure 3-1D). The biofilm could be loosened by increased stirring ($>500 \text{ rpm}$) for 1 minute, but this resulted in flakes coming loose and fluctuating the OD540 measurements. This made it difficult to estimate the true number of cells in the reactor at any given point and did not bode well for the efficacy and lifetime of the filter membrane.

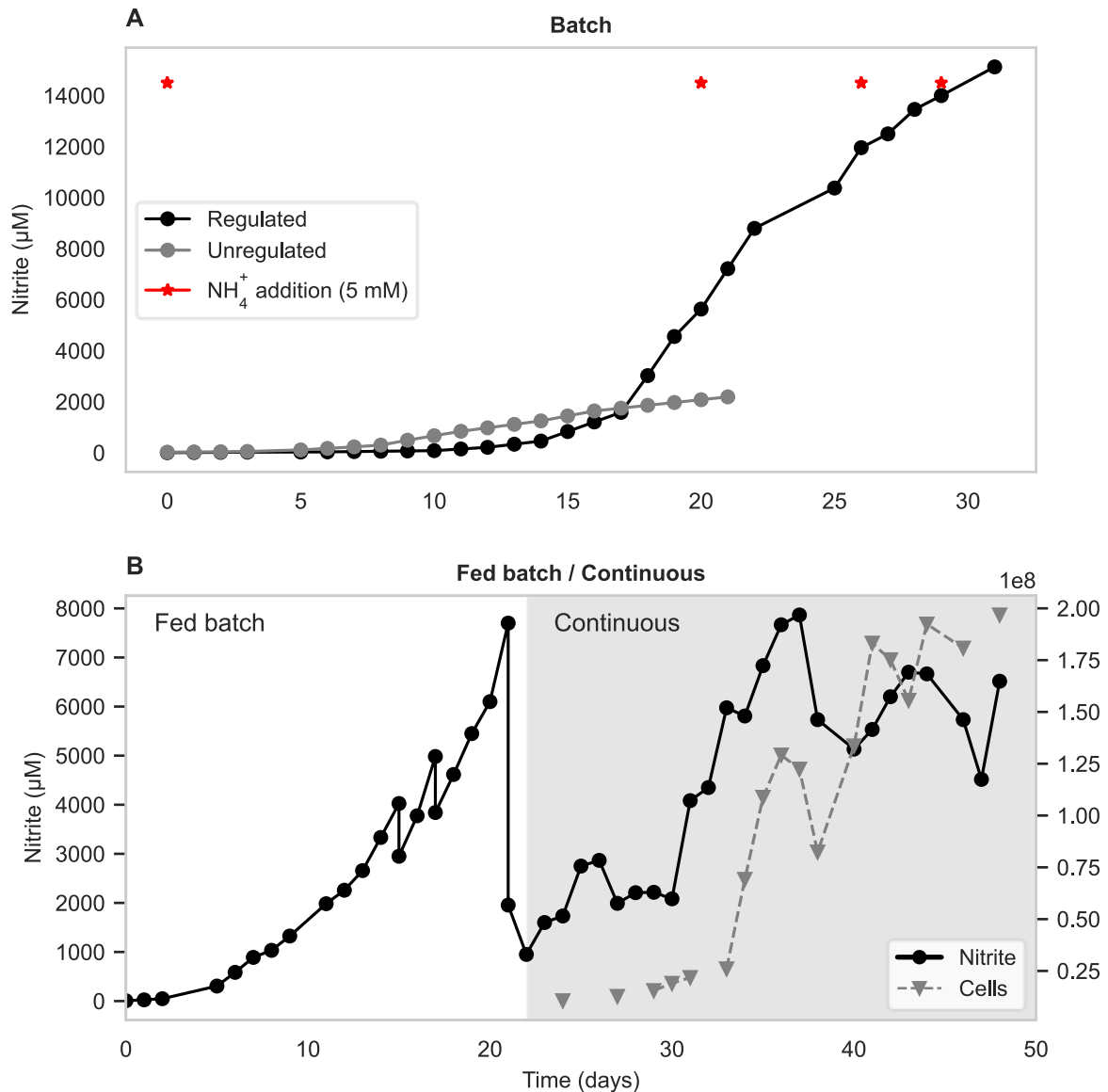


Figure 3-2 – Overview of the first two successful reactor runs. Batch mode (A) (Run 1) and fed batch (B, white) combined with continuous (B, grey) (Run 2). Unregulated: no pH and O_2 control; Regulated: with pH, O_2 control. A clear benefit from pH and O_2 regulation is visible. pH was regulated using 0.5M NaOH and HCl. Red stars indicate addition of NH_4Cl up to 5mM. Cell quantities are based on OD540 measurements.

During the first 10 days of continuous operation, nitrite in the effluent stabilised to ~ 2 mM. This was due to oxygen limitation because when the aeration rate was increased from 5 to 10 L / min on day 30, there was an immediate increase in nitrite production up to 5 mM. The NH_4^+ in the inflow was adjusted to 10 mM on day 33 to explore the maximum concentration of ammonia which could be tolerated. The nitrite in the effluent further increased but never reached 10mM.

To compare the activity of ‘Ca. N. franklandus’ cells grown in the bioreactor to those grown in batch culture, 20 mL culture was removed from the reactor (day 41) and 2 L of batch-grown culture was harvested. Both sets of cells were washed using HEPES-buffered salts and OD540 measured. OD was

adjusted to 0.440 in fresh medium. 1mM ammonium was added and nitrite production was measured every 30 min for 2 hours (Figure 3-3). The cells in the reactor showed 83.5% of the activity of the batch-grown cells after being in the reactor for 41 days. This was promising and showed a robustness in the cell viability and activity. However, the reactor system should aim to provide equally healthy or healthier cells compared to batch culture so the addition of a bleed to the system is essential to remove dead cells.

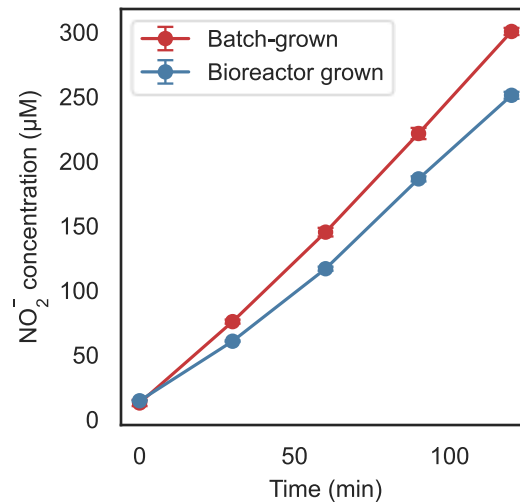


Figure 3-3 – Activity assay of batch-grown cells compared to reactor grown cells. Cell suspensions were normalised to an OD540 of 0.440 and nitrite production was measured every 30 min for 2 hours. Data of a single replicate is shown. The cells in the reactor showed 83.5% of the activity of the batch-grown cells after being in the reactor for 41 days.

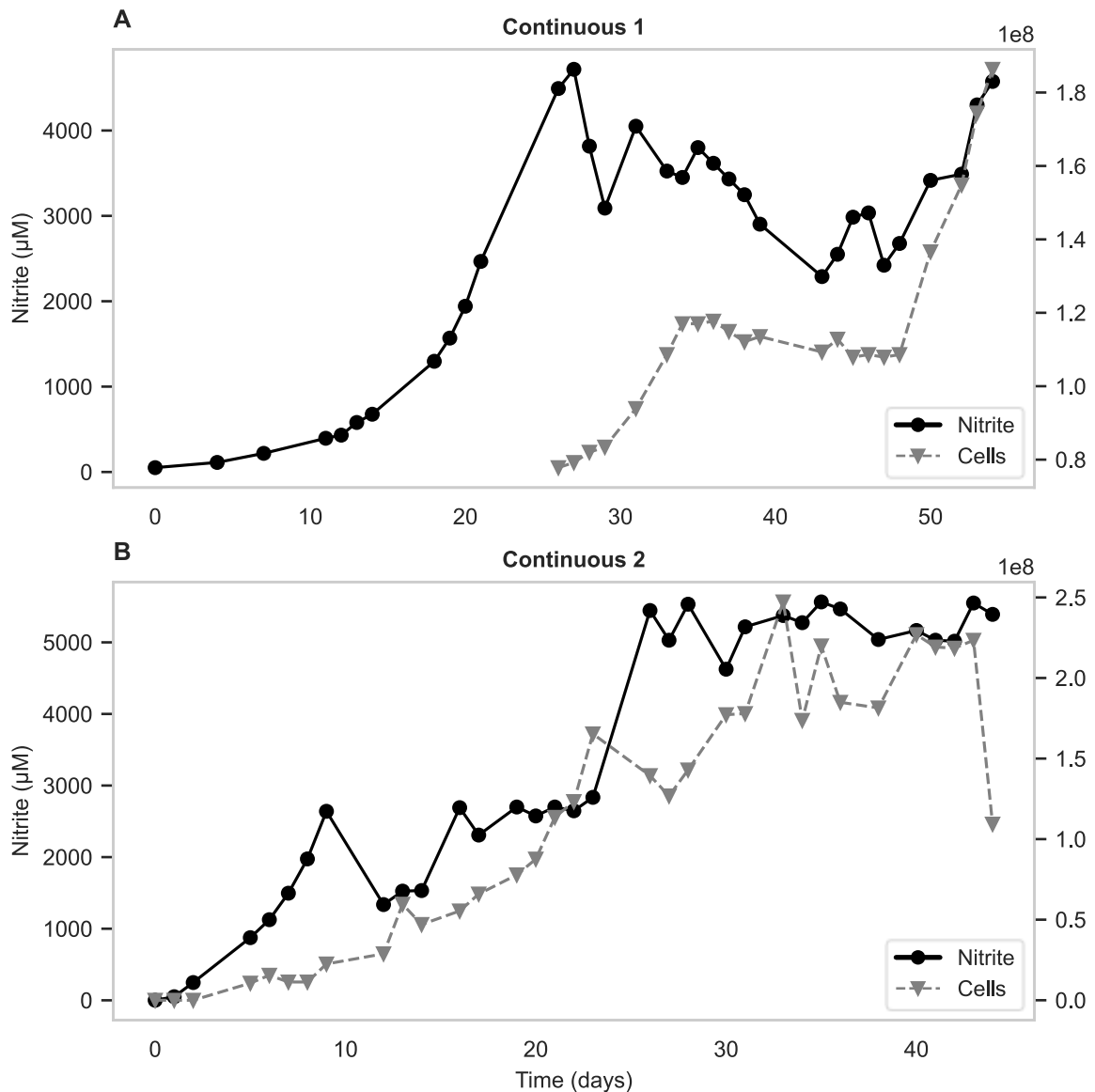
However, a pump malfunctioned overnight at day 50 and the reactor was pumped empty. The filter membrane lost its permeability due to being dry for a prolonged time and the run had to be stopped.

To ensure that cells were not inhibited by the nitrite in the reactor, NH₄⁺ in the influent was limited to 5 mM in subsequent runs. Despite limitations, the results were promising with the number of cells stabilising at ~2 x 10⁸ mL⁻¹, which is approximately 10-20x as much as in batch culture. It is likely that ‘Ca. N. franklandus’ can be grown to even higher cell densities using the bioreactor as there are still many improvements that can be implemented.

3.2.1.3 Run 3 and 4 (continuous)

The third run (Figure 3-4A) run was set up the same as the second, except instead of feeding in batches, continuous mode was started as soon as the reactor reached 5 mM nitrite and no antibiotics were added once continuous mode was started. At this stage, nitrite in the reactor decreased while the cell density increased as is expected until the cell density is high enough to consume all the ammonia that is fed. However, the nitrite and cell density stagnated and, likely due to biofilm

formation, the cell density even declined slightly. It was found that this was again due to oxygen limitation, and when the aeration rate was increased and the biofilm detached, nitrite production and cell density increased again. When the reactor finally reached 5 mM nitrite, consuming all the ammonia provided, the reactor overflowed and became contaminated due to a membrane failure. This meant that the run had to be terminated again before a bleed could be added.



mM in continuous mode on day 26, the cell density kept going up for a few more days but then stabilised. The cells may have been forming a biofilm on the filter again, but this was not visible. On day 30, 200 mL of the reactor volume was harvested, resulting in a drop in nitrite concentration but an unexpected increase in cell density the following day. This was either due to increased growth rate or because a piece of biofilm became detached. Another 200 mL was harvested on day 34, this time resulting in a drop in cell density but no drop in nitrite concentration. This suggests there must have been enough cells to maintain the consumption of all ammonia. This was promising as it indicated that the reactor was now in a state where 200 mL could be harvested regularly.

However, on day 36 the filter was blocked, and the reactor became pressured. 600 mL was pumped out, but nitrite remained stable and cell density was lower due to the dilution. The reactor was run for 8 more days and on day 43 another 400 mL was harvested but another filter block resulted in another overflow event and the reactor had to be shut down on day 44. It appears the filter has a lifetime of 30-40 days instead of the 50 claimed by the manufacturer. Runs should aim to stay below 30 days for that reason.

3.2.2 Evaluation of breakage methods

It is known that many archaea are resistant to widely used chemical lysis techniques (Salonen *et al.*, 2010), and the focus was therefore placed on mechanical breakage. Previously, mechanical breakage by French press in combination with osmotic stress was used in *Nitrosopumilus maritimus* with great success (Konneke *et al.*, 2014) and this technique, with some modifications, was applied to *N. franklandus*. Other breakage methods like freeze thawing, SDS, Proteinase K, CTAB and Tween have been attempted in the past but were fruitless. Cell breakage was evaluated by phase-contrast microscopy.

Table 3-1 Overview of tested breakage methods and their effectivity. Methods were evaluated by microscopy and SDS-PAGE. -: no lysis, +: slight lysis, ++: good but incomplete lysis, +++: complete lysis.

Lysis method	Effectivity
Sonication (3 x 10 sec, 50 kHz)	-
Sonication (3 x 30 sec, 50 kHz)	+
French press (20,000 psi)	++
Bead beating (40 sec at 6 m/sec)	+++
Osmotic stress (dH ₂ O) + French press	+++

Several mechanical breakage techniques were attempted (Table 3-1) and bead-beating and French press were the most efficient and least time-consuming techniques. Combination methods including boiling and adding SDS with the French press were attempted but made little difference. Alkaline boiling is an excellent lysis technique and efficient for '*Ca. N. franklandus*' but results in low yield of DNA and protein. The addition of a washing step with diluted salts to introduce osmotic stress to the cells improved the lysis in the French press similar to *N. maritimus* (Konneke *et al.*, 2014). An SDS-PAGE gel with the most efficient techniques was run to investigate the efficacy (Figure 3-5).

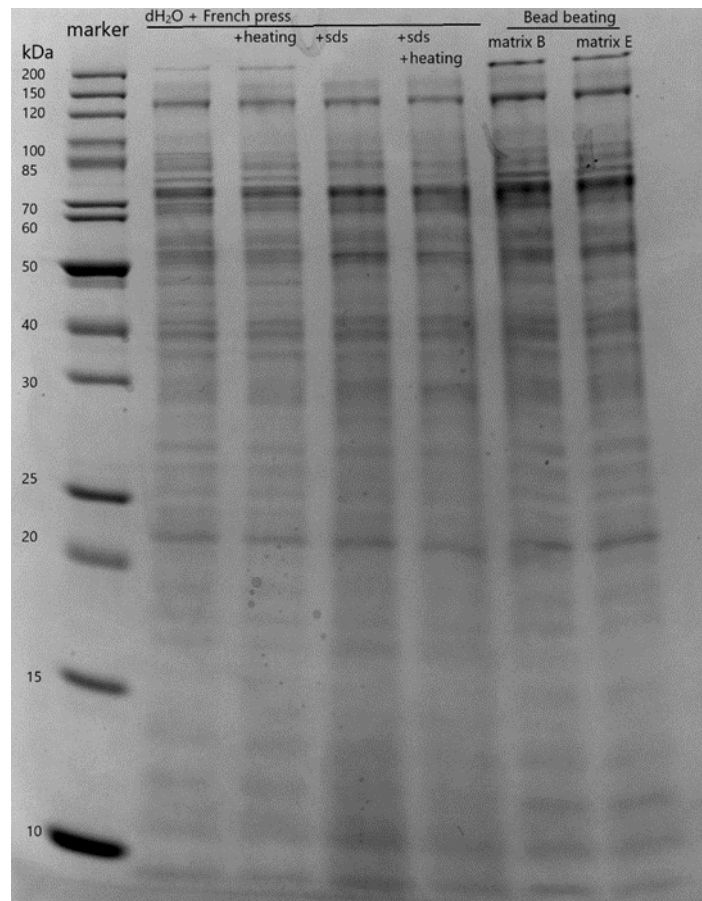


Figure 3-5 – Coomassie stained SDS-PAGE profiles of identical *N. franklandus* protein samples lysed with different mechanical lysis techniques.

When comparing the SDS-PAGE profiles of the two most successful lysis techniques (bead-beating and French press), samples lysed by bead-beating revealed several protein bands that were not detected in the samples lysed by French press (Figure 3-5) and the protein yield was slightly higher (based on band intensity). This technique may be preferable for fast and low volume protein extraction while the French press can more easily be scaled up and may be preferable when attempting to separate the membrane and cytoplasmic fractions. Finally cryo-grinding is a labour intense method that can yield high quality DNA but is hard to scale up (Nicol *et al.*, 2019).

3.2.3 Making cell-free protein extract and developing a hydroxylamine oxidation assay

Cell extracts were made by using the French press. Before lysis, cells were washed an additional time on the filter using diluted HEPES-buffered FWM salts (pH 7.5), 1:7 with H₂O. This osmotic stress enhanced the physical destruction of the cells (Konneke *et al.*, 2014). The cells were suspended in up to 4 mL of precooled buffer (Tris or HEPES) and were then passed 3 – 5 times through a chilled (4 °C) French press cell at 20 000 psi. Finally, the cell extracts were centrifuged (10 min, 17 000 g, 4 °C) to remove any insoluble components and large debris. This method was used for all further cell extract experiments.

3.2.3.1 Finding a suitable electron acceptor

In AOB, the activity of the HAO enzyme can be easily tested in cell extract with the addition of electron acceptors and substrate. The reduction of the electron acceptors can then be followed to determine the hydroxylamine oxidation activity. Several electron acceptors were tested in the AOA *N. franklandus* under aerobic conditions at room temperature in 50 mM Tris buffer at pH 8 and the reaction was started by adding 1 mM NH₂OH. Cell-free extract was prepared by lysing cells using the French press, osmotic shock combination and subsequent centrifugation as described above. The absorbance was measured at the respective wavelengths of the electron acceptors for 2 minutes (Table 3-2). The electron acceptors were chosen based on their efficacy as electron acceptors for HAO. 2,6-dichlorophenolindophenol (DCPIP), phenazine methosulfate (PMS) (Caranto & Lancaster, 2017) and ferricyanide have all been routinely used to determine HAO activity in cell extracts of AOB (Yamanaka & Sakano, 1980), anammox bacteria (Schalk *et al.*, 2000) and methanotrophs (Versantvoort *et al.*, 2020).

Table 3-2 – Electron acceptors tested with cell extract from ‘*Ca N. franklandus*’ and their concentration. Concentrations, compounds and wavelengths were chosen based on literature of AOB and MOB.

Electron acceptor/dye	Concentration (μM)	Wavelength (nm)	Activity observed	Reference
DCPIP	50	605	No	Caranto & Lancaster (2017)
DCPIP + PMS	50 + 50	605	No	Caranto & Lancaster, (2017)
PMS	100	388	No	Caranto & Lancaster, (2017)
Ferricyanide	500	420	Yes	Yamanaka & Sakano (1980), Schalk <i>et al.</i> (2000), Versantvoort <i>et al.</i> (2020)

Only ferricyanide showed any activity. While the conditions could be varied and different electron acceptors could be used, it was decided to look further into the ferricyanide to study hydroxylamine oxidation. The following assays were done by following the reduction of 500 μM ferricyanide at 420 nm.

3.2.3.2 Optimising pH and protein concentration

A pH range experiment was carried out to determine the optimal pH for the hydroxylamine oxidation assay. Only one replicate was performed to preserve precious material.

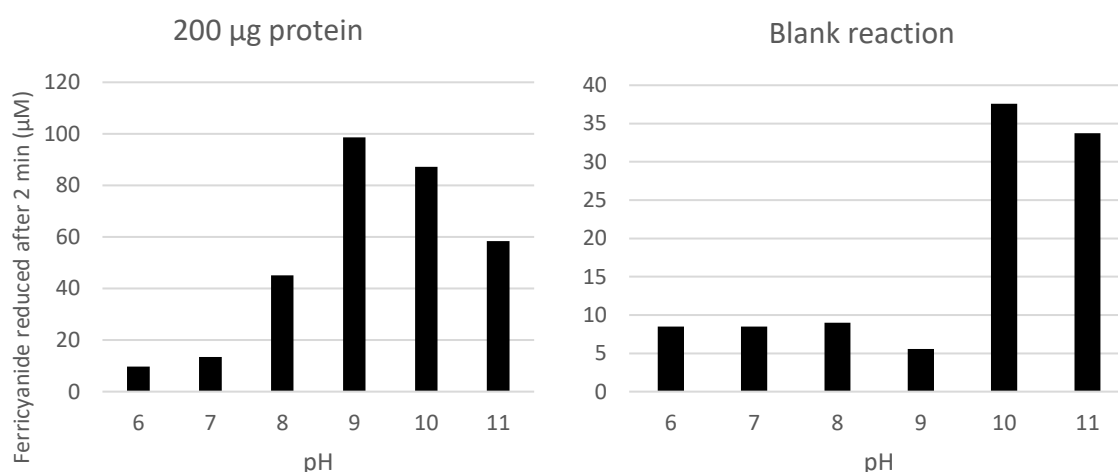


Figure 3-6 – pH optimum of the reduction of ferricyanide in cell free extracts of ‘*Ca N. franklandus*’ when using 200 μg protein in 50 mM Tris buffer. Bars are values of a single replicate as not enough material was available to do more.

The pH optimum appeared to be at pH 9, at 95 μM ferricyanide reduced after 2 minutes. However, at higher pH (>10), abiotic reactions resulted in reduction of more ferricyanide than in lower pH (<10). This interfering effect from the abiotic reaction seemed to be minimal at pH 9 so this pH was chosen for further experiments.

There is a fine balance between having enough sensitivity to detect activity and preserving hard to obtain protein extract. Therefore, three concentrations of cell free protein extract were tested, 100, 200 and 400 μg protein to determine an optimal concentration. They were tested at both pH 8 and 9 and extract of *Nitrosomonas europaea*, prepared in the same way, was used as a positive control (Figure 3-7).

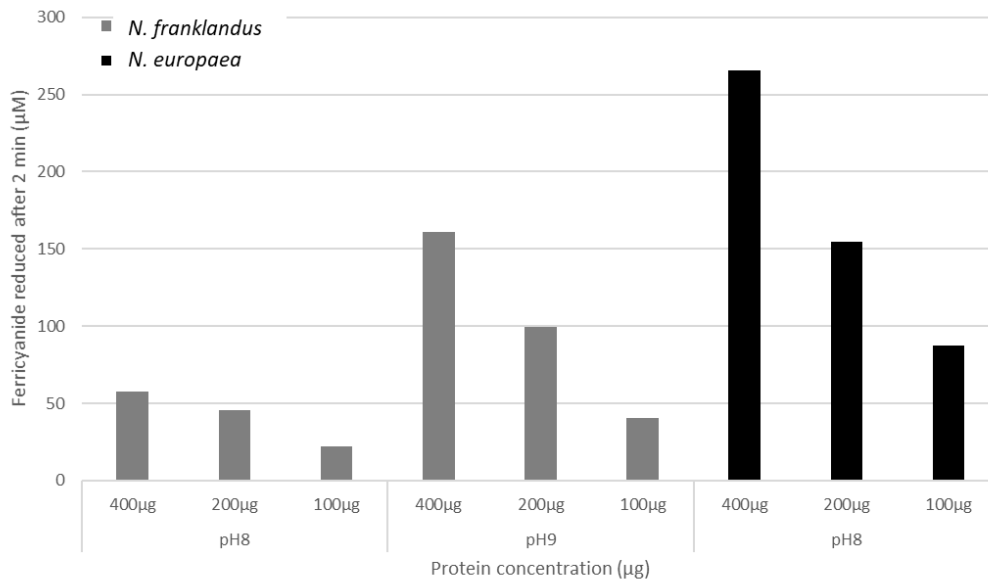


Figure 3-7 – The reduction of ferricyanide in cell free extracts of ‘*Ca N. franklandus*’ and *N. europaea* when using different protein concentrations in 50 mM Tris buffer. Bars are values of a single replicate as not enough material was available to do more.

From these results, 200 µg protein concentration was chosen to carry out further experiments as it showed sufficient activity but saved on material compared to 400 µg. This experiment also demonstrates a concentration-dependent activity as would be expected.

3.2.3.3 Fractionation

Next, an attempt was made to isolate the activity with the goal of getting a positive identification on the enzyme causing the activity. First, an anion exchange column was used to fractionate the cell extract (Figure 3-8). The sample was loaded on the column and eluted with equal volumes of different concentrations of NaCl. An attempt was made to measure protein in the different fractions, but this was almost always below detection limit, so unless otherwise specified, the fractions were used undiluted.

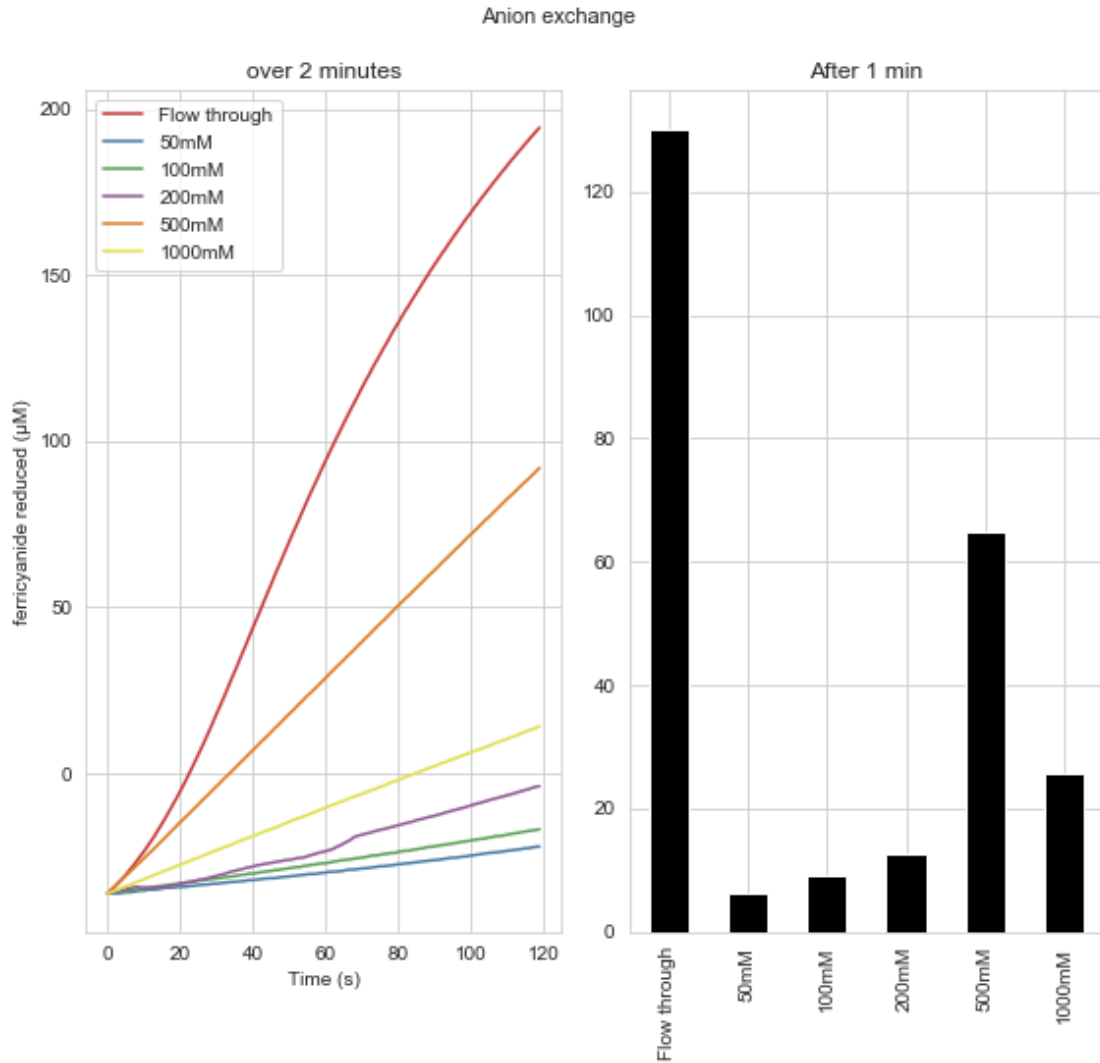


Figure 3-8 – Profile of the activity in the different fractions after anion exchange fractionation. Activity is expressed as concentration of ferricyanide reduced. The left panel shows the total ferricyanide reduced over time. The right panel shows the total ferricyanide reduced after 1 minute.

A significant amount of activity was observed in the 500 mM NaCl fractions but most of the activity appeared to be in the flow through fraction i.e., proteins that did not bind to the column. This was then repeated with identical results (not shown) and the flow-through was used to load on a cation exchange column. In this approach, the anion exchange column is used as an initial wash step to get rid of a portion of the proteins in the sample. The cation exchange column is then used to purify the protein of interest.

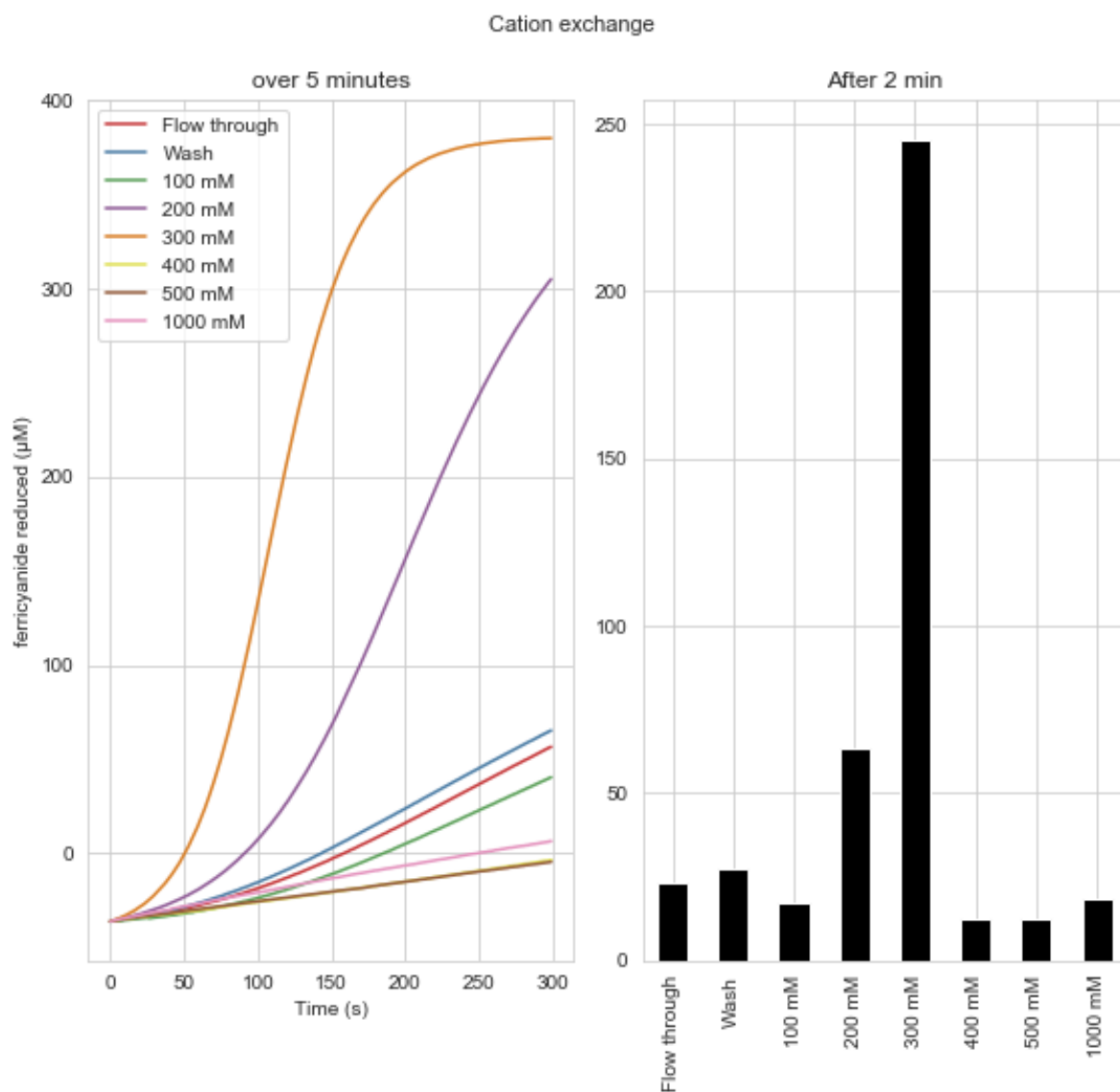


Figure 3-9 – Profile of the activity in the different fractions after cation exchange fractionation. The activity was determined using undiluted fractions. Activity is expressed as concentration of ferricyanide reduced. The left panel shows the total ferricyanide reduced over time. The right panel shows the total ferricyanide reduced after 2 minutes.

Almost all the activity was concentrated in the 200-300 mM NaCl fractions. The protein concentration was still below the detection limit in these samples however ($<8 \mu\text{g mL}^{-1}$ protein) and no bands were visible on a coomassie stained SDS-PAGE (not shown). Therefore, a SYPRO Ruby (Bio-Rad) protein stain was used which has a higher sensitivity of $\sim 1 \text{ ng}$ to visualise a protein band (Figure 3-10). The samples were also spin-concentrated using 5 kDa cut-off spin columns (Cytiva).

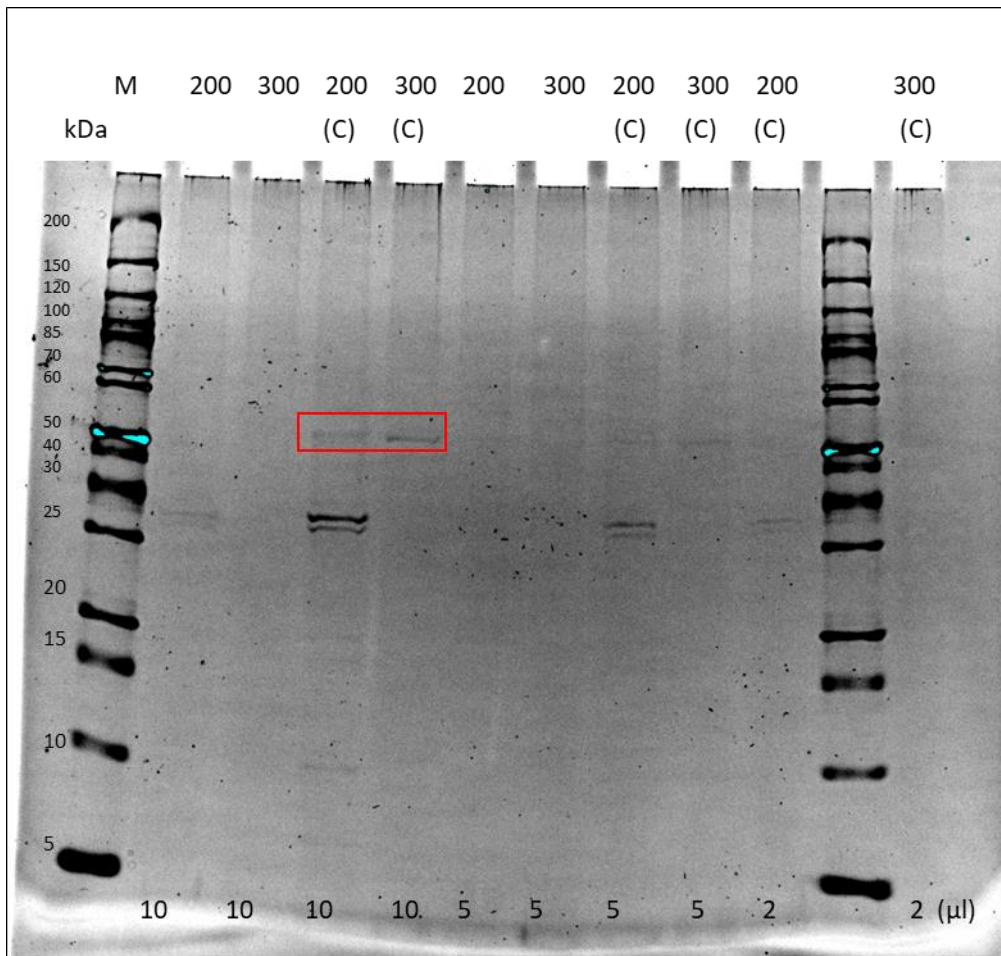


Figure 3-10 – SYPRO Ruby stained SDS-PAGE gel of active fractions after cation exchange fractionation. M: marker; (C) = spin concentrated ~10x; Top numbers: concentration NaCl in mM; Bottom number: μl loaded on gel; red box: cut out bands for identification.

Barely any bands were visible. At this point the low protein concentration combined with the high activity were highly suspicious but it was decided to move forward with an identification anyway. The protein band at ~50 kDa which was present in both the active fractions was cut out to be identified using an Orbitrap Eclipse (Thermo Fisher) by Dr. Gerhard Saalbach (John Innes Centre, Norwich, UK). The more intense bands at ~25 kDa from the 200 mM NaCl fraction were not identified as they were not present in the 300 mM fraction.

Identification

Table 3-3 shows the ten most abundant proteins in both the 200 and 300 mM NaCl samples.

Table 3-3 – The ten most abundant proteins identified in the samples cut out from an SDS-PAGE gel. * = Quantitative value based on normalized total spectra.

Identified Proteins	Accession Number	Molecular Weight	200 mM sample*	300 mM sample*
conserved protein of unknown function	NFRAN_v2_2353 ID:634 86736	16 kDa	94.189	46.447
30S ribosomal protein S27ae	NFRAN_v2_3128 ID:634 87511 rps27ae	7 kDa	51.209	14.515
F420-dependent glucose-6-phosphate dehydrogenase	NFRAN_v2_1211 ID:634 85594 fgd1	35 kDa	40.236	40.641
50S ribosomal protein L23	NFRAN_v2_3177 ID:634 87560 rpl	11 kDa	37.493	52.253
30S ribosomal protein S8e	NFRAN_v2_0088 ID:634 84471 rps8e	14 kDa	32.92	40.641
Methionine aminopeptidase	NFRAN_v2_1444 ID:634 85827 map	33 kDa	30.177	31.932
30S ribosomal protein S17e (modular protein)	NFRAN_v2_0737 ID:634 85120	12 kDa	18.746	20.321
Thioredoxin reductase	NFRAN_v2_3109 ID:634 87492 trxB	36 kDa	16.917	17.418
Pyridoxamine 5'-phosphate oxidase	NFRAN_v2_1087 ID:634 85470	16 kDa	16.917	11.612
50S ribosomal protein L30e	NFRAN_v2_2737 ID:634 87120	11 kDa	16.917	17.418

A large part of the '*Ca. N. franklandus*' genome is still unannotated, and many genes are annotated as conserved proteins of unknown function. The most abundant protein in both samples, NFRAN_v2_2353, is one of these. As far as the identification of a possible hydroxylamine oxidising enzyme goes, as mentioned in Chapter 1, likely candidates are F420-containing enzymes, multicopper oxidases and other oxidoreductases. The gene annotated as F420-dependent glucose-6-phosphate dehydrogenase (NFRAN_v2_1211), may be an interesting candidate. However, when some oxidised F420 was sourced (from Ghader Bashiri, University of Auckland), neither the glucose-6-phosphate nor hydroxylamine could reduce it using crude cell extract in the same assay conditions as with ferricyanide (data not shown).

3.2.3.4 Troubleshooting

To confirm that the cause of the activity in the fractions was in fact a protein and not an abiotic component in the buffer, spin tubes with a cut-off of 5 and 30 kDa were used to concentrate and separate the (larger) proteins from the buffer. Both fractions were then tested in the ferricyanide assay (Figure 3-11). Fractions that were saved from previous experiments were tested, including the 300 mM NaCl fraction that was identified, the 1 M NaCl fraction from the anion exchange column and the unbound protein from the cation exchange column.

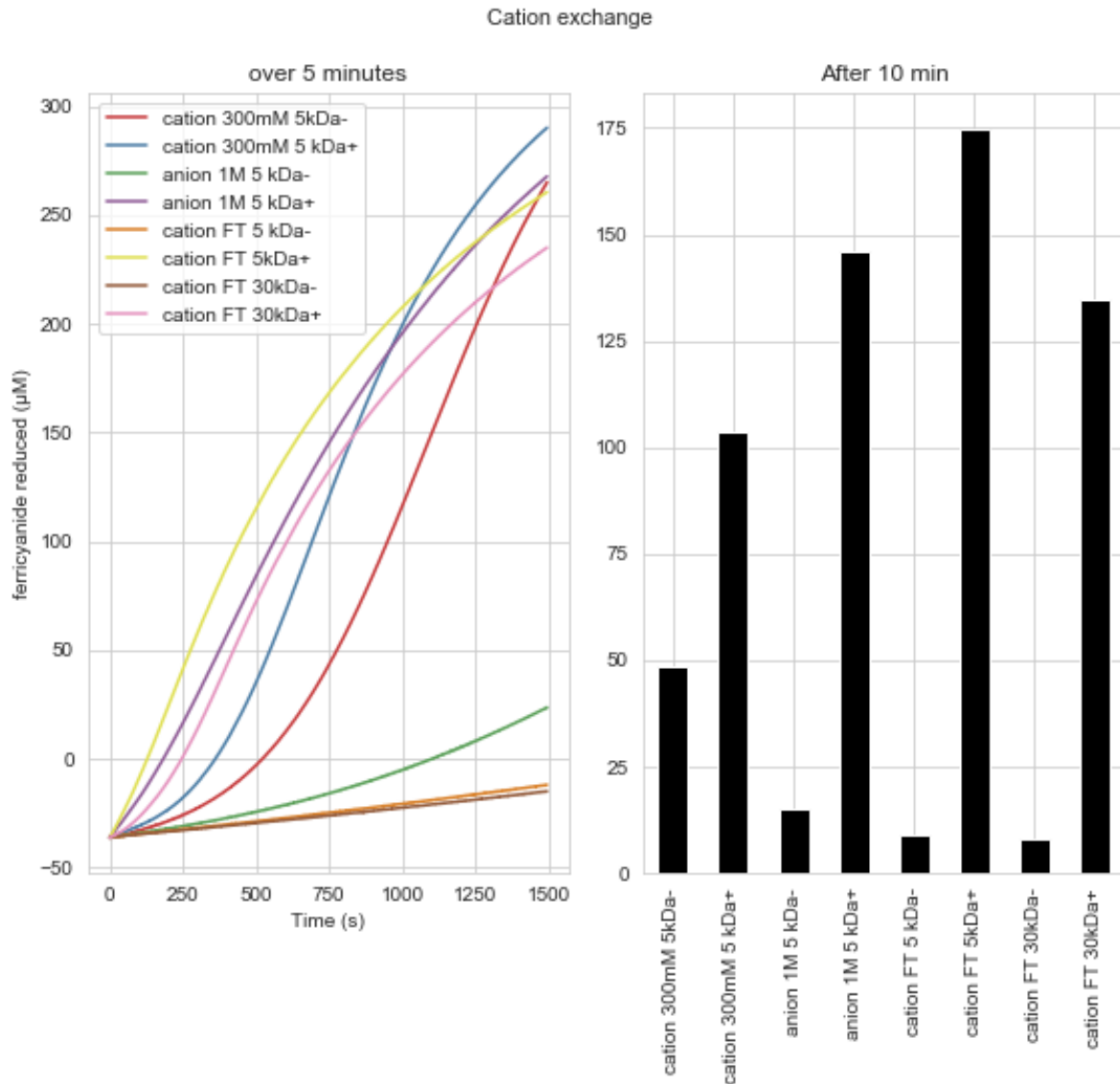


Figure 3-11 – Size exclusion fractionation of active fractions using spin tubes. Activity is expressed as concentration of ferricyanide reduced. -: smaller than; +: bigger than. The left panel shows the total ferricyanide reduced over time. The right panel shows the total ferricyanide reduced after 10 minutes.

Care should be taken in the interpretation of these results as 100 µl of the filtrate was used and all the remaining concentrated fraction (20-50 µl, >5 kDa). Activity in the <5 kDa fraction is therefore a low protein concentration and mild activity could be significant. The result shows that activity is present in the <5 kDa fraction of the 300 mM NaCl sample. This is unlikely to be enzymatic activity as enzymes <5 kDa are unlikely to exist (Storz *et al.*, 2014). The other fractions did show the expected pattern with no or little activity in the <5 kDa fraction and significant activity in the >5 kDa fractions. In the unbound protein from the cation experiment a cut-off of 30 kDa even yielded the same result indicating the activity was caused by a larger sized protein.

This result casts doubt on the identification experiment as this activity may not have been caused by a protein but instead could be due to some impurity such as a metal that was copurified (Heil *et al.*, 2016). However, this is slightly surprising as this result implies that an abiotic factor responsible for the activity was also fractionated by the columns. This also shows that the assay may have worked but that the activity was lower than expected. This approach could still be used to attempt to purify and identify a hydroxylamine oxidation enzyme if the assay is further optimised and non-enzymatic activity can be separated from the enzymatic activity using e.g., size exclusion chromatography.

3.2.4 Proteomics using growth on urea and ammonia

Ammonia monooxygenase subunits are among the most abundant proteins in the proteomes of ammonia oxidising archaea (Bayer *et al.*, 2019; Kerou *et al.*, 2016; Qin *et al.*, 2018). This is unsurprising, given that AMO is a key enzyme responsible for energy production in AOA. It was therefore hypothesised that other enzymes in the ammonia oxidation pathway, including the unknown hydroxylamine dehydrogenase, would also be some of the highly abundant proteins in the proteome.

There are only two known substrates on which *N. franklandus* can grow: ammonia and urea. Urea is hydrolysed to ammonia by the urease enzyme, which is found in some, but not all, ammonia oxidising archaea. To determine a baseline for protein expression and to identify the most abundant proteins, 'Ca. *N. franklandus*' was grown on urea and ammonia and the proteome was determined. This provides insights into the steady state operation of the cell and may identify some candidate enzymes that are important in the metabolism of this organism. The membrane and cytosolic proteins were extracted together and not separated. There are no published proteomes of any representatives of genus *Nitrosocosmicus*, and as such, a proteomic analysis is a valuable dataset to have and has the potential to provide insights into the metabolism in 'Ca. *N. franklandus*'.

3.2.4.1 Up and downregulated proteins in urea grown cells compared to ammonia grown cells

In the AOA 'Ca. *N. franklandus*', only 30 proteins were significantly upregulated and 70 were significantly downregulated in the presence of urea compared to ammonia. All significantly up or downregulated proteins are shown in

Figure 3-13. Many of the upregulated proteins are associated with the urea metabolism and include a putative nickel transporter (NFRAN_1480 – NFRAN_1483), urease subunits (NFRAN_1484 – NFRAN_1492), urea transporters (NFRAN_1493 – NFRAN_1494) and possible regulators (NFRAN_1495 – NFRAN_1496). These proteins are localised together in the genome and seem to be regulated similarly. Figure 3-12 shows a detail of these genes.

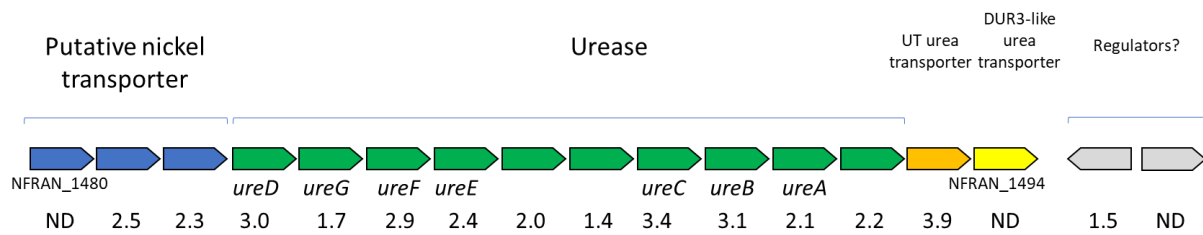


Figure 3-12 – Details of the urease operon in ‘Ca. N. franklandus’. The numbers under the figure indicate the fold change in cells grown on urea vs ammonia. ND: not detected. Urea related genes are upregulated during growth on urea. Results are the average fold change from triplicates of each conditions.

NFRAN_1480, NFRAN_1494 and NFRAN_1496 were not detected, it is unclear whether this is because they were not present or due to the extraction method. We expected these proteins to potentially be present due to the facts that NFRAN_1480 is a predicted subunit of the putative nickel ABC transporter, NFRAN_1494 is a putative urea transporter and these ORFs are syntenic with other genes involved in urea metabolism and upregulated in response to urea. Nickel is a co-factor for the urease enzyme and thus upregulation of nickel uptake was expected. In addition, urease is believed to be a cytoplasmic enzyme in AOA and upregulation of urea uptake was therefore also expected. The remainder of the upregulated proteins are mostly conserved proteins of unknown function, so it is hard to infer any function. A significant proportion of proteins encoded by genomes of AOA are conserved hypothetical proteins, which lack homology to proteins which have been biochemically characterised. Sensor proteins are among those up (NFRAN_2890), and down (NFRAN_2058) regulated which makes sense as the addition of urea in batch cultures will have influenced pH and ammonia sensing. There is no clear pattern of proteins responding to the pH except possibly for NFRAN_0652 which is among the most downregulated proteins and is identified as an inner membrane antiporter.

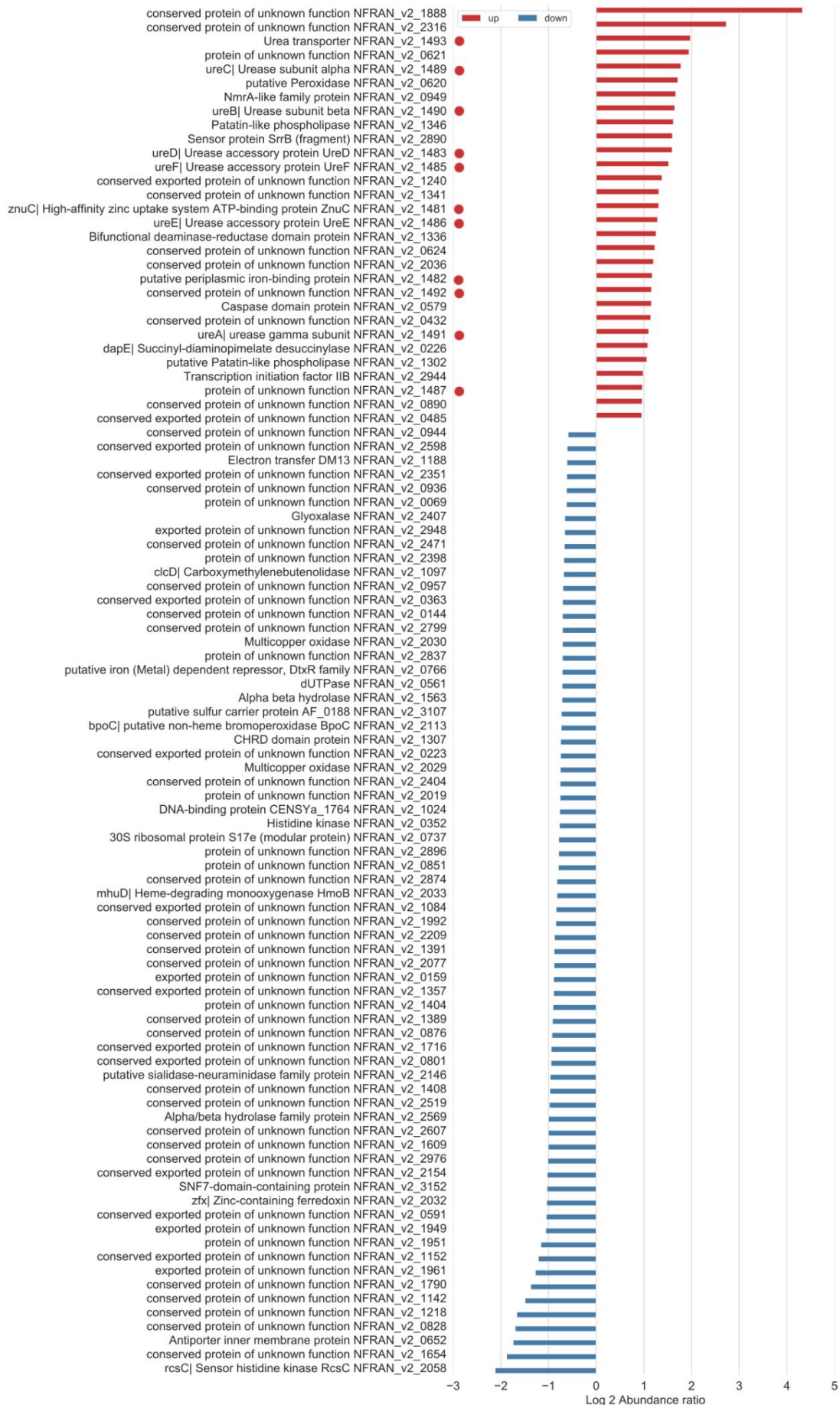


Figure 3-13 – All significantly up or downregulated proteins that were detected in the proteome of ‘*Ca. N. franklandus*’ when grown on urea versus ammonia. Proteins associated with the urea metabolism are highlighted with a red dot. Results based on triplicates of each condition; error bars were too low to be visible.

3.2.4.2 Most highly expressed in both conditions

The normalised absolute abundances of the 50 most highly expressed proteins detected in ammonia and urea grown cells are shown in Figure 3-14. Most of the abundant proteins are involved in the central carbon metabolism or information processing (replication, translation, transcription). The proteins related to the urea metabolism are among the most highly expressed in the urea grown cells as would be expected but interestingly, the urease genes were also detected in the ammonia grown conditions especially urease subunits B and C (NFRAN_1489 – 1490) were among the 50 most highly expressed proteins. This indicates that urease may be expressed constitutively but is upregulated when urea is present, which would be consistent with *ureC* transcription pattern in the AOA *N. agrestis* (L. Liu *et al.*, 2021). The AMO subunits were not as abundant as expected when compared to other AOA, e.g. in *N. viennensis* where AmoB was the second most abundant protein in the proteome (Kerou *et al.*, 2016). It is possible that this was due a bias in extraction method and because the membrane fractions were not separated from the intracellular fractions. In the most abundant proteins, there are less conserved proteins of unknown function compared to the most up-and down regulated proteins. It makes sense that the most highly expressed proteins would be well known proteins with homologues in other organisms, but it highlights how little we know of the AOA-specific proteins and their function.

One of the goals of this experiment was to identify possible hydroxylamine oxidation enzymes. As mentioned in section 1.7.2 of the introduction, prominent candidates are the multicopper oxidases (MCO). There are two multicopper oxidases among the 50 most abundant proteins in both growth conditions, namely NFRAN_2029 and NFRAN_2030. However, these are not conserved in other AOA and are therefore unlikely to be the hydroxylamine oxidising enzyme in all AOA. Among the other MCO detected were NFRAN_2792 and NFRAN_2798 with reasonably high abundances (130 and 135 most abundant, respectively) and finally in low abundances were NFRAN_2427 and NFRAN_0604 (983 and 1497 most abundant, respectively). These last two are homologues of the previously proposed ‘MCO1’ candidate hydroxylamine oxidation enzyme (Kerou *et al.*, 2016). Unless the protein extraction method was biased and we selected against these proteins, it seems unlikely that either of these would be the hydroxylamine oxidation enzyme as their abundance was very low. No other previously identified proteins were found among the most abundant proteins.

Many of the most highly expressed proteins in ‘*Ca. N. franklandus*’ are involved in either anabolism, energy generation or protection from oxidative stress. In addition to ammonia monooxygenase,

urease and multicopper oxidases, all of which are crucial for energy generation, subunit A of the V-type ATP synthase (NFRAN_0340) was also detected among the most highly expressed proteins. Thermosome and proteasome proteins are also among the proteins expressed most highly. Thermosome proteins are typical archaeal proteins involved in the folding of denatured proteins (Spang *et al.*, 2012), indicating '*Ca Nitrosocosmicus franklandus*' requires aid in protein folding while under the growth conditions used and may indicate some level of stress. Similarly, proteasome proteins were highly abundant, indicating a need for protein degradation. These could be misfolded proteins. An interesting protein that is among the most abundant proteins in both conditions is NFRAN_3193, which is annotated as DNA protection during starvation protein. In Chapter 6, this protein is discussed in detail, and it is shown that this protein is likely involved in the detoxification of H₂O₂, another stress response protein. Putative peroxiredoxin (NFRAN_2748) may also be involved in protection against oxidative stress. In addition, ferritin-like domain protein (NFRAN_1663) was among the most highly expressed proteins. Whilst it is not possible to infer the function of this protein, it is interesting to note that both the putative peroxiredoxin (NFRAN_2748) and the DNA protection during starvation protein (NFRAN_3193) also have structural similarity to ferritins.

Ammonia oxidising archaea use the hydroxypropionate-hydroxybutyrate pathway to fix inorganic HCO₃⁻, and several enzymes belonging to this pathway were detected in the proteomes. 3-hydroxypropionyl Co-A synthetase (NFRAN_0539), 4-hydroxybutyryl Co-A synthetase (NFRAN_1765) and crotonyl-CoA reductase (NFRAN_1025) were detected in the 50 most highly expressed proteins in both ammonia- and urea-grown cells. In addition, 4-hydroxybutyryl dehydratase / vinylacetyl-CoA delta-isomerase (NFRAN_0724) was detected in the 50 most highly expressed proteins in urea-grown cultures. Succinate-CoA ligase (NFRAN_0742) converts succinyl-CoA to succinate for incorporation into biomass. Glutamate dehydrogenase (NFRAN_0537) catalyses reversible conversion of ammonia and α -ketoglutarate into glutamate and was also among the highest expressed proteins (Figure 3-14).

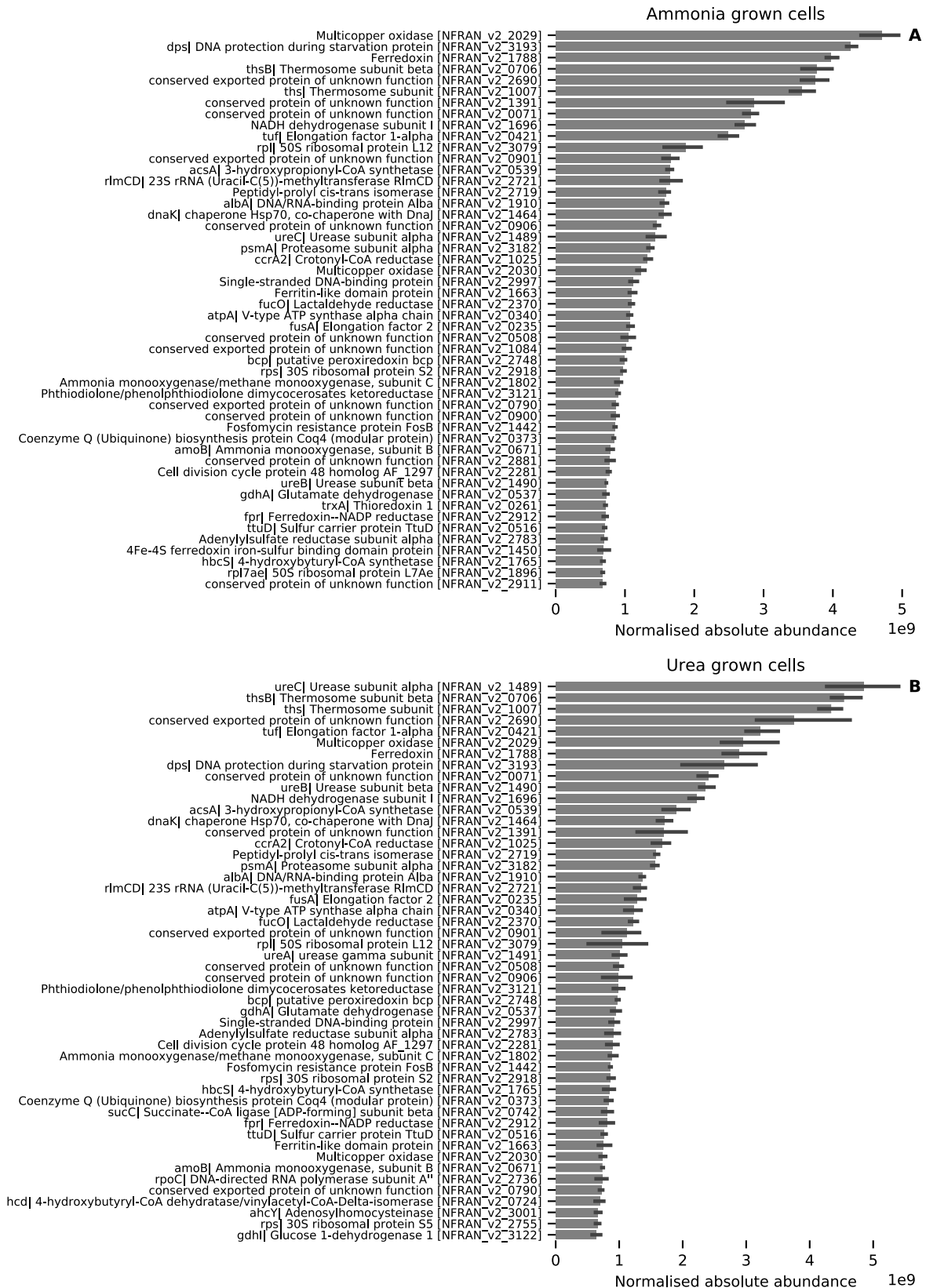


Figure 3-14 – The normalised absolute abundances of the 50 most highly expressed proteins detected in (A) ammonia grown cells and (B) urea grown cells. Values on the x-axis are abundances, normalised to all detected proteins in billions. Results obtained from triplicate samples, error bars represent standard deviation.

3.3 Discussion

3.3.1 A bioreactor system for the growth of AOA

While bioreactors could be a powerful tool for the growth and research of AOA, there are a lot of factors that need optimisation, and the use of bioreactors for growing AOA may not always be feasible. First, operating bioreactors requires a significant amount of know-how and while they are semi-autonomous, they need maintenance and observation. Therefore, it is important to have the necessary trained staff to help mind the reactors especially over long-term runs such as those required for AOA. Second, long runs come with their own problems. The longer the run, the more difficult it is to keep the reactor sterile, and the addition of antibiotics is an undesirable long-term solution because of the high cost and antibiotic waste. Furthermore, because of the long runs, equipment failures are especially detrimental, thus pumps and membranes need to be of sufficient quality to handle the long runs. Third, for optimal biomass production and utilisation, the bleed should be optimised as soon as there are enough cells to consume all the ammonia that is being fed, as this will be the highest growth rate achieved unless other parameters are changed. Having an optimised bleed may reduce pressure on the membrane as less volume would have to be pumped out through the membrane. Finally, it may also be possible to set up a reactor without a membrane if the solids retention time is kept higher than the doubling time. Practically this means that if the doubling time is 48 hours, half of the cells could theoretically be removed every 48 hours, resulting in 500 mL/ day from the 2 L reactor. It should be tested to see if the cells will be able to consume all the ammonia at this flow rate.

3.3.2 Hydroxylamine oxidation in cell extract

Using protein material from the ammonia oxidising archaea to purify and identify a hydroxylamine oxidation enzyme would be the most direct and conclusive way of identifying this enzyme. An attempt was made here to pave the way for future studies but it is clear that many challenges are still to be solved. These include, (i): Getting a reliable method for obtaining biomass. (ii): Dealing with the abiotic reactions that occur with the substrate (hydroxylamine) and likely also the product. (iii): Optimising a specific, sensitive, and reliable assay to detect the activity. This last point may be the most crucial, as a more sensitive and specific assay will require less biomass. The approach that was taken here, using different electron acceptors is viable and could be further explored, however rigorous controls would be needed to guarantee the observed activity is indeed what it appears to be. Including denatured protein extract in experiments is a good way to discern between abiotic and biotic activity and if it had been done in these experiments, the results could have been different. Overall, too many variables such as temperature, pH and electron acceptor, need to be adjusted to develop an assay such as this and the limiting factor is the availability of biomass. When ample biomass is present, more electron acceptors can be screened at different conditions and importantly more replicates can be done to

obtain robust results. An alternative way of developing an assay could be looking at substrate consumption or product formation, both of which have additional difficulties in the case of hydroxylamine oxidation, but could be solved. There have been reports of the development of a hydroxylamine sensor (Soler-Jofra *et al.*, 2021), depending on the sensitivity, this could be a way to detect activity. While there are many sensors capable of detecting nitrogen cycle intermediates with a high sensitivity, it is still unclear what exactly the intermediates are in the archaeal pathway and further studies in this direction will also aid with the development of a hydroxylamine oxidation assay suitable for AOA.

3.3.3 Proteome of *N. franklandus* grown with urea and ammonia

The proteome of '*Ca Nitrosocosmicus franklandus*' was determined under ammonia and urea grown conditions. This dataset will be used to check hypotheses and to get an understanding of the general metabolism of this organism. It is another tool to further develop '*Ca. Nitrosocosmicus franklandus*' as a model organism for soil AOA. Out of the 3180 proteins encoded in the genome (Nicol *et al.*, 2019), 1852 were recovered which is a decent coverage of 58% and significantly higher than the 48% recovered proteins in the *N. viennensis* proteome (Kerou *et al.*, 2016), but lower than the 74% recovered in *N. maritimus* (Qin *et al.*, 2018). This is not unexpected as the *Nitrososphaerales* have significantly expanded genomes compared to the the *Nitrosopumilales* (Abby *et al.*, 2020).

Overall, the cells responded to urea as predicted with an upregulation of the urea metabolism proteins. It is striking, however, how few proteins were differentially regulated. The pH of the medium of the ammonia grown cells was adjusted with bicarbonate to match that of the urea grown cells which could explain the limited difference in pH related proteins. No new hydroxylamine oxidation enzyme candidates were identified yet, but future candidates can be compared to the proteome and their abundance may indicate the likeliness of their involvement in the central metabolism of this AOA. An example of the value a proteome can contribute is shown in Chapter 6, where an enzyme was identified and could be traced back to one of the most abundant proteins in the proteome.

4 Hydrazines as substrates and inhibitors of the archaeal ammonia oxidation pathway

4.1 Introduction

Aerobic oxidation of ammonia (NH_3) to nitrite (NO_2^-) is the first step in nitrification and is carried out by ammonia-oxidising archaea (AOA) and bacteria (AOB) along with complete ammonia-oxidising bacteria (comammox). Comammox bacteria and nitrite-oxidising bacteria then further oxidise NO_2^- to nitrate (NO_3^-). Nitrifiers play a central role in the global nitrogen cycle, with important consequences in greenhouse gas emission and leaching of nitrate from terrestrial environments. AOA are ubiquitous and significantly contribute to nitrification in many ecosystems, including acidic soils, unfertilised soils, and the oligotrophic open ocean. Ammonia monooxygenase (AMO), a member of the copper membrane monooxygenase (CuMMO) superfamily, is found in ammonia-oxidising archaea and bacteria and initiates the nitrification process through the conversion of NH_3 to hydroxylamine (NH_2OH) (N. Vajjala *et al.*, 2013; YOSHIDA & ALEXANDER, 1964). Catalysis by AMO requires the input of two electrons which are supplied by downstream oxidation of hydroxylamine to NO_2^- , leaving two net electrons to enter the respiratory electron transport chain and making the oxidation of hydroxylamine the first energy yielding reaction in the pathway (Lancaster *et al.*, 2018; N. Vajjala *et al.*, 2013).

Functional and structural understanding of the archaeal AMO has improved through work exploring substrate analogues (Anne E. Taylor *et al.*, 2013; Wright *et al.*, 2020). This has led to applications such as the use of octyne to distinguish between archaeal and bacterial ammonia oxidation in soil microcosms (Anne E. Taylor *et al.*, 2013), and the use of alkadiynes in combination with click chemistry to label the AMO (Sakoula *et al.*, 2021). AMO has never been purified in its active form and virtually all knowledge about this enzyme comes from work on substrate analogues, highlighting the importance and potential of substrate analogues as tools in nitrification research. Very little is known about how hydroxylamine, produced from the initial oxidation of ammonia by the AMO, is converted to nitrite in archaea.

In AOB, hydroxylamine is converted to nitric oxide (NO) by hydroxylamine dehydrogenase (HAO) (Anderson, 1964; Caranto & Lancaster, 2017) and NO is then further oxidised to NO_2^- by an unknown mechanism (Lancaster *et al.*, 2018). HAO is a homotrimer with each subunit containing eight c-type hemes and one of these, the active site, is a P_{460} cofactor (Cedervall *et al.*, 2013). In the AOA, no genetic HAO homolog has been identified and the genetic inventory for production of c-type hemes is incomplete (Walker *et al.*, 2010), suggesting that a fundamentally different enzyme system for hydroxylamine oxidation is required. Based on proteomics and comparative genomics, several

candidate enzymes have been identified (Kerou *et al.*, 2016), including F₄₂₀-dependent enzymes and multicopper oxidases. However, no candidate enzymes have been experimentally verified.

Hydrazine (N₂H₄) is an alternative substrate for HAO from AOB. It competes with hydroxylamine for access to the HAO active site and thus can be described as a competitive inhibitor (Hooper & Nason, 1965). However, hydrazine can be used as an external source of reductant to supply the bacterial AMO with the electrons required for activity, making it possible to study the oxidation of a wide range of compounds by the AMO (M. R. Hyman *et al.*, 1990; M R Hyman *et al.*, 1988; Michael R. Hyman & Wood, 1984; Juliette *et al.*, 1993; W. K. Keener & Arp, 1994; William K. Keener & Arp, 1993; Rasche *et al.*, 1991). As opposed to HAO, the product of hydrazine oxidation by the HAO is dinitrogen gas (N₂) which causes no toxic build-up of products, making it such a potent tool to study the AMO (Maalcke *et al.*, 2014). Anaerobic ammonia-oxidising (anammox) bacteria also have a HAO homologue, hydrazine dehydrogenase, which catalyses the conversion of hydrazine to N₂ gas as part of their ammonia oxidation pathway (Schalk *et al.*, 2000).

Organohydrazines on the other hand, are irreversible suicide inhibitors of the HAO, covalently modifying the P₄₆₀ active site (Logan & Hooper, 1995). Phenylhydrazine has been used to characterise the HAO of different groups of AOB, showing differential responses between AOB groups (Nishigaya *et al.*, 2016). An attempt was made to use organohydrazines (phenylhydrazine, methylhydrazine and 2-hydroxyethylhydrazine) to distinguish between bacterial and archaeal ammonia oxidation in soil microcosms (Y. Wu *et al.*, 2012), relying on the absence of a genetic HAO homolog in the AOA. However, the authors found that the abundances of both AOA and AOB were affected. The inhibition of both AOA and AOB by organohydrazines was confirmed later in a different soil microcosm study (W. Yang *et al.*, 2017). However, the effect of organohydrazines on AOA cultures has not been studied and the inhibition of AOA by hydrazines warrants further investigation. If hydrazines inhibit AOA, they would be valuable tools for investigating the archaeal ammonia oxidation pathway.

The objectives of this study were to investigate the effect of hydrazines on ammonia and hydroxylamine oxidation using three strains of soil AOA and to compare the hydrazine metabolism of AOA and AOB. Specifically, we aimed to address the following questions: 1. Do hydrazines inhibit archaeal hydroxylamine and ammonia oxidation? 2. Are hydrazines reversible or irreversible inhibitors in AOA? 3. Are hydrazines oxidised and do they yield ATP in AOA? and 4. Can AOA oxidise hydrazine to N₂ like AOB do?

4.2 Results

4.2.1 The effect of phenylhydrazine on NH_3 and hydroxylamine-dependent nitrite production by ammonia oxidisers

To investigate the effect of phenylhydrazine on NH_3 and hydroxylamine oxidation by three different AOA strains and *N. europaea*, NO_2^- production, as proxy for activity, was compared after exposure to different concentrations of phenylhydrazine (Figure 4-1). Both NH_3 -dependent and hydroxylamine-dependent NO_2^- production were used to characterise and compare the inhibitory thresholds of the AOA and *N. europaea*.

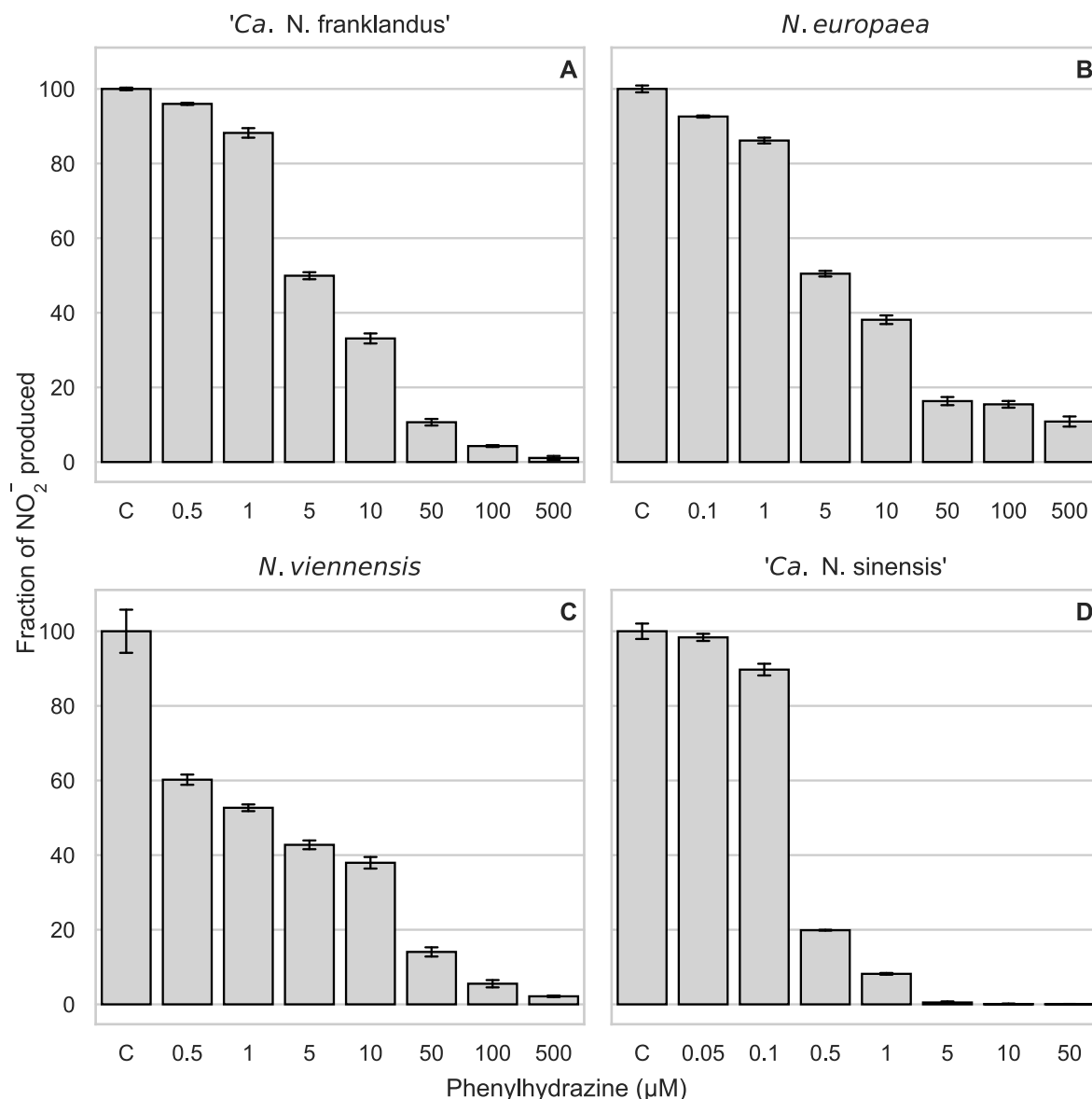


Figure 4-1 - Percentage NO_2^- production compared to the uninhibited control (C) after 1 h incubation with different concentrations of phenylhydrazine using $100 \mu\text{M}$ NH_4^+ as substrate. NO_2^- was measured 1 h after addition of the substrate. Nitrite accumulation in the uninhibited control treatment represents 100% activity, and the treatments with phenylhydrazine are shown as the

percentage of activity compared to this control. Error bars represent standard deviation (n = 3). 100% activity corresponded to 100 μM, 58 μM, 53 μM and 61 μM nitrite accumulated after one hour in 'Ca. N. franklandus', *N. europaea*, *N. viennensis* and 'Ca. N. sinensis', respectively.

The inhibition threshold of 'Ca. Nitrosocosmicus franklandus' (Figure 4-1A) and *N. europaea* (Figure 4-1B) was similar, but 'Ca. Nitrosocosmicus franklandus' was less sensitive to phenylhydrazine inhibition compared to *N. viennensis* (Figure 4-1A, C). The acidophilic AOA 'Ca. Nitrosotalea sinensis' was more sensitive than the other AOA tested and 5 μM phenylhydrazine inhibited NH₃-dependent NO₂⁻ production completely (Figure 4-1D).

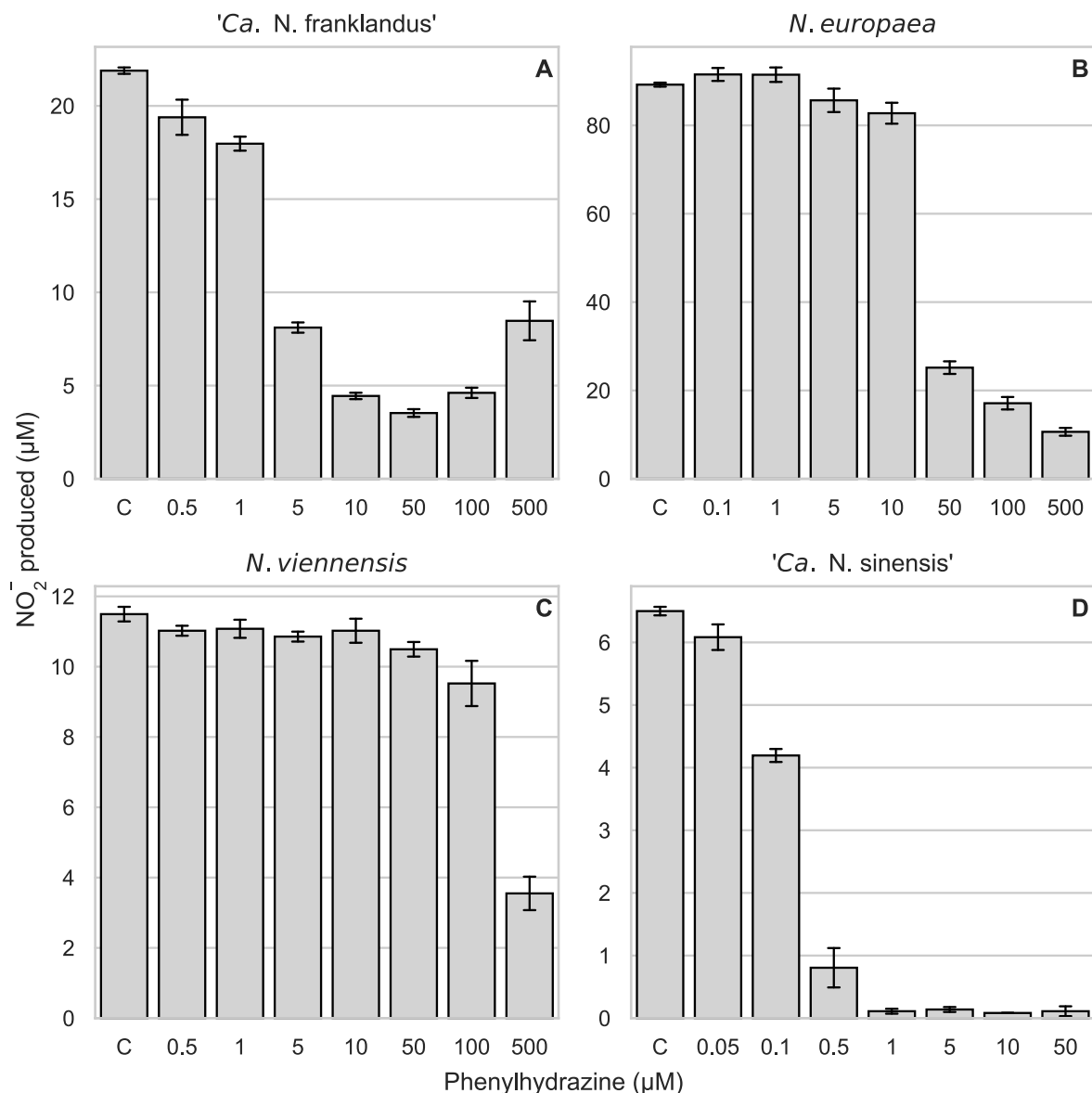


Figure 4-2 - NO₂⁻ production after 1 h incubation with different concentrations of phenylhydrazine using 100 μM NH₂OH as substrate for *N. europaea* and 'Ca. Nitrosotalea sinensis' and 200 μM for 'Ca. Nitrosocosmicus franklandus' and *N. viennensis*. NO₂⁻ was measured 1 h after addition of the substrate. Error bars represent standard deviation (n = 3).

The inhibitory range of phenylhydrazine was similar between NH_3 -dependent and hydroxylamine-dependent NO_2^- accumulation (Figure 4-1 and Figure 4-2), although the threshold for phenylhydrazine inhibition was higher when hydroxylamine was used as the substrate in *N. europaea* and *N. viennensis*. From these results, 100 μM phenylhydrazine was chosen to inhibit all strains in subsequent experiments, except for '*Ca. Nitrosotalea sinensis*', where 10 μM phenylhydrazine was used. The lowest concentrations that resulted in nearly full inhibition were chosen to minimise abiotic interactions and toxic effects (Misra & Fridovich, 1976). In addition, hydroxylamine is reactive, potentially toxic and may participate in abiotic reactions. To mitigate toxic effects and abiotic reactions, a suitable hydroxylamine concentration (200 μM for '*Ca. N. franklandus* and *N. viennensis*', 100 μM for *N. europaea* and '*Ca. N. sinensis*') was chosen by pre-screening a range of hydroxylamine concentrations.

4.2.2 The effect of hydrazine on NH_3 and hydroxylamine-dependent NO_2^- production

Hydrazine was tested to determine whether it inhibits NH_3 -dependent (Figure 4-3) and hydroxylamine-dependent (Figure 4-4) NO_2^- production. It was hypothesised that hydrazine would compete with hydroxylamine as a substrate due to its similar chemical properties (Sakamoto *et al.*, 2004).

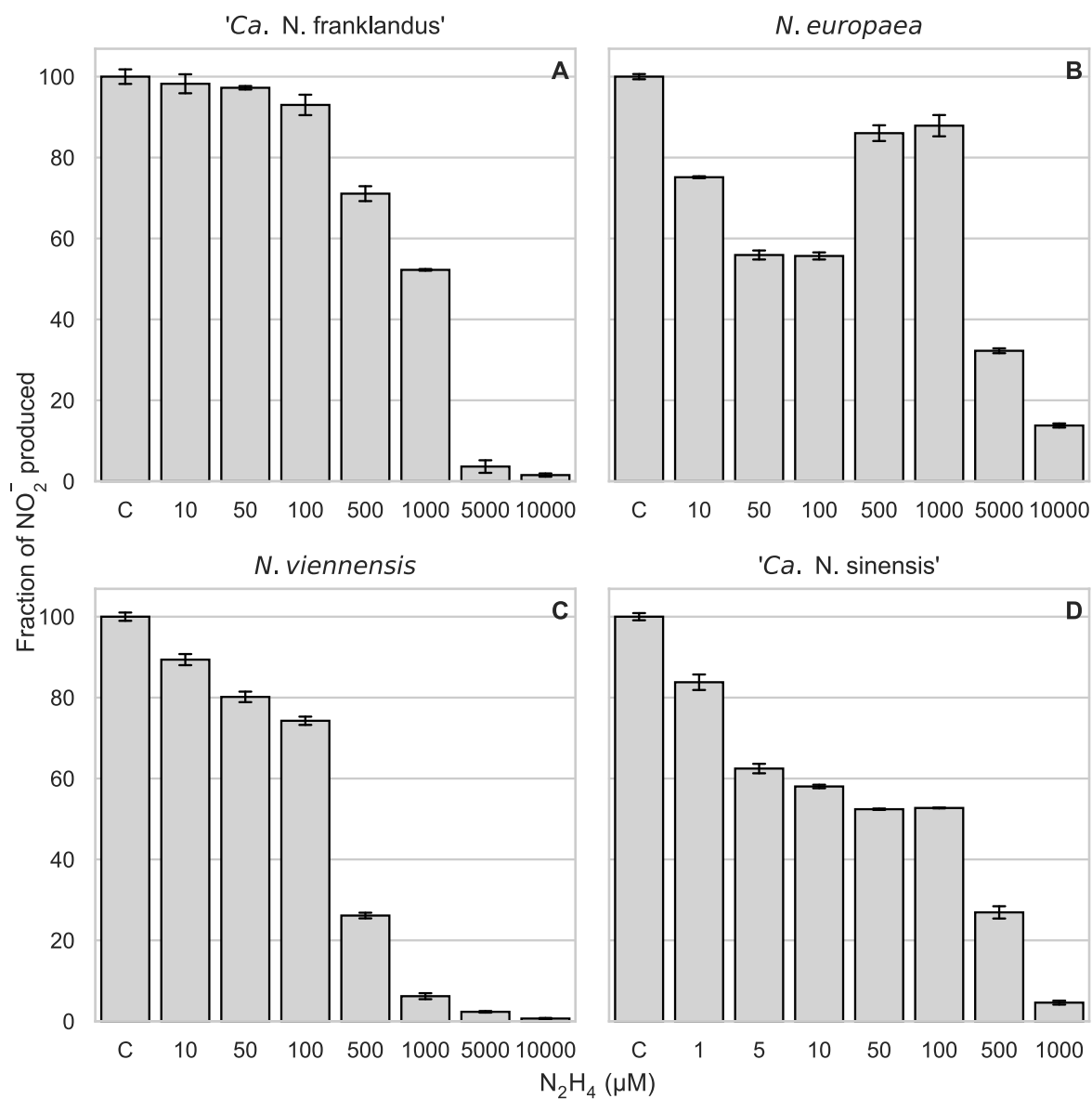


Figure 4-3 - Percentage NO_2^- production compared to the uninhibited control (C) after 1 h incubation with different concentrations of hydrazine using $100 \mu\text{M NH}_4^+$ as substrate. NO_2^- was measured 1 h after addition of the substrate. Nitrite accumulation in the uninhibited control treatment represents 100% activity, and the treatments with hydrazine are shown as the percentage of activity compared to this control. Error bars represent standard deviation (n = 3). 100% activity corresponded to $100 \mu\text{M}$, $59 \mu\text{M}$, $54 \mu\text{M}$ and $63 \mu\text{M}$ nitrite accumulated after one hour in '*Ca. N. franklandus*', *N. europaea*, *N. viennensis* and '*Ca. N. sinensis*', respectively.

Higher concentrations of hydrazine than phenylhydrazine were required to inhibit NO_2^- production in all ammonia oxidisers (Figure 4-3 and 4-4). In *N. europaea* (Figure 4-3B), hydrazine is known to be a competitive inhibitor of the HAO (Hooper & Nason, 1965) and increasing hydrazine concentrations inhibited the ammonia oxidation activity to a greater extent. Interestingly, 500 and 1,000 μM phenylhydrazine inhibited NO_2^- production less than lower concentrations in *N. europaea*.

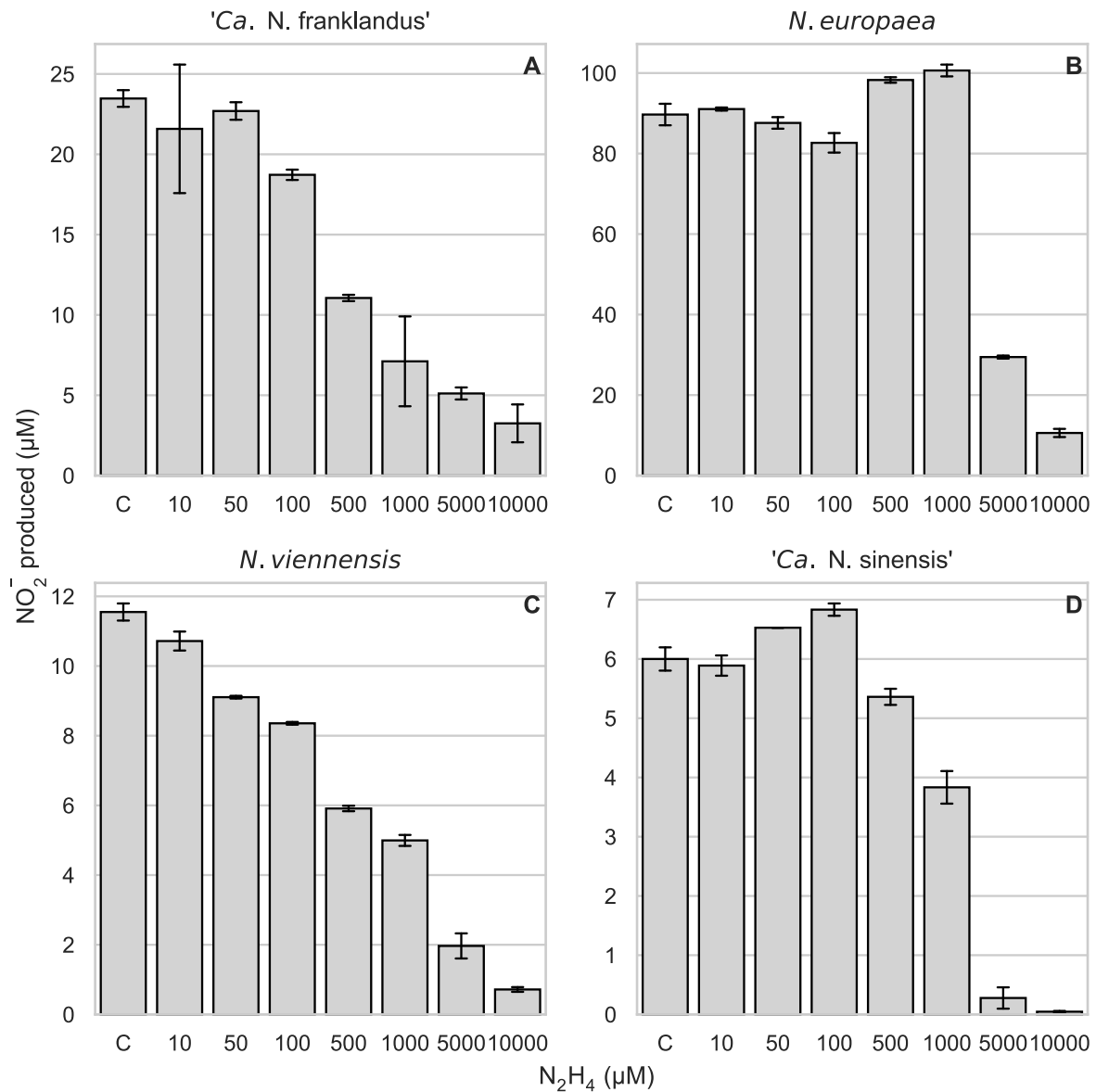


Figure 4-4 - NO_2^- production after 1 h incubation with different concentrations of N_2H_4 using 100 μM NH_2OH as substrate for *N. europaea* and 'Ca. Nitrosotalea sinensis' and 200 μM for 'Ca. Nitrosocosmicus franklandus' and *N. viennensis*. NO_2^- was measured 1 h after addition of the substrate. Error bars represent standard deviation (n = 3).

This profile was less pronounced, but also apparent when hydroxylamine was used as substrate (Figure 4-4B). The AOA tested also showed decreasing nitrite production with increasing hydrazine concentrations (Figure 4-4 A, C and D). When supplied with NH_3 as substrate, the sensitivity of *N. viennensis* and '*Ca. Nitrosotalea sinensis*' to 500 μM N_2H_4 was very similar, but in comparison '*Ca. Nitrosocosmicus franklandus*' was only inhibited slightly (Figure 4-3A, C, D). As with phenylhydrazine, '*Ca. Nitrosotalea sinensis*' was more sensitive to hydrazine than the other strains (Figure 4-3D). The highest concentrations tested, 5,000 μM and 10,000 μM N_2H_4 , strongly inhibited all the ammonia oxidiser strains tested and were likely toxic.

4.2.3 Recovery of NO_2^- production by '*Ca. Nitrosocosmicus franklandus*' following inhibition with phenylhydrazine or hydrazine

Having confirmed that phenylhydrazine and hydrazine inhibited both NH_3 oxidation and hydroxylamine oxidation in AOA and AOB, the inhibition was further characterised by testing whether phenylhydrazine and hydrazine act as reversible or irreversible inhibitors. '*Ca. Nitrosocosmicus franklandus*' was selected as the model AOA for recovery experiments with phenylhydrazine and hydrazine because of its relative ease of growth and high biomass production. Cells were treated with phenylhydrazine (100 μM) or hydrazine (1,000 μM or 10,000 μM) for 1 hour and the inhibitors were subsequently removed by washing. When an enzyme is inhibited with an irreversible inhibitor, *de novo* protein synthesis is required for restoration of enzyme activity, resulting in a lag in recovery as was seen after acetylene inhibition in '*Ca. Nitrosocosmicus franklandus*' (Wright *et al.*, 2020). With a reversible inhibitor, recovery is instantaneous as seen after 1-octyne inhibition in '*Ca. Nitrosocosmicus franklandus*' (Wright *et al.*, 2020) and two *Nitrososphaera* species (A. E. Taylor *et al.*, 2015).

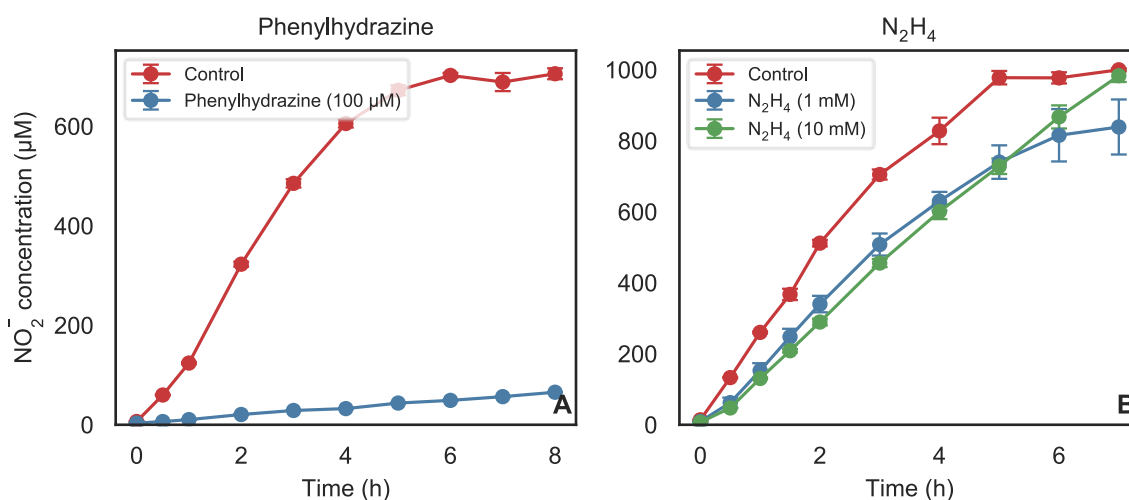


Figure 4-5 - Time course of the recovery of NO₂⁻ production from 1 mM NH₄⁺ in ‘*Ca. Nitrosocosmicus franklandus*’ after removal of 100 μM phenylhydrazine (A) or 1 mM and 10 mM N₂H₄ (B) by washing. Error bars represent the standard deviation (n = 3).

‘*Ca. Nitrosocosmicus franklandus*’ did not recover from inhibition by 100 μM phenylhydrazine (Figure 4-5A), indicating that phenylhydrazine is an irreversible inhibitor.

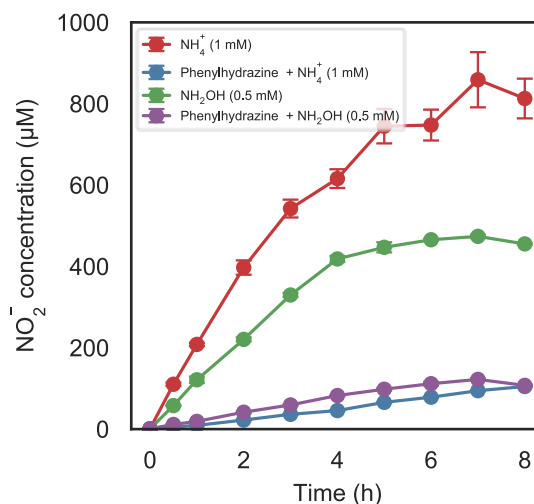


Figure 4-6 - Time course of the recovery of NO₂⁻ production in *N. europaea* with 1 mM NH₄⁺ or 0.5 mM NH₂OH as substrate after removal of 100 μM phenylhydrazine by washing. Error bars represent the standard deviation (n = 3).

Similarly, *N. europaea* showed no recovery when inhibited with 100 μM phenylhydrazine (Figure 4-6). In contrast, inhibition with 1,000 μM and even 10,000 μM N₂H₄ was readily reversible in ‘*Ca.*

Nitrosocosmicus franklandus' (Figure 4-5B). This also indicates that the inhibition was not due to toxic effects but more likely due to substrate competition.

4.2.4 Hydrazine-dependent O₂ consumption in 'Ca. Nitrosocosmicus franklandus'

Hydrazine is an alternative substrate for the HAO in AOB and competes with hydroxylamine for the active site (Hooper & Nason, 1965). To test if hydrazine is also a substrate for the equivalent enzyme in AOA, hydrazine-dependent O₂ uptake by "Ca. Nitrosocosmicus franklandus" cells was measured and compared to hydroxylamine-dependent O₂ uptake. Additionally, cells were preincubated with phenylhydrazine with the expectation that it would inhibit both hydrazine- and hydroxylamine-dependent O₂ uptake. *N. europaea* was used for comparison as similar experiments have previously been performed with this nitrifier (Logan & Hooper, 1995).

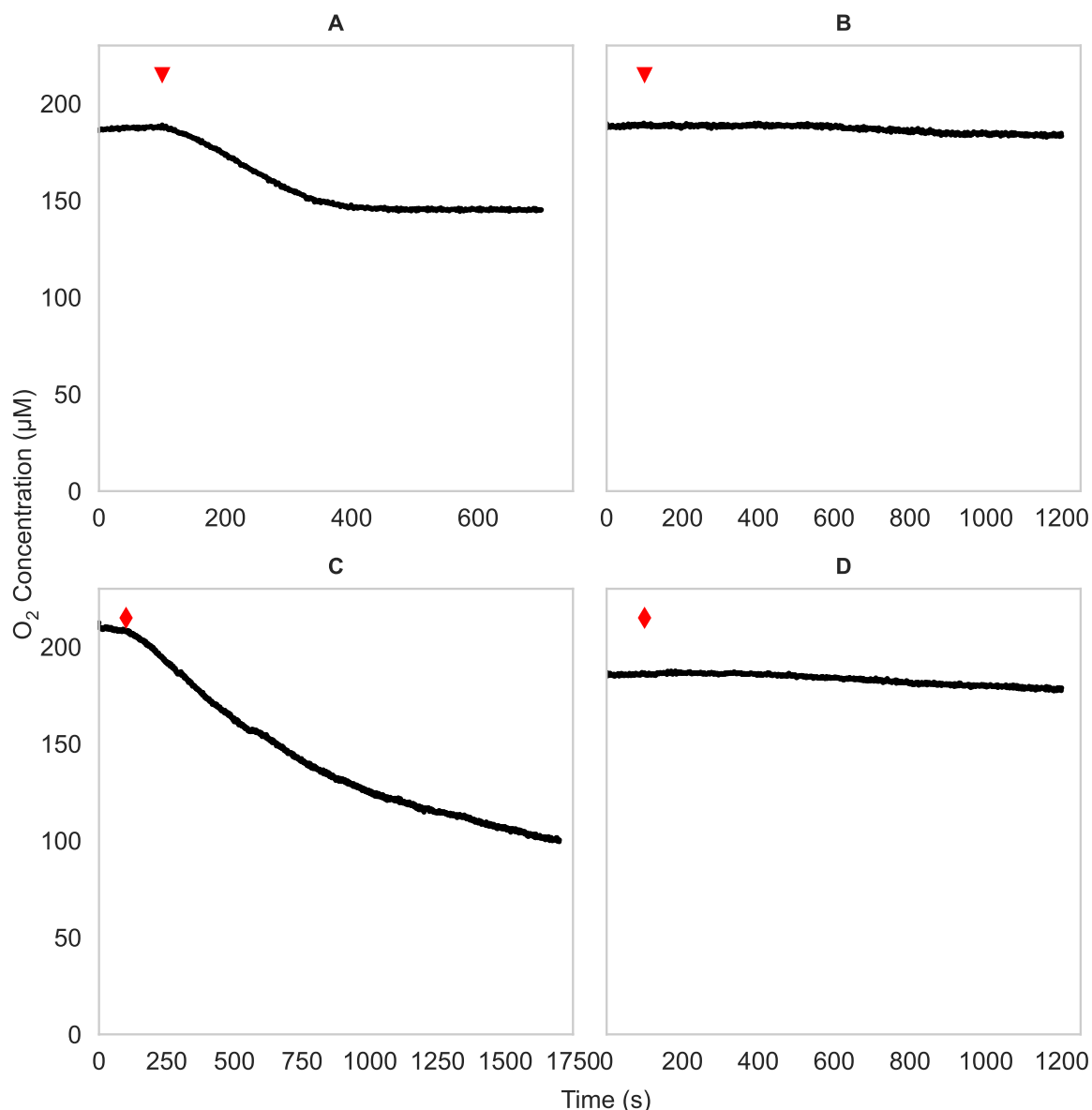


Figure 4-7 - Oxygen uptake measurements in cell suspensions of ‘*Ca. Nitrosocosmicus franklandus*’. Concentrations of 200 µM NH₂OH (A and B, red triangles) or 600 µM N₂H₄ (C and D, red diamonds) were added. Control cells (A and C) are compared to cells incubated with 100 µM phenylhydrazine (B and D). Experiments were performed at least three times with similar results.

First, hydroxylamine-induced O₂ uptake was investigated. For ‘*Ca. Nitrosocosmicus franklandus*’, the optimal concentration of hydroxylamine was 200 µM, since a higher concentration reduced the O₂ uptake rate, and the induced rate was not linear (Figure 4-8A). When cells were given 200 µM NH₂OH as substrate, ‘*Ca. Nitrosocosmicus franklandus*’ O₂ uptake ceased when 49 ± 4 µM O₂ had been consumed (Figure 4-7A). Subsequent spiking with 200 µM NH₂OH caused O₂ uptake to resume, and this could be repeated until all O₂ was consumed (Figure 4-8B), indicating that the cessation of O₂ uptake after a reduction of 49 ± 4 µM O₂ was due to the depletion of hydroxylamine. Consumption of 49 ± 4 µM O₂ coincided with the production of 23 ± 1 µM NO₂⁻, close to a 2:1 O₂ to NO₂⁻ stoichiometry

instead of a 1:1 stoichiometry reported previously for other AOA strains (Kozlowski, Stieglmeier, *et al.*, 2016; N. Vajrala *et al.*, 2013). This difference in stoichiometry could indicate a difference in pathways between the AOA and should be further investigated.

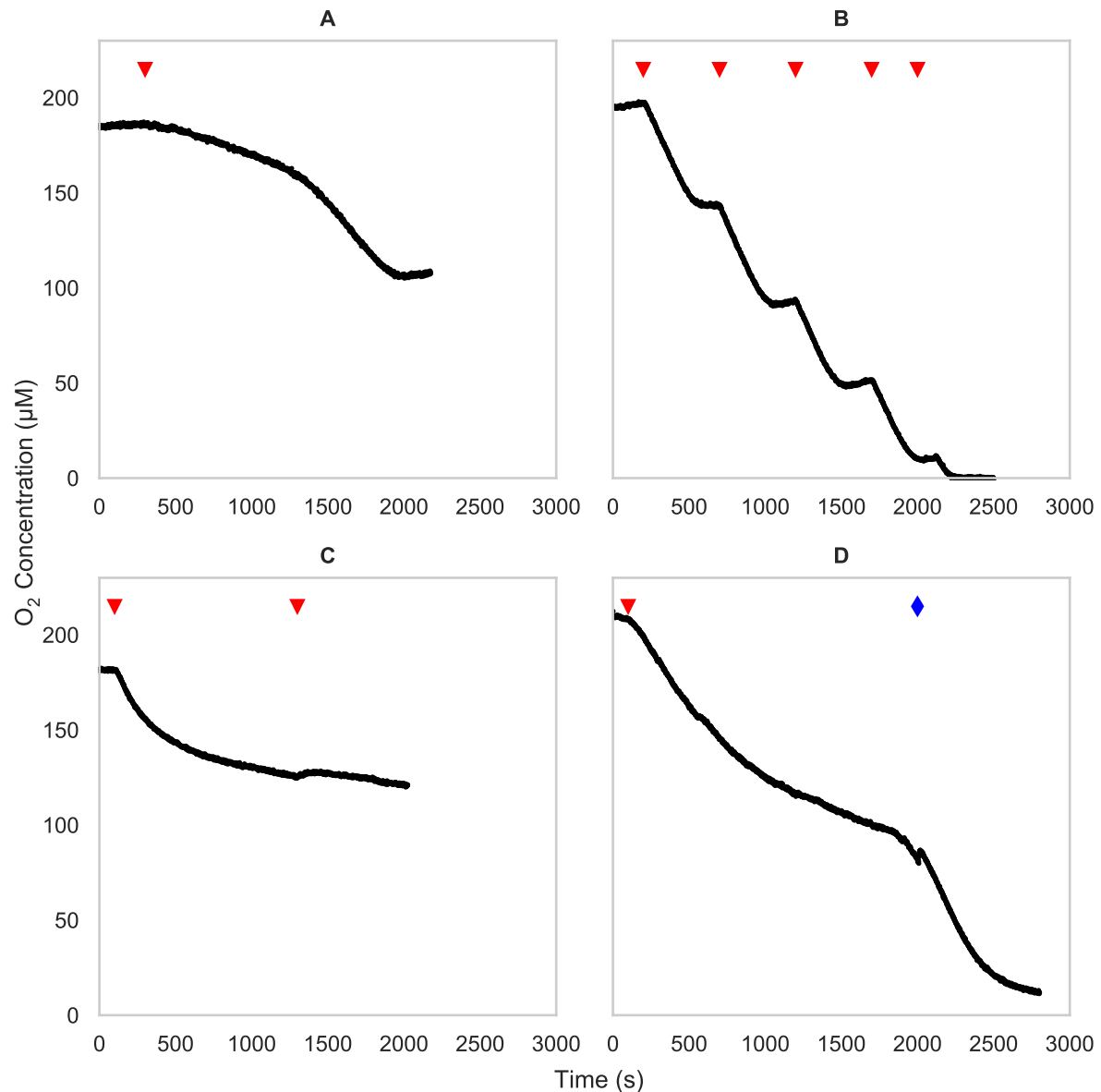


Figure 4-8 - Oxygen uptake measurements by cell suspensions of 'Ca. Nitrosocosmicus franklandus'. A: addition of 400 μM NH_2OH (red triangle); B: repeated spiking with 200 μM NH_2OH (red triangles) until anoxic; C: spiking with 600 μM N_2H_4 (red triangles); D: addition of 600 μM N_2H_4 (red triangle) followed by 500 μM NH_4^+ (blue diamond). Second, a concentration range of 200 – 1,000 μM N_2H_4 was tested to determine if higher concentrations were inhibitory like hydroxylamine (Figure 4-9). Only a slight increase in the initial rate was observed at concentrations over 600 μM , so for further experiments 'Ca. Nitrosocosmicus franklandus' cells were spiked with 600 μM N_2H_4 which was also chosen to allow comparison with *N. europaea*, where 600 μM N_2H_4 was saturating, and higher concentrations did not increase the O_2 uptake rates (Michael R. Hyman & Wood, 1984).

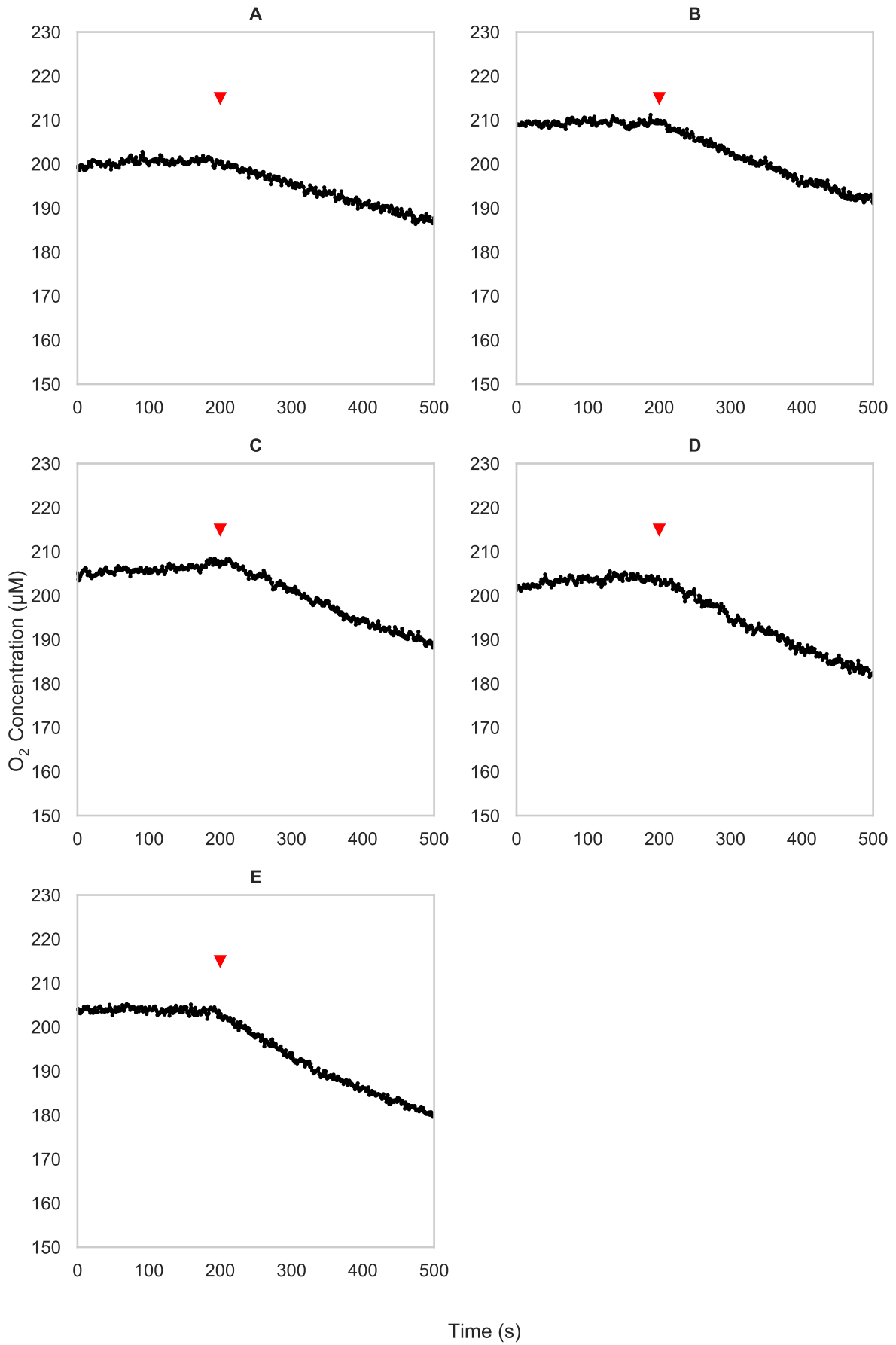


Figure 4-9 - Initial rates of oxygen consumption in cell suspensions of 'Ca. Nitrosocosmicus franklandus' after addition of different concentrations of N₂H₄ (red triangles). A: 200 μM N₂H₄; B: 400 μM N₂H₄; C: 600 μM; N₂H₄; D: 800 μM; N₂H₄; E: 1000 μM N₂H₄.

The initial rate of O₂ uptake in the presence of 600 μM N₂H₄ in 'Ca. Nitrosocosmicus franklandus' was $9.51 \pm 0.69 \mu\text{M O}_2 \text{ min}^{-1}$, similar to the initial rate of hydroxylamine-dependent O₂ uptake with 200 μM NH₂OH ($10.54 \pm 0.21 \mu\text{M O}_2 \text{ min}^{-1}$). Notably, the hydrazine-induced rate was not linear and started to decrease after 10 min, reaching a steady rate of $1.15 \mu\text{M O}_2 \text{ min}^{-1}$ after 20 min, close to the abiotic rate (Figure 4-7C). In contrast to hydroxylamine, spiking with more hydrazine did not restore the initial rate (Figure 4-8C), although addition of NH₄⁺ did cause oxygen consumption to resume (Figure 4-8D). As anticipated, preincubating cells with 100 μM phenylhydrazine inhibited O₂ consumption coupled to both hydroxylamine and hydrazine in 'Ca. Nitrosocosmicus franklandus' (Figure 4-7B, D, respectively), suggesting that the same enzyme oxidises both substrates, as it does in *N. europaea* (Maalcke *et al.*, 2014)(Figure 4-10B, D), or that different enzymes are similarly affected. In contrast with AMO-specific inhibitors (e.g. acetylene), phenylhydrazine did inhibit hydroxylamine oxidation activity (Wright *et al.*, 2020).

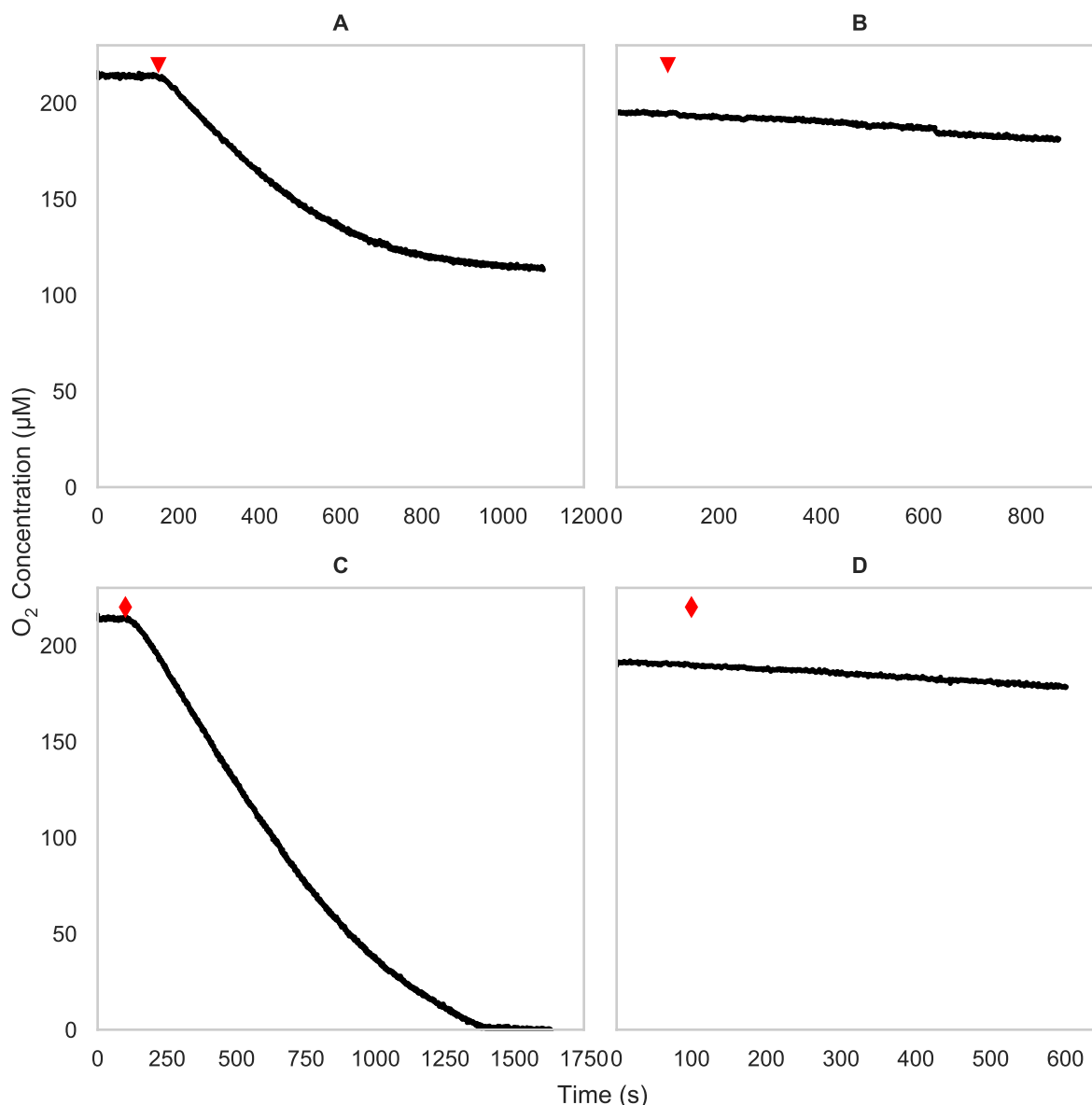


Figure 4-10 - Oxygen uptake measurements by cell suspensions of *N. europaea*. Concentrations of 100 µM NH₂OH (A and B, red triangles) or 600 µM N₂H₄ (C and D, red diamonds) were added. Control cells (A and C) are compared to cells incubated with 100 µM phenylhydrazine (B and D). Experiments were performed at least three times with similar results.

4.2.5 ATP production in response to hydrazine and phenylhydrazine

To investigate whether the oxidation of hydrazines is coupled to energy conservation, ATP levels were determined in '*Ca. Nitrosocosmicus franklandus*' and *N. europaea*, incubated with known substrates (NH₃ or hydroxylamine) or with hydrazine or phenylhydrazine (Figure 4-11). We hypothesised that both hydroxylamine and hydrazine would yield more ATP than ammonia. The oxidation of ammonia by AMO consumes two electrons and these electrons are normally produced from the downstream pathway of hydroxylamine oxidation. Therefore, it is expected that the net yield of electrons and ATP would be higher with hydroxylamine and hydrazine as substrates. Higher ATP yield from hydroxylamine compared to ammonia in the marine AOA *N. maritimus* supports this notion (N. Vajrala

et al., 2013). Comparisons were made between cells preincubated with or without 100 μM phenylhydrazine for 1 h. All treatments were also performed using heat-killed cells as abiotic controls, which showed no variation in ATP concentration (data not shown).

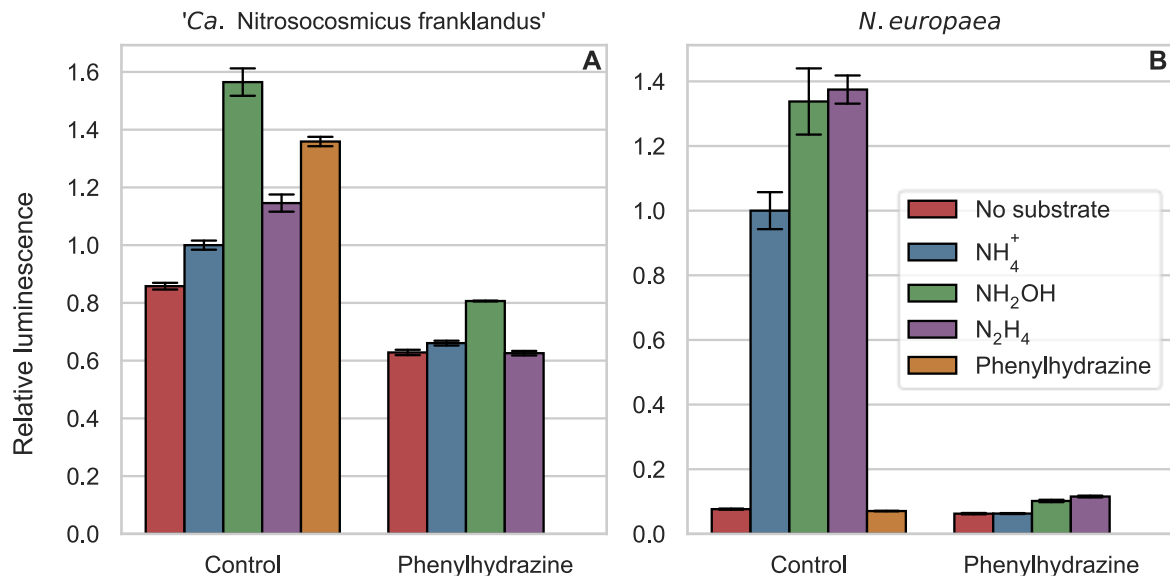


Figure 4-11 - Relative ATP-dependent luminescence, with NH_4^+ controls normalised to 1. All treatments were added in 100 μM concentrations and the cells were incubated for 10 min before ATP was measured. Bars on the left and right of each panel show cells pre-incubated without or with phenylhydrazine, respectively. Error bars represent the standard deviation (n = 3).

In *'Ca. Nitrosocosmicus franklandus'*, without preincubation with phenylhydrazine, hydroxylamine yielded more ATP than NH_3 (Figure 4-11A) as was previously reported for the marine AOA *N. maritimus* (N. Vajjala *et al.*, 2013). Moreover, the addition of hydrazine generated ATP in *'Ca. Nitrosocosmicus franklandus'*, confirming that hydrazine was not only oxidised but also produced energy in this AOA. The ATP concentration from hydrazine was greater than that from NH_3 , but lower than from hydroxylamine. Unexpectedly, short-term incubations with phenylhydrazine caused an increase in ATP in *'Ca. Nitrosocosmicus franklandus'* (Figure 4-11A), whereas preincubation for one hour with phenylhydrazine depleted ATP to even lower levels than in cells incubated with no substrate, suggesting that ATP, initially generated, was subsequently consumed and that these cells had an even greater requirement for ATP than control cells. In *N. europaea*, the amount of ATP production in response to hydroxylamine and hydrazine was very similar (Figure 4-11B). In contrast to *'Ca. Nitrosocosmicus franklandus'*, *N. europaea* produced no ATP in response to phenylhydrazine and ATP values were comparable to the starved cells.

4.2.6 N₂ is a product of hydrazine oxidation in '*Ca. Nitrosocosmicus franklandus*'

To test if N₂ is a product of hydrazine oxidation in the AOA as it is in the AOB (Maalcke *et al.*, 2014), ¹⁵N-labelled hydrazine was added to cell suspensions of '*Ca. Nitrosocosmicus franklandus*' and *N. europaea*.

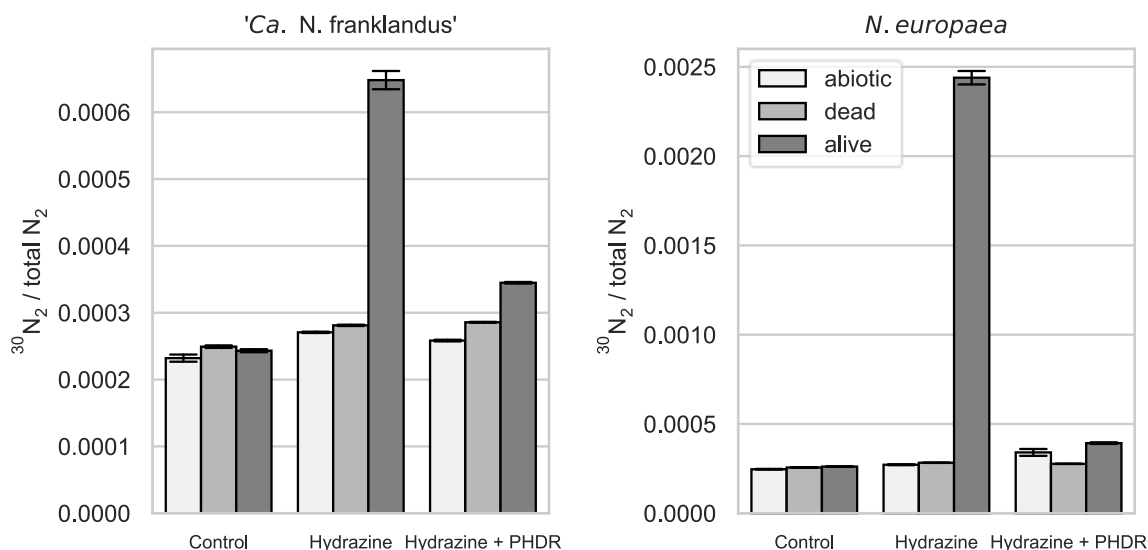


Figure 4-12 - ³⁰N₂/total N₂ ratio after 1 h incubation of cell suspensions of '*Ca. Nitrosocosmicus franklandus*' (A) and *N. europaea* (B) with 500 μM ¹⁵N-N₂H₄. Abiotic and dead cells were included as controls. Error bars represent the standard (n = 3).

As expected, ²⁹N₂/²⁸N₂ ratios of the abiotic, killed control and live cell incubations did not differ from the natural abundance in the atmosphere. In contrast, there was a clear enrichment of ³⁰N₂ with both '*Ca. N. franklandus* C13' (Figure 4-12A) and *N. europaea* (Figure 4-12B), indicating that both organisms produced ³⁰N₂ when ¹⁵N-hydrazine was added. Additionally, the production of ³⁰N₂ from ¹⁵N-hydrazine was inhibited when 100 μM phenylhydrazine was included in the incubations. From the total 1 500 nanomoles of ¹⁵N-hydrazine added, 129 (±2) and 1 049 (± 23) nanomoles of ³⁰N₂ were produced by '*Ca. Nitrosocosmicus franklandus*' and *N. europaea*, respectively, during the one-hour incubation. This is equal to ~8.8 % and 71.4 % of the total added ¹⁵N-hydrazine being oxidised to ³⁰N₂ by '*Ca. Nitrosocosmicus franklandus*' and *N. europaea*, respectively. This is consistent with the oxygen electrode data shown above (Figure 4-7A, C) and suggests that *N. europaea* was able to consume most of the ¹⁵N-hydrazine during the experiment, whereas '*Ca. Nitrosocosmicus franklandus*' was only able to oxidise hydrazine transiently. It is likely that 71.4%, rather than 100% of the hydrazine was recovered as N₂ in *N. europaea*, due to abiotic degradation of hydrazine.

4.3 Discussion

4.3.1 Hydrazines as inhibitors of AOA

While the enzyme that catalyses hydroxylamine oxidation in AOA has not been identified, hydrazine and phenylhydrazine seem to have similar effects on NH_3 and hydroxylamine oxidation by AOA and AOB. Phenylhydrazine and hydrazine inhibited hydroxylamine and NH_3 oxidation in AOA as they do in the AOB, *N. europaea*. The variability in inhibition thresholds between different AOA and AOB strains clearly demonstrates the value of using more than one model microorganism, preferably from different clades when evaluating inhibitors, as has been described with AOB (Kaur-Bhambra et al., 2022). A recent study revealed a similar pattern in the affinity for ammonia as was found for the sensitivity to hydrazines in this study (Jung et al., 2021), indicating that these different sensitivities may reflect the niche in the environment with the organisms with higher ammonia affinities being more sensitive to inhibition by hydrazines.

The inhibition of ammonia oxidation by hydrazine has been extensively studied in AOB, and more specifically *N. europaea* (Anderson, 1964; Kane & Williamson, 1983; YOSHIDA & ALEXANDER, 1964). Hydrazine is a reversible competitive inhibitor of the HAO enzyme (Hooper & Nason, 1965) which explains the inhibition of NO_2^- production by *N. europaea* at higher concentrations (Figure 4-4B). However, the inhibition pattern where 500 – 1 000 μM hydrazine inhibited NO_2^- production in *N. europaea* less than hydrazine concentrations below 500 μM is difficult to explain and is probably caused by an interplay of hydrazine-driven NO_2^- reduction (Remde & Conrad, 1990), abundance of reductant (Michael R. Hyman & Wood, 1984) and interactions of the HAO and cytochrome P_{460} with hydrazine (Erickson & Hooper, 1972).

In AOA, hydrazine interfered with NO_2^- production from both NH_3 and hydroxylamine, likely due to competition with hydroxylamine for the substrate binding site. It was not possible to unequivocally demonstrate competitive inhibition as hydroxylamine concentrations higher than 200 μM reduced the hydroxylamine oxidation rate (Figure 4-8A). The inhibition with hydrazine in AOA was readily reversible in a manner similar to AOB.

Organohydrazines were characterised in *N. europaea* as irreversible suicide substrates of the HAO enzyme using purified protein (Logan & Hooper, 1995). They have been successfully used to inhibit both archaeal and bacterial nitrification in soil microcosms (Wu et al., 2012; Yang et al., 2017) and here we provide insight into the archaeal inhibition mechanism. Phenylhydrazine would likely have a short-lived inhibitory effect on nitrification due to its role as an irreversible inhibitor of AOA and AOB. However, the use of phenylhydrazine as a HAO-specific nitrification inhibitor for long-term experiments (>24h) should be cautioned as it is sensitive to light and unstable in aqueous solutions

(Misra & Fridovich, 1976). Nevertheless, it is interesting to consider that hydrazine and its derivatives could potentially enter soil environments either through anthropogenic routes or, to a much lesser extent, via biological production by diazotrophs and some fungi. Whilst the potential for environmental applications and impacts of hydrazines are unknown, at least in theory, it may be possible that AOA could oxidise hydrazine and gain ATP from this reaction.

While it was not possible to use pure enzyme from AOA, phenylhydrazine was identified as an inhibitor of hydroxylamine oxidation in the three tested AOA strains. The inhibition specific to hydroxylamine/hydrazine oxidation was verified and characterised in '*Ca. Nitrosocosmicus franklandus*' using several approaches including NO_2^- accumulation assays, oxygen consumption and ATP assays. As in the AOB, the inhibition by phenylhydrazine in '*Ca. Nitrosocosmicus franklandus*' was irreversible, and the cells did not recover even after several hours (Logan & Hooper, 1995; Wright *et al.*, 2020). Consistent with these approaches, the production of ^{15}N -labelled N_2 was also inhibited by phenylhydrazine. One caveat is that it was impossible to verify that phenylhydrazine inhibits the hydroxylamine oxidation enzyme directly and it could also be affecting downstream enzymes.

4.3.2 Hydrazine as a substrate in AOA

Oxygen consumption in response to hydrazine confirmed that hydrazine was used as a substrate. However, hydrazine-induced oxygen uptake decreased over time (Figure 4-7C), indicating that an unknown mechanism limits the oxidation of hydrazine. The product of hydrazine oxidation is likely N_2 , as it is in AOB (Maalcke *et al.*, 2014), making product inhibition unlikely. The incubations with ^{15}N -labelled hydrazine confirmed that N_2 is a product of hydrazine oxidation in the AOA but it is possible there are other products such as NO or N_2O . In future work, these compounds should be measured as well. In addition, while challenging, NH_2OH could be measured in more assays to complete the nitrogen balance and get a more complete overview.

ATP was produced after hydrazine addition in AOA and future studies should investigate the use of hydrazine in growth experiments and as a source of reductant in physiological experiments. In both *N. europaea* and '*Ca. Nitrosocosmicus franklandus*', hydroxylamine and hydrazine produced higher ATP concentrations than NH_3 , which was expected. However, in *N. europaea* the amount of ATP produced from both substrates was similar while in '*Ca. Nitrosocosmicus franklandus*' it was vastly different. This could be due to differences in the NH_3 oxidation pathways in AOA and AOB, or differences in the rates of oxidation, as hydrazine had a lower initial oxidation rate in the AOA and the rate decreased over time (Figure 4-7C). Interestingly, ATP values increased in '*Ca. Nitrosocosmicus franklandus*' after short-term incubations with phenylhydrazine, which was not observed in the AOB. A possible explanation is that phenylhydrazine can serve as a substrate, but its product, or

phenylhydrazine itself, becomes toxic. Hemoproteins such as the HAO of AOB are thought to be inhibited by organohydrazine derivatives by the formation of a cation radical (Logan & Hooper, 1995). It is likely that a similar radical is formed in the AOA.

4.4 Outlook for applications of hydrazines in ammonia oxidation research

The fact that the hydrazine inhibitors affect AOA and AOB could aid in the development of the next generation of nitrification inhibitors. The availability of crystal structures for the bacterial HAO provide an advantage in the development of new nitrification inhibitors, compared to the AMO for which no structures are available (Cedervall *et al.*, 2013; Nishigaya *et al.*, 2016). It is important however, not to overlook other nitrifiers such as AOA and comammox in these studies, but to investigate further potential inhibitors which target all ammonia oxidisers.

While it is known that organohydrazines inhibit a broad range of enzymes with both oxidative (Binda *et al.*, 2008; Logan & Hooper, 1995) and electrophilic (Datta *et al.*, 2003) cofactors via a covalent mechanism, it is interesting that they inhibit hydroxylamine oxidation in AOA, which are thought not to have the same heme cofactor as AOB. The inhibition of the archaeal hydroxylamine oxidation mechanism by organohydrazines could be used to finally identify this long sought-after enzyme either by using ¹⁴C phenylhydrazine (Logan & Hooper, 1995) or by using hydrazine probes as activity-based protein profiling probes (Bennett *et al.*, 2016; Matthews *et al.*, 2017).

In conclusion, this study provides evidence that hydrazine can be oxidised by AOA and that N₂ is a product of its oxidation. Phenylhydrazine was shown to be an inhibitor of archaeal hydroxylamine oxidation. The inhibition by hydrazines was tested in several environmentally relevant strains of terrestrial AOA and further characterisation was done in '*Ca. Nitrosocosmicus franklandus*'. We demonstrate that 1. Hydrazine and phenylhydrazine inhibit archaeal NH₃ and hydroxylamine oxidation at concentrations comparable to AOB and 2. Hydrazine acts as a reversible inhibitor and phenylhydrazine as an irreversible inhibitor in both AOA and AOB. Further, we demonstrate that 3. Hydrazine is oxidised by AOA and this reaction yields ATP and 4. N₂ is produced from hydrazine oxidation by AOA, as is the case in AOB and anammox. Despite the profound differences in the enzymology of archaeal and bacterial NH₃ oxidation pathways, this study demonstrates that hydrazine metabolism in AOB and AOA is surprisingly similar: Both AOA and AOB were inhibited by hydrazines in a similar manner and with similar thresholds, and both groups of ammonia oxidisers were able to generate ATP by oxidising hydrazine to N₂. Future studies should focus on identifying the enzymes affected by phenylhydrazine and the use of hydrazine in growth experiments and as a source of reductant.

5 Identification of novel enzymes in the archaeal ammonia oxidation pathway using activity-based protein profiling (ABPP)

5.1 Introduction

Activity-based protein profiling (ABPP) makes use of chemical probes to profile enzymatic activities of related enzymes within a complex environment. The probes are typically small molecules that covalently modify active enzymes through reaction with a 'warhead' group which is specifically designed for the target enzyme. Probes contain a linker group, which can be used to control specificity and to link the warhead to a tag, which is used for identification or purification (Berger *et al.*, 2004) (Figure 5-2).

The AMO enzyme of archaeal and bacterial ammonia oxidisers has been shown to interact with a broad range of molecules (Wright *et al.*, 2020, and references therein). These substrate analogues could be used to design suitable ABPP probes for e.g. visualising the AMO using a fluorescent tag or performing a pull-down of the AMO protein complex and its interacting partners using an affinity tag. Of particular interest are the terminal alkynes which bind irreversibly with the AMO, by forming a ketene intermediate (Gilch, Vogel, *et al.*, 2009). In *Nitrosomonas europaea*, the exact amino acid where acetylene binds is known (His-191 on subunit A of the ammonia monooxygenase), however, this residue is not present in the archaeal AMO. Linear alkynes have been used to investigate the substrate range of the AMO in different AOA and AOB (M R Hyman *et al.*, 1988; Wright *et al.*, 2020). Linear alkynes inhibit the archaeal and bacterial AMO. The archaeal AMO is inhibited by short-chain-length alkynes (<C₅), whereas the bacterial AMO has a broader range for alkynes and is inhibited by alkynes of up to C₈ (Anne E. Taylor *et al.*, 2013; Wright *et al.*, 2020). This has led to the use of 1-octyne to differentiate between AOA and AOB activity in the environment due to the lower sensitivity of AOA to this compound (Giguere *et al.*, 2017; Hink *et al.*, 2017; Lu *et al.*, 2015; Anne E. Taylor *et al.*, 2017, 2013)

Click (Copper(I)-catalyzed alkyne-azide cycloaddition (CuAAC)) reactions are used to bind an alkyne and an azide molecule together efficiently with few by-products (Liang & Astruc, 2011). A diyne probe can be used as a bifunctional probe where one ethynyl group reacts with the monooxygenase and the other ethynyl group is then used in the CuAAC reaction to click a tag to the probe. 1,7-octadiyne (17OD; Figure 5-1A), a linear alkadiyne with a triple bond on each side, has been used as an ABPP probe in combination with "click" reactions to fluorescently label the AMO of *Nitrosomonas europaea* (Bennett *et al.*, 2016). In addition, 17OD was used in *N. europaea* for a pull-down assay which successfully detected the AMO and several proteins which interact with the AMO, including the HAO (Bennett *et al.*, 2016). Recently, 17OD was used to fluorescently label whole cells of ammonia- and

alkane-oxidizing bacteria by binding to their monooxygenases (Sakoula *et al.*, 2021). However, labelling of AOA using 17OD was not successful, which is consistent with the higher threshold of inhibition by longer chain alkynes in AOA and a more limited substrate range of AOA compared to AOB (Wright *et al.*, 2020). It was hypothesised that a smaller chain linear diyne may be able to bind the archaeal AMO, however, diynes smaller than 1,5-hexadiyne (15HD; Figure 5-1B) are extremely reactive and difficult to synthesise (Sakoula *et al.*, 2021). Although 1-hexyne showed very little inhibition in AOA (Wright *et al.*, 2020), it is possible that its respective diyne does inhibit the AOA and it is worth investigating 15HD as an ABPP probe. Labelling the archaeal AMO has the potential to provide important insights into interaction of substrate analogues with the AMO enzyme and localisation of the AMO enzyme in the archaeal cell. Furthermore, a pulldown of the archaeal AMO may reveal several interacting proteins, including the unknown hydroxylamine oxidising enzyme, as was reported in *N. europaea* (Bennett *et al.*, 2016).

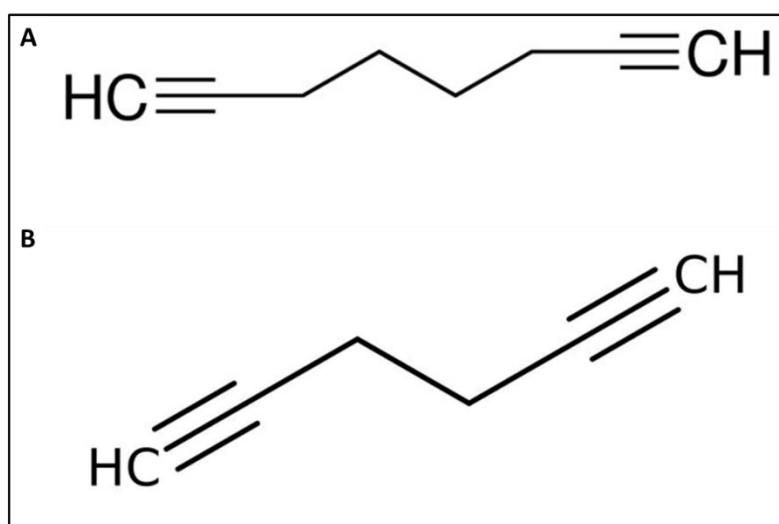
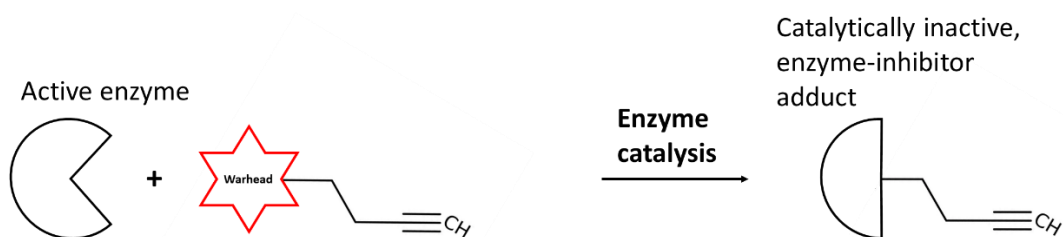


Figure 5-1 – Chemical structures of 1,7-octadiyne (A) and 1,5-hexadiyne (B).

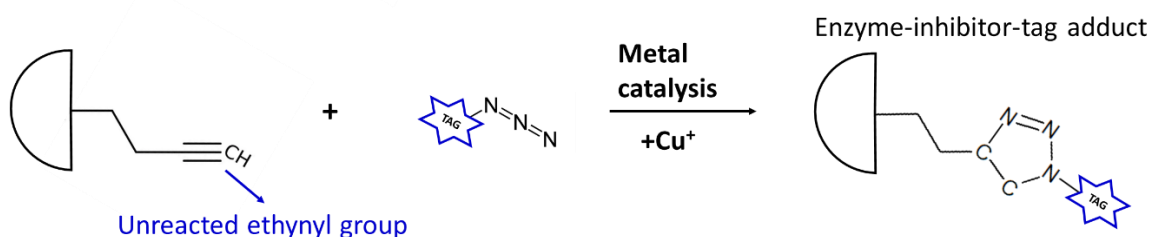
In the previous chapter, hydrazines were shown to inhibit archaeal hydroxylamine oxidation. It was hypothesised that hydrazines would be suitable ABPP probes using the hydrazine group as a warhead. A hydrazine-ABPP probe could provide insights into the inhibition mechanism of hydrazines and could lead to the identification of the elusive archaeal hydroxylamine oxidation enzyme. Moreover, it could also be used to label the bacterial hydroxylamine dehydrogenase (HAO) enzyme if successful.

In this chapter, several ABPP probes were evaluated for labelling archaeal enzymes. (I) 1,5-hexadiyne was used to label the AMO and (II) hydrazine probes were used to label candidate hydroxylamine oxidation enzymes.

a) Mechanism based enzyme inhibition



b) Copper-catalysed azide-alkyne cycloaddition (CuAAC) reaction



c) Downstream applications

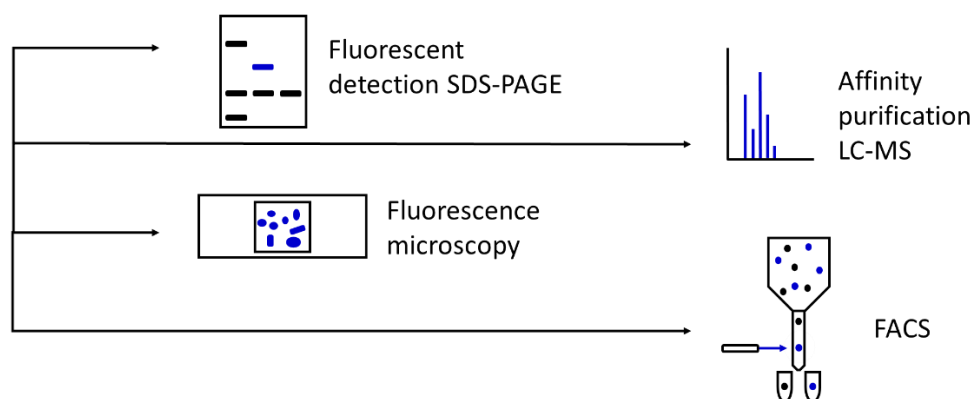


Figure 5-2 – ABPP schematic for enzyme labelling using bifunctional inhibitor-alkyne probes. (a) A warhead group forms a covalent bond through a mechanism-based reaction with the enzyme resulting in a catalytically inactive enzyme-inhibitor adduct. (b) CuAAC reaction clicking the unreacted ethynyl group to an azide-tag. (c) Downstream applications using the tag to visualise, purify or identify the labelled proteins.

5.2 Results

The data below, showing the inhibition and specificity of the 15HD probe on *Nitrosocosmicus franklandus*, contributed to a study by Sakoula and colleagues showing the potential of 15HD in the labelling of monooxygenases in bacteria and archaea. This study will be published in the future. Fluorescence pictures were taken by Dimitra Sakoula. In addition, the data reporting the recovery of 'Ca. N. franklandus' from inhibition by acetylene and the effects of cycloheximide were published in the journal Applied and Environmental Microbiology (Wright *et al.*, (2020)).

5.2.1 Inhibition of ammonia oxidation in the archaeon '*Ca. N. franklandus*' by 1,5-Hexadiyne (15HD)

To investigate whether 15HD will bind to the ammonia monooxygenase (AMO) enzyme, the inhibition of this enzyme was tested in the model organism *Nitrosocosmicus franklandus*. Previous work has shown that 100 μM octyne was sufficient to inhibit the AMO completely in two *Nitrososphaera* species (A. E. Taylor *et al.*, 2015) and this concentration was therefore chosen for 15HD inhibition experiments. Pentane was included as a control because the commercially available 15HD is only available in a 1:1 (v/v) solution with pentane. Nitrite was used as a proxy for ammonia oxidation to measure the inhibition and ammonia consumption was also measured using the colorimetric ammonia assay. Full methods have been described in Chapter 2.

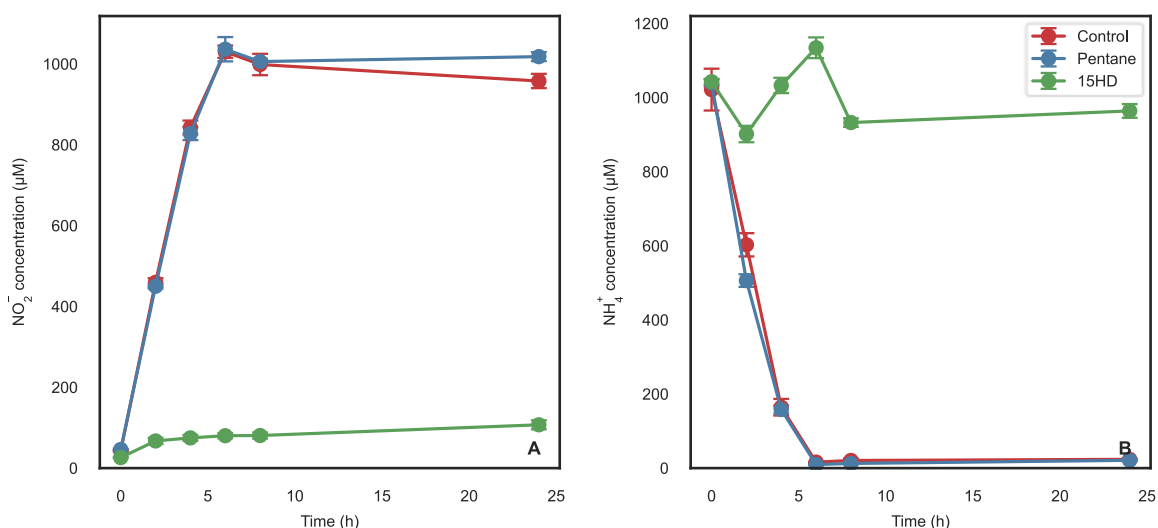


Figure 5-3 – Time course of the inhibition of NO₂⁻ production (A) and NH₃ consumption (B) from 1 mM NH₄⁺ in '*Ca. Nitrosocosmicus franklandus*' after addition of 100 μM 15HD and 100 μM pentane. Cell concentrations were 7.55×10^7 cells mL⁻¹. Error bars represent the standard deviation of biological triplicates (n = 3).

Mid-exponential cultures of '*Ca. N. franklandus*' were harvested, concentrated, and washed before testing the inhibition by 15HD in a short-term activity assay. Nitrite production was completely inhibited by 100 μM 15HD (Figure 5-3). The ammonia consumption corresponded to the inhibition of nitrite production and the stoichiometry was 1:1 as expected. Pentane had no effect on the ammonia oxidation activity of '*Ca. N. franklandus*' compared to the uninhibited control. All ammonia (1 mM) was consumed within 6 h in both uninhibited control treatment and the pentane control treatment.

5.2.2 15HD inhibition is AMO-specific

To ensure that the inhibition by 15HD was due to specific interaction with the AMO enzyme and not a general toxicity or inhibition of a downstream enzymes, the oxidation of hydroxylamine was assayed. If the inhibition is specific to the AMO, hydroxylamine oxidation should not be inhibited. Hydroxylamine was used as a substrate in short-term activity assays to investigate the inhibition by 15HD and both nitrite production and hydroxylamine consumption were assayed.

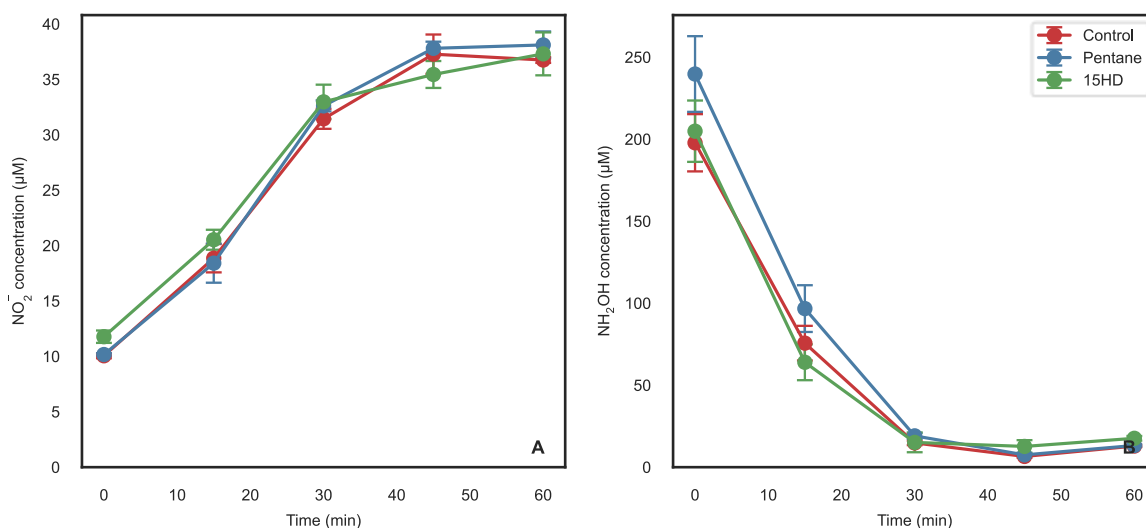


Figure 5-4 – Time course of the inhibition of NO₂⁻ production (A) and NH₂OH consumption (B) from 200 μM NH₂OH in ‘*Ca. Nitrosocosmicus franklandus*’ after addition of 100 μM 15HD and 100 μM pentane. Error bars represent the standard deviation (n = 3).

As discussed in Chapter 4, hydroxylamine conversion to nitrite is not stoichiometric and only about 25 μM nitrite is produced for every 200 μM hydroxylamine consumed. The stoichiometry observed in this experiment was consistent with the previous findings. The 15HD had no effect on hydroxylamine oxidation (Figure 5-4B) by ‘*Ca. N. franklandus*’ and all hydroxylamine was consumed, resulting in 25 μM nitrite (Figure 5-4A). This indicates that the inhibition by 15HD is indeed AMO-specific in ‘*Ca. N. franklandus*’, and 15HD does not interfere with the downstream ammonia oxidation pathway.

5.2.3 15HD inhibition is irreversible

To be suitable as a ABPP probe, 15HD should bind covalently to the enzyme of interest, the AMO. Irreversible (as opposed to reversible) inhibition of enzyme activity is a good indication that the inhibitor binds covalently. The following experiments were designed to test the recovery of ‘*Ca. N. franklandus*’ from inhibition and to determine whether inhibition was reversible or irreversible. Acetylene was included in these experiments as it has been previously shown to be an irreversible inhibitor of the AMO in both AOB and AOA.

If the inhibition is irreversible, the cells will need to synthesise new protein *de novo* and this will result in a delay in the recovery. Usually, when evaluating reversibility, a translational inhibitor is included as a negative control. This way, when protein synthesis is needed to recover it will not be able to recover when the inhibitor is included. No such inhibitor was available for *Nitrosocosmicus franklandus*. To this end, cycloheximide (CHX) was tested as a translation inhibitor. This fungicide has been shown to inhibit translation in the AOA *Nitrosopumilus maritimus* (Neeraja Vajrala *et al.*, 2014) but in the soil AOA *Nitrososphaera viennensis*, the same concentration ($200 \mu\text{g mL}^{-1}$) only slowed the recovery (A. E. Taylor *et al.*, 2015). To test whether CHX is suitable for recovery assays in '*Ca. N. franklandus*' and to investigate the mode of inhibition by 15HD, mid-exponential '*Ca. N. franklandus*' cells were harvested, washed, and incubated for 1 h in the presence of 15HD. Inhibitor was removed by multiple rounds of washing in FWM, and cells were re-suspended in fresh medium in the presence of $200 \mu\text{g mL}^{-1}$ CHX.

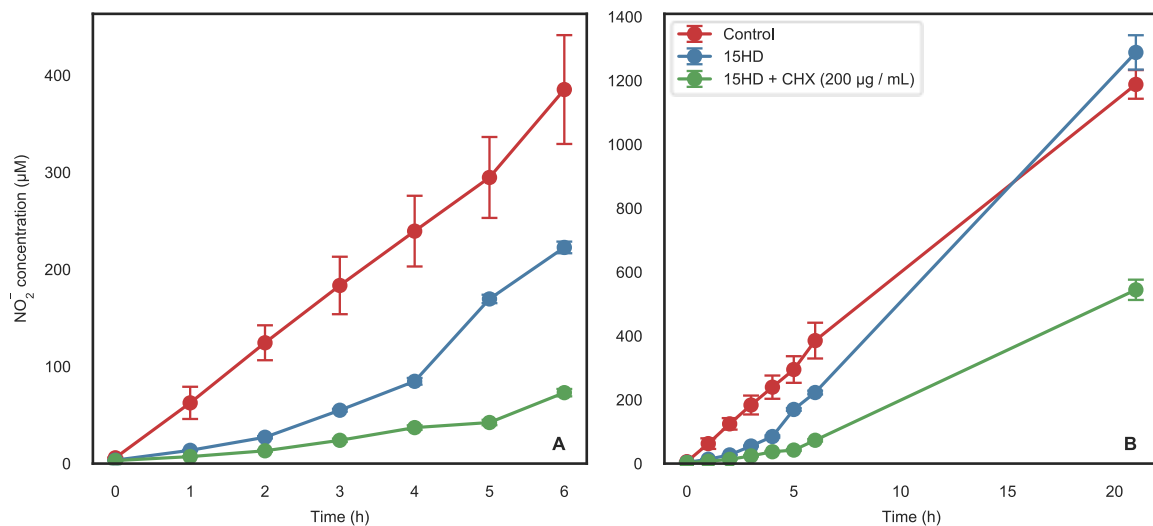


Figure 5-5 – Six (A) and 21 (B) hour time course of the recovery of NO_2^- production from 1 mM NH_4^+ in '*Ca. Nitrosocosmicus franklandus*' after removal of $100 \mu\text{M}$ 15HD with and without $200 \mu\text{g mL}^{-1}$ CHX. Error bars represent the standard deviation ($n = 3$).

There was a clear delay of up to 4 hours in the recovery after washing of 15HD treated cells (Figure 5-5A). This indicated that the inhibition was indeed irreversible, as seen for example in the recovery of AOA from inhibition by acetylene (Wright *et al.*, 2020). The cycloheximide treated samples recovered more slowly but eventually started recovering and after 21 h (Figure 5-5B) they had recovered completely. The irreversibility was a promising sign for the potential of using 15HD as an ABPP probe. However, it was not clear whether cycloheximide would be a suitable translational inhibitor for *Nitrosocosmicus franklandus* as $200 \mu\text{g mL}^{-1}$ CHX did not fully inhibit the recovery of ammonia oxidation.

To further investigate whether CHX could be used as a translation inhibitor in '*Ca. N. franklandus*', a range of CHX concentrations (200 $\mu\text{g mL}^{-1}$ to 2 mg mL^{-1} CHX) was tested in '*Ca. N. franklandus*' (Figure 5-6A). Acetylene treatment was performed to compare the inhibition pattern of 15HD. As acetylene is an irreversible inhibitor of the AMO, similar recovery response would be expected for both acetylene and 15HD. Although higher concentrations of CHX resulted in slightly stronger inhibition of ammonia oxidation than lower CHX concentrations in the short-term incubations, the inhibition was not complete. A high concentration (1 mg mL^{-1} CHX) was used to test recovery from acetylene inhibition (Figure 5-6B). Again, although the CHX treated AOA cells recovered more slowly than the treatment without CHX, the inhibition was incomplete. There was an initial inhibition of recovery but eventually, the cells did recover. Nevertheless, the recovery from acetylene followed a similar pattern to that of 15HD, providing further support that 15HD is an irreversible inhibitor.

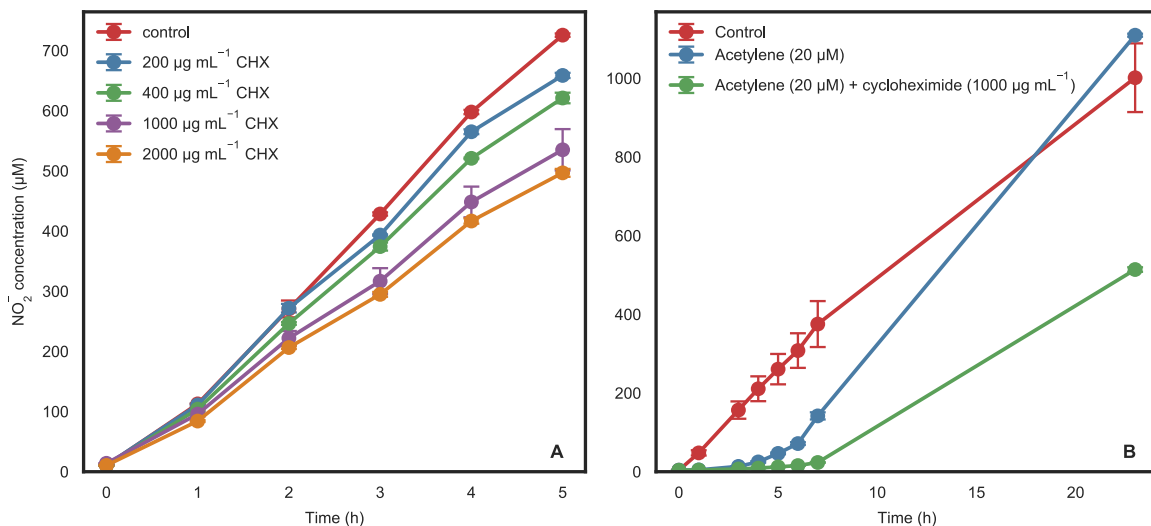


Figure 5-6 – Time course of the inhibition of NO_2^- production with different concentrations of CHX (A) and recovery of NO_2^- production from 1 mM NH_4^+ in '*Ca. Nitrosocosmicus franklandus*' after removal of 20 μM acetylene with and without 1000 $\mu\text{g mL}^{-1}$ CHX (B). Error bars represent the standard deviation ($n = 3$).

It is possible the CHX was not stable over long periods of time, however this was not the case in *Nitrosopumilus maritimus* (Neeraja Vajjala *et al.*, 2014). Alternatively, the concentration may have been too low. However, the concentration used was already at the limit of what the solubility allowed, and it is likely that if higher concentrations are needed, CHX is not an effective translational inhibitor. In conclusion, cycloheximide is not suitable as a translation inhibitor in '*Ca. N. franklandus*'. Despite this, it was possible to demonstrate that both acetylene and 15HD are irreversible inhibitors by observing the delay in recovery compared to uninhibited control treatments. These data were published in Wright *et al.* (2020).

5.2.4 A fluorescent tag reveals labelled cells by fluorescent microscopy

Having confirmed that 15HD specifically and irreversibly inhibits the archaeal AMO, effectiveness of the 15HD probe for ABPP was evaluated in whole cells of '*Ca. N. franklandus*'. This was done using click chemistry to attach a fluorescent azide compound (fluorescein azide) to the free terminal triple bond. If successful, this approach should result in fluorescent labelling of the AMO enzyme. Whole cells of '*Ca. N. franklandus*' were first inhibited with 15HD as in the activity assays. A copper-catalysed azide–alkyne cycloaddition (CuAAC) was then carried out to fluorescently label the AMO.

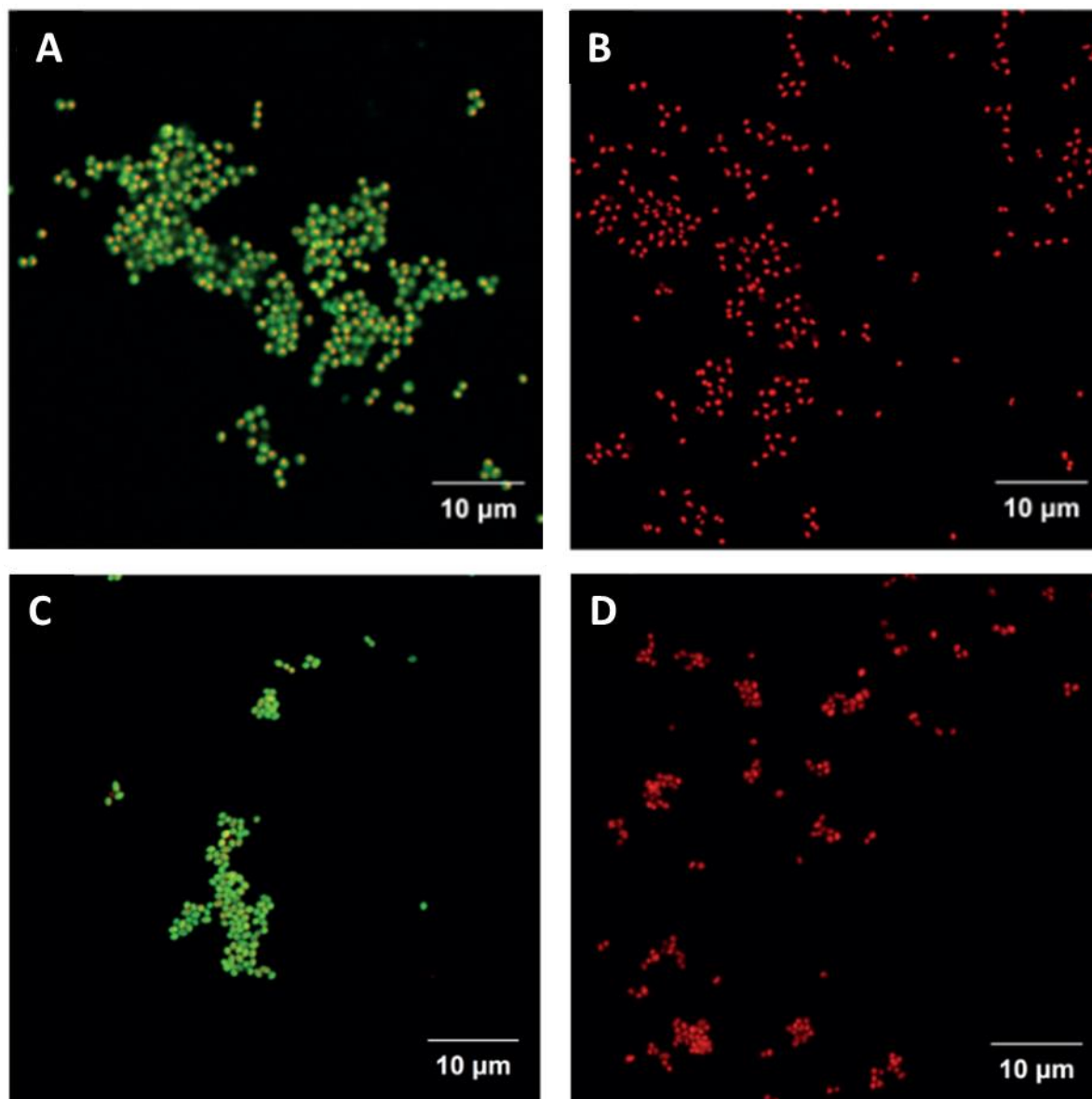


Figure 5-7 - ABPP-based fluorescent labelling of active '*Ca. N. franklandus*' (A and B) and *N. europaea* (C and D). Cells pre-incubated with 15HD (A and C), cells without 15HD pre-incubation (B and D). Fluorescein was clicked to the alkyne from 15HD probe and is shown in green. DAPI stained DNA is shown in red.

The technique proved a success, and the 15HD-inhibited cells of '*Ca. N. franklandus*' and *N. europaea* showed a clear fluorescent signal (Figure 5-7A, C). Nearly all cells showed a fluorescent signal, consistent with the finding that >90% of active *N. europaea* cells were stained when inhibited with 18OD (Sakoula *et al.*, 2022). '*Ca. N. franklandus*' and *N. europaea* cells without 15HD treatment had no fluorescent signal (Figure 5-7B, D), indicating that the signal was not due to autofluorescence or artefacts from the click reaction. This was a promising indication that ABPP with 15HD was working and could be used to identify the AMO subunit responsible for the 15HD binding.

5.2.5 Fluorescent SDS-PAGE

To investigate whether the fluorescent labelling with 15HD and fluorescein azide was specific to the AMO or if more proteins were labelled, cell extracts of '*Ca. N. franklandus*' and *N. europaea* were prepared using 15HD-labelled cells and the proteins were clicked using the fluorescent tag. The protein extracts were then run on an SDS-PAGE gel and the fluorescence was visualised. *Nitrosomonas europaea* was used as a positive control using both 17OD and 15HD (Figure 5-8).

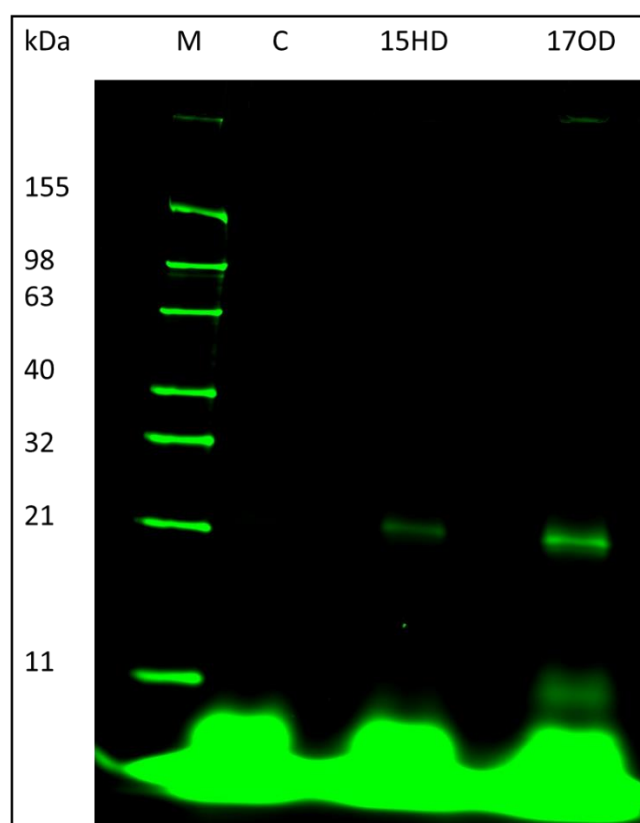


Figure 5-8 – Fluorescent SDS-PAGE of cell extracts of *N. europaea*. M: marker; C: untreated control; 15HD: cells pre-treated with 1,5-hexadiyne; 17OD: cells pre-treated with 1,7-octadiyne.

Both with 15HD and 17OD, there was one bright fluorescent band around 22 kDa. This is at a smaller size than the 28 kDa that was observed previously (Bennett *et al.*, 2016), although a different fluorophore and fluorescent marker were used.

However, when this was attempted in '*Ca. N. franklandus*' (Figure 5-9), there was no clear single band as there was in *N. europaea*. Moreover, when the experiment was repeated with *N. europaea*, additional fluorescent bands were visible.

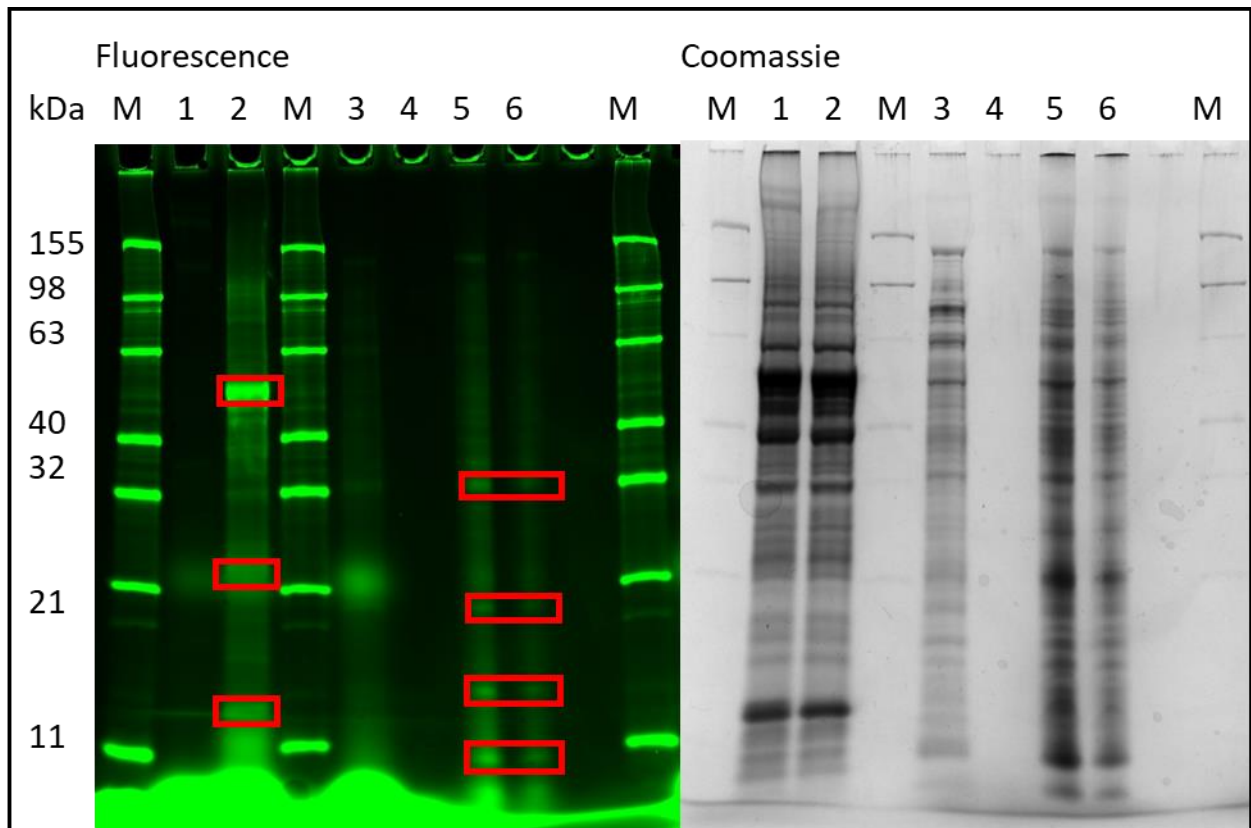


Figure 5-9 – Fluorescent (left) and Coomassie stained (right) SDS-PAGE gel. M: marker; 1: untreated *N. europaea* cell extract; 2: 15HD treated *N. europaea* cell extract; 3-6: 15HD treated '*Ca. N. franklandus*' cell extract. 4 and 5 were samples concentrated by precipitation. Red rectangles highlight excised bands for identification.

This fluorescence profile did not correspond to our expectations and was inconsistent with the initial attempt results in *N. europaea* where only one protein band was visible. Especially in *N. franklandus*, there were no clear bands and additional protein precipitation was necessary to observe the fluorescence due to low amounts of protein. To verify whether the AMO was labelled in either '*Ca. N. franklandus*' or *N. europaea*, the bands with the brightest fluorescent signal were excised and analysed using MALDI-TOF (Table 5-1).

Table 5-1 – Identification of proteins by MALDI-TOF from excised SDS-PAGE protein bands.

Band	Hit mass	Hit score	Identified proteins
NC1	0	158	Mixture from proteins: "03::NFRAN_v2_2912 ID:63487295 fpr ", "03::NFRAN_v2_0657 ID:63485040 ttuD ", "03::NFRAN_v2_0886 ID:63485269 pcn "
NC2	22545	84	NFRAN_v2_3193 ID:63487576 dps DNA protection during starvation protein
NC3	15427	95	NFRAN_v2_1813 ID:63486196 conserved protein of unknown function
NC4	40260	53	NFRAN_v2_0865 ID:63485248 tyrS Tyrosine--tRNA ligase
NE1	53222	223	NE1921 ID:1724877 cbbL Ribulose biphosphate carboxylase large chain
NE2	20999	93	NE2465 ID:1723823 Alkyl hydroperoxide reductase/ Thiol specific antioxidant/ Mal allergen
NE3	13860	103	NE1920 ID:1724876 cbbS ribulose biphosphate carboxylase, small chain

None of the AMO subunits was among the identified proteins in either '*Ca. N. franklandus*' (amoA: 24 kDa, amoB: 21 kDa, amoC: 21 kDa) or *N. europaea* (amoA: 28 kDa, amoB: 43 kDa, amoC: 31 kDa). This does not correspond to previous reports (Bennett *et al.*, 2016; Sakoula *et al.*, 2021). A possible explanation is that the AMO behaves inconsistently in SDS-PAGE gels which is not uncommon for membrane proteins. The labelling protocol was shown to be highly specific to monooxygenases (Sakoula *et al.*, 2021) and therefore it is unlikely that none of the AMO was labelled in these extracts. However, the presence of multiple fluorescent bands suggests potential non-target effects of 15HD on proteins other than AMO. 15HD is highly reactive, and reactions with other enzymes cannot be ruled out. Further work could attempt to pull-down the labelled proteins using a biotin probe instead of a fluorescent probe. Using the pull-down approach, biotin probe could be bound to streptavidin-coated magnetic beads and protein of interest recovered.

5.2.6 Hydrazine-based ABPP probes

After it was shown that hydrazine is oxidised in '*Ca. N. franklandus*' and organohydrazines inhibit hydroxylamine oxidation, this class of compounds seemed like a perfect candidate to use as ABPP probes. By using ABPP with hydrazine probes, the inhibition by hydrazines could be further elucidated by identifying the proteins these hydrazines bind to. In addition, it could also help identify the elusive hydroxylamine oxidation protein in the AOA, as it would be expected to be one of the proteins bound by the probe.

5.2.7 Inhibition of 'Ca. N. franklandus' by biotin-hydrazides

A first attempt was made using biotin-hydrazides in *Nitrosocosmicus franklandus*. They were chosen because they are commercially available and because of the presence of the biotin, which would make the need for the CuAAC unnecessary. It was hypothesised that the warhead group was similar enough to have the same inhibition mechanism as phenylhydrazine which was tested in the previous chapter. Two probes were used, one with the biotin bound to the hydrazine group (Figure 5-10A) and one with 4 polyethylene glycol groups as spacers (Figure 5-10B) in case there was steric hindrance.

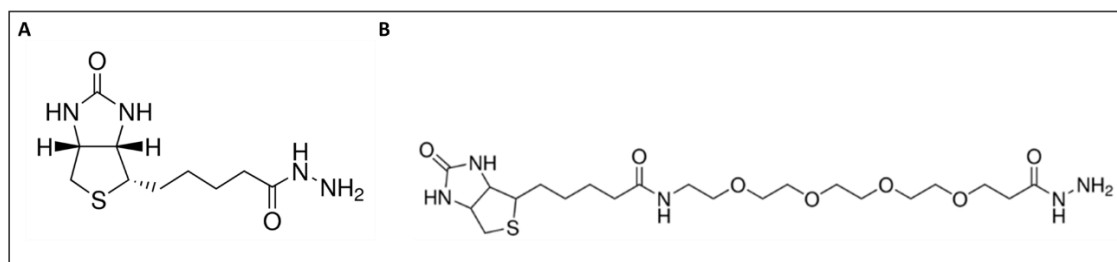


Figure 5-10 - Chemical structures of the two biotin-hydrazine probes used. A: biotin hydrazide (BHDR); B: Biotin-dPEG₄-hydrazide (BPHDR)

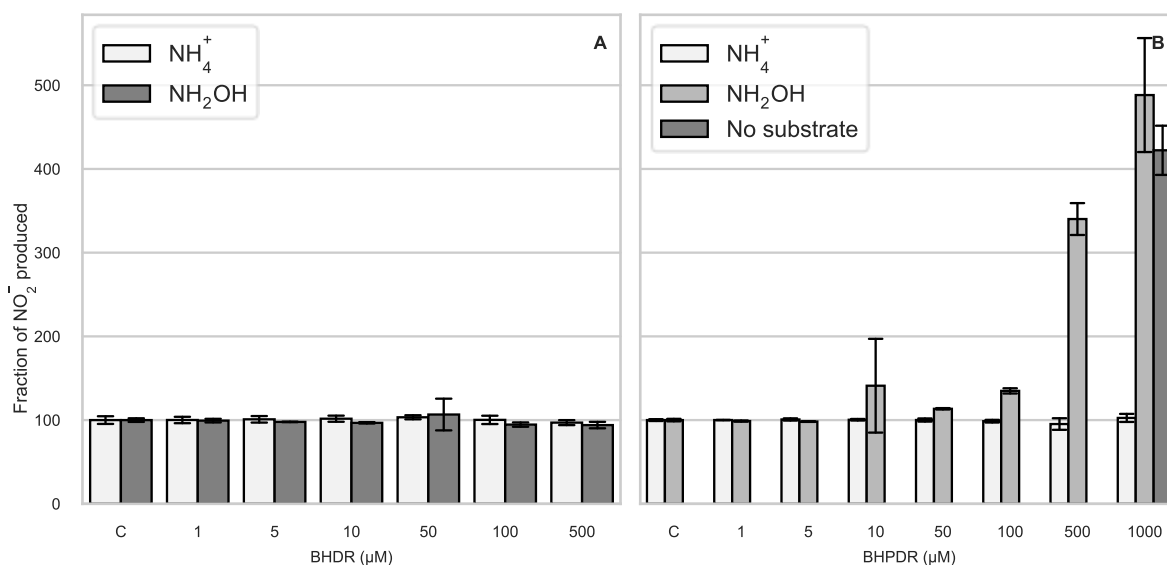


Figure 5-11 - Percentage NO₂⁻ production compared to the uninhibited control (C) after 1 h incubation with different concentrations of biotin-hydrazine probe using 100 μM NH₄⁺ or 200 μM NH₂OH as substrate. NO₂⁻ was measured 1 h after addition of the substrate. Nitrite accumulation in the uninhibited control treatment represents 100% activity, and the treatments with hydrazine are shown as the percentage of activity compared to this control. Error bars represent standard deviation (n = 3). BHDR: biotin hydrazide; BHPDR: biotin hydrazide with spacer.

The first biotin hydrazide probe did not show any inhibition at any of the concentrations tested (Figure 5-11). This was discouraging because concentrations > 100 μM of phenylhydrazine completely inhibited hydroxylamine oxidation (chapter 4). The spacer probe also did not show any inhibition and

strangely apparently enhanced nitrite production at higher concentrations. A control treatment without substrate was carried out. This revealed that the apparent increase in nitrite production was not a result of ammonia or hydroxylamine oxidation and was probably a result from reaction with the probe. It is not clear whether this is true nitrite production or a reaction with the assay reagent. However, this reaction must be biological because an abiotic control did not show the increase in absorbance in the nitrite assay (data not shown). It is possible that an amine oxidase released ammonium from the probe which would then be further converted to nitrite and provide extra substrate in the assay. This effect would only be visible in the hydroxylamine conditions as there substrate was fully consumed while in the ammonia conditions there was substrate in excess. It is strange that this would only have happened in the probe with the spacer, although the amine group may be more accessible.

5.2.8 Hydrazine-alkyne ABPP probes

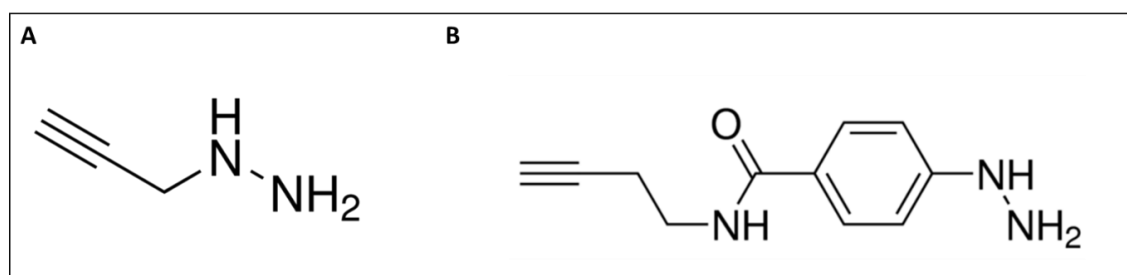


Figure 5-12 – Chemical structures of hydrazine probes: (A): prop-2-yn-1-ylhydrazine (alkyl probe); (B): N-(But-3-yn-1-yl)-4-hydrazineylbenzamide (aryl probe).

Recently, clickable hydrazine probes were synthesised and verified to discover protein electrophiles (Matthews *et al.*, 2017) and they were later used as a proof-of-concept for drug discovery (Lin *et al.*, 2020). These probes have a higher similarity to the hydrazines tested in Chapter 4 and could be suitable probes for this instance, using the hydrazine group as warhead and the alkyne group as click target. The alkyl probe (prop-2-yn-1-ylhydrazine; Figure 5-12A) was not commercially available at the time of the experiments so the aryl probe (N-(But-3-yn-1-yl)-4-hydrazineylbenzamide; Figure 5-12) was used. The aryl probe has a high structural similarity to phenylhydrazine and could therefore be a suitable probe to investigate the inhibition targets of this compound.

5.2.9 Inhibition of '*Ca. N. franklandus*' by a hydrazine-alkyne

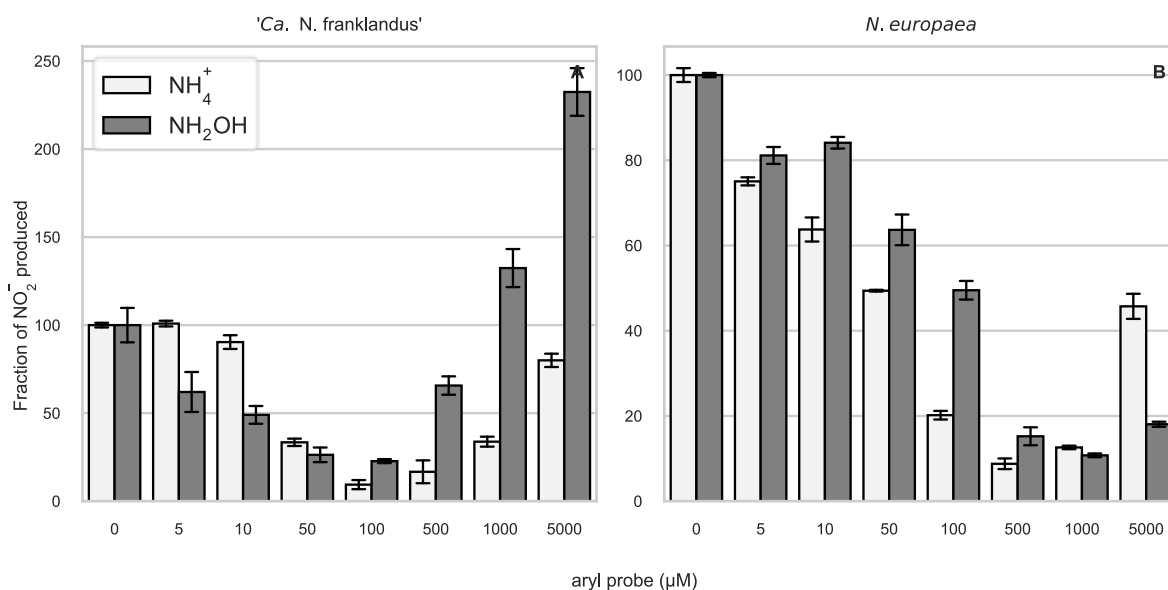


Figure 5-13 – Relative NO₂⁻ production compared to the control after 1 h incubation with different concentrations of aryl probe using 100 μM NH₄⁺ or 200 μM NH₂OH as substrate. NO₂⁻ was measured 1 h after addition of the substrate. Nitrite accumulation in the uninhibited control treatment represents 100% activity, and the treatments with aryl probe are shown as the percentage of activity compared to this control. Error bars represent standard deviation (n = 3).

Just as with the hydrazines tested in Chapter 4, higher concentrations resulted in progressively higher inhibition of ammonia and hydroxylamine oxidation in both '*Ca. N. franklandus*' and *N. europaea* (Figure 5-13). However, in '*Ca. N. franklandus*' concentrations higher than 100 μM started showing higher absorbance in the nitrite assays and even an apparent increase compared to the control with no added aryl probe was observed (Figure 5-13A), similar to that by BHPDR (Figure 5-11B). In *N. europaea*, this effect was less pronounced and only the highest concentration (5,000 μM) resulted in lower inhibition. Initially it was suspected that the apparent increase in nitrite production at high concentration of the aryl probe was due to a reaction with the buffer, but this does not explain the difference between *N. europaea* and '*Ca. N. franklandus*'. Moreover, while the blank reaction showed increased absorbance in the nitrite assay at higher concentrations (Figure 5-14), this was only up to the level that was observed in *N. europaea*. Thus, abiotic reactions alone cannot account for the increased nitrite production by '*Ca. N. franklandus*' in the presence of >500 μM aryl probe. Therefore, it is likely that '*Ca. N. franklandus*' metabolises the inhibitor to another compound that further reacts with the nitrite assay reagents to change colour. It is unclear whether this would influence protein labelling.

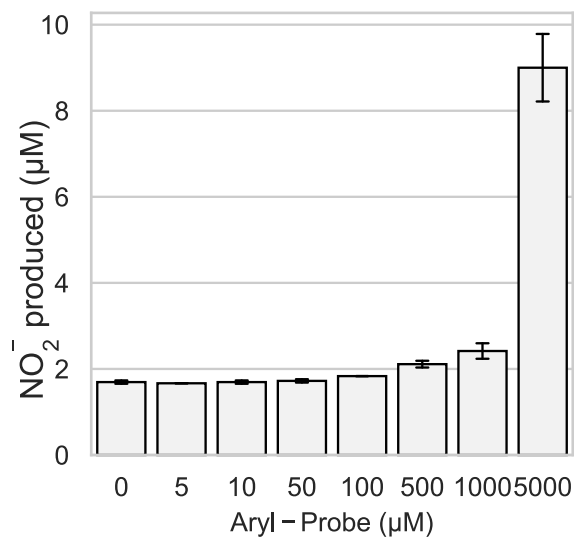


Figure 5-14 – Abiotic nitrite measurements with different concentrations of Aryl probe.

5.2.10 Click-fluorescence

To investigate which proteins were labelled, a fluorescent azide probe was clicked to the terminal triple bond of the probe and a fluorescent SDS-PAGE was carried out. This experiment has the potential caveat that the terminal triple bond may also react with the AMO. A preincubation with phenylhydrazine was performed as a control because it is expected to inhibit in the same enzyme with the same mode of action and therefore by irreversibly binding the target proteins it should prevent labelling.

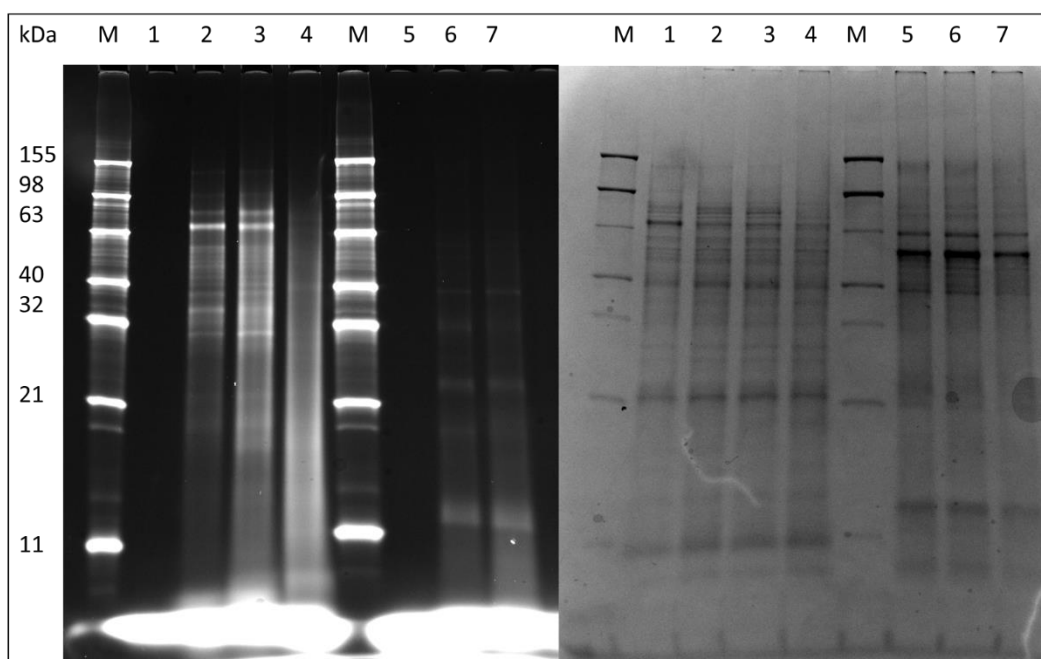


Figure 5-15 - Fluorescent labelling profiles by the aryl probe after clicking (left) and corresponding expression profiles after Coomassie staining (right) of protein extract from ‘*Ca. N. franklandus*’ (1-4) and *N. europaea* (5-7) (3µg protein/sample). 1: untreated protein extract; 2: 100 µM aryl probe; 3: 500 µM aryl probe; 4: 500 µM phenylhydrazine; 5: untreated protein extract; 6: 100 µM aryl probe; 7: 500 µM aryl probe; M: fluorescent protein marker.

There was no fluorescence in the samples without the aryl probe. Samples preincubated with phenylhydrazine had no fluorescent bands but they did show a fluorescent smear which could be caused by abiotic interactions between phenylhydrazine and the aryl probe. In ‘*Ca. N. franklandus*’ many proteins were labelled both with 100 µM and 500 µM probe. Some bands were very abundant and would be interesting to identify as they are potential candidate proteins for the archaeal hydroxylamine dehydrogenase. Lower concentrations could be tested as it is expected that the hydroxylamine oxidising protein is highly abundant and sensitive to this probe and using a lower concentration might improve the likelihood of identifying it this way. In *N. europaea*, labelling was less prominent and fewer protein bands were discernible. Importantly, the HAO which has a size of ~64 kD was expected to fluoresce significantly but no bands were visible at this size.

5.3 Discussion

This chapter provides the initial basis for the further investigation of ABPP probes in AOA.

5.3.1 Labelling of the archaeal AMO with 1,5-Hexadiyne

Diynes as probes for monooxygenases have been successfully used in microscopy experiments and have been shown to be powerful tools (Bennett *et al.*, 2016; Sakoula *et al.*, 2021). 15HD, however, showed mixed results in terms of labelling proteins with click chemistry. 15HD can effectively label the

archaeal AMO in whole cells (Figure 5-7), which is a huge step forward, but when attempting to visualise the protein difficulties arise. It is possible that further optimisation of the protocol can overcome these difficulties as was done in *Nitrosomonas europaea* (Bennett *et al.*, 2016). Here we characterised 15HD as an inhibitor and demonstrate its potential as a ABPP probe for the archaeal AMO. However, we fail to conclusively identify AMO subunits in the labelled proteins. A pull-down using a biotin tag may solve this issue and should be attempted in the future. NFRAN_v2_3193 was one of the proteins identified by fluorescent labelling with 15HD and was shown to be highly abundant in the proteome of '*Ca. N. franklandus*' (see Chapter 3). This protein is suspected to function as a catalase (chapter 6) but it may have other functions and it seems to play an important role in the growth of '*Ca. N. franklandus*'.

We evaluated the use of cycloheximide as a translational inhibitor in '*Ca. N. franklandus*' and concluded that while it shows some inhibition, it is unfit to be used as the concentrations needed to obtain inhibition are too high. The solubility in water is too low to obtain the concentrations needed for inhibition.

5.3.2 Labelling of archaeal hydroxylamine oxidising enzymes using hydrazine probes

Two biotin hydrazide probes were tested to see if they inhibited nitrite production from ammonia or hydroxylamine. The probes did not show the desired inhibition which is likely due to the oxygen on the first carbon which would create a different functional group compared to phenylhydrazine after oxidation of the hydrazine group. Instead of a radical, an aldehyde would be formed which does not have the same reactivity and is unlikely to inactivate the enzyme.

The aryl probe that was evaluated here showed more promising results although a lot more work will be needed to evaluate this molecule as a probe. The labelling appears to be non-specific, so as a probe for the hydroxylamine oxidation enzyme it might not be ideal. However, this does not mean it cannot be used to identify this enzyme as it is likely to be labelled. Using a biotin-azide, a pull down could be done and by using a quantitative approach, likely candidates for the enzyme could be identified. Another thing to consider is the terminal alkyne group in the aryl probe. The AMO reacts with terminal alkynes which would render the probe useless as there would be no clickable group. It is possible this is why the labelling in *N. europaea* was less pronounced than in '*Ca. N. franklandus*', because *N. europaea* has been shown to be ten times more sensitive to the aromatic alkyne phenylacetylene (Wright *et al.*, 2020).

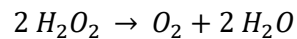
Future work should include: (I) optimisation of the optimal labelling concentration of the aryl probe. (II) a biotin pull-down using 15HD and the aryl probe, followed by proteomics to identify the targets

they bind to. (III) further optimisation to the 15HD labelling protocol in the AOA to visualise the targeted proteins and (IV) the aryl probe labelling in the AOB to label the HAO.

6 Identification of a Catalase isozyme from '*Ca. N. franklandus*' C13

6.1 Introduction

Hydrogen peroxide (H_2O_2) is a reactive oxygen species that can be formed as a by-product of aerobic metabolism, as a signalling molecule or as a weapon for intercellular warfare. H_2O_2 is toxic and most aerobic organisms have defence mechanisms against it, the most well-known being the catalase enzyme. Catalase catalyses the disproportionation of H_2O_2 :



The name catalase reflects its historical importance at the basis of biological enzyme catalysis (Nicholls, 2012). The heme-containing catalase has been characterised extensively and is found in nearly all organisms that are exposed to oxygen. However, another catalase was discovered in lactic acid bacteria lacking hemes and cytochromes, but still showing catalase activity (Delwiche, 1961; Johnston & Delwiche, 1965). This unusual catalase contains manganese (Mn) instead of a heme at the active site (Kono & Fridovich, 1983). This novel catalase was initially named a "pseudocatalase" but was later renamed to Mn-catalase. Very little is known about Mn-catalases and only a few have been characterised (Shaeer *et al.* (2019), and references therein). Mn-catalases are widespread among prokaryotes but, notably, are absent in eukaryotes (Whittaker, 2012) and are thought to provide advantages over heme catalases in certain environmental context such as iron limitation, microaerophilic oxidative stress, thermostability, and cyanide resistance (Whittaker, 2012).

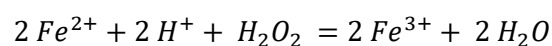
In ammonia oxidising archaea (AOA), H_2O_2 detoxification has attracted significant research interest. In the marine environment, AOA were shown to be highly sensitive to H_2O_2 , despite H_2O_2 being a common by-product of aerobic metabolism (Tolar *et al.*, 2016). Genes for H_2O_2 detoxification are absent from many AOA genomes (Tolar *et al.*, 2016), and different closely related AOA strains were shown to have different degrees of sensitivity to H_2O_2 , which may contribute to their niche differentiation (Bayer *et al.*, 2019). It is unclear if AOA have peroxidases capable of detoxifying H_2O_2 (Tolar *et al.*, 2016).

For several years, many terrestrial AOA were thought to be mixotrophic because they required α -keto acids such as pyruvate or oxaloacetate to grow (Qin *et al.*, 2014; Tourna *et al.*, 2011). This view was revised after the discovery that the requirement of the α -keto acids was due to their hydrogen peroxide detoxification capacity (Kim *et al.*, 2016). Over the years, many more AOA strains have been isolated and more genomic information has become available providing new insights into the role of reactive oxygen in AOA (Abby *et al.*, 2020; Ren *et al.*, 2019; Sheridan *et al.*, 2020).

A recent genomic study based on 39 complete or nearly complete genomes of *Thaumarchaeota* highlighted the evolution of Mn-catalases in the *Nitrososphaerales* (Abby *et al.*, 2020). Intriguingly, *Nitrososphaerales* is the only clade in the *Thaumarchaeota* which has acquired a Mn-catalase. The lack of any catalase homologues in other *Thaumarchaeota* clades is curious considering that it is deemed a crucial enzyme in aerobic metabolism. It has been hypothesised that AOA instead rely on alkyl hydroperoxide reductase for the detoxification of H₂O₂ during exponential growth (Abby *et al.*, 2020; Seaver & Imlay, 2001). Alternatively, AOA may rely on other catalase-containing microorganisms in the environment to detoxify H₂O₂ (Bayer *et al.*, 2019). Perhaps it is unsurprising that there would be multiple mechanisms and adaptations for H₂O₂ detoxification as oxygen availability and by proxy H₂O₂ detoxification is thought to have played a major role in the evolution of AOA (Ren *et al.*, 2019).

Of the cultured *Nitrososphaerales* representatives, only *N. viennensis* EN76^T and ‘*Ca. N. franklandus*’ C13 do not contain a catalase. However, only *N. viennensis* relies on pyruvate or other additives for H₂O₂ detoxification (Tourna *et al.*, 2011) while ‘*Ca. N. franklandus*’ can grow without any added H₂O₂ detoxification compounds (Lehtovirta-Morley *et al.*, 2016).

According to the study by Abby and colleagues, the last common ancestor of the AOA acquired DNA protection during starvation family protein genes (Dps), and this repertoire was later expanded in the *Nitrososphaerales*. Dps proteins are usually dodecameric (Bellapadrona *et al.*, 2010), and have been characterised in several organisms where they bind to the chromosome, forming DNA-Dps co-crystals and protecting the DNA from damage including oxidative stress (Wolf *et al.*, 1999). Oxidative stress protection occurs by consuming both substrates from the Fenton reaction (Fe²⁺ and H₂O₂), preventing the production of hydroxyl radicals (Bellapadrona *et al.*, 2010):



However, Dps proteins are also known to have a weak catalase activity (Zhao *et al.*, 2002) and a distinct cluster within the ferritin family of Dps proteins, named Dps-like (DpsL) proteins, are known archaeal antioxidants (Wiedenheft *et al.*, 2005). The active site, which is thought to contain Fe, shows a close similarity to bacterioferritin and Mn-catalase (Gauss *et al.*, 2006). Importantly, it was shown that the Dps protein from *Kineococcus radiotolerans* could bind both Fe and Mn at the active site (Ardini *et al.*, 2013) and the DpsL protein from the archaeon *Sulfolobus solfataricus* showed catalase activity when bound with Mn (Hayden & Hendrich, 2010). These observations show that Dps and DpsL proteins have multiple functions including the detoxification of reactive oxygen species and the protection of DNA and they could play an important role in the AOA, especially those lacking catalases.

In this study, a DpsL protein from ‘*Ca. N. franklandus*’ was identified after partial purification, based on its significant catalase activity. Sequence analysis showed similarity to other DpsL proteins and a

conservation of a bacterioferritin-like active site. This protein was also one of the most abundant proteins in the proteome of '*Ca. N. franklandus*' under normal growth conditions which highlights its importance. The catalase function of DpsL proteins is severely understudied with, to our knowledge, only one study characterising it (Hayden & Hendrich, 2010). Therefore, the identification of a DpsL protein functioning as a catalase in an AOA devoid of other catalase isozymes is of particular interest.

6.2 Results

6.2.1 '*Ca. N. franklandus*' has a H₂O₂ detoxification enzyme

To investigate if '*Ca. N. franklandus*' had an enzyme responsible for H₂O₂ detoxification, an in-gel activity stain was used. The activity stain relies on the conversion of ferricyanide (III) to ferrocyanide (II) by H₂O₂. Ferric chloride is then added and reacts with the ferrocyanide to form a stable insoluble Prussian Blue pigment. Areas where catalase is active will have had less H₂O₂ and therefore less potassium ferrocyanide resulting in less or no blue colour. In the following experiments, colourless native PAGE was done, followed by an activity stain, and by a Coomassie stain.

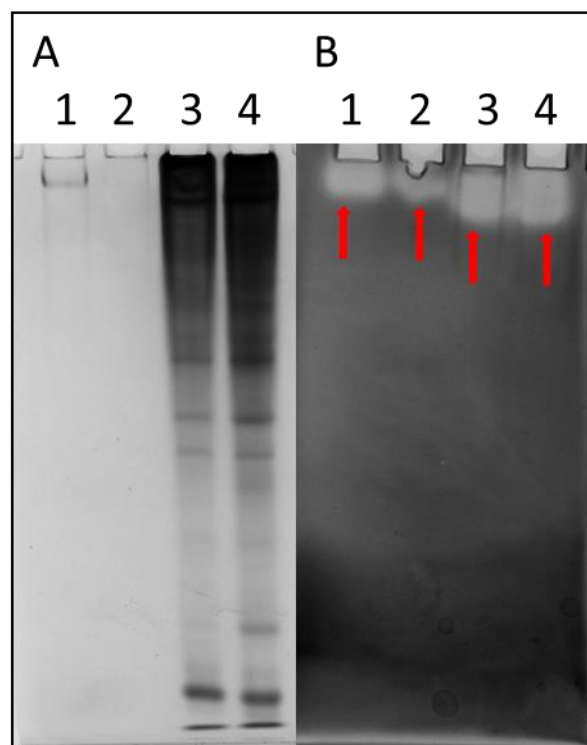


Figure 6-1 - Colourless native PAGE (10%) stained with Coomassie (A) and activity stained (B). 1: 25 units of catalase; 2: 2.5 units of catalase; 3: 80 µg crude cell extract (frozen); 4: 80 µg crude cell extract (fresh) The activity is yellow-green on a blue background and light areas indicate catalase activity (red arrow). The Coomassie stain is blue as well, and the sensitivity was therefore limited due to background staining. Heme-catalase from bovine liver (Merck, cat no. C9322) was included as a positive control.

A light band, indicating catalase activity, was observed in the crude extract samples (Figure 6-1B). This coincided with an abundant band in the Coomassie stained gel (Figure 6-1A). The fact that both the

fresh extract and the frozen extract showed activity was promising for subsequent experiments because it allowed growing several batches of cells and extract to be frozen before use.

6.2.2 Partial purification of the catalase enzyme

Before attempting to identify the catalase enzyme, two purification techniques were used to partially purify the protein, increasing the chance of getting a correct identification. It was not possible to do a complete native purification as biomass is hard to obtain and it would have been prohibitively time-consuming.

6.2.2.1 Ammonium sulfate $\{(NH_4)_2SO_4\}$ precipitation

As a first purification strategy, 10 mL cell extract containing 7.33 mg protein was fractionated by salting out using $(NH_4)_2SO_4$ in increments of 20% saturation. The precipitated protein was isolated by centrifugation and was resuspended in Tris-buffer (50 mM, pH 8) and the protein concentration in each fraction was determined (Table 6-1).

Table 6-1 - Protein concentrations of different fractions after $(NH_4)_2SO_4$ precipitation

% Saturation	Protein concentration (mg mL⁻¹)
20	0.0866
40	2.459
60	4.599
80	1.191
100	< 0.008
100 (liquid)	< 0.008

Perhaps unsurprisingly, most of the protein precipitated in the 40 and 60 % saturated fractions. Next, an SDS-PAGE was performed (Figure 6-2) to evaluate whether fractions were significantly different. Where possible (40 – 80 % fractions), 5 µg protein per well was loaded onto the gel. For fractions with less than 5 µg protein available, 10 µl of the fraction was loaded. After addition of 5 µl loading buffer the total sample volume was 15 µl.

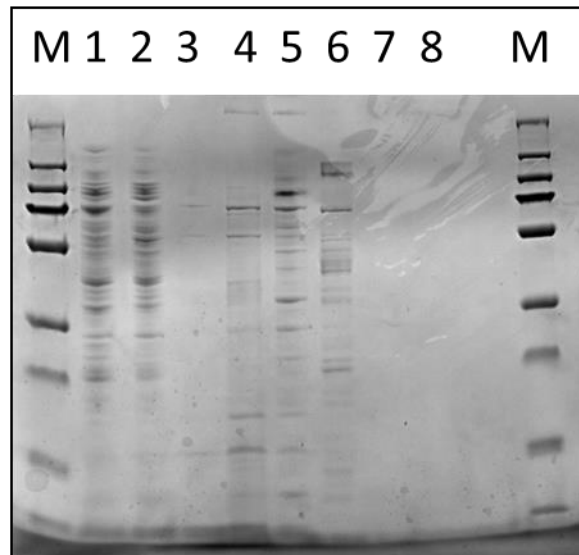


Figure 6-2 Coomassie-stained 10% SDS-PAGE gel with $(\text{NH}_4)_2\text{SO}_4$ precipitated fractions. M: marker; 1: Crude cell extract from batch-grown cells; 2: Crude cell extract from bioreactor-grown cells; 3: 20% saturated fraction; 4: 40% saturated fraction; 5: 60% saturated fraction; 6: 80% saturated fraction; 7: 100% saturated fraction; 8: 100% saturated fraction (liquid).

Fractions were different from each other as seen by the band patterns. Strongest bands in the different fractions were not necessarily abundant in the crude extract, indicating that the fractionation was successfully selecting for different proteins in different fractions. To test if the catalase activity was still present after precipitation, an activity stain was performed using the fractions. To increase the likelihood of observing activity, the highest volume possible (10 μL) was used irrespective of the protein concentration.

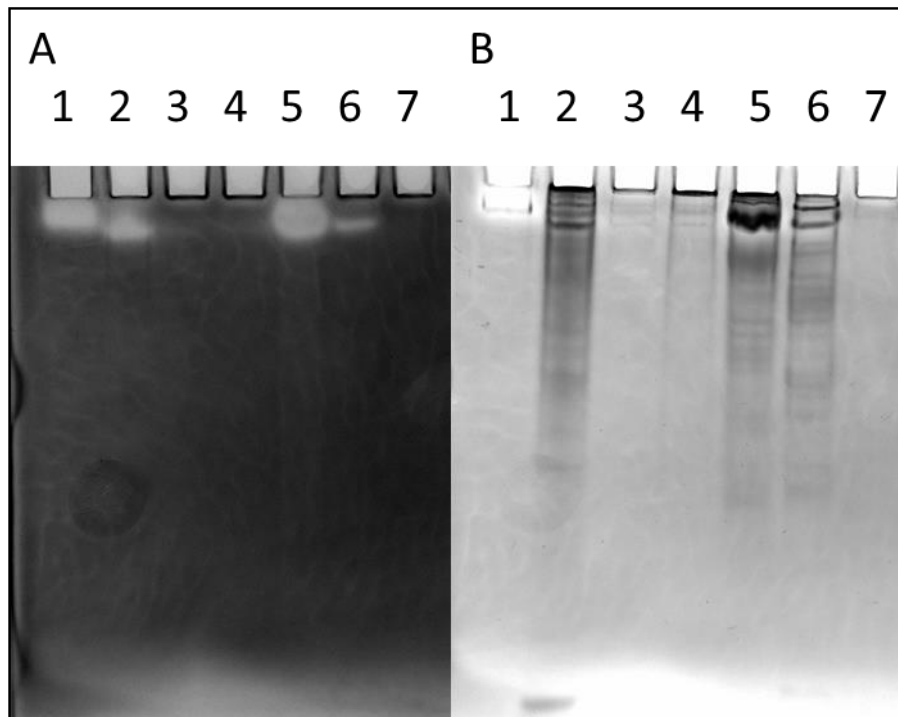


Figure 6-3 – Colourless native PAGE (10%) activity stained for catalase activity (A) and Coomassie stained (B). 1: 25 units catalase; 2: Crude cell extract from batch-grown cells; 3: 20% saturated fraction; 4: 40% saturated fraction; 5: 60% saturated fraction; 6: 80% saturated fraction; 7: 100% saturated fraction.

The activity stain clearly showed activity in the 60 and 80% fractions. The difference in intensity was probably due to the different amount of protein in the samples. While the activity was clear, the samples did not migrate readily in the 10% acrylamide gel. This technique relies on the proteins having a native negative charge so proteins with a low negative charge or a positive charge will migrate slowly or not at all (Wittig & Schägger, 2005). This is also obvious in the Coomassie stain where most of the proteins remain in the well without migrating (e.g., in lane 4, Figure 6-3). Subsequent gels were run using 5% gels to increase the mobility of the proteins in the gels.

6.2.2.2 Anion exchange purification

Before attempting to identify the active protein in the gel, a second purification strategy was used to increase the chance of isolating the protein responsible for the catalase activity. Anion exchange chromatography relies on the charge of the proteins instead of the solubility, providing a different property to fractionate the crude extract. A total of 28.76 mg protein was loaded onto an anion exchange column and fractions were eluted in 100 mM NaCl increments from the column in 5mL buffer (Table 6-2).

Table 6-2 - Protein concentrations of different fractions after anion exchange fractionation

NaCl concentration (mM)	Protein concentration (mg mL ⁻¹)
100	0.480
200	1.064
300	0.637
400	0.471
500	0.031
1000	< 0.008

Again, an activity stain was performed followed by Coomassie staining. Where possible, 10 µg protein was loaded per well (200 – 300 mM fractions), or 20 µL extract when the concentration was too low. This time, 5% acrylamide gels were used.

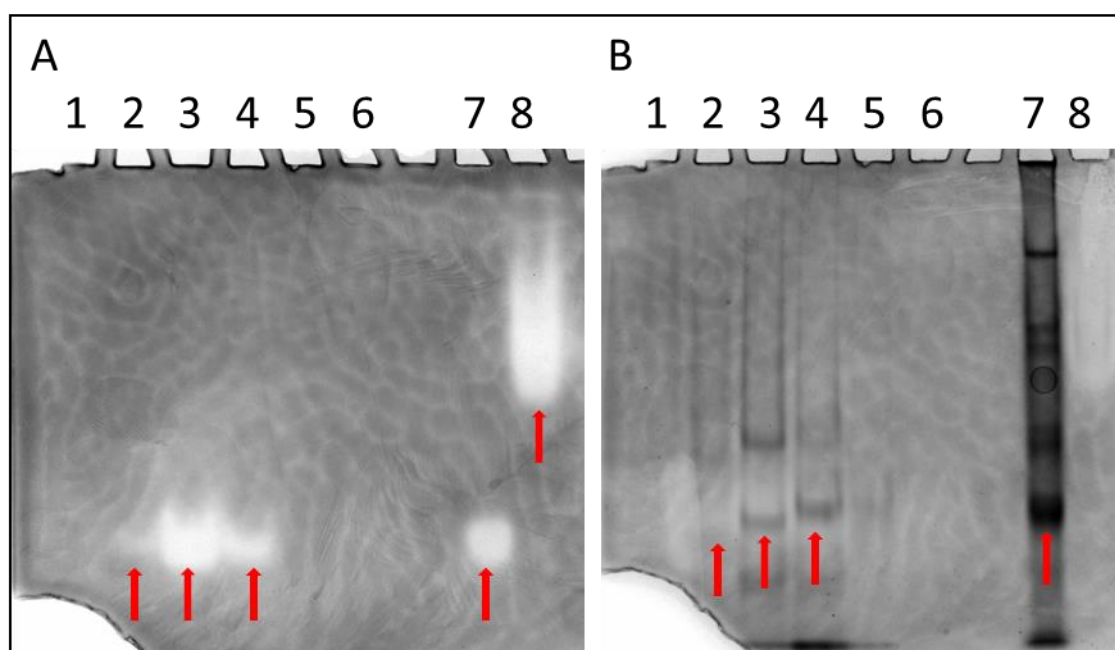


Figure 6-4 - Colourless native PAGE (5%) activity stained for catalase activity (A) and Coomassie stained (B). 1: 100 mM NaCl fraction; 2: 200 mM NaCl fraction; 3: 300 mM NaCl fraction; 4: 400 mM NaCl fraction; 5: 500 mM NaCl fraction; 6: 1000 mM NaCl fraction; 7: crude cell extract from batch-grown cells (40 µg); 8: 25 units catalase. Zones of activity and their corresponding protein bands are highlighted with red arrows.

The use of a 5% gel instead of 10% allowed for the proteins to migrate further into the gel. This highlighted the difference between the heme-catalase that was used as a control and the catalase from '*Ca N. franklandus*'. Activity was observed in the 200-400 mM NaCl fractions with most of the activity in the 300 mM fraction. Excitingly, distinct protein bands were observed after Coomassie

staining at the spots of activity. Interestingly, the bands differed slightly in position. The spot showing activity in the crude cell extract sample corresponded to a highly abundant protein band, indicating a high abundance of this catalase isozyme.

6.2.3 Identification of the candidate catalase isozyme

The fractions from $(\text{NH}_4)_2\text{SO}_4$ precipitation and anion exchange containing the activity were loaded onto a clear native PAGE gel (5%) and were run as previously (Figure 6-5). No activity staining was carried out because the chemicals could have interfered with the identification. The bands previously corresponding to the activity spots were excised and analysed using MALDI-TOF and LC-MS analysis.

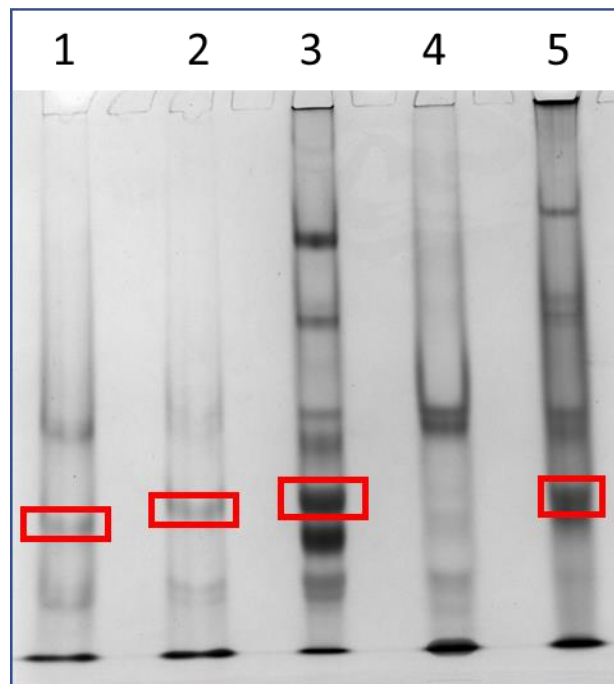


Figure 6-5 - Colourless native PAGE (5%) Coomassie-stained. 1: 300 mM NaCl fraction from anion exchange fractionation (12 μg protein); 2: 400 mM NaCl fraction from anion exchange fractionation (9 μg protein); 3: 60% $(\text{NH}_4)_2\text{SO}_4$ saturated fraction (40 μg protein); 4: 80% $(\text{NH}_4)_2\text{SO}_4$ saturated fraction (20 μg protein); 5: crude cell extract (40 μg protein). Bands indicated in red were cut out.

6.2.3.1 Matrix-assisted laser desorption/ionization time of flight (MALDI-TOF) analysis

A first attempt to identify the gel bands was done using peptide mass fingerprinting after trypsin digestion on a Maldi-TOF mass spectrometer. The identification results are shown in Table 6-3.

Table 6-3 - MALDI-TOF analysis results. *: >51 is significant (p < 0.05)

Sample	Sample name	Accession	Hit Mass (Da)	Hit Score*	Description
1	Anion exchange 300 mM	NFRAN_v2_3193	22545	<u>57</u>	DNA protection during starvation protein
2	Anion exchange 400 mM	NFRAN_v2_1329	7996	28	conserved protein of unknown function
3	(NH ₄) ₂ SO ₄ 60% saturated	Q9R0H5	57860	38	Keratin, type II cytoskeletal
4	Crude extract	NFRAN_v2_3193	22545	<u>133</u>	DNA protection during starvation protein

Only two of the samples yielded a significant identification, NFRAN_v2_3193. Lack of significant identification is to be expected when using complex samples on a MALDI-TOF mass spectrometer.

6.2.3.2 Liquid Chromatography - Tandem Mass Spectrometry (LC-MS-MS)

To gain a better understanding of proteins in the samples, LC-MS/MS on an Orbitrap Tribrid was used after trypsin digestion. This technique allows the identification and quantification of proteins in complex samples. Based on the previous experiments, the catalase isozyme was expected to be abundant in the analysed samples. Therefore, the top 5 most abundant proteins are shown (Table 6-4).

Table 6-4 - The top five most abundant identified proteins in each sample, NFRAN_v2_3193 is highlighted as it was identified in all samples in the top five most abundant proteins. *: Quantitative value (normalised total spectra).

Predicted function	Sample 1	accession number	QV*
DNA protection during starvation protein		NFRAN_v2_3193	369.7
Multicopper oxidase		NFRAN_v2_2029	176.62
Lactaldehyde reductase		NFRAN_v2_2370	94.296
Inorganic pyrophosphatase		NFRAN_v2_0425	94.296
Tetratricopeptide repeat protein		NFRAN_v2_2876	70.348
Sample 2			
Copper-containing nitrite reductase		NFRAN_v2_1409	275.08
Multicopper oxidase		NFRAN_v2_2029	146.86
DNA protection during starvation protein		NFRAN_v2_3193	116.56
conserved exported protein of unknown function		NFRAN_v2_0790	41.961
putative sialidase-neuraminidase family protein		NFRAN_v2_2146	37.299
Sample 3			
Copper-containing nitrite reductase		NFRAN_v2_1409	217.24
Bacterial extracellular solute-binding proteins, family 5 Middle		NFRAN_v2_3011	160.73
DNA protection during starvation protein		NFRAN_v2_3193	114.27
chaperone Hsp70, co-chaperone with DnaJ		NFRAN_v2_1464	67.809
Multicopper oxidase, type 3		NFRAN_v2_2792	59.019
Sample 4			
DNA protection during starvation protein		NFRAN_v2_3193	231.18
putative enzyme		NFRAN_v2_2718	145.26
Lactaldehyde reductase		NFRAN_v2_2370	131.02
fumarate reductase (anaerobic) catalytic and NAD/ flavoprotein subunit		NFRAN_v2_1904	112.03
Copper-containing nitrite reductase		NFRAN_v2_1409	77.377

Only NFRAN_v2_3193, which was annotated as a 'DNA protection during starvation protein' (dps), was detected in the top five most abundant identified proteins of every sample. A second gene, NFRAN_v2_2370, which was annotated as a 'Lactaldehyde reductase', was identified in all samples in the ten most abundant identified proteins but was significantly less abundant than NFRAN_v2_3193. NFRAN_v2_3193 is a 22 kDa protein from the ferritin family group of proteins putatively annotated as a Dps protein. These proteins are known to be involved in the detoxification of reactive oxygen species and some have been shown to have catalase activity (Hayden & Hendrich, 2010; Zhao *et al.*, 2002). However, the observed catalase activity seemed to be significant. No Fe²⁺ addition was necessary for catalase activity, which implies a different cofactor is required for this catalase. This is in contrast to majority of previously characterised catalases which are heme-dependent and warrants further

investigation. Moreover, this protein was one of the most abundant proteins in the proteome of '*Ca N. franklandus*' during normal growth (Chapter 3).

6.2.4 Sequence analysis

The Dps protein (NFRAN_3193) from '*Ca N. franklandus*' clusters with DpsL proteins as opposed to other Dps proteins, indicating it is a member of this subclass of proteins (Wiedenheft *et al.*, 2005). This DpsL cluster is most closely related to Dps proteins but has an active site resembling that of other members of the ferritin-like superfamily such as ferritins, bacterioferritins and manganese catalase (Gauss *et al.*, 2006). Possessing features of both Dps and bacterioferritin, the DpsL cluster may be an intermediate in the ferritin family evolution (Bai *et al.*, 2015). Importantly, the DpsL protein from *Sulfolobus solfataricus* has been shown to have catalase activity when bound with Mn instead of Fe (Hayden & Hendrich, 2010). To investigate the features from the '*Ca N. franklandus*' DpsL protein, a protein sequence alignment was made with ferritins, bacterioferritins, Dps and DpsL proteins (Figure 6-6). Three representative sequences from each subclass were used and the sequences were aligned using MUSCLE (Edgar, 2004). Characteristic motifs or residues (Andrews, 2010) are highlighted when amino acid charge and motif spacing are conserved.

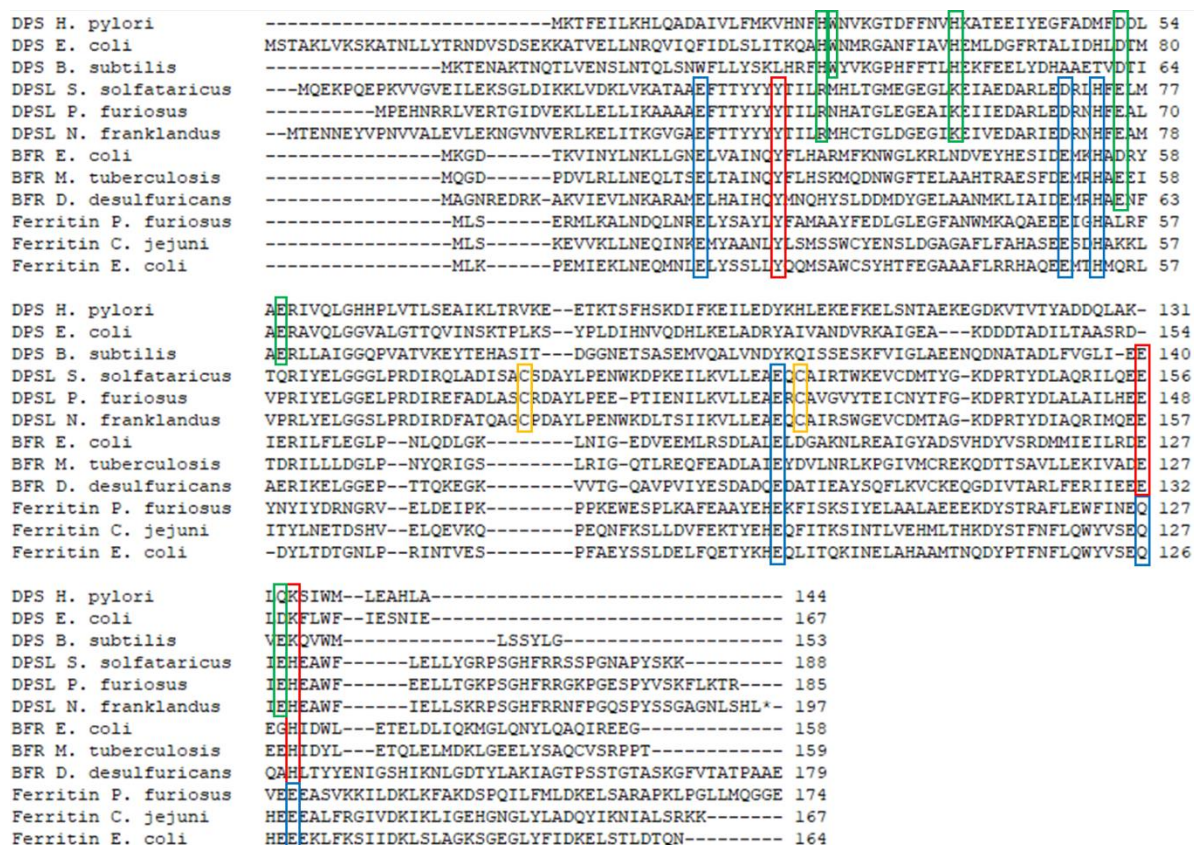


Figure 6-6 - Sequence alignment of three representative sequences of the Ferritins, bacterioferritins (BFR), Dps and DpsL proteins. Blue: Residues associated with metal binding in ferritins and bacterioferritins; Red: conserved motifs in ferritins and/or bacterioferritins; Green: conserved motifs in Dps proteins; Yellow: DpsL-specific residues.

The alignment revealed that most residues involved in metal binding in ferritins and especially bacterioferritins were conserved or underwent conservative mutations in the DpsL proteins (Figure 6-6, blue). On the contrary, the typical motifs in Dps proteins were only partially conserved (Figure 6-6, green) and conserved motifs characteristic for (bacterio)ferritins (Figure 6-6, red) were conserved in DpsL proteins but not in Dps proteins. Finally, two cysteine residues were highlighted (Figure 6-6, Yellow), that are thought to be unique to DpsL proteins and may play a redox active role.

These results indicate that NFRAN_v2_3193 is indeed a DpsL protein as it has the right amino acid residues and activity of this cluster of poorly characterised proteins.

6.2.5 Blue native polyacrylamide gel electrophoresis (BN-PAGE)

To have an indication of the quaternary structure of the active protein, a BN-PAGE was done (Figure 6-7). In this technique, proteins are coated with an anionic Coomassie dye, providing them with a charge (Wittig *et al.*, 2006). The proteins then separate on the gel based only on the size as they all have the same charge. Half of the gel was used for activity staining while the other half was de-stained

to enable the observation of the Coomassie-stained proteins. The expectation was that the protein would be dodecameric like other Dps and DpsL proteins as opposed to hexa or 24-meric like Mn catalases and ferritins, respectively. As the monomer is predicted to be 22 330 Da, the dodecamer would be 267 960 Da.

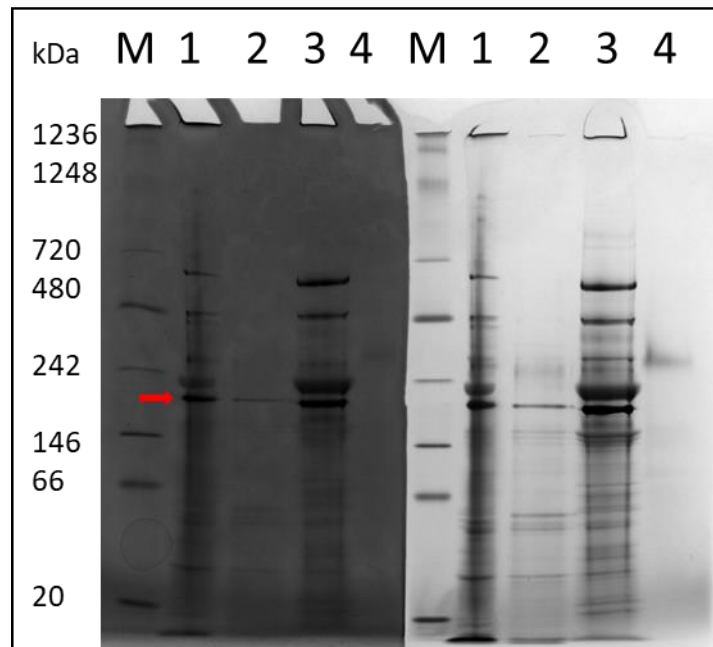


Figure 6-7 - BN-PAGE from different fractions of protein with catalase activity. Activity stain (left) destained (right). M: marker; 1: crude cell extract (60 μ g); 2: 300 mM NaCl fraction from anion exchange fractionation (9 μ g protein); 3: 60% (NH₄)₂SO₄ saturated fraction (60 μ g protein); 4: Catalase (25 units); red arrow: possible decamer.

Unfortunately, the catalase activity stain (Figure 6-7, left) was not successful either due to the Coomassie G250 dye interfering with activity or the colour difference being invisible as the activity stain and Coomassie dyes are both blue. On the de-stained gel, (Figure 6-7, right) some bands that were abundant in all fractions were present and could be good candidates for the DpsL enzyme. The most prominent band is visible around 210 kDa (Figure 6-7, red arrow) which does not agree with the 268 kDa predicted size but more closely resembles a decamer (223 kDa). To ascertain the mass of the protein, pure protein should be used for future characterisation.

6.2.6 Growth with pyruvate and catalase

The DpsL protein was one of the most highly expressed proteins identified in the proteome and a significant number of cellular resources must be used to produce this protein. This suggest that the Dps protein is likely to be very important for the growth of '*Ca N. franklandus*'. Therefore, we hypothesised that if the H₂O₂ stress is relieved by the addition of pyruvate or catalase, '*Ca N. franklandus*' would grow better as less resources would need to be invested into producing Dps. To

test this hypothesis, '*Ca N. franklandus*' was grown in normal growth conditions, with the addition of 0.5 mM pyruvate or with 1 μ M catalase. Growth was monitored by measuring nitrite and an SDS-PAGE was carried out to investigate if there was a visible difference in protein expression.

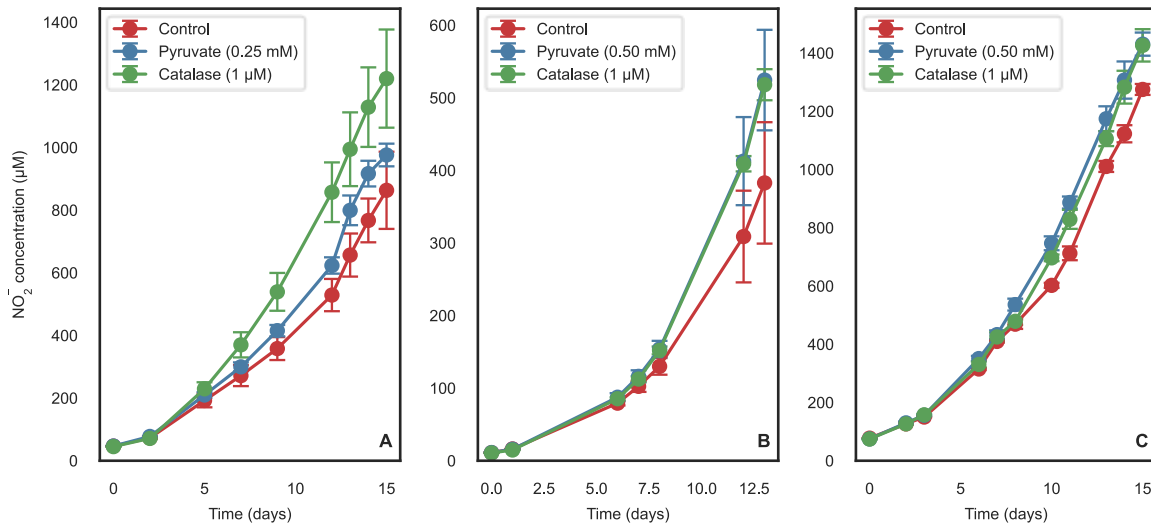


Figure 6-8 - Growth, quantified by nitrite accumulation, of three separate experiments (A, B, C) where triplicate cultures of each treatment were grown. In panel B, the catalase and pyruvate treatments overlap.

Cultures grown with pyruvate or catalase accumulated more NO_2^- in the first 12 – 15 days of the incubations (Figure 6-8). This indicates that the H_2O_2 stress response indeed used a significant amount of resources and the removal of H_2O_2 by catalase or pyruvate had a beneficial effects on ammonia oxidation and growth. In the first experiment (Figure 6-8A), only 0.25 mM pyruvate was used, and the growth was intermediate between that of the control and the catalase, indicating the H_2O_2 stress relief was incomplete. In subsequent experiments 0.5 mM pyruvate was used (Figure 6-8B, C) and the effect was comparable to that of the added catalase.

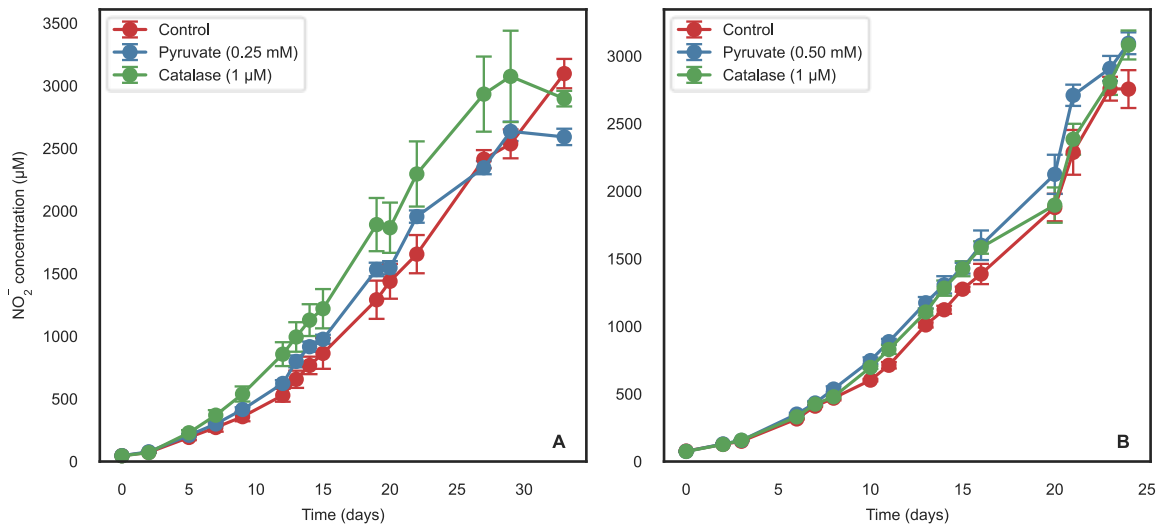


Figure 6-9 – Growth, quantified by nitrite accumulation, of the Figure 6-8 A and C experiments over a longer time, A and B, respectively where triplicate cultures of each treatment were grown.

When growth was tracked for longer, the effect was less clear (Figure 6-9). This could be because when cell abundances are higher, H_2O_2 toxicity is less severe (Bayer *et al.*, 2019). This is a known phenomenon in other organisms (Morris *et al.*, 2011) and while the exact mechanism is not known, it may be due to a quorum sensing response.

On an SDS-PAGE (Figure 6-10), all treatments looked similar, including the area where the 22 kDa DpsL protein would be expected to be located. It may be better to grow the cells in the presence of added H_2O_2 to see a difference in protein expression. Alternatively, each condition could be further investigated by carrying out proteome or RNA-seq which are more sensitive techniques. If only the DpsL protein is of interest, an RT-QPCR experiment could be carried out.

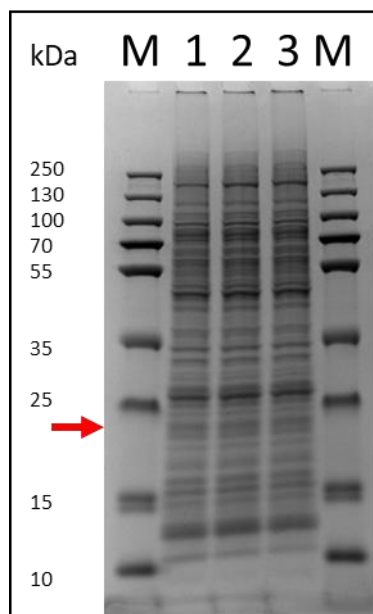


Figure 6-10 – SDS-PAGE of protein extracts from ‘*Ca N. franklandus*’ cells grown in normal growth conditions (1), with 0.5 mM pyruvate (2) or 1 μM catalase. M: protein marker. The red arrow indicates where NFRAN_3193 would be expected to migrate to.

6.3 Discussion

The work described in this chapter came about when trying to adapt the catalase activity stain to detect hydroxylamine oxidation. This hypothesis relied upon the chemical similarities between hydroxylamine and hydrogen peroxide. In the catalase stain, hydrogen peroxide reacts with ferricyanide (III) to form ferrocyanide (II) and O₂. The ferrocyanide then reacts with ferric chloride to form Prussian Blue pigment. Preliminary experiments showed that hydroxylamine could also form the Prussian Blue pigment and hence it was hypothesised the assay could be adapted to be used with hydroxylamine instead of hydrogen peroxide. While the catalase stain was not suitable for studying hydroxylamine oxidation, it surprisingly revealed a protein with an apparent catalase function in the model AOA ‘*Ca N. franklandus*’. This was unexpected because the genome of ‘*Ca N. franklandus*’ does not contain recognisable catalase homologues, whilst on the other hand this AOA strain can grow without addition of pyruvate or other α-keto acids which are required for H₂O₂ detoxification in other catalase-negative AOA. This led to the identification of the DpsL protein as a novel catalase in ‘*Ca N. franklandus*’.

The identification of this H₂O₂ detoxification mechanism could be important for the AOA as closely related sequences are found in other clades including the marine AOA. Other *Nitrosocosmicos* strains do have a Mn-catalase as well as dps(L) genes, it would be interesting to find out whether both or either are expressed and functional. The high abundance of the DpsL protein in the proteome of *N. franklandus* highlighted that it has an important function during growth. It would be interesting to investigate whether this detoxification mechanism provides an advantage over other AOA without

catalase. However, *N. viennensis*, has *dps* genes in its genome but needs H₂O₂ detoxification compounds to grow. It is also not clear whether having both catalase and *dpsL* genes would be beneficial and if they would work in different conditions especially because the rate of the *dpsL* protein is expected to be 10-100 times lower than Mn-catalase (Hayden & Hendrich, 2010).

The high abundance in the proteome, could indicate H₂O₂ stress during growth. The experiments where '*Ca N. franklandus*' was grown with H₂O₂ detoxifying compounds indicated they may assist during the exponential growth phase but later on the effect seemed minimal or absent. This is in contrast with results from other AOA strains where H₂O₂ scavengers were crucial for growth (Kim et al., 2016). This further highlights how dealing with reactive oxygen stress in AOA may have been a driver for adaptation to different environments.

Other functions of the DpsL enzyme should be considered too. The high abundance in the proteome indicates it may be involved in more than just H₂O₂ detoxification. The *dps* proteins have been implicated in protection and stabilisation of DNA (Wolf *et al.*, 1999) and it would be interesting to investigate whether this *dpsL* protein can do the same. Finally, it may have a function in iron detoxification (Chiancone & Ceci, 2010).

Whether the protein binds iron, manganese or both could be vital as well. Similar proteins have been shown to have different functions depending on the metal they bind (Ardini *et al.*, 2013) and Mn-catalase is thought to have an advantage compared to heme-catalase in Fe limited environments (Whittaker, 2012).

Further research should investigate the DpsL protein and characterise it. Purification from the native host or after expression in a different host would be beneficial to study the protein in isolation. In particular: (i) Finding out which metal residues it binds, Fe or Mn or both. (ii) Investigating whether the activity is purely catalase activity (producing oxygen) or whether Fe is needed for H₂O₂ detoxification. (iii) Characterising the optimal conditions and compare with other catalases to see if it has biotechnological value. And finally, (iv) does it bind DNA? Furthermore, to investigate the expression and importance of this protein in the growth of *N. franklandus*, the use of RT-QPCR or a quantitative proteome in conditions with and without H₂O₂ could be done, although it may be challenging to see a difference as the DpsL protein is already highly expressed.

In conclusion, the DpsL protein from '*Ca N. franklandus*' was shown to have a catalase function which provides this AOA with a previously unknown mechanism for H₂O₂ detoxification in AOA and explains why '*Ca N. franklandus*' can grow without the addition of H₂O₂ detoxification compounds.

7 Conclusions and prospects for future research

7.1 Development of '*Ca. N. franklandus*' as a model organism

In Chapter 3, techniques were developed with the aim to make studying '*Ca. N. franklandus*' on the protein level more accessible. To do this, growth in a bioreactor system was evaluated. A continuous system with biomass retention resulted in biomass yields significantly greater than what is possible to achieve in batch cultures. The continuous out and inflow of medium could be regulated to prevent the toxic build-up of nitrite. Moreover, due to the way this continuous system works, cells will always be substrate limited and in a healthy physiological state. Thus, providing a constant supply of large amounts of cells and protein for experiments. However, growing AOA in a bioreactor system requires long runs of often 30 – 60 days. These long growth times made the reactor more prone to contamination and the reactor requires daily maintenance throughout the whole run.

To study the proteins of '*Ca. N. franklandus*', a reliable technique to lyse the cells was necessary. The cells are extremely tough to break and after evaluating several methods a mechanical lysis technique was chosen as the preferred and most efficient method. Several passes through a French press after washing the cells with hypoosmotic buffer yielded the best results. Additionally, when only small-scale lysis was necessary, bead beating was a good option. Cell-free extract was used to develop an assay to detect the activity of a hydroxylamine oxidising enzyme. Ferricyanide was selected as an electron acceptor. While the assay could not be developed to a point where it was reliable, it may be worth investigating further.

Finally, a proteome of '*Ca. N. franklandus*' was determined with cells grown on ammonia and urea, the only two known growth substrates. This dataset will be used as a baseline protein profile of '*Ca. N. franklandus*' in both growing conditions. While the dataset did not reveal any hydroxylamine oxidation enzymes yet, it will be used in the future to refer to and can be included in future data analyses.

To facilitate future physiological experiments in AOA, further efforts should be made to improve biomass yields. Current protocols grow the AOA in static glass bottles in the dark. The bioreactor cultivations show that the oxygen availability becomes limiting when biomass is increasing. It is therefore unlikely that the cultures grown in static incubators have sufficient oxygen. When ambitious attempts are made to investigate these organisms, such as native purification of proteins or activity assays, it is imperative that protocols to grow them are improved. Bioreactors can be a powerful tool and solution to discover limiting factors and to improve yields. Chemostat runs could be used to optimise things such as the optimal pH, substrate concentration or inhibitory nitrite concentration.

These experiments have only been done using batch cultures which are not controlled circumstances. Once optimised, the biomass retention system can be used to produce biomass for experiments.

As a final note on this topic, it might be more beneficial to attempt to isolate a more appropriate laboratory AOA strain from the environment. Conditions could be selected to select for fast growing AOA capable of reaching high cell densities. Considering the progress that *N. europaea* has enabled on the study of AOB, a similar AOA isolate could accelerate AOA research a lot.

7.2 Hydrazines as inhibitors and substrates in the AOA

In Chapter 4, hydrazines were shown to interact with the hydroxylamine oxidation mechanisms of ‘*Ca. N. franklandus*’ and two other AOA. Hydrazine was shown to be oxidised by measuring oxygen consumption and the product, dinitrogen gas, was verified directly by providing ^{15}N -hydrazine and measuring $^{30}\text{N}_2$. Phenylhydrazine, an organohydrazine, was shown to irreversibly inhibit the mechanism. The inhibition was demonstrated by measuring three separate parameters namely, nitrite production, oxygen consumption and N_2 production from hydrazine. This knowledge was used in Chapter 5 to select ABPP probes for the identification of the enzyme(s) responsible. Finally, ATP measurements were used to show that the AOA could generate ATP from both hydrazine and even phenylhydrazine, although only for a short period of time for the latter.

To further investigate hydrazines in the AOA, it would be interesting to see if they can grow on either hydrazine or hydroxylamine as a sole substrate. Due to the toxicity and instability of these compounds these experiments are challenging but not impossible. It is unlikely sufficient growth could be observed in a batch culture with a non-toxic concentration within the time it takes for the compound to degrade due to instability. Therefore, a continuous bioreactor system could be set up with a biomass retention system. This way, low concentrations of substrate can be fed continuously while growth will be easy to observe. Only one instance of a similar experiment is known where *Nitrosomonas europaea* was grown on a mixture of ammonia and hydroxylamine, resulting in higher growth than on ammonia alone (Bruijn et al., 1995; Soler-Jofra et al., 2021). No AOB or AOA has been shown to be capable of growing on hydroxylamine alone.

Finally, products of the oxidation of hydrazine and hydroxylamine should be investigated in more detail. It was shown that N_2 is a product, but a full characterisation of the nitrogen compounds should be done to get a complete nitrogen balance. This way, the abiotic interactions can be quantified, and it can be determined if other products are formed biotically or not. Especially the non-stoichiometric conversion of hydroxylamine to nitrite which was observed should be investigated as it was not observed in either *N. maritimus* or *N. viennensis* (Kozłowski, Stieglmeier, et al., 2016; N. Vajrala et al., 2013).

7.3 Activity based protein profiling in AOA

A method for the labelling of ammonia and alkane monooxygenase was recently developed (Sakoula *et al.*, 2021), which was based on a proof-of-concept study in *Nitrosomonas europaea* (Bennett *et al.*, 2016). In the first part of Chapter 5, an attempt was made to further develop this method with a new bifunctional alkydiyne probe: 1,5-hexadiyne (15HD). The inhibition of 15HD was characterised as AMO specific and irreversible, as is typical for alkyne inhibitors. The labelling of the AMO, however, could not be observed on a protein gel. Further development of this method will be necessary for future use. The fluorescence obtained after labelling the AMO with diyne probes demonstrates the potential of the technique (Sakoula *et al.*, 2021), but further optimisation to the protocol is necessary to determine precisely what happens on the molecular level. A pull-down followed by proteomics should be the next step to find out which proteins or even amino acids are bound by the probes.

In the second part of this chapter, hydrazine probes were evaluated with the goal to label the hydroxylamine oxidising enzyme of the AOA. Based on the results from Chapter 4, we hypothesised that organohydrazine probes would be able to inhibit the oxidation of hydroxylamine in a similar way as phenylhydrazine did. An alkyne group on the probe would then provide a click site to connect fluorophores or other useful tags to the complex. Indeed, the hydrazine-alkyne probe inhibited hydroxylamine oxidation and a fluorescent profile was observed on an SDS-PAGE gel after clicking a fluorescent probe to the probe. As opposed to what was observed for the AMO of *N. europaea* (Bennett *et al.*, 2016), the probe was not specific to just one protein but a range of proteins was labelled. To follow up this work, a pull-down followed by proteomics could be done to show which proteins are affected by the probes, and by proxy by organohydrazines such as phenylhydrazine. This experiment could not only provide insights into the inhibition mechanism and specificity of (organo)hydrazines but it could also identify the hydroxylamine oxidation enzyme.

7.4 The role of a H₂O₂ detoxification mechanism in 'Ca. N. franklandus'

'Ca. N. franklandus' does not encode for an annotated catalase in its genome, yet as opposed to *Nitrososphaera viennensis*, it does not need added pyruvate or catalase to grow. In Chapter 6, the H₂O₂ detoxification mechanism of 'Ca. N. franklandus' was investigated. A Dps-like enzyme was identified as a possible catalase isozyme. This protein was one of the most abundant proteins in the proteome determined in Chapter 3. This highlights its importance in the growth conditions that 'Ca. N. franklandus' was grown in, and it demonstrates the value of having a proteome dataset to verify enzymes of interest. Further research is needed to finalise this work. First, to unequivocally demonstrate this protein has catalase activity, it should be heterologously expressed, and the activity should be verified using pure protein. Then, the metal residues bound should be investigated as there could be an interplay of iron and manganese metals. The other proposed functions such as DNA

protection and iron detoxification could be investigated as well. Finally, a detailed analysis of Dps(L) proteins in AOA could be made to infer the importance of these proteins in this group of organisms.

7.5 Prospects for future research

As with all research, it is never finished, and this thesis is no exception. The main objective, to identify new enzymes in the central ammonia oxidation pathway of AOA, was not achieved. However, a lot of progress was made to establish how these enzymes could be identified, and insight into alternative substrates and inhibitors was obtained. Methods for growing this model AOA and investigating the ammonia oxidation pathway were developed. Substrates and inhibitors for the unknown hydroxylamine oxidation enzyme were characterised and can be used to further investigate this pathway. While a lot of development and improvement is still needed, a start was made, and future work will be able to build upon this thesis.

References

- Abalos, D., Jeffery, S., Sanz-Cobena, A., Guardia, G., & Vallejo, A. (2014). Meta-analysis of the effect of urease and nitrification inhibitors on crop productivity and nitrogen use efficiency. *Agriculture, Ecosystems and Environment*, *189*, 136–144. <https://doi.org/10.1016/j.agee.2014.03.036>
- Abby, S. S., Kerou, M., & Schleper, C. (2020). Ancestral Reconstructions Decipher Major Adaptations of Ammonia-Oxidizing Archaea upon Radiation into Moderate Terrestrial and Marine Environments. *MBio*, *11*(5), 2020.06.28.176255. <https://doi.org/10.1128/mBio.02371-20>
- Abby, S. S., Melcher, M., Kerou, M., Krupovic, M., Stieglmeier, M., Rossel, C., ... Schleper, C. (2018). *Candidatus Nitrosocaldus cavascurensis*, an Ammonia Oxidizing, Extremely Thermophilic Archaeon with a Highly Mobile Genome. *Frontiers in Microbiology*, *9*(January), 1–19. <https://doi.org/10.3389/fmicb.2018.00028>
- Amberger, A. (1989). Research on dicyandiamide as a nitrification inhibitor and future outlook. *Communications in Soil Science and Plant Analysis*, *20*(19–20), 1933–1955. <https://doi.org/10.1080/00103628909368195>
- Anderson, J. (1964). The metabolism of hydroxylamine to nitrite by *Nitrosomonas*. *Biochemical Journal*, *91*(1), 8–17. <https://doi.org/10.1042/bj0910008>
- Andrews, S. C. (2010). The Ferritin-like superfamily: Evolution of the biological iron storeman from a rubrerythrin-like ancestor. *Biochimica et Biophysica Acta - General Subjects*, *1800*(8), 691–705. <https://doi.org/10.1016/j.bbagen.2010.05.010>
- Ardini, M., Fiorillo, A., Fittipaldi, M., Stefanini, S., Gatteschi, D., Ilari, A., & Chiancone, E. (2013). *Kineococcus radiotolerans* Dps forms a heteronuclear Mn–Fe ferroxidase center that may explain the Mn-dependent protection against oxidative stress. *Biochimica et Biophysica Acta (BBA) - General Subjects*, *1830*(6), 3745–3755. <https://doi.org/10.1016/j.bbagen.2013.02.003>
- Bai, L., Xie, T., Hu, Q., Deng, C., Zheng, R., & Chen, W. (2015). Genome-wide comparison of ferritin family from Archaea, Bacteria, Eukarya, and Viruses: Its distribution, characteristic motif, and phylogenetic relationship. *Science of Nature*, *102*(9). <https://doi.org/10.1007/s00114-015-1314-3>
- Balasubramanian, R., Smith, S. M., Rawat, S., Yatsunyk, L. A., Stemmler, T. L., & Rosenzweig, A. C. (2010). Oxidation of methane by a biological dicopper centre. *Nature*, *465*(7294), 115–119. <https://doi.org/10.1038/nature08992>
- Bartossek, R., Spang, A., Weidler, G., Lanzen, A., & Schleper, C. (2012). Metagenomic analysis of

- ammonia-oxidizing archaea affiliated with the soil group. *Frontiers in Microbiology*, 3(JUN).
<https://doi.org/10.3389/fmicb.2012.00208>
- Bayer, B., Pelikan, C., Bittner, M. J., Reinthaler, T., Könneke, M., Herndl, G. J., & Offre, P. (2019). Proteomic Response of Three Marine Ammonia-Oxidizing Archaea to Hydrogen Peroxide and Their Metabolic Interactions with a Heterotrophic Alphaproteobacterium. *MSystems*, 4(4), 1–15.
<https://doi.org/10.1128/msystems.00181-19>
- Bayer, B., Vojvoda, J., Offre, P., Alves, R. J. E., Elisabeth, N. H., Garcia, J. A. L., ... Herndl, G. J. (2016). Physiological and genomic characterization of two novel marine thaumarchaeal strains indicates niche differentiation. *ISME Journal*, 10(5), 1051–1063. <https://doi.org/10.1038/ismej.2015.200>
- Beaumont, H. J. E., Hommes, N. G., Sayavedra-Soto, L. A., Arp, D. J., Arciero, D. M., Hooper, A. B., ... van Spanning, R. J. M. (2002). Nitrite Reductase of *Nitrosomonas europaea* Is Not Essential for Production of Gaseous Nitrogen Oxides and Confers Tolerance to Nitrite. *Journal of Bacteriology*, 184(9), 2557–2560. <https://doi.org/10.1128/JB.184.9.2557-2560.2002>
- Beaumont, H. J. E., van Schooten, B., Lens, S. I., Westerhoff, H. V., & van Spanning, R. J. M. (2004). *Nitrosomonas europaea* Expresses a Nitric Oxide Reductase during Nitrification. *Journal of Bacteriology*, 186(13), 4417–4421. <https://doi.org/10.1128/JB.186.13.4417-4421.2004>
- Beeckman, F., Motte, H., & Beeckman, T. (2018). Nitrification in agricultural soils: impact, actors and mitigation. *Current Opinion in Biotechnology*, 50, 166–173.
<https://doi.org/10.1016/j.copbio.2018.01.014>
- Bellapadrona, G., Ardini, M., Ceci, P., Stefanini, S., & Chiancone, E. (2010). Dps proteins prevent Fenton-mediated oxidative damage by trapping hydroxyl radicals within the protein shell. *Free Radical Biology and Medicine*, 48(2), 292–297.
<https://doi.org/10.1016/j.freeradbiomed.2009.10.053>
- Belser, L. W., & Schmidt, E. L. (1981). Inhibitory effect of nitrapyrin on three genera of ammonia-oxidizing nitrifiers. *Applied and Environmental Microbiology*, 41(3), 819–821.
<https://doi.org/10.1016/j.enbuild.2010.09.028>
- Bennett, K., Sadler, N. C., Wright, A. T., Yeager, C., & Hyman, M. R. (2016). Activity-Based Protein Profiling of Ammonia Monooxygenase in *Nitrosomonas europaea*. *Applied and Environmental Microbiology*, 82(8), 2270–2279. <https://doi.org/10.1128/AEM.03556-15>
- Berger, A. B., Vitorino, P. M., & Bogoy, M. (2004). Activity-Based Protein Profiling. *American Journal of Pharmacogenomics*, 4(6), 371–381. <https://doi.org/10.2165/00129785-200404060-00004>

- Berube, P. M., & Stahl, D. A. (2012). The divergent amoc3 subunit of ammonia monooxygenase functions as part of a stress response system in *Nitrosomonas europaea*. *Journal of Bacteriology*, *194*(13), 3448–3456. <https://doi.org/10.1128/JB.00133-12>
- Binda, C., Wang, J., Li, M., Hubalek, F., Mattevi, A., & Edmondson, D. E. (2008). Structural and Mechanistic Studies of Arylalkylhydrazine Inhibition of Human Monoamine Oxidases A and B. *Biochemistry*, *47*(20), 5616–5625. <https://doi.org/10.1021/bi8002814>
- Bintrim, S. B., Donohue, T. J., Handelsman, J., Roberts, G. P., & Goodman, R. M. (1997). Molecular phylogeny of Archaea from soil. *Proceedings of the National Academy of Sciences of the United States of America*, *94*(1), 277–282. <https://doi.org/10.1073/pnas.94.1.277>
- Brochier-Armanet, C., Boussau, B., Gribaldo, S., & Forterre, P. (2008). Mesophilic crenarchaeota: Proposal for a third archaeal phylum, the Thaumarchaeota. *Nature Reviews Microbiology*, *6*(3), 245–252. <https://doi.org/10.1038/nrmicro1852>
- Broda, E. (1977). Two kinds of lithotrophs missing in nature. *Zeitschrift Für Allgemeine Mikrobiologie*, *17*(6), 491–493. <https://doi.org/10.1002/jobm.3630170611>
- Bruijn, P., de Graaf, A. A., Jetten, M. S. M., Robertson, L. A., & Kuenen, J. G. (1995). Growth of *Nitrosomonas europaea* on hydroxylamine. *FEMS Microbiology Letters*, *125*(2–3), 179–184. <https://doi.org/10.1111/j.1574-6968.1995.tb07355.x>
- Burris, R. H., & Roberts, G. P. (1993). Biological Nitrogen Fixation. *Annual Review of Nutrition*, *13*(1), 317–335. <https://doi.org/10.1146/annurev.nu.13.070193.001533>
- Cantera, J. J. L., & Stein, L. Y. (2007). Role of nitrite reductase in the ammonia-oxidizing pathway of *Nitrosomonas europaea*. *Archives of Microbiology*, *188*(4), 349–354. <https://doi.org/10.1007/s00203-007-0255-4>
- Caranto, J. D., & Lancaster, K. M. (2017). Nitric oxide is an obligate bacterial nitrification intermediate produced by hydroxylamine oxidoreductase. *Proceedings of the National Academy of Sciences*, *114*(31), 8217–8222. <https://doi.org/10.1073/pnas.1704504114>
- Cassman, K. G., Dobermann, A., & Walters, D. T. (2002). Agroecosystems, nitrogen-use efficiency, and nitrogen management. *Ambio*, *31*(2), 132–140. <https://doi.org/10.1579/0044-7447-31.2.132>
- Castignetti, D., & Gunner, H. B. (1980). Sequential nitrification by an *Alcaligenes* sp. and *Nitrobacter agilis*. *Canadian Journal of Microbiology*, *26*(9), 1114–1119. <https://doi.org/10.1139/m80-184>
- Cedervall, P., Hooper, A. B., & Wilmot, C. M. (2013). Structural studies of hydroxylamine

- oxidoreductase reveal a unique heme cofactor and a previously unidentified interaction partner. *Biochemistry*, 52(36), 6211–6218. <https://doi.org/10.1021/bi400960w>
- Chain, P., Lamerdin, J., Larimer, F., Regala, W., Lao, V., Land, M., ... Arp, D. (2003). Complete genome sequence of the ammonia-oxidizing bacterium and obligate chemolithoautotroph *Nitrosomonas europaea*. *Journal of Bacteriology*, 185(9), 2759–2773. <https://doi.org/10.1128/JB.185.9.2759-2773.2003>
- Chapuis-Lardy, L., Wrage, N., Metay, A., Chotte, J.-L., & Bernoux, M. (2007). Soils, a sink for N₂O? A review. *Global Change Biology*, 13(1), 1–17. <https://doi.org/10.1111/j.1365-2486.2006.01280.x>
- Chen, Q., & Ni, J. (2011). Heterotrophic nitrification–aerobic denitrification by novel isolated bacteria. *Journal of Industrial Microbiology & Biotechnology*, 38(9), 1305–1310. <https://doi.org/10.1007/s10295-010-0911-6>
- Chiancone, E., & Ceci, P. (2010). The multifaceted capacity of Dps proteins to combat bacterial stress conditions: Detoxification of iron and hydrogen peroxide and DNA binding. *Biochimica et Biophysica Acta - General Subjects*, 1800(8), 798–805. <https://doi.org/10.1016/j.bbagen.2010.01.013>
- Cho, C. M. H., Yan, T., Liu, X., Wu, L., Zhou, J., & Stein, L. Y. (2006). Transcriptome of a *Nitrosomonas europaea* mutant with a disrupted nitrite reductase gene (*nirK*). *Applied and Environmental Microbiology*, 72(6), 4450–4454. <https://doi.org/10.1128/AEM.02958-05>
- Chu, Y. J., Lee, J. Y., Shin, S. R., & Kim, G. J. (2015). A Method for Cell Culture and Maintenance of Ammonia-Oxidizing Archaea in Agar Stab. *Indian Journal of Microbiology*, 55(4), 460–463. <https://doi.org/10.1007/s12088-015-0536-6>
- Ciais, P., Sabine, C., Bala, G., Bopp, L., Brovkin, V., Canadell, J., ... Thornton, P. (2014). Carbon and Other Biogeochemical Cycles. *Climate Change 2013 – The Physical Science Basis: Working Group I Contribution to the Fifth Assessment Report of the Intergovernmental Panel on Climate Change*, 465–570. [https://doi.org/DOI: 10.1017/CBO9781107415324.015](https://doi.org/DOI:10.1017/CBO9781107415324.015)
- Cole, J. A., & Brown, C. M. (1980). Nitrite Reduction to Ammonia by Fermentative Bacteria: a Short Circuit in the Biological Nitrogen Cycle. *FEMS Microbiology Letters*, 7(2), 65–72. <https://doi.org/10.1111/j.1574-6941.1980.tb01578.x>
- Coskun, D., Britto, D. T., Shi, W., & Kronzucker, H. J. (2017). Nitrogen transformations in modern agriculture and the role of biological nitrification inhibition. *Nature Plants*, 3(June), 1–10. <https://doi.org/10.1038/nplants.2017.74>

- Costa, E., Pérez, J., & Kreft, J. U. (2006). Why is metabolic labour divided in nitrification? *Trends in Microbiology*, *14*(5), 213–219. <https://doi.org/10.1016/j.tim.2006.03.006>
- Culpepper, M. A., & Rosenzweig, A. C. (2012). Architecture and active site of particulate methane monoxygenase. *Critical Reviews in Biochemistry and Molecular Biology*, *47*(6), 483–492. <https://doi.org/10.3109/10409238.2012.697865>
- Daebeler, A., Herbold, C. W., Vierheilig, J., Sedlacek, C. J., Pjevac, P., Albertsen, M., ... Wagner, M. (2018). Cultivation and genomic analysis of “*Candidatus Nitrosocaldus islandicus*,” an obligately thermophilic, ammonia-oxidizing thaumarchaeon from a hot spring biofilm in Graendalur valley, Iceland. *Frontiers in Microbiology*, *9*(FEB), 1–16. <https://doi.org/10.3389/fmicb.2018.00193>
- Daims, H., Lebedeva, E. V., Pjevac, P., Han, P., Herbold, C., Albertsen, M., ... Wagner, M. (2015). Complete nitrification by *Nitrospira* bacteria. *Nature*, *528*(7583), 504–509. <https://doi.org/10.1038/nature16461>
- Daims, H., Lücker, S., & Wagner, M. (2016). A New Perspective on Microbes Formerly Known as Nitrite-Oxidizing Bacteria. *Trends in Microbiology*, *24*(9), 699–712. <https://doi.org/10.1016/j.tim.2016.05.004>
- Datta, S., Ikeda, T., Kano, K., & Mathews, F. S. (2003). Structure of the phenylhydrazine adduct of the quinoxinoprotein amine dehydrogenase from *Paracoccus denitrificans* at 1.7 Å resolution. *Acta Crystallographica Section D Biological Crystallography*, *59*(9), 1551–1556. <https://doi.org/10.1107/S090744490301429X>
- de Almeida, N. M., Neumann, S., Mesman, R. J., Ferousi, C., Keltjens, J. T., Jetten, M. S. M., ... van Niftrik, L. (2015). Immunogold Localization of Key Metabolic Enzymes in the Anammoxosome and on the Tubule-Like Structures of *Kuenenia stuttgartiensis*. *Journal of Bacteriology*, *197*(14), 2432–2441. <https://doi.org/10.1128/JB.00186-15>
- DeLong, E. F. (1992). Archaea in coastal marine environments. *Proceedings of the National Academy of Sciences of the United States of America*, *89*(12), 5685–5689. <https://doi.org/10.1073/pnas.89.12.5685>
- Delwiche, E. A. (1961). Catalase of *Pediococcus cerevisiae*. *Journal of Bacteriology*, *81*(3), 416–418. <https://doi.org/10.1128/jb.81.3.416-418.1961>
- Di, H. J., & Cameron, K. C. (2002). Nitrate leaching in temperate agroecosystems: Sources, factors and mitigating strategies. *Nutrient Cycling in Agroecosystems*, *64*(3), 237–256. <https://doi.org/10.1023/A:1021471531188>

- Di, Hong Jie, & Cameron, K. C. (2016). Inhibition of nitrification to mitigate nitrate leaching and nitrous oxide emissions in grazed grassland: a review. *Journal of Soils and Sediments*, *16*(5), 1401–1420. <https://doi.org/10.1007/s11368-016-1403-8>
- Doane, T. A. (2017). The Abiotic Nitrogen Cycle. *ACS Earth and Space Chemistry*, *1*(7), 411–421. <https://doi.org/10.1021/acsearthspacechem.7b00059>
- Edgar, R. C. (2004). MUSCLE: multiple sequence alignment with high accuracy and high throughput. *Nucleic Acids Research*, *32*(5), 1792–1797. <https://doi.org/10.1093/nar/gkh340>
- Erickson, R. H., & Hooper, A. B. (1972). Preliminary characterization of a variant co-binding heme protein from *Nitrosomonas*. *BBA - Bioenergetics*, *275*(2), 231–244. [https://doi.org/10.1016/0005-2728\(72\)90044-8](https://doi.org/10.1016/0005-2728(72)90044-8)
- Erismann, J. W., Sutton, M. A., Galloway, J., Klimont, Z., & Winiwarter, W. (2008). How a century of ammonia synthesis changed the world. *Nature Geoscience*, *1*(10), 636–639. <https://doi.org/10.1038/ngeo325>
- Ettwig, K. F., Butler, M. K., Le Paslier, D., Pelletier, E., Mangenot, S., Kuypers, M. M. M., ... Strous, M. (2010). Nitrite-driven anaerobic methane oxidation by oxygenic bacteria. *Nature*, *464*(7288), 543–548. <https://doi.org/10.1038/nature08883>
- Fowler, D., Coyle, M., Skiba, U., Sutton, M. A., Cape, J. N., Reis, S., ... Voss, M. (2013). The global nitrogen cycle in the Twentyfirst century. *Philosophical Transactions of the Royal Society B: Biological Sciences*, *368*(1621), 1–13. <https://doi.org/10.1098/rstb.2013.0164>
- Frankland, P., & Frankland, G. (1890). The Nitrifying Process and Its Specific Ferment. *Proceedings of the Royal Society of London (1854-1905)*, *47*, 296–298. Retrieved from <http://dx.doi.org/10.1098/rspl.1889.0096>
- Fuhrman, J. A., & McCallum, K. (1992). Novel major archaeobacterial group from marine plankton. *Nature*, *356*(6365), 148–149. <https://doi.org/10.1038/356148a0>
- Gauss, G. H., Benas, P., Wiedenheft, B., Young, M., Douglas, T., & Lawrence, C. M. (2006). Structure of the DPS-Like Protein from *Sulfolobus solfataricus* Reveals a Bacterioferritin-Like Dimetal Binding Site within a DPS-Like Dodecameric, (eq I), 10815–10827.
- Giguere, A. T., Taylor, A. E., Suwa, Y., Myrold, D. D., & Bottomley, P. J. (2017). Uncoupling of ammonia oxidation from nitrite oxidation: Impact upon nitrous oxide production in non-cropped Oregon soils. *Soil Biology and Biochemistry*, *104*, 30–38. <https://doi.org/10.1016/j.soilbio.2016.10.011>

- Gilch, S., Meyer, O., & Schmidt, I. (2009). A soluble form of ammonia monooxygenase in *Nitrosomonas europaea*. *Biological Chemistry*, 390(9), 863–873. <https://doi.org/10.1515/BC.2009.085>
- Gilch, S., Vogel, M., Lorenz, M. W., Meyer, O., & Schmidt, I. (2009). Interaction of the mechanism-based inactivator acetylene with ammonia monooxygenase of *Nitrosomonas europaea*. *Microbiology*, 155(1), 279–284. <https://doi.org/10.1099/mic.0.023721-0>
- Green, M. J., & Hill, H. A. O. (1984). [1] Chemistry of dioxygen. In *Methods in Enzymology* (Vol. 105, pp. 3–22). [https://doi.org/10.1016/S0076-6879\(84\)05004-7](https://doi.org/10.1016/S0076-6879(84)05004-7)
- Grizzetti, B., Bouraoui, F., Billen, G., van Grinsven, H., Cardoso, A. C., Thieu, V., ... Johnes, P. (2011). Nitrogen as a threat to European water quality. *The European Nitrogen Assessment*, 379–404. <https://doi.org/10.1017/CBO9780511976988.020>
- Guo, Y. J., Di, H. J., Cameron, K. C., Li, B., Podolyan, A., Moir, J. L., ... He, J. Z. (2013). Effect of 7-year application of a nitrification inhibitor, dicyandiamide (DCD), on soil microbial biomass, protease and deaminase activities, and the abundance of bacteria and archaea in pasture soils. *Journal of Soils and Sediments*, 13(4), 753–759. <https://doi.org/10.1007/s11368-012-0646-2>
- Hakemian, A. S., Kondapalli, K. C., Telsler, J., Hoffman, B. M., Stemmler, T. L., & Rosenzweig, A. C. (2008). The metal centres of particulate methane mono-oxygenase. *Biochemical Society Transactions*, 36(6), 1134–1137. <https://doi.org/10.1042/bst0361134>
- Haroon, M. F., Hu, S., Shi, Y., Imelfort, M., Keller, J., Hugenholtz, P., ... Tyson, G. W. (2013). Anaerobic oxidation of methane coupled to nitrate reduction in a novel archaeal lineage. *Nature*, 500(7464), 567–570. <https://doi.org/10.1038/nature12375>
- Hayden, J. A., & Hendrich, M. P. (2010). EPR spectroscopy and catalase activity of manganese-bound DNA-binding protein from nutrient starved cells. *JBIC Journal of Biological Inorganic Chemistry*, 15(5), 729–736. <https://doi.org/10.1007/s00775-010-0640-3>
- Heil, J., Vereecken, H., & Brüggemann, N. (2016). A review of chemical reactions of nitrification intermediates and their role in nitrogen cycling and nitrogen trace gas formation in soil. *European Journal of Soil Science*, 67(1), 23–39. <https://doi.org/10.1111/ejss.12306>
- Herbold, C. W., Lehtovirta-Morley, L. E., Jung, M.-Y., Jehmlich, N., Hausmann, B., Han, P., ... Gubry-Rangin, C. (2017). Ammonia-oxidising archaea living at low pH: Insights from comparative genomics. *Environmental Microbiology*, 19(12), 4939–4952. <https://doi.org/10.1111/1462-2920.13971>
- Hink, L., Nicol, G. W., & Prosser, J. I. (2017). Archaea produce lower yields of N₂O than bacteria during

- aerobic ammonia oxidation in soil. *Environmental Microbiology*, 19(12), 4829–4837.
<https://doi.org/10.1111/1462-2920.13282>
- Hooper, A. B., & Nason, A. (1965). Characterization of hydroxylamine-cytochrome c reductase from the chemoautotrophs *Nitrosomonas europaea* and *Nitrosocystis oceanus*. *Journal of Biological Chemistry*, 240(10), 4044–4057.
- Hosseinzadeh, P., Tian, S., Marshall, N. M., Hemp, J., Mullen, T., Nilges, M. J., ... Lu, Y. (2016). A Purple Cupredoxin from *Nitrosopumilus maritimus* Containing a Mononuclear Type 1 Copper Center with an Open Binding Site. *Journal of the American Chemical Society*, 138(20), 6324–6327.
<https://doi.org/10.1021/jacs.5b13128>
- Hu, Z., Wessels, H. J. C. T., van Alen, T., Jetten, M. S. M., & Kartal, B. (2019). Nitric oxide-dependent anaerobic ammonium oxidation. *Nature Communications*, 10(1), 1244.
<https://doi.org/10.1038/s41467-019-09268-w>
- Hyman, M. R., Kim, C. Y., & Arp, D. J. (1990). Inhibition of ammonia monooxygenase in *Nitrosomonas europaea* by carbon disulfide. *Journal of Bacteriology*, 172(9), 4775–4782.
<https://doi.org/10.1128/jb.172.9.4775-4782.1990>
- Hyman, M R, Murton, I. B., & Arp, D. J. (1988). Interaction of Ammonia Monooxygenase from *Nitrosomonas europaea* with Alkanes, Alkenes, and Alkynes. *Applied and Environmental Microbiology*, 54(12), 3187–3190. <https://doi.org/10.1021/es3042912>
- Hyman, M R, & Wood, P. M. (1985). Suicidal inactivation and labelling of ammonia mono-oxygenase by acetylene. *Biochemical Journal*, 227(3), 719–725. <https://doi.org/10.1042/bj2270719>
- Hyman, Michael R., & Wood, P. M. (1984). Ethylene oxidation by *Nitrosomonas europaea*. *Archives of Microbiology*, 137(2), 155–158. <https://doi.org/10.1007/BF00414458>
- Iizumi, T., Mizumoto, M., & Nakamura, K. (1998). A bioluminescence assay using *Nitrosomonas europaea* for rapid and sensitive detection of nitrification inhibitors. *Applied and Environmental Microbiology*, 64(10), 3656–3662.
- Johnston, M. A., & Delwiche, E. A. (1965). Isolation and Characterization of the Cyanide-Resistant and Azide-Resistant Catalase of *Lactobacillus plantarum*. *Journal of Bacteriology*, 90(2), 352–356.
<https://doi.org/10.1128/jb.90.2.352-356.1965>
- Jones, C. M., Graf, D. R. H., Bru, D., Philippot, L., & Hallin, S. (2013). The unaccounted yet abundant nitrous oxide-reducing microbial community: a potential nitrous oxide sink. *The ISME Journal*, 7(2), 417–426. <https://doi.org/10.1038/ismej.2012.125>

- Juliette, L. Y., Hyman, M. R., & Arp, D. J. (1993). Inhibition of Ammonia Oxidation in *Nitrosomonas europaea* by Sulfur Compounds: Thioethers Are Oxidized to Sulfoxides by Ammonia Monooxygenase. *Applied and Environmental Microbiology*, 59(11), 3718–3727. <https://doi.org/10.1128/aem.59.11.3718-3727.1993>
- Jung, M. Y., Sedlacek, C. J., Kits, K. D., Mueller, A. J., Rhee, S. K., Hink, L., ... Wagner, M. (2021). Ammonia-oxidizing archaea possess a wide range of cellular ammonia affinities. *ISME Journal*, (March), 2021.03.02.433310. <https://doi.org/10.1038/s41396-021-01064-z>
- Kampschreur, M. J., Temmink, H., Kleerebezem, R., Jetten, M. S. M., & van Loosdrecht, M. C. M. (2009). Nitrous oxide emission during wastewater treatment. *Water Research*, 43(17), 4093–4103. <https://doi.org/10.1016/j.watres.2009.03.001>
- Kane, D. A., & Williamson, K. J. (1983). Bacterial toxicity and metabolism of hydrazine fuels. *Archives of Environmental Contamination and Toxicology*, 12(4), 447–453. <https://doi.org/10.1007/BF01057588>
- Karner, M. B., Delong, E. F., & Karl, D. M. (2001). Archaeal dominance in the mesopelagic zone of the Pacific Ocean. *Nature*, 409(6819), 507–510. <https://doi.org/10.1038/35054051>
- Kartal, B., & Keltjens, J. T. (2016). Anammox Biochemistry: a Tale of Heme c Proteins. *Trends in Biochemical Sciences*, 41(12), 998–1011. <https://doi.org/10.1016/j.tibs.2016.08.015>
- Kaur-Bhambra, J., Wardak, D. L. R., Prosser, J. I., & Gubry-Rangin, C. (2022). Revisiting plant biological nitrification inhibition efficiency using multiple archaeal and bacterial ammonia-oxidising cultures. *Biology and Fertility of Soils*, 58(3), 241–249. <https://doi.org/10.1007/s00374-020-01533-1>
- Keener, W. K., & Arp, D. J. (1994). Transformations of aromatic compounds by *Nitrosomonas europaea*. *Applied and Environmental Microbiology*, 60(6), 1914–1920. <https://doi.org/10.1128/aem.60.6.1914-1920.1994>
- Keener, William K., & Arp, D. J. (1993). Kinetic Studies of Ammonia Monooxygenase Inhibition in *Nitrosomonas europaea* by Hydrocarbons and Halogenated Hydrocarbons in an Optimized Whole-Cell Assay. *Applied and Environmental Microbiology*, 59(8), 2501–2510. <https://doi.org/10.1128/aem.59.8.2501-2510.1993>
- Kerou, M., Offre, P., Valledor, L., Abby, S. S., Melcher, M., Nagler, M., ... Schleper, C. (2016). Proteomics and comparative genomics of *Nitrososphaera viennensis* reveal the core genome and adaptations of archaeal ammonia oxidizers. *Proceedings of the National Academy of Sciences*,

113(49), E7937–E7946. <https://doi.org/10.1073/pnas.1601212113>

- Kim, J.-G., Park, S.-J., Sinninghe Damsté, J. S., Schouten, S., Rijpstra, W. I. C., Jung, M.-Y., ... Rhee, S.-K. (2016). Hydrogen peroxide detoxification is a key mechanism for growth of ammonia-oxidizing archaea. *Proceedings of the National Academy of Sciences*, 113(28), 7888–7893. <https://doi.org/10.1073/pnas.1605501113>
- Kits, K. D., Jung, M.-Y., Vierheilig, J., Pjevac, P., Sedlacek, C. J., Liu, S., ... Daims, H. (2019). Low yield and abiotic origin of N₂O formed by the complete nitrifier *Nitrospira inopinata*. *Nature Communications*, 10(1), 1836. <https://doi.org/10.1038/s41467-019-09790-x>
- Klein, T., Poghosyan, L., Barclay, J. E., Murrell, J. C., Hutchings, M. I., & Lehtovirta-Morley, L. E. (2022). Cultivation of ammonia-oxidising archaea on solid medium. *FEMS Microbiology Letters*, 369(1), 1–9. <https://doi.org/10.1093/femsle/fnac029>
- Klotz, M. G., & Stein, L. Y. (2014). Genomics of Ammonia-Oxidizing Bacteria and Insights into Their Evolution. *Nitrification*, 57–94. <https://doi.org/10.1128/9781555817145.ch4>
- Kobayashi, S., Hira, D., Yoshida, K., Toyofuku, M., Shida, Y., Ogasawara, W., ... Oshiki, M. (2018). Nitric Oxide Production from Nitrite Reduction and Hydroxylamine Oxidation by Copper-containing Dissimilatory Nitrite Reductase (NirK) from the Aerobic Ammonia-oxidizing Archaeon, *Nitrososphaera viennensis*. *Microbes and Environments*, 33(4), 428–434. <https://doi.org/10.1264/jsme2.ME18058>
- Koch, H., van Kessel, M. A. H. J., & Lücker, S. (2019). Complete nitrification: insights into the ecophysiology of comammox *Nitrospira*. *Applied Microbiology and Biotechnology*, 103(1), 177–189. <https://doi.org/10.1007/s00253-018-9486-3>
- Könneke, M., Bernhard, A. E., De La Torre, J. R., Walker, C. B., Waterbury, J. B., & Stahl, D. A. (2005). Isolation of an autotrophic ammonia-oxidizing marine archaeon. *Nature*, 437(7058), 543–546. <https://doi.org/10.1038/nature03911>
- Konneke, M., Schubert, D. M., Brown, P. C., Hugler, M., Standfest, S., Schwander, T., ... Berg, I. A. (2014). Ammonia-oxidizing archaea use the most energy-efficient aerobic pathway for CO₂ fixation. *Proceedings of the National Academy of Sciences*, 111(22), 8239–8244. <https://doi.org/10.1073/pnas.1402028111>
- Kono, Y., & Fridovich, I. (1983). Isolation and characterization of the pseudocatalase of *Lactobacillus plantarum*. *The Journal of Biological Chemistry*, 258(10), 6015–6019. Retrieved from <http://www.ncbi.nlm.nih.gov/pubmed/6853475>

- Kozłowski, J. A., Kits, K. D., & Stein, L. Y. (2016). Genome Sequence of *Nitrosomonas communis* Strain Nm2, a Mesophilic Ammonia-Oxidizing Bacterium Isolated from Mediterranean Soil, *4*(1), 2–3. <https://doi.org/10.1128/genomeA.01541-15>. Copyright
- Kozłowski, J. A., Price, J., & Stein, L. Y. (2014). Revision of N₂O-producing pathways in the ammonia-oxidizing bacterium *Nitrosomonas europaea* ATCC 19718. *Applied and Environmental Microbiology*, *80*(16), 4930–4935. <https://doi.org/10.1128/AEM.01061-14>
- Kozłowski, J. A., Stieglmeier, M., Schleper, C., Klotz, M. G., & Stein, L. Y. (2016). Pathways and key intermediates required for obligate aerobic ammonia-dependent chemolithotrophy in bacteria and Thaumarchaeota. *The ISME Journal*, *10*(8), 1836–1845. <https://doi.org/10.1038/ismej.2016.2>
- Kraft, B., Tegetmeyer, H. E., Sharma, R., Klotz, M. G., Ferdelman, T. G., Hettich, R. L., ... Strous, M. (2014). The environmental controls that govern the end product of bacterial nitrate respiration. *Science*, *345*(6197), 676–679. <https://doi.org/10.1126/science.1254070>
- Kuypers, M. M. M., Marchant, H. K., & Kartal, B. (2018). The microbial nitrogen-cycling network. *Nature Reviews Microbiology*, *16*(5), 263–276. <https://doi.org/10.1038/nrmicro.2018.9>
- Ladha, J. K., Pathak, H., J. Krupnik, T., Six, J., & van Kessel, C. (2005). Efficiency of Fertilizer Nitrogen in Cereal Production: Retrospects and Prospects. In *Advances in Agronomy* (Vol. 87, pp. 85–156). [https://doi.org/10.1016/S0065-2113\(05\)87003-8](https://doi.org/10.1016/S0065-2113(05)87003-8)
- Lancaster, K. M., Caranto, J. D., Majer, S. H., & Smith, M. A. (2018). Alternative Bioenergy: Updates to and Challenges in Nitrification Metalloenzymology. *Joule*, *2*(3), 421–441. <https://doi.org/10.1016/j.joule.2018.01.018>
- Landreau, M., You, H. J., Stahl, D. A., & Winkler, M. K. H. (2021). Immobilization of active ammonia-oxidizing archaea in hydrogel beads. *Npj Clean Water*, *4*(1). <https://doi.org/10.1038/s41545-021-00134-1>
- Lawton, T. J., Ham, J., Sun, T., & Rosenzweig, A. C. (2014). Structural conservation of the B subunit in the ammonia monooxygenase/particulate methane monooxygenase superfamily. *Proteins: Structure, Function and Bioinformatics*, *82*(9), 2263–2267. <https://doi.org/10.1002/prot.24535>
- Lehtovirta-Morley, L. E. (2018). Ammonia oxidation: Ecology, physiology, biochemistry and why they must all come together. *FEMS Microbiology Letters*, *365*(9), 1–9. <https://doi.org/10.1093/femsle/fny058>
- Lehtovirta-Morley, L. E., Ge, C., Ross, J., Yao, H., Nicol, G. W., & Prosser, J. I. (2014). Characterisation

- of terrestrial acidophilic archaeal ammonia oxidisers and their inhibition and stimulation by organic compounds. *FEMS Microbiology Ecology*, *89*(3), 542–552. <https://doi.org/10.1111/1574-6941.12353>
- Lehtovirta-Morley, L. E., Ross, J., Hink, L., Weber, E. B., Gubry-Rangin, C., Thion, C., ... Nicol, G. W. (2016). Isolation of ‘*Candidatus Nitrosocosmicus franklandus*’, a novel ureolytic soil archaeal ammonia oxidiser with tolerance to high ammonia concentration. *FEMS Microbiology Ecology*, *92*(5), fiw057. <https://doi.org/10.1093/femsec/fiw057>
- Lehtovirta-Morley, L. E., Sayavedra-Soto, L. A., Gallois, N., Schouten, S., Stein, L. Y., Prosser, J. I., & Nicol, G. W. (2016). Identifying Potential Mechanisms Enabling Acidophily in the Ammonia-Oxidizing Archaeon “*Candidatus Nitrosotalea devanattera*.” *Applied and Environmental Microbiology*, *82*(9), 2608–2619. <https://doi.org/10.1128/AEM.04031-15>
- Lehtovirta-Morley, L. E., Stoecker, K., Vilcinskas, A., Prosser, J. I., & Nicol, G. W. (2011). Cultivation of an obligate acidophilic ammonia oxidizer from a nitrifying acid soil. *Proceedings of the National Academy of Sciences*, *108*(38), 15892–15897. <https://doi.org/10.1073/pnas.1107196108>
- Lehtovirta-Morley, L. E., Verhamme, D. T., Nicol, G. W., & Prosser, J. I. (2013). Effect of nitrification inhibitors on the growth and activity of *Nitrosotalea devanattera* in culture and soil. *Soil Biology and Biochemistry*, *62*, 129–133. <https://doi.org/10.1016/j.soilbio.2013.01.020>
- Levičnik-Höfferle, Š., Nicol, G. W., Ausec, L., Mandić-Mulec, I., & Prosser, J. I. (2012). Stimulation of thaumarchaeal ammonia oxidation by ammonia derived from organic nitrogen but not added inorganic nitrogen. *FEMS Microbiology Ecology*, *80*(1), 114–123. <https://doi.org/10.1111/j.1574-6941.2011.01275.x>
- Liang, L., & Astruc, D. (2011). The copper(I)-catalyzed alkyne-azide cycloaddition (CuAAC) “click” reaction and its applications. An overview. *Coordination Chemistry Reviews*, *255*(23–24), 2933–2945. <https://doi.org/10.1016/j.ccr.2011.06.028>
- Lieberman, R. L., Arciero, D. M., Hooper, A. B., & Rosenzweig, A. C. (2001). Crystal structure of a novel red copper protein from *Nitrosomonas europaea*. *Biochemistry*, *40*(19), 5674–5681. <https://doi.org/10.1021/bi0102611>
- Lieberman, R. L., & Rosenzweig, A. C. (2005). Crystal structure of a membrane-bound metalloenzyme that catalyses the biological oxidation of methane. *Nature*, *434*(7030), 177–182. <https://doi.org/10.1038/nature03311>
- Lin, Z., Wang, X., Bustin, K. A., He, L., Suci, R. M., Schek, N., ... Matthews, M. L. (2020). Hydrazines as

- versatile chemical biology probes and drug-discovery tools for cofactor-dependent enzymes. *BioRxiv*, 1–15. <https://doi.org/10.1101/2020.06.17.154864>
- Liu, L., Li, S., Han, J., Lin, W., & Luo, J. (2019). A Two-Step Strategy for the Rapid Enrichment of *Nitrosocosmicus*-Like Ammonia-Oxidizing Thaumarchaea. *Frontiers in Microbiology*, *10*(APR), 1–10. <https://doi.org/10.3389/fmicb.2019.00875>
- Liu, L., Liu, M., Jiang, Y., Lin, W., & Luo, J. (2021). Production and Excretion of Polyamines To Tolerate High Ammonia, a Case Study on Soil Ammonia-Oxidizing Archaeon “*Candidatus Nitrosocosmicus agrestis*.” *MSystems*, *6*(1), 1–17. <https://doi.org/10.1128/mSystems.01003-20>
- Liu, T., Hu, S., & Guo, J. (2019). Enhancing mainstream nitrogen removal by employing nitrate/nitrite-dependent anaerobic methane oxidation processes. *Critical Reviews in Biotechnology*, *39*(5), 732–745. <https://doi.org/10.1080/07388551.2019.1598333>
- Liu, T., Hu, S., Yuan, Z., & Guo, J. (2019). High-level nitrogen removal by simultaneous partial nitrification, anammox and nitrite/nitrate-dependent anaerobic methane oxidation. *Water Research*, *166*, 115057. <https://doi.org/10.1016/j.watres.2019.115057>
- Logan, M. S. P., & Hooper, A. B. (1995). Suicide Inactivation of Hydroxylamine Oxidoreductase of *Nitrosomonas europaea* by Organohydrazines. *Biochemistry*, *34*(28), 9257–9264. <https://doi.org/10.1021/bi00028a039>
- Lu, X., Bottomley, P. J., & Myrold, D. D. (2015). Contributions of ammonia-oxidizing archaea and bacteria to nitrification in Oregon forest soils. *Soil Biology and Biochemistry*, *85*, 54–62. <https://doi.org/10.1016/j.soilbio.2015.02.034>
- Luesken, F. A., Sánchez, J., van Alen, T. A., Sanabria, J., Op den Camp, H. J. M., Jetten, M. S. M., & Kartal, B. (2011). Simultaneous Nitrite-Dependent Anaerobic Methane and Ammonium Oxidation Processes. *Applied and Environmental Microbiology*, *77*(19), 6802–6807. <https://doi.org/10.1128/AEM.05539-11>
- Maalcke, W. J., Dietl, A., Marritt, S. J., Butt, J. N., Jetten, M. S. M., Keltjens, J. T., ... Kartal, B. (2014). Structural basis of biological nitrogen generation by octaheme oxidoreductases. *Journal of Biological Chemistry*, *289*(3), 1228–1242. <https://doi.org/10.1074/jbc.M113.525147>
- Magri, A., Rusalleda, M., Vil, A., Akaboci, T. R. V, Balaguer, M. D., & Llenas, J. M. (2021). Partial Nitrification-Anammox System Treating Landfill Leachate.
- Marchant, H. K., Lavik, G., Holtappels, M., & Kuypers, M. M. M. (2014). The Fate of Nitrate in Intertidal Permeable Sediments. *PLoS ONE*, *9*(8), e104517. <https://doi.org/10.1371/journal.pone.0104517>

- Marsden, K. A., Marín-Martínez, A. J., Vallejo, A., Hill, P. W., Jones, D. L., & Chadwick, D. R. (2016). The mobility of nitrification inhibitors under simulated ruminant urine deposition and rainfall: a comparison between DCD and DMPP. *Biology and Fertility of Soils*, 52(4), 491–503. <https://doi.org/10.1007/s00374-016-1092-x>
- Marsden, K. A., Scowen, M., Hill, P. W., Jones, D. L., & Chadwick, D. R. (2015). Plant acquisition and metabolism of the synthetic nitrification inhibitor dicyandiamide and naturally-occurring guanidine from agricultural soils. *Plant and Soil*, 395(1–2), 201–214. <https://doi.org/10.1007/s11104-015-2549-7>
- Martens-Habbena, W., Qin, W., Horak, R. E. A., Urakawa, H., Schauer, A. J., Moffett, J. W., ... Stahl, D. A. (2015). The production of nitric oxide by marine ammonia-oxidizing archaea and inhibition of archaeal ammonia oxidation by a nitric oxide scavenger. *Environmental Microbiology*, 17(7), 2261–2274. <https://doi.org/10.1111/1462-2920.12677>
- Matthews, M. L., He, L., Horning, B. D., Olson, E. J., Correia, B. E., Yates, J. R., ... Cravatt, B. F. (2017). Chemoproteomic profiling and discovery of protein electrophiles in human cells. *Nature Chemistry*, 9(3), 234–243. <https://doi.org/10.1038/nchem.2645>
- Meiklejohn, J. (1950). The isolation of *Nitrosomonas europaea* in pure culture. *Journal of General Microbiology*, 4(2), 185–191. <https://doi.org/10.1099/00221287-4-2-185>
- Misra, H. P., & Fridovich, I. (1976). The oxidation of phenylhydrazine: superoxide and mechanism. *Biochemistry*, 15(3), 681–687. <https://doi.org/10.1021/bi00648a036>
- Mkhabela, M. S., Gordon, R., Burton, D., Madani, A., & Hart, W. (2006). Effect of lime, dicyandiamide and soil water content on ammonia and nitrous oxide emissions following application of liquid hog manure to a marshland soil. *Plant and Soil*, 284(1–2), 351–361. <https://doi.org/10.1007/s11104-006-0056-6>
- Morris, J. J., Johnson, Z. I., Szul, M. J., Keller, M., & Zinser, E. R. (2011). Dependence of the cyanobacterium *Prochlorococcus* on hydrogen peroxide scavenging microbes for growth at the ocean's surface. *PLoS ONE*, 6(2). <https://doi.org/10.1371/journal.pone.0016805>
- Nicholls, P. (2012). Classical catalase: Ancient and modern. *Archives of Biochemistry and Biophysics*, 525(2), 95–101. <https://doi.org/10.1016/j.abb.2012.01.015>
- Nicol, G. W., Hink, L., Gubry-Rangin, C., Prosser, J. I., & Lehtovirta-Morley, L. E. (2019). Genome Sequence of “*Candidatus Nitrosocosmicus franklandus*” C13, a Terrestrial Ammonia-Oxidizing Archaeon. *Microbiology Resource Announcements*, 8(40), 1–3.

<https://doi.org/10.1128/MRA.00435-19>

- Nishigaya, Y., Fujimoto, Z., & Yamazaki, T. (2016). Optimized inhibition assays reveal different inhibitory responses of hydroxylamine oxidoreductases from beta- and gamma-proteobacterial ammonium-oxidizing bacteria. *Biochemical and Biophysical Research Communications*, 476(3), 127–133. <https://doi.org/10.1016/j.bbrc.2016.05.041>
- Palomo, A., Pedersen, A. G., Fowler, S. J., Dechesne, A., Sicheritz-Pontén, T., & Smets, B. F. (2018). Comparative genomics sheds light on niche differentiation and the evolutionary history of comammox *Nitrospira*. *ISME Journal*, 12(7), 1779–1793. <https://doi.org/10.1038/s41396-018-0083-3>
- Pan, B., Lam, S. K., Mosier, A., Luo, Y., & Chen, D. (2016). Ammonia volatilization from synthetic fertilizers and its mitigation strategies: A global synthesis. *Agriculture, Ecosystems and Environment*, 232, 283–289. <https://doi.org/10.1016/j.agee.2016.08.019>
- Papen, H., von Berg, R., Hinkel, I., Thoene, B., & Rennenberg, H. (1989). Heterotrophic nitrification by *Alcaligenes faecalis*: NO₂⁻, NO₃⁻, N₂O, and NO production in exponentially growing cultures. *Applied and Environmental Microbiology*, 55(8), 2068–2072. <https://doi.org/10.1128/aem.55.8.2068-2072.1989>
- Picone, N., Pol, A., Mesman, R., van Kessel, M. A. H. J., Cremers, G., van Gelder, A. H., ... Op den Camp, H. J. M. (2021). Ammonia oxidation at pH 2.5 by a new gammaproteobacterial ammonia-oxidizing bacterium. *The ISME Journal*, 15(4), 1150–1164. <https://doi.org/10.1038/s41396-020-00840-7>
- Pjevac, P., Schauburger, C., Poghosyan, L., Herbold, C. W., van Kessel, M. A. H. J., Daebeler, A., ... Daims, H. (2017). AmoA-targeted polymerase chain reaction primers for the specific detection and quantification of comammox *Nitrospira* in the environment. *Frontiers in Microbiology*, 8(AUG), 1–11. <https://doi.org/10.3389/fmicb.2017.01508>
- Powell, S. J., & Prosser, J. I. (1986). Inhibition of ammonium oxidation by nitrapyrin in soil and liquid culture. *Applied and Environmental Microbiology*, 52(4), 782–787. <https://doi.org/10.1128/aem.52.4.782-787.1986>
- Purwantini, E., & Mukhopadhyay, B. (2009). Conversion of NO₂ to NO by reduced coenzyme F420 protects mycobacteria from nitrosative damage. *Proceedings of the National Academy of Sciences*, 106(15), 6333–6338. <https://doi.org/10.1073/pnas.0812883106>
- Qin, W., Amin, S. A., Lundeen, R. A., Heal, K. R., Martens-Habbena, W., Turkarslan, S., ... Stahl, D. A.

- (2018). Stress response of a marine ammonia-oxidizing archaeon informs physiological status of environmental populations. *ISME Journal*, 12(2), 508–519. <https://doi.org/10.1038/ismej.2017.186>
- Qin, W., Amin, S. A., Martens-Habbena, W., Walker, C. B., Urakawa, H., Devol, A. H., ... Stahl, D. A. (2014). Marine ammonia-oxidizing archaeal isolates display obligate mixotrophy and wide ecotypic variation. *Proceedings of the National Academy of Sciences*, 111(34), 12504–12509. <https://doi.org/10.1073/pnas.1324115111>
- Rasche, M. E., Hyman, M. R., & Arp, D. J. (1991). Factors Limiting Aliphatic Chlorocarbon Degradation by *Nitrosomonas europaea*: Cometabolic Inactivation of Ammonia Monooxygenase and Substrate Specificity. *Applied and Environmental Microbiology*, 57(10), 2986–2994. <https://doi.org/10.1128/aem.57.10.2986-2994.1991>
- Remde, A., & Conrad, R. (1990). Production of nitric oxide in *Nitrosomonas europaea* by reduction of nitrite. *Archives of Microbiology*, 154(2), 187–191. <https://doi.org/10.1007/BF00423331>
- Ren, M., Feng, X., Huang, Y., Wang, H., Hu, Z., Clingenpeel, S., ... Luo, H. (2019). Phylogenomics suggests oxygen availability as a driving force in Thaumarchaeota evolution. *ISME Journal*, 13(9), 2150–2161. <https://doi.org/10.1038/s41396-019-0418-8>
- Rinke, C., Chuvochina, M., Mussig, A. J., Chaumeil, P.-A., Davín, A. A., Waite, D. W., ... Hugenholtz, P. (2021). A standardized archaeal taxonomy for the Genome Taxonomy Database. *Nature Microbiology*, 6(7), 946–959. <https://doi.org/10.1038/s41564-021-00918-8>
- Rockström, J., Steffen, W., Noone, K., Persson, Å., Chapin, F. S., Lambin, E. F., ... Foley, J. A. (2009). A safe operating space for humanity. *Nature*, 461(7263), 472–475. <https://doi.org/10.1038/461472a>
- Ruser, R., & Schulz, R. (2015). The effect of nitrification inhibitors on the nitrous oxide N₂O release from agricultural soils—a review. *Journal of Plant Nutrition and Soil Science*, 178(2), 171–188. <https://doi.org/10.1002/jpln.201400251>
- Rütting, T., Boeckx, P., Müller, C., & Klemedtsson, L. (2011). Assessment of the importance of dissimilatory nitrate reduction to ammonium for the terrestrial nitrogen cycle. *Biogeosciences*, 8(7), 1779–1791. <https://doi.org/10.5194/bg-8-1779-2011>
- Sakamoto, H., Higashimoto, Y., Hayashi, S., Sugishima, M., Fukuyama, K., Palmer, G., & Noguchi, M. (2004). Hydroxylamine and hydrazine bind directly to the heme iron of the heme–heme oxygenase-1 complex. *Journal of Inorganic Biochemistry*, 98(7), 1223–1228.

<https://doi.org/10.1016/j.jinorgbio.2004.02.028>

- Sakoula, D., Smith, G. J., Frank, J., Mesman, R. J., Kop, L. F. M., Blom, P., ... Lücker, S. (2021). Universal activity-based labeling method for ammonia- and alkane-oxidizing bacteria. *The ISME Journal*, (February), 1–14. <https://doi.org/10.1038/s41396-021-01144-0>
- Salonen, A., Nikkilä, J., Jalanka-Tuovinen, J., Immonen, O., Rajilić-Stojanović, M., Kekkonen, R. A., ... de Vos, W. M. (2010). Comparative analysis of fecal DNA extraction methods with phylogenetic microarray: Effective recovery of bacterial and archaeal DNA using mechanical cell lysis. *Journal of Microbiological Methods*, 81(2), 127–134. <https://doi.org/10.1016/j.mimet.2010.02.007>
- Schalk, J., de Vries, S., Kuenen, J. G., & Jetten, M. S. M. (2000). Involvement of a Novel Hydroxylamine Oxidoreductase in Anaerobic Ammonium Oxidation. *Biochemistry*, 39(18), 5405–5412. <https://doi.org/10.1021/bi992721k>
- Schatteman, A., Wright, C. L., Crombie, A. T., Murrell, J. C., & Lehtovirta-Morley, L. E. (2022). Hydrazines as Substrates and Inhibitors of the Archaeal Ammonia Oxidation Pathway. *Applied and Environmental Microbiology*, 88(8). <https://doi.org/10.1128/aem.02470-21>
- Schleper, C., & Nicol, G. W. (2010). Ammonia-oxidising archaea - physiology, ecology and evolution. *Advances in Microbial Physiology*, 57(C), 1–41. <https://doi.org/10.1016/B978-0-12-381045-8.00001-1>
- Seaver, L. C., & Imlay, J. A. (2001). Alkyl Hydroperoxide Reductase Is the Primary Scavenger of Endogenous Hydrogen Peroxide in Escherichia coli. *Journal of Bacteriology*, 183(24), 7173–7181. <https://doi.org/10.1128/JB.183.24.7173-7181.2001>
- Shaeer, A., Aslam, M., & Rashid, N. (2019). A highly stable manganese catalase from *Geobacillus thermopakistaniensis*: molecular cloning and characterization. *Extremophiles*, 23(6), 707–718. <https://doi.org/10.1007/s00792-019-01124-5>
- Shen, T., Stieglmeier, M., Dai, J., Urich, T., & Schleper, C. (2013). Responses of the terrestrial ammonia-oxidizing archaeon *Ca. Nitrososphaera viennensis* and the ammonia-oxidizing bacterium *Nitrosospira multiformis* to nitrification inhibitors. *FEMS Microbiology Letters*, 344(2), 121–129. <https://doi.org/10.1111/1574-6968.12164>
- Sheridan, P. O., Raguideau, S., Quince, C., Holden, J., Zhang, L., Gaze, W. H., ... Gubry-Rangin, C. (2020). Gene duplication drives genome expansion in a major lineage of Thaumarchaeota. *Nature Communications*, 11(1), 1–12. <https://doi.org/10.1038/s41467-020-19132-x>
- Soler-Jofra, A., Pérez, J., & van Loosdrecht, M. C. M. (2021). Hydroxylamine and the nitrogen cycle: A

- review. *Water Research*, *190*, 116723. <https://doi.org/10.1016/j.watres.2020.116723>
- Spang, A., Hatzenpichler, R., Brochier-Armanet, C., Rattei, T., Tischler, P., Spieck, E., ... Schleper, C. (2010). Distinct gene set in two different lineages of ammonia-oxidizing archaea supports the phylum Thaumarchaeota. *Trends in Microbiology*, *18*(8), 331–340. <https://doi.org/10.1016/j.tim.2010.06.003>
- Spang, A., Poehlein, A., Offre, P., Zumbärgel, S., Haider, S., Rychlik, N., ... Wagner, M. (2012). The genome of the ammonia-oxidizing *Candidatus Nitrososphaera gargensis*: Insights into metabolic versatility and environmental adaptations. *Environmental Microbiology*, *14*(12), 3122–3145. <https://doi.org/10.1111/j.1462-2920.2012.02893.x>
- Stahl, D. A., & de la Torre, J. R. (2012). Physiology and Diversity of Ammonia-Oxidizing Archaea. *Annual Review of Microbiology*, *66*(1), 83–101. <https://doi.org/10.1146/annurev-micro-092611-150128>
- Stein, L. Y., & Arp, D. J. (1998). Loss of ammonia monooxygenase activity in *Nitrosomonas europaea* upon exposure to nitrite. *Applied and Environmental Microbiology*, *64*(10), 4098–4102. <https://doi.org/10.1128/AEM.70.3.1555-1562.2004>
- Stieglmeier, M., Klingl, A., Alves, R. J. E., Rittmann, S. K.-M. R., Melcher, M., Leisch, N., & Schleper, C. (2014). *Nitrososphaera viennensis* gen. nov., sp. nov., an aerobic and mesophilic, ammonia-oxidizing archaeon from soil and a member of the archaeal phylum Thaumarchaeota. *International Journal of Systematic and Evolutionary Microbiology*, *64*(Pt_8), 2738–2752. <https://doi.org/10.1099/ijs.0.063172-0>
- Storz, G., Wolf, Y. I., & Ramamurthi, K. S. (2014). Small Proteins Can No Longer Be Ignored. *Annual Review of Biochemistry*, *83*(1), 753–777. <https://doi.org/10.1146/annurev-biochem-070611-102400>
- Strous, M., Fuerst, J. A., Kramer, E. H. M., Logemann, S., Muyzer, G., Van De Pas-Schoonen, K. T., ... Jetten, M. S. M. (1999). Missing lithotroph identified as new planctomycete. *Nature*, *400*(6743), 446–449. <https://doi.org/10.1038/22749>
- Subbarao, G. V., Sahrawat, K. L., Nakahara, K., Ishikawa, T., Kishii, M., Rao, I. M., ... Lata, J. C. (2012). *Biological nitrification inhibition-a novel strategy to regulate nitrification in agricultural systems. Advances in Agronomy* (1st ed., Vol. 114). Elsevier Inc. <https://doi.org/10.1016/B978-0-12-394275-3.00001-8>
- Tahon, G., Geesink, P., & Ettema, T. J. G. (2021). Expanding Archaeal Diversity and Phylogeny: Past, Present, and Future. *Annual Review of Microbiology*, *75*(1), 359–381.

<https://doi.org/10.1146/annurev-micro-040921-050212>

- Tappe, W., Laverman, A., Bohland, M., Braster, M., Rittershaus, S., Groeneweg, J., & Van Verseveld, H. W. (1999). Maintenance energy demand and starvation recovery dynamics of *Nitrosomonas europaea* and *Nitrobacter winogradskyi* cultivated in a retentostat with complete biomass retention. *Applied and Environmental Microbiology*, 65(6), 2471–2477. <https://doi.org/10.1128/aem.65.6.2471-2477.1999>
- Taylor, A. E., Taylor, K., Tennigkeit, B., Palatinszky, M., Stieglmeier, M., Myrold, D. D., ... Bottomley, P. J. (2015). Inhibitory Effects of C 2 to C 10 1-Alkynes on Ammonia Oxidation in Two *Nitrososphaera* Species. *Applied and Environmental Microbiology*, 81(6), 1942–1948. <https://doi.org/10.1128/AEM.03688-14>
- Taylor, Anne E., Giguere, A. T., Zobelein, C. M., Myrold, D. D., & Bottomley, P. J. (2017). Modeling of soil nitrification responses to temperature reveals thermodynamic differences between ammonia-oxidizing activity of archaea and bacteria. *ISME Journal*, 11(4), 896–908. <https://doi.org/10.1038/ismej.2016.179>
- Taylor, Anne E., Vajrala, N., Giguere, A. T., Gitelman, A. I., Arp, D. J., Myrold, D. D., ... Bottomley, P. J. (2013). Use of Aliphatic n -Alkynes To Discriminate Soil Nitrification Activities of Ammonia-Oxidizing Thaumarchaea and Bacteria. *Applied and Environmental Microbiology*, 79(21), 6544–6551. <https://doi.org/10.1128/AEM.01928-13>
- Tolar, B. B., Powers, L. C., Miller, W. L., Wallsgrove, N. J., Popp, B. N., & Hollibaugh, J. T. (2016). Ammonia Oxidation in the Ocean Can Be Inhibited by Nanomolar Concentrations of Hydrogen Peroxide. *Frontiers in Marine Science*, 3(NOV). <https://doi.org/10.3389/fmars.2016.00237>
- Tourna, M., Stieglmeier, M., Spang, A., Konneke, M., Schintlmeister, A., Urich, T., ... Schleper, C. (2011). *Nitrososphaera viennensis*, an ammonia oxidizing archaeon from soil. *Proceedings of the National Academy of Sciences*, 108(20), 8420–8425. <https://doi.org/10.1073/pnas.1013488108>
- Tourna, Maria, Stieglmeier, M., Spang, A., Konneke, M., Schintlmeister, A., Urich, T., ... Schleper, C. (2011). *Nitrososphaera viennensis*, an ammonia oxidizing archaeon from soil. *Proceedings of the National Academy of Sciences*, 108(20), 8420–8425. <https://doi.org/10.1073/pnas.1013488108>
- Townsend, A. R., Howarth, R. W., Bazzaz, F. A., Booth, M. S., Cleveland, C. C., Collinge, S. K., ... Wolfe, A. H. (2003). Human health effects of a changing global nitrogen cycle. *Frontiers in Ecology and the Environment*, 1(5), 240–246. Retrieved from <https://esajournals.onlinelibrary.wiley.com/doi/abs/10.1890/1540->

9295%282003%29001%5B0240%3AHHEOAC%5D2.0.CO%3B2

- Treusch, A. H., Leininger, S., Kietzin, A., Schuster, S. C., Klenk, H. P., & Schleper, C. (2005). Novel genes for nitrite reductase and Amo-related proteins indicate a role of uncultivated mesophilic crenarchaeota in nitrogen cycling. *Environmental Microbiology*, *7*(12), 1985–1995. <https://doi.org/10.1111/j.1462-2920.2005.00906.x>
- Vajrala, N., Martens-Habbena, W., Sayavedra-Soto, L. A., Schauer, A., Bottomley, P. J., Stahl, D. A., & Arp, D. J. (2013). Hydroxylamine as an intermediate in ammonia oxidation by globally abundant marine archaea. *Proceedings of the National Academy of Sciences*, *110*(3), 1006–1011. <https://doi.org/10.1073/pnas.1214272110>
- Vajrala, Neeraja, Bottomley, P. J., Stahl, D. A., Arp, D. J., & Sayavedra-Soto, L. A. (2014). Cycloheximide prevents the de novo polypeptide synthesis required to recover from acetylene inhibition in *Nitrosopumilus maritimus*. *FEMS Microbiology Ecology*, *88*(3), 495–502. <https://doi.org/10.1111/1574-6941.12316>
- van Kessel, M. A. H. J., Speth, D. R., Albertsen, M., Nielsen, P. H., Op den Camp, H. J. M., Kartal, B., ... Lücker, S. (2015). Complete nitrification by a single microorganism. *Nature*, *528*(7583), 555–559. <https://doi.org/10.1038/nature16459>
- van Kessel, M. A., Stultiens, K., Slegers, M. F., Guerrero Cruz, S., Jetten, M. S., Kartal, B., & Op den Camp, H. J. (2018). Current perspectives on the application of N-damo and anammox in wastewater treatment. *Current Opinion in Biotechnology*, *50*, 222–227. <https://doi.org/10.1016/j.copbio.2018.01.031>
- Venter, J. C., Remington, K., Heidelberg, J. F., Halpern, A. L., Rusch, D., Eisen, J. A., ... Smith, H. O. (2004). Environmental Genome Shotgun Sequencing of the Sargasso Sea. *Science*, *304*(5667), 66–74. <https://doi.org/10.1126/science.1093857>
- Versantvoort, W., Pol, A., Jetten, M. S. M., van Niftrik, L., Reimann, J., Kartal, B., & Op den Camp, H. J. M. (2020). Multiheme hydroxylamine oxidoreductases produce NO during ammonia oxidation in methanotrophs. *Proceedings of the National Academy of Sciences of the United States of America*, *117*(39), 24459–24463. <https://doi.org/10.1073/pnas.2011299117>
- Vitousek, P. M., Porder, S., Houlton, B. Z., & Chadwick, O. A. (2010). Terrestrial phosphorus limitation: mechanisms, implications, and nitrogen–phosphorus interactions. *Ecological Applications*, *20*(1), 5–15. <https://doi.org/10.1890/08-0127.1>
- Walker, C. B., de la Torre, J. R., Klotz, M. G., Urakawa, H., Pinel, N., Arp, D. J., ... Stahl, D. A. (2010).

- Nitrosopumilus maritimus genome reveals unique mechanisms for nitrification and autotrophy in globally distributed marine crenarchaea. *Proceedings of the National Academy of Sciences*, 107(19), 8818–8823. <https://doi.org/10.1073/pnas.0913533107>
- Whittaker, J. W. (2012). Non-heme manganese catalase - The “other” catalase. *Archives of Biochemistry and Biophysics*, 525(2), 111–120. <https://doi.org/10.1016/j.abb.2011.12.008>
- Wiedenheft, B., Mosolf, J., Willits, D., Yeager, M., Dryden, K. A., Young, M., & Douglas, T. (2005). An archaeal antioxidant: Characterization of a Dps-like protein from *Sulfolobus solfataricus*. *Proceedings of the National Academy of Sciences of the United States of America*, 102(30), 10551–10556. <https://doi.org/10.1073/pnas.0501497102>
- Wijma, H. J., Canters, G. W., De Vries, S., & Verbeet, M. P. (2004). Bidirectional catalysis by copper-containing nitrite reductase. *Biochemistry*, 43(32), 10467–10474. <https://doi.org/10.1021/bi0496687>
- Winogradsky, S. (1890). Recherches sur les Organismes des la Nitrification (Parts 4-5). *Annales de l'Institut Pasteur*, 5, 92–100.
- Wittig, I., Braun, H. P., & Schägger, H. (2006). Blue native PAGE. *Nature Protocols*, 1(1), 418–428. <https://doi.org/10.1038/nprot.2006.62>
- Wittig, I., & Schägger, H. (2005). Advantages and limitations of clear-native PAGE. *PROTEOMICS*, 5(17), 4338–4346. <https://doi.org/10.1002/pmic.200500081>
- Wolf, S. G., Frenkiel, D., Arad, T., Finkeil, S. E., Kolter, R., & Minsky, A. (1999). DNA protection by stress-induced biocrystallization. *Nature*, 400(6739), 83–85. <https://doi.org/10.1038/21918>
- Wood, N. (2001). Catalase and superoxide dismutase activity in ammonia-oxidising bacteria. *FEMS Microbiology Ecology*, 38(1), 53–58. [https://doi.org/10.1016/S0168-6496\(01\)00173-8](https://doi.org/10.1016/S0168-6496(01)00173-8)
- Woodbury, W., Spencer, A. K., & Stahmann, M. A. (1971). An improved procedure using ferricyanide for detecting catalase isozymes. In Intergovernmental Panel on Climate Change (Ed.), *Analytical Biochemistry* (Vol. 44, pp. 301–305). Cambridge: Cambridge University Press. [https://doi.org/10.1016/0003-2697\(71\)90375-7](https://doi.org/10.1016/0003-2697(71)90375-7)
- Wright, C. L., Schatteman, A., Crombie, A. T., Murrell, J. C., & Lehtovirta-Morley, L. E. (2020). Inhibition of ammonia monooxygenase from ammonia-oxidizing archaea by linear and aromatic alkynes. *Applied and Environmental Microbiology*, 86(9), 1–14. <https://doi.org/10.1128/AEM.02388-19>
- Wu, M.-R., Miao, L.-L., Liu, Y., Qian, X.-X., Hou, T.-T., Ai, G.-M., ... Liu, S.-J. (2022). Identification and

- characterization of a novel hydroxylamine oxidase, DnfA, that catalyzes the oxidation of hydroxylamine to N₂. *Journal of Biological Chemistry*, 298(9), 102372. <https://doi.org/10.1016/j.jbc.2022.102372>
- Wu, M., Hou, T., Liu, Y., Miao, L., Ai, G., Ma, L., ... Liu, S. (2021). Novel *Alcaligenes ammonioxydans* sp. nov. from wastewater treatment sludge oxidizes ammonia to N₂ with a previously unknown pathway. *Environmental Microbiology*, 00. <https://doi.org/10.1111/1462-2920.15751>
- Wu, Y., Guo, Y., Lin, X., Zhong, W., & Jia, Z. (2012). Inhibition of Bacterial Ammonia Oxidation by Organohydrazines in Soil Microcosms. *Frontiers in Microbiology*, 3(JAN), 1–8. <https://doi.org/10.3389/fmicb.2012.00010>
- Yamanaka, T., & Sakano, Y. (1980). Oxidation of hydroxylamine to nitrite catalyzed by hydroxylamine oxidoreductase purified from *Nitrosomonas europaea*. *Current Microbiology: An International Journal*, 4(4), 239–244. <https://doi.org/10.1007/BF02605864>
- Yang, M., Fang, Y., Sun, D., & Shi, Y. (2016). Efficiency of two nitrification inhibitors (dicyandiamide and 3, 4-dimethylpyrazole phosphate) on soil nitrogen transformations and plant productivity: A meta-analysis. *Scientific Reports*, 6(February), 1–10. <https://doi.org/10.1038/srep22075>
- Yang, W., Wang, Y., Tago, K., Tokuda, S., & Hayatsu, M. (2017). Comparison of the Effects of Phenylhydrazine Hydrochloride and Dicyandiamide on Ammonia-Oxidizing Bacteria and Archaea in Andosols. *Frontiers in Microbiology*, 8(NOV). <https://doi.org/10.3389/fmicb.2017.02226>
- Yoshida, T., & Alexander, M. (1964). Hydroxylamine Formation by *Nitrosomonas europaea*. *Canadian Journal of Microbiology*, 10(6), 923–926. <https://doi.org/10.1139/m64-121>
- Zacherl, B., & Amberger, A. (1990). Effect of the nitrification inhibitors dicyandiamide, nitrapyrin and thiourea on *Nitrosomonas europaea*. *Fertilizer Research*, 22(1), 37–44. <https://doi.org/10.1007/BF01054805>
- Zerulla, W., Barth, T., Dressel, J., Erhardt, K., Horchler von Locquenghien, K., Pasda, G., ... Wissemeyer, A. (2001). 3,4-Dimethylpyrazole phosphate (DMPP) - A new nitrification inhibitor for agriculture and horticulture. An introduction. *Biology and Fertility of Soils*, 34(2), 79–84. <https://doi.org/10.1007/s003740100380>
- Zhao, G., Ceci, P., Ilari, A., Giangiacomo, L., Laue, T. M., Chiancone, E., & Dennis Chasteen, N. (2002). Iron and hydrogen peroxide detoxification properties of DNA-binding protein from starved cells. A ferritin-like DNA-binding protein of *Escherichia coli*. *Journal of Biological Chemistry*, 277(31), 27689–27696. <https://doi.org/10.1074/jbc.M202094200>

